The functional interplay between TNPO3, CPSF6 and HIV-1 CA

THE FUNCTIONAL INTERPLAY BETWEEN TNPO3, CPSF6 AND HIV-1 CA

A dissertation presented

by

Ilker Oztop

to

The Division of Medical Sciences

in partial fulfillment of the requirements

for the degree of

Doctor of Philosophy

in the subject of

Virology

Harvard University

Cambridge, Massachusetts

July, 2014

Advisor: Dr. Alan Engelman **Author: Ilker Oztop**

THE FUNCTIONAL INTERPLAY BETWEEN TNPO3, CPSF6 AND HIV-1 CA

ABSTRACT

Lentiviruses can infect postmitotic cells, indicative of a role for the nucleocytoplasmic transport machinery. Genome-wide RNA interference screens identified transportin 3 (TNPO3) that may regulate human immunodeficiency virus type 1 (HIV-1) preintegration complex (PIC) nuclear import but plays no role during murine leukemia virus (MLV) infection. Independently, TNPO3 was shown to bind HIV-1 integrase (IN), a PIC component, suggesting a potential mechanism for nuclear import. We demonstrated direct binding between TNPO3 and several retroviral INs, which did not correlate with TNPO3 dependency profiles of the respective retroviruses. Infectivity assays employing HIV-1/MLV chimeric viruses ascertained that the capsid (CA) domain, but not IN, was the functional determinant of TNPO3 dependence. A carboxy-terminal truncation mutant of the serine-arginine rich (SR) protein family member, cleavage and polyadenylation specific factor 6 (CPSF6), CPSF6-358, which lacks its RS domain, was shown to restrict HIV-1 PIC nuclear import. We demonstrated that CPSF6 interacts with HIV-1 CA, and a single point mutation in CA, Asn74Asp (N74D), abolished this interaction. N74D also rendered HIV-1 TNPO3-independent and impaired cyclophilin A (CypA) binding to CA. The CA:CPSF6 binding interface, as described in a partial co-crystal structure, defined a surface pocket on CA that faces the CA hexamer:hexamer interspace. Infectivities and CA binding profiles of CA mutants within this pocket or with aberrant CypA-related phenotypes were assessed to compare their CPSF6-358 sensitivity and TNPO3 dependence, which largely

correlated. We showed an overall correlation between the CPSF6/CPSF6-358 binding profiles of these HIV-1 CA mutants and their CPSF6-358 sensitivity, whereas TNPO3 binding and TNPO3 dependence did not correlate. Based on similar infectivity profiles of CA mutants and the loss of the RS domain from CPSF6-358 we tested for a direct interaction between CPSF6 and TNPO3. We demonstrated specific binding between recombinant TNPO3 and the CPSF6.RS domain. Mutagenesis experiments suggested a multicontact binding interface. The interaction was downmodulated by Ras-related nuclear protein (Ran)-GTP, indicating that CPSF6 is a *bona fide* import substrate of TNPO3. Our results support a model where TNPO3 regulates nuclear CPSF6 localization and that in its absence CPSF6 may restrict infection by directly interacting with HIV-1 CA at the hexamer:hexamer interface.

TABLE OF CONTENTS

TABLE OF FIGURES

LIST OF ABBREVIATIONS

AIDS	Acquired immunodeficiency syndrome
ALIX	Apoptosis-linked gene 2-interacting protein X
APOBEC3G	Apolipoprotein B mRNA-editing, enzyme-catalytic, polypeptide-like 3G
ASF/SF2	serine/arginine-rich splicing factor 1 / pre-mRNA splicing factor 2
BIV	Bovine immunodeficiency virus
CA	Capsid
Cas9	CRISPR associated nuclease 9
CCD	Catalytic core domain
CCHC	Cysteine-X_2-Cysteine-X_4-Histidine-X_4-Cysteine motif
CCR5	Cysteine-Cysteine chemokine receptor type 5
CD3	Cluster of differentiation 3 glycoprotein
CD4	Cluster of differentiation 4 glycoprotein
CDK	Cyclin dependent kinase
cPPT	Central polypurine tract
CPSF6/ CFIm68	Cleavage and polyadenylation specific factor 6, mammalian cleavage factor I 68 kD subunit
CRISPR	Clustered regularly interspaced short palindromic repeats
CRL	Cullin–RING finger E3 ubiquitin ligase
CRM1/XPO1	Chromosome region maintenance 1, exportin 1
CsA	Cyclosporine A
CTD	Carboxyl terminal domain
CTL	Cytotoxic T-lymphocyte
CTS	Central termination signal
CXCR4	Cysteine-X-Cysteine chemokine receptor type 4
CypA	Cylophilin A
EIAV	Equine infectious anemia virus
EM	Electron microscopy
Env/*env*	Envelope glycoprotein
ER	Endoplasmic reticulum
ERT	Early reverse transcript
ESCRT	Endosomal sorting complex required for transport
FG-repeat	Phenylalanine-glycine repeat
FIV	Feline immunodeficiency virus
Fv1	Friend virus susceptibility 1
Gag/*gag*	Group specific antigen
GDP	Guanosine diphosphate
GFP	Green fluorescent protein
GST	Glutathione S-transferase
gRNA	Genomic RNA
GTP	Guanosine triphosphate
HAART	Highly active antiretroviral therapy
HIV	Human immunodeficiency virus
HMW	High molecular weight
HSCT	Hematopoietic stem cell transplantation

IN	Integrase
KARS	Lysyl-tRNA synthetase
KD	Knockdown
KPN	Karyopherin
LEDGF/p75	Lens epithelium-derived growth factor
LRT	Late reverse transcript
LTR	Long terminal repeat
MA	Matrix
MG132	N-(benzyloxycarbonyl)-leucinyl-leucinyl-leucinal
MHC-I	Major histocompatibility complex class I
MHIV	MLV/HIV
MLV	Murine leukemia virus
MMTV	Mouse mammary tumor virus
MPMV	Mason-Pfizer monkey virus
MOI	Multiplicity of infection
Mx2/MxB	Myxovirus resistance 2
NC	Nucleocapsid
Nef/*nef*	Negative regulatory factor
NES	Nuclear export signal
NHEJ	Non-homologous end-joining
NLS	Nuclear localization signal
NPC	Nuclear pore complex
NTD	Amino terminal domain
NTF2	Nuclear transport factor 2
NUP/Nup	Nucleoporin
PBS	Primer binding sequence
PDZD8	PDZ domain containing 8
PFV	Prototype foamy virus
PIC	Preintegration complex
Pol/*pol*	Polymerase
PPT	Polypurine tract
PR	Protease
PTAP	Proline-threonine-alanine-proline-proline
P-TEFb	Positive transcription elongation factor b
qPCR	Quantitative PCR
Ran	Ras-related nuclear protein
RanBP1/2	Ran binding protein 1/2
RanGAP	Ran GTPase activating protein
RanGEF	Ran guanine nucleotide exchange factor
RCC1	Regulator of chromosome condensation 1
RD	Arginine-aspartate
RE	Arginine-glutamate
Rev/*rev*	Regulator of expression of viral proteins
RFP	Red fluorescent protein
RNAi	RNA interference
RNase H	Ribonuclease H

RRE	Rev response element
RRM	RNA recognition motif
RS	Arginine-serine rich
RSV	Rous sarcoma virus
RT	Reverse transcriptase
RTC	Reverse transcription complex
SAMHD1	SAM domain and HD domain-containing protein 1
SDM	Site directed mutagenesis
SEM	Standard errors of the means
shRNA	Small hairpin RNA
siRNA	Small interfering RNA
SIV	Simian immunodeficiency virus
SR	Serine-arginine rich
SU/gp120	Surface attachment glycoprotein
SV40	Simian vacuolating virus 40
TAR	Trans-active response element
Tat/t*at*	Trans-activator of transcription
TCR	T cell receptor
TG	Thymine-guanine
TM/gp41	Transmembrane glycoprotein
TNPO3/TRN-SR2	Transportin 3, importin 12
TRIM5α	Tripartite motif-containing Motif 5
TRIMCyp	TRIM5-CypA fusion protein
tRNALys,3	Lysine tRNA, 3
Tsg101	Tumor susceptibility gene 101
TU	Transcriptional unit
U3	Unique 3’ sequence
U5	Unique 5’ sequence
vDNA	Viral DNA
Vif/*vif*	Viral infectivity factor
VLP	Viral like particles
Vpr/*vpr*	Viral protein R
Vpu/*vpu*	Viral protein unique
Vpx/*vpx*	Vpr-related viral protein x
vRNA	Viral RNA
VSV-G	Vesicular stomatitis virus G envelope glycoprotein
WT	Wild type
YPX_nL	Tyrosine-proline-X_n-leucine
ZFN	Zinc finger nuclease

To my mom,
Füsun Mutlusoy Öztop

and my late grandma,
'ananem' Selma Mutlusoy

ACKNOWLEDGMENTS

I would like to start with acknowledging my dissertation examiners Drs. David Knipe, Karl Münger, Ann Sheehy and my chair Dana Gabuzda for agreeing to serve on my committee on a tight schedule. I want to thank Drs. Gabuzda, Knipe and Münger, along with the Dean of the Division of Medical Sciences, Dr. David Cardozo, especially, from whose instrumental mentorship I benefited on several critical occasions during grad school.

I am grateful to Drs. Dana Gabuzda, who chaired both my dissertation examination and advisory committees, Thomas Schwartz and Joe Sodroski for their scientific advice and supervision over the years. Without the challenging advisory meetings I would not have grown into the young scientist I am today.

I would like to extend my gratitude to Drs. Vineet KewalRamani, KyeongEun Lee, Zandrea Ambrose, Chris Aiken, Peter Cherepanov, Goedele Maertens, Jinwoo Ahn and Tatyana Polenova, whom I had the privilege to collaborate with on several projects. Peter, a former Engelmanite himself, gratuitously hosted me in his lab at the London Research Institute briefly and gave me crucial technical and intellectual advice during the course of this project. An exceptional and exemplary expat scientist, he is a great role model I look up to.

Drs. Jim Cunningham, Welkin Johnson, Sean Whelan and Don Coen each had a major influence on me building up my self-confidence as a student-scientist during the initial phase of grad school. I want to give special credit to Jim, Welkin and Don for their inspiring mentorship, for their love of science for the sake of science and for being unique and successful role models, who do not fit into given stereotypes.

My decision to pursue a PhD in virology was a result of several past research experiences. I would like to acknowledge Dr. Aslı Tolun from my *alma mater* Boğaziçi

University, who inspired me to do biomedical research. Dr. Peter Daniel at Max Delbrück Center for Molecular Medicine in Berlin introduced me to the high standards of the international world of academia. Dr. Walther Mothes at Yale University offered me a post-baccalaureate research position in his retrovirology lab under his passionate scientific supervision and encouraging mentorship that have lasted up until today.

Luis Menendez's incredible insight into all things research, his inspiring passion for science, his exceptional bench skills and selfless support have set the bar really high for me and kept me motivated all along. Both as a great scientist and a great friend, I am looking forward to keep learning from you. Muchos gracias, amigo.

Allison Ballandras-Colas has not only been an extraordinary role model to me for her excellent biochemistry skills, her intelligence and her mentorship, but also for her continuous academic (and PyMol!) support and companionship in and outside the lab. I "Got Lucky" for numerous reasons to have met you. Merci pour tout.

I cannot appreciate enough my bros Oğuz Semerci, Arda Halu and Mehmet Akçakaya. Thank you for your sincere and 'bro-tastic' camaraderie and thanks for helping me tackle many academic and personal challenges over the years.

My past and present roommates at Chez 199, Wilhelm Weihofen, Catarina Moniz Alves and Gabi Aguilar; and our close circle of friends Eva Fast, Sonu Parikh Mehta, Manav Mehta and Daniela Panakova deserve much gratitude for creating a 'home away from home' for me.

I also want to thank my former roommate, Gaye Soley, with whom I both enjoyed and suffered the ups and downs of grad school at Harvard together for many years. Now a faculty herself at our *alma mater*, she set me an example of a successful academic that I aspire to become myself one day.

I am deeply grateful to cikletoğlan Gökcan Demirkazık for his gratuitous love and support during demanding times in grad school. I cherish your selfless companionship and your insightful remarks that allowed me to grow into the person I am today.

Kenny Matreyek. Be it for your nonjudgmental and supportive presence in and outside the lab or for your absence during the Dark Ages, your friendship was certainly a defining part of my time at Harvard. Thank you for all the intellectual conversations we had, for making me feel less of an international student and for setting a great example of a diligent and successful young scientist. Don't be a stranger.

I would also like to thank my virology cohort, of whom I am the last man standing. Alex Guth deserves a special shout out for his genuine support and friendship over the years; and so does Jennifer Spangle, who was also the best travel companion and makeshift landlord extraordinaire when needed. I am also grateful to the Harvard Virology Program for creating a close-knit environment. I feel lucky to have overlapped with my brother-in-capsid Kevin McCarthy, whose unflickering love of science, unwavering enthusiasm about all things capsid and indescribable joy for ejecting strategically placed micropipette tips have been a constant motivation all along.

I want to acknowledge all my past and present fellow Engelmanites, but especially Kellie Jurado, Erik Serrao, Amanda Dudek and Lavanya Krishnan for making the lab and the CIA floor an amicable working environment (and also for all of our blastful weekend getaways!). I also like to thank Nicole Espy for believing in me as a scientist and a human being more than I do myself and to Andrés Finzi for continuously challenging and supporting me as a researcher during his time at DFCI.

I am glad to have met and mentored Suna Yücel and Duygu Sarı, both summer interns at Harvard, from whom I have learned as much as I taught them.

I am grateful for the guidance and mentorship I received from postdoctoral researchers Jeremy Kamil and My Sam at the very beginning of grad school, when I barely had any biochemistry bench skills and basically learned everything from them.

As known by many in Longwood, "I am the terror that flaps in the night". But no way on earth could I have survived those nightshifts, if it weren't for the sandwiches Doreen prepared at Au Bon Pain (free hugs included), or for the late night cab vouchers Eleanor handed out to me at Vandy Security over and over again. I also like to thank the HMS Campus Maintenance for letting me regularly sleep in TMEC and Vandy lounges!

Talking of my need for impromptu sleeping accommodations, I want to thank Ece Turnator and her wife Amanda Green, who have gratuitously hosted me in their home during stressful times in grad school. Ever since our days back in Istanbul and at IKSV, I have always found support in the company of you both and your son, Sinan Finnigan.

I have not had that many role models in my academic training, but Dr. Jon Beckwith is undoubtedly one. In him I see a dedicated scientist, a socially responsible thought leader/activist and also a devoted science communicator, who is willing to experiment with the arts to reach these ends. I am honored that he recruited me to be one of the cofounders of the Science-Theater Board at Harvard, a joint Harvard-American Repertory Theater (ART) initiative aiming to communicate science in unorthodox ways to reach as diverse and (science-) naive audiences as possible.

Stage acting has always been my creative outlet and it has also helped me balance out the exhausting and demanding hours in the lab. I consider myself lucky for having had many acting

opportunities through the Harvard-Radcliffe Dramatic Club (HRDC) over the years. I especially want to acknowledge directors életem Vanda Gyuris, James Leaf, Matt Stone, Renée Michelle Ragin, Jan Lukšič, Sonia Koman and Calla Videt for their inspiring theater making. Michael van Devere's production of William Wilson, a short movie based on the eponymous short story by Edgar Allen Poe, was a rewarding (and rewarded) acting experience that I am proud of, especially.

The last year of graduate school overlapped with a sensitive period in modern Turkish political history ripe with anti-governmental, pro-democratization mass protests. This part grim, part highly celebrated series of events garnered international support from citizens and friends of Turkey in many corners of the world, including in Boston. I am honored and proud to be one of the founding members and spokespeople of our Turkish human rights NGO, Bostonbullular that came to existence during these historical times.

I am deeply grateful for the friendship and support Bostonbullular provided me with during grad school: My old and bold bro-ette Selen 'Başgan' Yanmaz; 'annem' Esen Şefik and 'babam' gourmet Kutay Karatepe, who even staged a disturbed sleep schedule intervention for my benefit; my comrade Emrah(izm) Altındiş; Semir Beyaz, whom I still owe a Weissbier; Güneş Bozkurt, who was always there to help me get through the troughs of academia; Didem İlter, without whose company M2 rides would just be incomplete; Gülfer Göze and Beste Kamalı, with whom I share a predilection for all things absurd and intelligent; and finally Nihal Terzi, who always shared with me her advice on things both academic and beyond, ever since she became my GSAS-appointed buddy 8 years ago.

The final stretch of dissertation writing was simply impossible to imagine without Alp Sipahigil, Efe Murat Balıkçıoğlu, Akif Ercihan Yerlioğlu, Dilan Yıldırım, Kıvanç Birsoy, Bikem

Akten, Ali Bilgin Arslan, Lerzan Coşkun and especially Zeynep Oğuz and Burak Tekin. You guys were there to check on my progress, to give me a pat on the shoulder and to get me going whenever I struggled to see the light at the end of the tunnel. Alp Sipahigil deserves a special mention for all the logistical and culinary support he willingly (!) provided in this process.

My brother and kanka I have only got to meet late in life, Umur Aksel, and his unbiased, wise and witty perspective have been a tremendous support to me over the years. Knowing that you and *manevi annem*, Reyyan Aksel, were cheering for me all along this tough rite of passage was invaluable.

Grad school is unimaginable without my partner in crime, my best friend and my most honest critic, Aysu Uygur. You have been the most defining and vital companion I have had at Harvard. I cherish our shared passion for not only pursuing knowledge but also spreading it to those who may not have had the access to our resources, our absurd sense of humor and our uniquely successful science communication initiative, Bilim Kazanı. I am proud of everything we created together. Çok yaşa, Kraliçem.

Atılgan Yılmaz is a true selfless friend, a true devoted academic and a true crusader of science I have nothing else but to look up to. You have had my back countless times in academic and personal matters ever since we committed ourselves to study science back in college. I cannot appreciate enough your nonjudgmental yet honestly piercing insight into everything I do. Getting to this point in my career would have just been impossible without your belief in me as an academic. Daha nice başarıları ve mutlulukları paylaşmak ve ileride gene bir üniversitede buluşmak dileğiyle…

I cannot thank enough my aunt Serap Alsaç, my uncle Ongun Alsaç, and my cousins Güray Alsaç and Biray Seitz, who provided me with another ‘home away from home’ in the US

and also did a pretty good job of always feeding me well - a rather formidable task. I am glad Ken Seitz joined the family and decided to expand this supportive network further by fathering our youngest, Erkan Seitz.

My parents Füsun and Orhan Öztop provided me with the best educational and training resources available to me all my life. They always encouraged my pursuit of knowledge, taught me the importance of self-determination and gave me their unconditional support which shaped me into the person I am today. Over these years, my little brother Özer Öztop surpassed me in regard to life experiences and maturity, and became a strong role model for me. Thanks for having my back all the time.

Lastly and, without a doubt, most importantly, I want to thank my supervisor, Dr. Alan Engelman. In German, a PhD supervisor is called a Doktorvater - literally a 'PhD-father'. I find it ironic that it implies the exact kind of relationship you tried hard to avoid during my 6+ years in the lab. To my luck, you failed miserably.

You have not only been a careful and insightful scientific advisor, who instilled a strong sense of perfectionism – a rather double-edged sword – in me, but you have also unprecedently stepped out of your professional and personal comfort zone over and over again to mentor and support me to any length I needed, even though it was not your responsibility. You helped me plug into the esteemed network of retrovirologists and made sure that my intellectual and practical work got acknowledged with due credit at every occasion. You nurtured my scientific self-confidence (even if by employing reverse psychology at times - and deservingly so), and you inspired and fired me all along by constantly and rightfully challenging my scientific thinking and research practice. All along my dissertation work and in the final stretch of writing,

especially, your role has simply been indispensable. I am hoping to be able to share my future success stories with you. Teşekkürler, Alan.

CHAPTER 1

INTRODUCTION

A. Epidemiology and evolutionary origins of HIV/AIDS

Acquired immunodeficiency syndrome (AIDS), caused by the retrovirus human immunodeficiency virus (HIV), was first described in 1981 when the Center for Disease Control reported 5 individual cases of *Pneumocystis carinii* pneumonia, an opportunistic infection that only leads to disease occurrence in immunosuppressed patients. In about 2 years HIV particles were isolated from AIDS patients and declared the causative agent of the disease (Gallo et al., 1983, Barre-Sinousi et al., 1983; Levy et al., 1984). HIV is transmitted via mucosal exposure during sex, direct blood-to-blood contact, and also breastfeeding. AIDS progresses by debilitating the adaptive immune defenses of the body by targeted killing of CD4 (cluster of differentiation 4 glycoprotein)+ T lymphocytes, macrophages and dendritic cells, and by inflicting irreversible damage to lymphoid tissues, which leave immunodeficient patients vulnerable to otherwise benign infections that may become life-threatening if left untreated.

There are two types of HIV (HIV-1 and HIV-2) identified so far that circulate in the human population. Molecular epidemiology and viral phylogeny analyses on viral genetic sequences map the evolutionary roots of the globally circulating virulent HIV-1 group M to Old World *Pan troglodytes troglodytes* populations in West Africa about 100 years ago (Korber et al,. 2000), where the related parental primate retrovirus, chimpanzee simian immunodeficiency virus (SIVcpz), is believed to have made a zoonotic jump into humans by means of bush meat consumption (Gao et al., 1999; Hahn et al,. 2000). HIV-1 subgroups N and O are thought to have derived from SIVcpz via independent zoonotic jumps, though HIV-1 Group O also bears some resemblance to SIVgor that infects gorillas (Sharp et al., 2011). The more recently discovered HIV-1 Group P has a clear independent evolutionary history that can be traced back to SIVgor sequences (Sharp et al., 2011). In the case of the less virulent HIV-2 epidemic that is mainly

contained to West Africa, the parental simian virus is believed to be SIVsmm that is endemic to sooty mangabees (Figure 1.1) (Hirsch et al; 1989; Sharp et al., 2011).

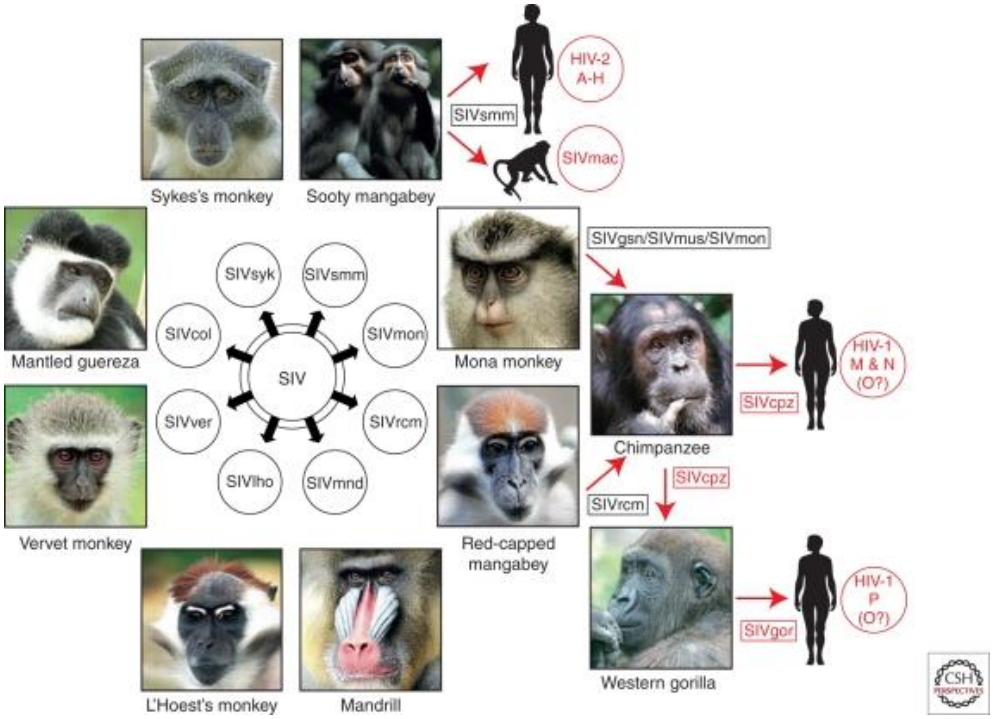

Figure 1.1 Evolutionary origin of HIV. A simplified schematic of the phylogenetic origins of HIV-1 and HIV-2 strains is shown (Adapted from Sharp et al., 2011).

Today, AIDS is a major pandemic associated with high morbidity and mortality. In 2012, the World Health Organization (WHO) and United Nations AIDS Programme (UNAIDS) estimated that there were 35.3 million people worldwide infected with HIV-1, of which ~29 million live in Sub-Saharan Africa and East and South Asia (WHO/UNAIDS, 2013). Most (95%) of the affected population resides in low- and middle-income countries with limited access to medication. It was estimated that AIDS has caused ~1.6 million deaths in 2012, still a significant decrease from ~2.3 million in 2005, thanks to the continuous development of post-exposure prophylactic strategies in the past ~20 years that culminated in a multiple drug regimen called highly active antiretroviral therapy (HAART). A high mutation rate of the virus enables quick generation of diverse HIV-1 quasispecies within an infected host. This in turn increases the

probability of viral resistance arising against antiretrovirals if they are not administered in a timely fashion and in combination to curb viral replication at independent stages, thereby limiting the occurrence of multiple resistance mutations. The continuous depletion of immune cells upon HIV-1 infection renders patients with a weakened immunity to fight back both HIV-1 itself and other associated opportunistic infections. HAART, however, has been successful in suppressing active viral replication and spread (OARAC, 2014), but AIDS still is practically an incurable disease due to non-replicating latent infections in HIV-1 reservoirs in the body that cannot be targeted by currently available drugs. This in turn enables HIV-1 to bounce back if the patients are taken off of HAART (Chun et al., 1997), requiring a life-long dependence on potentially high-cost medication and medical care.

Seminal recent reports, however, have shown that aggressive HAART in infected newborns may cure HIV-1 infection, possibly because the virus did not have the chance to form latent infection reservoirs yet (Persaud et al., 2013; Persaud et al., 2014). Additionally, the exceptional proof-of-principle case of "the Berlin Patient" showed that practical eradication of HIV-1 in a chronically infected individual may be possible (Yukl et al., 2013; Symons et al., 2014): Timothy Ray Brown, an HIV+ patient of 11 years on HAART, who concomitantly developed acute myeloid leukemia, was given two bone marrow transplants bearing hematopoietic stem cells from a donor who was selected for natural resistance to HIV-1 (Huetter et al., 2009). These HIV-1 resistant individuals have a nonfunctional CCR5 (Cys-Cys chemokine receptor type 5) protein with a 32 amino acid (aa) deletion (CCR5 Δ32) due to a rare homozygous mutation (Liu et al., 1996). CXCR4 (Cys-X-Cys chemokine receptor type 4), which is the coreceptor on CD4+ T cells required for HIV-1 attachment and entry (Feng et al., 1996) whereas another coreceptor, CCR5, is more abundantly found on macrophages (Deng et al.,

1996; Alkhatib et al., 1996) and microglial cells (He et al., 1997), a critical late target of HIV-1 during the course of systemic pathogenesis and progression to AIDS (Gartner et al., 1986). Following the repopulation of transplanted CCR5 Δ32 T cells (Huetter et al., 2009), Brown's viral load decreased to undetectable levels and even after discontinuation of HAART remained as such, prompting him to be declared the first person to be cured of chronic HIV-1 infection in 2006. Currently, several gene therapy strategies are being developed based on the success of the Berlin Patient that involve autologous hematopoietic stem cell transplantation (HSCT) combined with *ex vivo* CCR5 Δ32 genomic engineering (Li et al., 2013). They utilize the zinc finger nuclease (ZFN) and more recently the CRISPR/Cas9 (clustered regularly interspaced short palindromic repeats/CRISPR associated nuclease 9) technology (Cradick et al., 2013). Alternative approaches such as excision of the provirus from an infected cell are also being pursued with the goal of eradicating the disease (Hauber et al., 2013). With these experimental therapies still in the pipelines waiting to be optimized for both efficacy and safety (Manjunath et al., 2013; Zou et al., 2013), the search for further pharmacological prophylaxes to expand our arsenal of antiretrovirals targeting HIV-1 in its early phases of infection is of utmost importance.

B. HIV-1 virion structure

B.i. Genomic composition

Among the seven genera within the family of exogenous *Retroviridae; α-* through *ε-*, spumaviruses and lentiviruses, HIV-1 is the prototypical primate lentivirus (Figure 1.2). Exogenous retroviruses are found to infect both invertebrate insects and vertebrate animals from fishes to mammals, and evolutionarily they have a shared history with endogenous retroviruses, which are established upon extant retroviral infection of germline cells, are derivatives of retrotransposons bearing long terminal repeats (LTRs). The signature evolutionary adaptation from LTR-retrotransposons to retroviruses is that the latter acquired an open reading frame coding for an envelope (*env*) gene granting them the ability to jump from one cell to another (Malik *et al.*, 2000, Kim *et al.*, 2004). HIV-1 is believed to have evolved from chimpanzee SIV (SIVcpz; Figure 1.1) around the turn of the 20th century. Molecular clock analyses based on viral sequence comparisons claimed lentiviral SIVs to be at least about 32,000 years old (Worobey *et al.*, 2010; Worobey *et al.*, 2008). This finding, however, is probably a gross underestimate, as evidenced by the evolutionary history of anti-lentiviral host restriction factors that have to co-evolve with lentiviruses (Duggal and Emerman et al., 2012) and can be traced back to 10 Mya (Compton *et al.*, 2013).

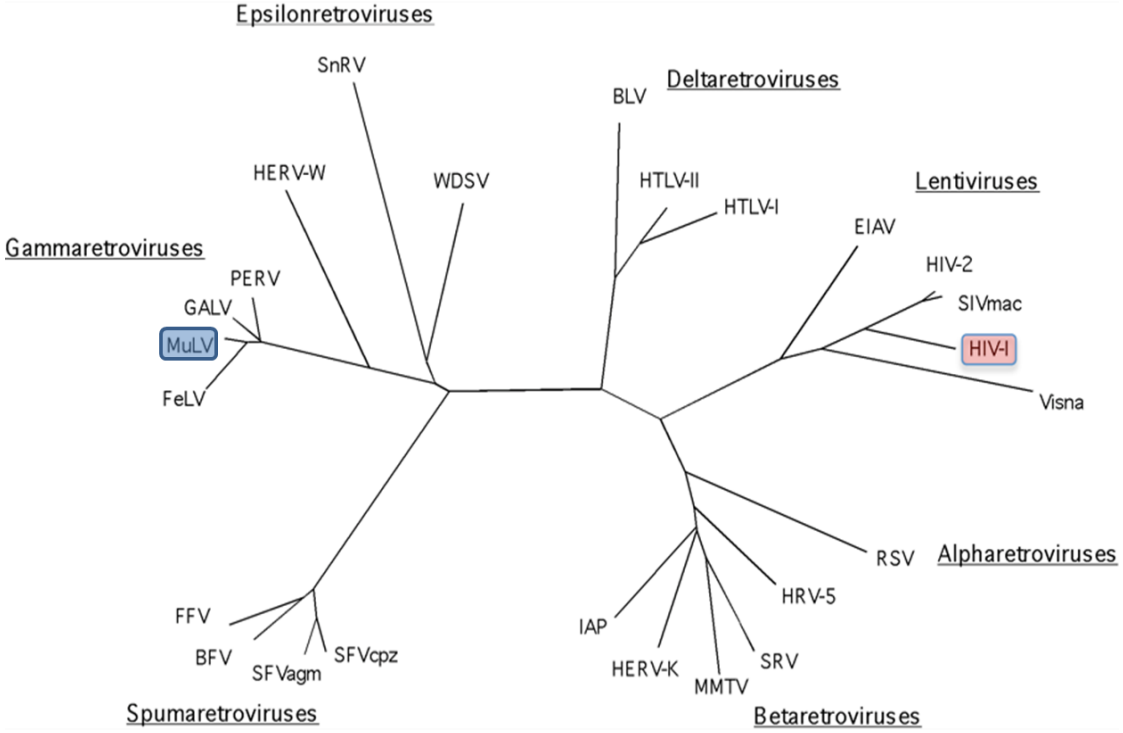

Figure 1.2 Evolutionary tree of *Retroviridae*. The seven genera of *Retroviridae* and related endogenous retroviruses based on an alignment of the amino acid residues of the RT domain of the *pol* gene. SFVcpz, simian foamy virus isolated from chimpanzee; SFVagm, simian foamy virus isolated from African green monkey; BFV, bovine foamy virus; FFV, feline foamy virus, FeLV, feline leukemia virus; MuLV/MLV, murine leukemia virus; GALV, gibbon ape leukemia virus; PERV, porcine endogenous retrovirus; HERV-W, human endogenous retrovirus W; SnRV, snake retrovirus; WDSV, walleye dermal sarcoma virus; BLV, bovine leukemia virus; HTLV, human T-lymphotropic virus; EIAV, equine infectious anemia virus; Visna, maedi-visna ovine lentivirus; RSV, Rous sarcoma virus; HRV-5, human retrovirus 5; SRV, simian retrovirus; MMTV, mouse mammary tumor virus, HERV-K, human endogenous retrovirus K; IAP, intracisternal A type particle of mouse. Adapted and modified from Weiss, 2006.

HIV-1, like all retroviruses, contains a positive-strand RNA genome, and once inside the target cells it needs to be reverse-transcribed into a double-stranded DNA genome by the viral reverse transcriptase (RT), a hallmark enzyme of all retroviruses. The viral DNA (vDNA) eventually gains access to host chromatin and with the aid of another retroviral hallmark enzyme, integrase (IN) (Panganiban et al., 1984), it gets integrated into the host genome. The distinguishing characteristics of HIV-1 and lentiviruses is that they can efficiently infect non-dividing cells such as resting CD4+ T cells (Zack et al., 1990) and differentiated tissue

macrophages (Von Schwedler et al., 1994), where the host chromatin would be inaccessible to most other retroviruses (Konstantoulas et al., 2014) within the post-mitotic nuclear envelope. This lentiviral property is readily taken advantage of by gene delivery vector development (Follenzi et al., 2000). More recently, the β-retrovirus MMTV was also shown to be able to transduce non-dividing dendritic cells (Konstantoulas et al., 2014).

HIV-1 virions carry two identical copies of an approximately 9.2 kilobase (kb) single-stranded, positive-sense genomic RNA (gRNA) that bears terminal repeat (R) elements abutting unique 5'- and 3'-end sequences named U5 and U3, respectively. The vDNA genome bears three structural and six regulatory/accessory genes flanked by a 5'- and a 3'- end LTR region, a result of U5 and U3 sequence duplication while reverse transcribing the gRNA; i.e. each LTR is composed of U3-R-U5 sequences. The primary genes, group-specific antigen (*gag*), polymerase (*pol*), and *env* encode protein products that are initially synthesized as polyproteins. Upon posttranslational modifications by viral or cellular proteases, respective polyprotein products **Gag** (55 kD), **Gag-Pol** (160 kD; resulting from a controlled translational frameshift), and glycoprotein (gp) **Env** (gp160, 160 kD) are processed into mature viral proteins that either become structural components of progeny virions (**Gag**; matrix (MA), capsid (CA), nucleocapsid (NC), protein (p) 6, and **Env**; surface gp120 (SU, 120 kD), transmembrane gp41 (TM, 41 kD), which remain noncovalently associated on the viral membrane after maturation) (Kowalski et al., 1987) or catalyze key enzymatic reactions of the viral life cycle (**Gag-Pol**: protease (PR), RT, IN). The other six HIV-1 regulatory and accessory genes, however, are primary translation products of alternatively spliced mRNAs: viral infectivity factor (Vif), viral protein R (Vpr), trans-activator of transcription (Tat), regulator of expression of virion proteins (Rev), viral protein unique (Vpu), and negative regulatory factor (Nef) that perform both cell-type specific

and non-specific functions to aid with HIV-1 infection and counteract innate host restriction mechanisms (Figure 1.3) (Coffin et al., 1997).

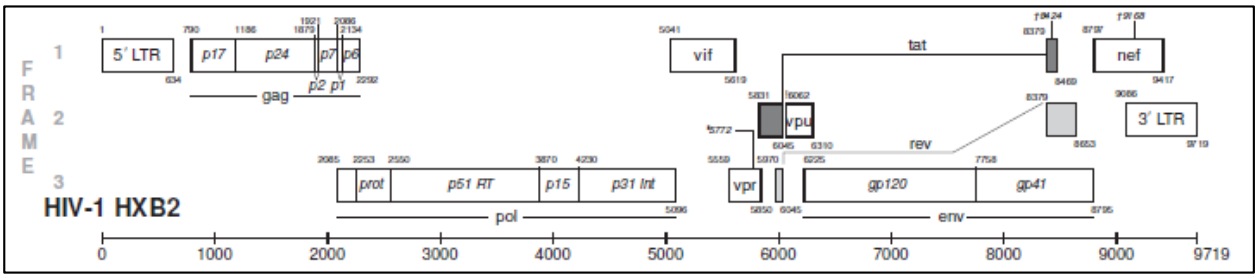

Figure 1.3 Genomic organization of HIV-1. The ~9.7 kb DNA genome harbors three structural genes; *gag*, *pol*, and *env*, which are flanked by identical 5'- and 3'-end LTR regions. Alternatively spliced transcripts from all three reading frames collectively encode two regulatory; *tat* and *rev*, and four accessory genes; *vif*, *vpu*, *vpr* and *nef*. The sequence of the HXB2 strain is taken as a reference for numbering. Adapted from Los Alamos National Laboratory HIV Sequence Compendium, 2013.

The HIV-1 RNA genome is generated by cellular RNA polymerase II and host transcriptional machinery and thus bears hallmarks of cellular mRNAs, such as the 7-methylguanosine cap at the 5' end and an approximately 200 nucleotide (nt) long poly(A) tail at the 3' end. There is an 18 nt long primer binding sequence (PBS) abutting the 5' LTR, complementary to the 3' terminal sequence of the cellular lysine transfer RNA (tRNALys,3) where reverse transcription is initiated upon tRNALys,3 binding. Downstream of the PBS is the *cis*-acting Psi (Ψ) packaging signal, composed of four stem loop structures, required for physical association with Gag and incorporation of the viral gRNA into assembling virions. Other critical secondary and tertiary structural motifs, named trans-activator response element (TAR) and Rev response element (RRE), are regulatory binding sites for viral accessory proteins Tat and Rev, respectively. The TAR element is a hairpin structure that serves as a negative regulator of transcriptional initiation and read-through elongation, unless bound by Tat (Kao et al., 1987). RRE is an approximately 350 nt long RNA secondary structure within the *env*-coding region of the vRNA and Rev to RRE binding is required for unspliced viral mRNAs to utilize the CRM1

(chromosome region maintenance 1)-dependent mRNA nucleocytoplasmic export pathway (Emerman et al., 1989).

B.ii. Structural components

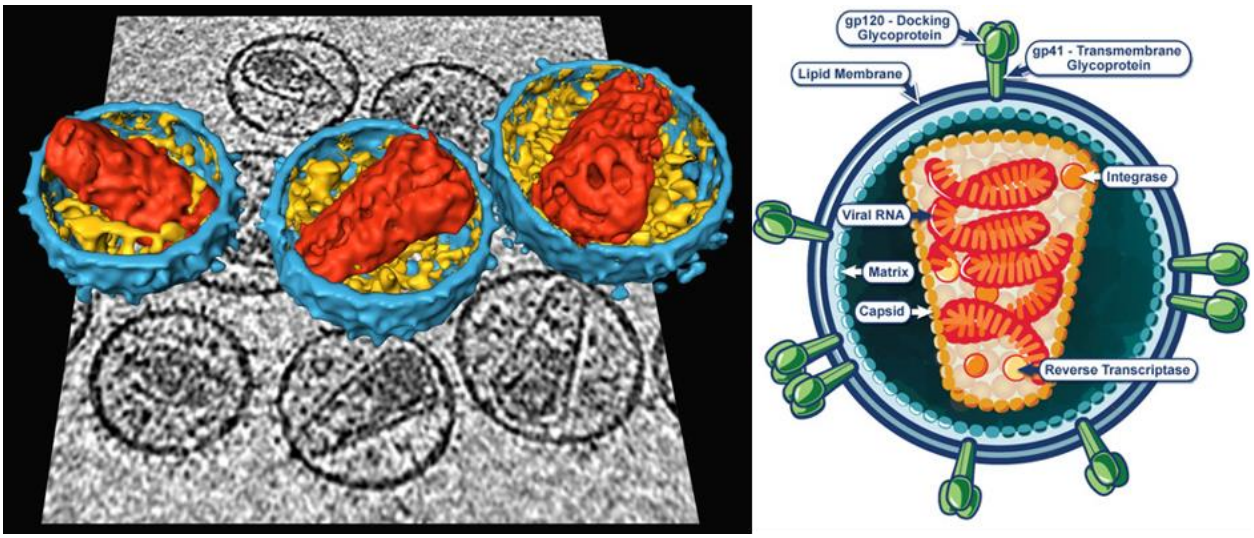

Figure 1.4 HIV-1 virion structure. On the left, 3D reconstruction and a reference cryoelectron tomography section of mature HIV-1 particles. Viral envelope is depicted in *blue*, matrix in *yellow* and capsid core in *red* (Briggs *et al.,* 2006). On the right, schematic representation of a mature HIV-1 particle. Adapted from National Institute of Allergy and Infectious Diseases, 2013.

Mature HIV-1 particles are enveloped in a spherical lipid bilayer (Ø ~145 nm) that is formed upon budding from specialized membrane microdomains. The viral envelope membrane is enriched in 'raft lipids', i.e. sphingomyelin, cholesterol, and plasmalogen-phosphatidyl ethanol; and saturated fatty acids are also more abundant than in the producer cell membrane (Waheed et al., 2009). The viral envelope is studded with the envelope glycoprotein (Env) formed by the noncovalently bonded TM gp41 and the SU attachment glycoprotein gp120 (Figure 1.4).

The proteolytically cleaved Gag polyprotein product (Figure 1.3) MA (17 kD, p17) forms a discontinuous submembrane layer that encloses the mature capsid core particle in the shape of a Fullerene cone composed of ~1100 copies of CA (24 kD, p24) (Figure 1.4). The core houses

the diploid gRNA in a dense ribonucleoprotein complex with NC (7 kD, p7), p6, and also cellular tRNALys,3, which is packaged into assembling virions via Lysyl-tRNA synthetase (KARS):Gag interactions (Guo et al., 2003; Kovaleski et al., 2006), to subsequently serve as the primer of reverse transcription in target cells. Other major components are the Gag-Pol polyprotein products responsible for key enzymatic reactions in the viral life cycle, namely RT for reverse transcribing the vRNA into vDNA and IN for eventually integrating the vDNA into the host genome (Figure 1.4, right).

When expressed by itself in absence of other viral proteins, unprocessed Gag is capable of generating immature virus like particles (VLPs) that do not form the conical core (Gheysen et al., 1989). The formation of these structures relies on the CA domain of the Gag polyprotein. VLPs will spontaneously bud off from producer cells and can also be non-specifically taken up by target cells, yet are replication-incompetent.

B.ii.1. Gag and the capsid core

MA spans the first 132 amino acid residues of the unprocessed Gag polyprotein, that upon myristoylation at its N-terminus and thanks to a highly basic domain between residues 17 and 31 targets Gag to viral assembly sites at the cell membrane (Hill et al, 1996). In the assembling virion it serves to bridge membrane-bound Env (specifically gp41) proteins with Gag proteins lining up under the membrane. Upon maturation initiated by PR proteolytic cleavage of Gag, MA forms trimeric and hexameric structures that act as protective barriers beneath the viral envelope around the capsid core. It is also reported to be associated with the reverse transcription complex (RTC) that forms upon delivery of the capsid core to the target cell cytoplasm and later co-purifies with cytoplasmic fractions that contain in vitro integration activity, suggesting it may

also be associated with the pre-integration complex (PIC) in infected cells (Fassati et al., 2001). Accordingly MA was proposed to play a role in the early phase post-entry events such as nuclear import of the PIC, but such a function has been subsequently contested (Yamashita et al., 2005).

In a mature HIV-1 particle, the conical capsid core serves as a protective vehicle that delivers the viral replication machinery to the host nucleus (Figure 1.4). It is made up of mature CA, a 231 aa long post-cleavage product of the Gag polyprotein. Each single CA molecule is composed of two independently folded domains; an amino-terminal domain (NTD) comprising seven α-helices and a β-hairpin (Mortuza et al., 2004), a carboxy-terminal domain (CTD) comprising four α-helices (Gamble et al., 1997), and a flexible linker with a 3_{10}-helix connecting the two structural domains (Figure 1.5D, E) (Berthet-Colominas et al., 1999). Upon maturation, approximately 1200 copies of CA, about half the number of the Gag proteins that make up the immature virion, multimerize into a conical shell that measures approximately 119 x 60 nM (Briggs *et al.*, 2003; Pornillos *et al.*, 2011; Figure 1.5A). The conical capsid structure results from the assembly of self-associating CA hexamers into a hexagonal lattice (Figure 1.5B) interspersed with an exact number of 12 CA pentamers (5 at the narrow and 7 at the broader end of the cone) that enable surface declinations and closure of an otherwise quasi-cylindrical topology with variable curvature (Figure 1.5A). Original calculations estimated the core to contain ~ 1500 CA molecules (Ganser *et al.*, 1999). Higher resolution structures and structural modeling efforts corrected this number to be ~ 1200 (Briggs *et al.*, 2003, Ganser-Pornillos et al., 2004) and then to ~ 1200 (Briggs et al., 2011; Pornillos *et al.*, 2011; Zhao *et al.*, 2013).

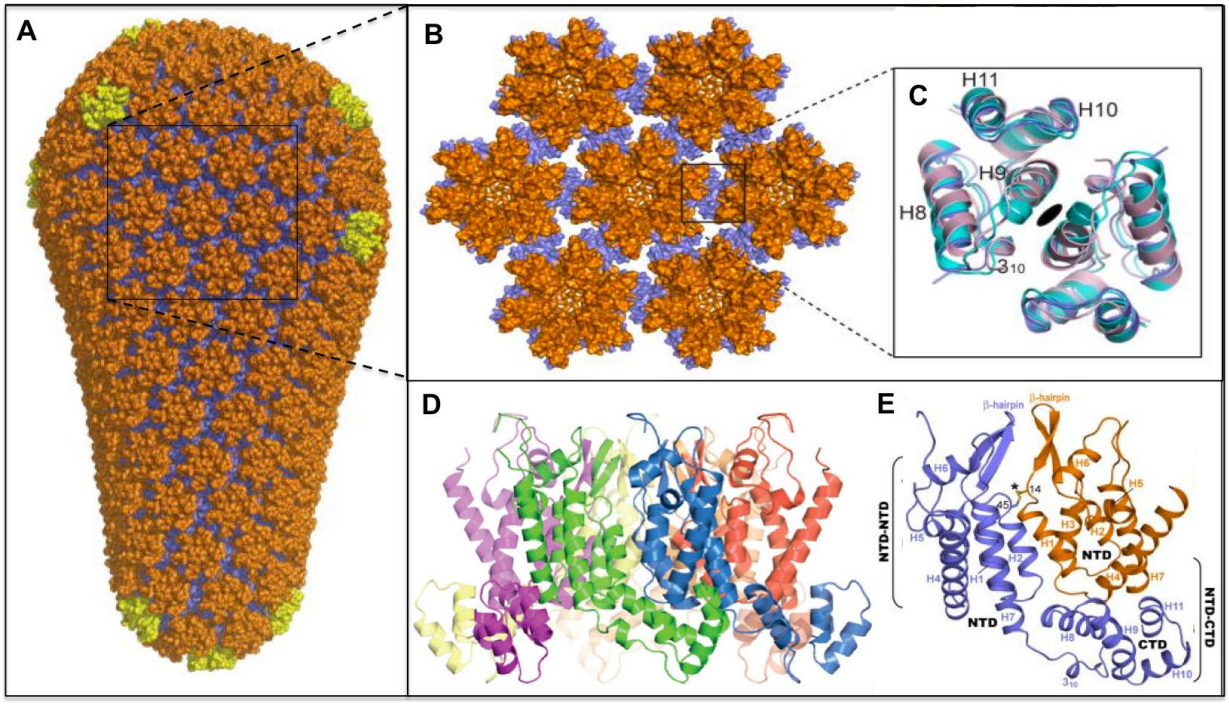

Figure 1.5. Atomic-level modeling of the HIV-1 capsid core. **(A)** Atomic structures of around 250 CA hexamers (orange NTDs, blue CTDs) and 12 CA pentamers (yellow NTDs, blue CTDs) are modelled together to render the conical capsid core (Adapted and modified from Pornillos *et al.*, 2011). **(B)** Expanded view of a central CA hexamer and six neighboring CA hexamers within a planar capsid lattice; resolved experimentally (Adapted from Pornillos *et al.*, 2009). **(C)** Expanded view of the CA CTD-CTD dimer interface between two neighboring CA hexamers. CTD α-helix (H) 9 mediates intermultimeric interactions (Adapted from Pornillos *et al.*, 2009). **(D)** Side view of a ribbon diagram of a single CA hexamer. Each CA subunit is colored differently (Adapted from Pornillos *et al.*, 2011). **(E)** Detailed view of the interaction surface between two neighboring capsid subunits within a hexamer. One full length CA (blue), and the NTD of an adjacent CA (orange) are depicted. Intermolecular NTD-NTD and NTD-CTD interfaces are highlighted (Adapted from Pornillos *et al.*, 2009).

While the hexameric symmetric rings of NTDs and their outward emanating flexible loops create the cytoplasmically exposed facade of the viral core available for interaction with cellular factors (Figure 1.5B), the inner-facing CTDs, and specifically α-helices 9 (H9s) of neighboring multimers are responsible for intermultimeric contacts at 2-fold symmetry axes enabling the formation of the conical capsid lattice (Figure 1.5A-C). Additional hydrophobic residues on CTD H10s at the hexameric three-fold symmetry centers contribute further critical interactions required for lattice formation. Intermolecular interactions between contiguous CAs within a multimer (Figure15.D) are mediated by intermolecular NTD-NTD and NTD-CTD

contacts of adjoining molecules (Figure 1.5E). Within each CA multimer, every CTD is packed against the NTD of the adjacent CA molecule where amino acid residues of the helix 4 in the NTD line up against a groove in the CTD formed by helices 8, 9 and 11 (Figure 1.5E) (Pornillos et al., 2009).

Extensive intrahexameric and intrapentameric packing ensures multimeric stability, whereas rather flexible intermultimeric interactions serve to enable modulation of capsid core stability. Such flexibility is essential (Forshey et al., 2002) as the viral core is slated for conformational and compositional changes upon its entry into the cytoplasm: The intact capsid shell is supposed to disassemble in a controlled fashion, i.e. 'uncoat', in order to allow sufficient shielding and timely delivery of the subviral RTC.

CA alone has self-assembling properties that enable mature lattice formation. This phenomenon can be utilized to reconstitute topologically closed (spherical) and open (cylindrical) CA assemblies *in vitro* that display native capsid surface architecture and thus can be used as a surrogate quaternary substrate in biochemical and structural studies (Gross et al., 1997; Gross et al., 1998). In a similar vein, the CA domain, when present within the context of unprocessed Gag polyprotein, is responsible for self-association of Gag at the inner surface of the cellular membrane during viral assembly.

Inside the capsid core, the viral RNA genome is complexed with the 55 aa residue long basic nucleic acid-binding protein NC. The hallmark feature of NC is two 14 aa residue long Cys-X_2-Cys-X_4-His-X_4-Cys (CCHC) 'Gag-knuckle' zinc finger domains (Morellet et al., 1992). Zn^{2+} coordination induces conformational changes in these knuckles within the central globular domain of NC that allows it to act as a critical molecular chaperone in the early stages of viral replication (Buckman et al., 2003), mainly reverse transcription (Levin et al., 2010). It

chaperones tRNALys,3 binding to the complementary PBS, aids with initiation and strand transfer of reverse transcription (Tsuchihashi et al., 1994), increases the efficiency of reverse transcription by destabilizing the secondary structure of TAR, and thereby relieves a structural block to minus-strand transfer during reverse transcription, adding to the stability of RTC and PIC by shielding the viral genome from cellular nucleases. NC, within the context of Gag, bears the major responsibility in mediating contact with ψ, which is crucial for gRNA encapsidation during viral assembly (Berkowitz et al., 1995). Multimerization of NC contributes to Gag self-assembly (Burniston et al., 1999) and plays a role in plasma membrane targeting of Gag during viral egress. NC may also be partially important during viral budding due to its limited ability to recruit components of the cellular membrane budding and scission machinery, which will be described below (Bieniasz, 2006).

P6, the carboxy-terminal protein domain of Gag, is a 52 aa residue long, proline-rich sequence that is responsible for budding at assembly sites on the plasma membrane (Goettlinger et al., 1991; Huang et al., 1995). Two distinct late assembly (L) domains within p6, namely the major Pro-Thr-Ala-Pro-Pro (PTAP), and the Tyr-Pro-X_n-Leu (YPX_nL) motifs, carry out this function (Strack et al., 2003; Von Schwedler et al., 2003). The PTAP motif is responsible for recruiting tumor susceptibility gene 101 (Tsg101), which then brings in other members of the cellular endosomal sorting complex required for transport (ESCRT) machinery to viral assembly sites (Garrus et al., 2001). ESCRT machinery coordinates outward plasma membrane budding at viral assembly sites and membrane scission by a complex set of molecular steps. The YPX_nL motif, on the other hand, binds another ESCRT component; apoptosis-linked gene 2-interacting protein X (ALIX), which itself can bind TSG101 and again recruit the full complement of the ESCRT machinery (Strack et al., 2003; Von Schwedler et al., 2003). Mutations in these two

domains result in a 'late' block to viral budding, where progeny viral particles fail to sever the membrane neck connecting them to cellular membranes; hence the 'L-domain' nomenclature. Besides its crucial role in budding, the p6 domain of Gag is also responsible for Vpr incorporation into viral particles (Kondo et al., 1996).

B.ii.2. Gag-Pol and the replication machinery

Gag-Pol expression results from a translational frameshift event (due to a single nucleotide backsliding of the ribosome) at the junction of *gag* and *pol* coding regions on the viral mRNA (Jacks et al., 1988). The frequency of this frameshift event determines the amount of Gag vs. Gag-Pol expression, and thus yields a critical 10-20:1 ratio required for efficient viral assembly (Jacks et al., 1988).

PR is responsible for maturational cleavage of both Gag and Gag-Pol (in the case of Gag-Pol in an autocatalytic fashion) upon viral budding, which yields mature Gag (MA, CA, NC, p6) and Pol (PR, RT, IN) proteins. In the absence of a functional PR or PR cleavage sites within Gag and Gag-Pol, progeny virions cannot undergo maturation and are rendered non-infectious (Kohl et al., 1988). HIV-1 PR is a homodimeric aspartyl protease, where each subunit contributes one catalytic aspartic acid residue (Asp25) to the active site (Wlodawer et al., 1989). PR activation and viral maturation is coupled to viral budding, presumably due to the high local concentration of Gag-Pol in assembling virions. Transient overexpression of Gag-Pol in virion producing cells leads to premature intracellular protease activity that is detrimental to viral assembly and budding (Karacostas et al., 1993).

HIV-1 gRNA undergoes reverse transcription to generate the double-stranded (ds) vDNA genome (Temin et al., 1970; Baltimore, 1970) that can be integrated into host chromatin. This

signature step of the retroviral life cycle, which originally challenged the central dogma of molecular biology, is catalyzed by the viral RT holoenzyme, a post-cleavage product of the Pol domain in Gag-Pol. The three enzymatic reactions that RT catalyzes are (i) RNA-dependent DNA polymerization (required for minus-strand synthesis), (ii) RNA degradation as a result of the non-specific endonuclease activity of the C-terminal RNase H domain, and (iii) DNA-dependent DNA polymerization, which is required for plus-strand synthesis and completion of reverse transcription (Hu and Hughes., 2012).

The RT holoenzyme is a heterodimer consisting of one p66 and one p51 subunit, where p51 is a PR post-cleavage product of a single RT molecule (p66) with the C-terminal RNase H domain removed (Di Marzo Veronese et al., 1996). As a result, p51 and p66 share identical amino acid sequences, yet within the context of the RT holoenzyme, the subdomains of each molecule adopt different conformations - to the extent that p51 lacks a functional nucleic acid binding cleft and a polymerase active site, and rather serves a structural role within the p66/p51 heterodimer (Kohlstaedt et al., 1992).

HIV-1 IN comprises three separate functional domains (Engelman et al. 1993): an NTD with a zing finger motif that serves a structural role; a catalytic core domain (CCD) that harbors DNA-binding sites and the catalytic DDE triad (D64, D116 and E152) (Engelman et al., 1992; Dyda et al., 1994) required for divalent cation (Mg^{2+} *in vivo*) coordination and enzymatic function (Goldgur et al., 1998); and finally a CTD with nonspecific DNA-binding properties (Dar et al,. 2009). The 3D structure of the full length HIV-1 IN, the active IN-tetramer, and the active IN-tetramer:vDNA complex; namely the intasome, have been elusive. Breakthrough structural studies with the prototype foamy virus (PFV) intasome yielded valuable insight into

the molecular underpinnings of the integration reaction (Hare et al., 2010; Maertens et al., 2010), which was later utilized to model the HIV-1 intasome (Krishnan et al., 2010b).

Upon completion of vDNA synthesis, the HIV-1 genome is slated for integration into the host chromatin to generate a provirus (Li et al., 2006). HIV-1 IN, encoded at the 3' end of the the *pol* gene, forms a nucleoproteinacious PIC together with the vDNA and other viral and cellular accessory proteins, and mediates two separate enzymatic reactions *in vivo* that enable integration (Figure 1.6; Engelman et al., 1991).

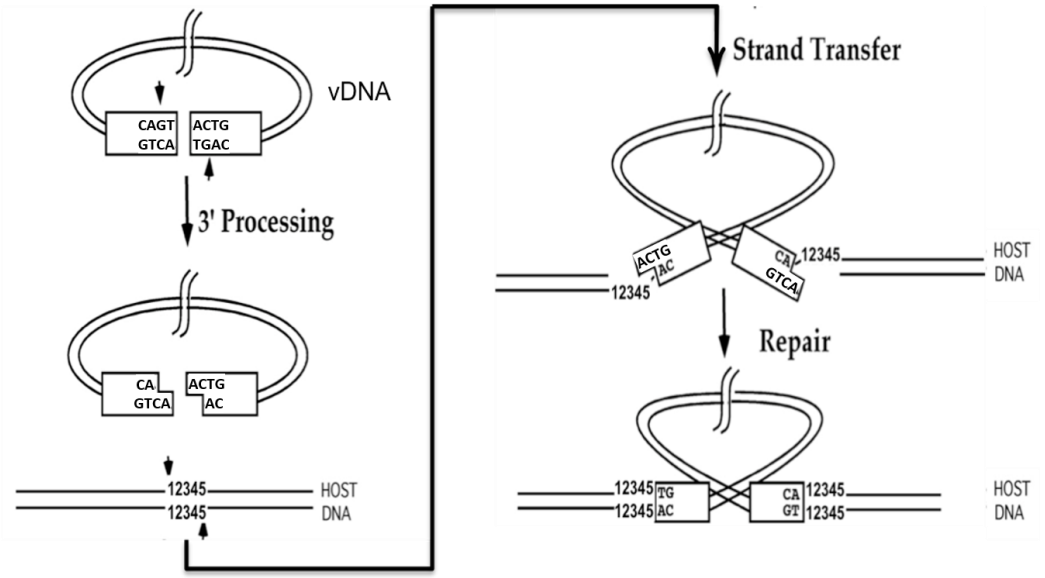

Figure 1.6 Mechanism of HIV-1 integration. The two enzymatic reactions carried out by IN *in vivo*, namely 3' processing of vDNA ends and strand transfer into host chromatin, are followed by nick repair by host DNA repair machinery. This in turn yields an integrated viral genome. Formation of a provirus is accompanied by a 5 bp duplication at the DNA target site, a signature of HIV-1 integration. Adapted and modified from Knipe and Howley, 2006.

During the initial '3' processing', IN removes a dinucleotide from both 3' termini of the ds vDNA in a specific endonucleolytic cleavage reaction, exposing a pair of palindromic CA dinucleotides and their 3-hydroxyl groups (Fujiwara et al., 1988). Upon gaining access to the host chromatin, IN catalyzes the insertion of the exposed 3'-OH ends into opposing strands of the host genomic DNA via a nucleophilic attack, which is dubbed "DNA strand transfer", a step

subject to pharmacological inhibition (Koh et al., 2011). The resulting nicked proviral ends are eventually repaired by host DNA repair machinery, and are flanked by a 5 bp long host DNA duplication (Figure 1.6) (Brown et al., 1989).

B.ii.3. Env and the viral envelope glycoprotein complex

Each HIV-1 Env trimer subunit is composed of a surface gp120 and a transmembrane gp41 that are post-cleavage products of the *env*-encoded polyprotein. Gp120 and gp41 are non-covalently attached to each other in a metastable state on the mature virion surface (Figure 1.4). Specifically, gp120 is responsible for initial attachment to the viral receptor CD4 (Dalgleish et al., 1984; McDougal et al 1986) and major coreceptors CCR5 or CXCR4 on target cells, whereas gp41 plays a crucial role during membrane fusion by juxtaposing the cellular and viral membranes upon major conformational changes (Vishwanathan et al., 2008). Sequential gp120/CD4/coreceptor interactions (Lasky et al., 1987) license gp41 to expose a previously buried fusion peptide (Buzon et al., 2010) that gets inserted into the target membrane akin to a spring loaded mechanism. This is immediately followed by additional conformational changes leading to parts of gp41 to snap back unto itself and form stable six helix bundles along the trimeric axis that pull the two membranes upon each other and initiate fusion (Melikyan et al., 2000).

The cytoplasmic tail of gp41, on the other hand, is necessary for contacting the MA domain of self-assembling Gag proteins at the plasma membrane allowing their incorporation into progeny virions (Freed et al., 1996). The ability of gp120 to recognize different viral coreceptors determines HIV-1 tropism; e.g. R5 isolates refer to viruses that bear a gp120 capable of binding to CCR5, whereas X4 isolates bind to CXCR4.

The metastable structure of the gp120/gp41 trimer, flexible surface regions called variable loops (V1-V5), heavy glycosylation and masking of the native Env trimer have all been confounding factors in structural efforts and, thus, solving the full length atomic structure of a native Env trimer has been formidable. Gradual progress was achieved by studies that utilized stable substructures (Furuta et al., 1998) and partial ligand:receptor complexes (Kwong et al., 1998), and more recently state-of-the-art technological advancements in 3D structure determination such as single particle cryo-electron microscopy coupled with traditional X-Ray crystallography yielded the first ever atomic resolution structural information about the Env trimer (Mao et al., 2013; Julien et al., 2013; Khayat et al., 2013; Lyumkis et., 2013). Env proteins mediate the first physical contact with the host and display immunogenic epitopes to the host adaptive immune system (Popovic et al., 1984; Wyatt et al., 1998). As a result, structural and biochemical details into their functioning are absolutely essential to our understanding of their mechanism of action and to our vaccine development efforts, which have to involve generating neutralizing antibodies, however difficult it may be.

B.ii.4. Regulatory proteins

Following provirus formation, the cellular transcription machinery expresses the viral genome. Host RNA polymerase II drives the transcription of the HIV-1 genome; however only abortive short viral transcripts are made initially. These transcripts allow expression of the regulatory Tat and Rev proteins. By binding to the TAR element within the 5' LTR of nascent viral transcripts, Tat recruits Cyclin T1 and cyclin-dependent kinase (CDK) 9 (Gaynor et al., 1992) that phosphorylates the CTD of RNA polymerase II (Ping et al., 2001), enabling increased processivity and transcriptional elongation (Laspia et al., 1989; Zhu et al., 1997; Mancebo et al., 1997). The Tat:TAR interaction thus acts as a switch from abortive to productive transcription of

the full complement of viral RNAs, including the unspliced gRNA (Feinberg et al., 1986). Lack of splicing poses a block to nuclear export of viral long RNAs, however this is relieved by Rev recruitment to RRE within the *env* on the viral gRNA that allows the utilization of the cellular CRM1-mediated mRNA nuclear export pathway even in absence of coupled splicing (Malim et al., 1989).This is critical for the late stage expression of viral structural polyproteins and for eventual gRNA incorporation into progeny virions.

B.ii.5. Accessory proteins

A characteristic feature of HIV-1, among other primate lentiviruses, is the expression of accessory proteins that aid in the evasion from host adaptive and innate immune defenses (Neil and Bieniasz, 2009). Vif, Vpu and Vpr each antagonize a separate intracellular intrinsic resistance factor (Malim et al., 2008) by inducing their polyubiquitination and proteasomal degradation via joint recruitment of the members of the modular Cullin–RING finger E3 ubiquitin ligases (CRLs). In otherwise non-permissive cells, Vif binds and targets (Marin et al., 2003; Sheehy et al., 2003) the restriction factor APOBEC3G (apolipoprotein B mRNA-editing, enzyme-catalytic, polypeptide-like 3G) in hematopoietic cells that induce hypermutations in vDNA by cytosine deamination (Sheehy et al., 2002; Harris et al., 2003; Bishop et al., 2004). Vpu counteracts the type II transmembrane protein tetherin (Van damme et al., 2008; Neil et al., 2008) that blocks viral release via membrane anchoring of budding virions. Vpr/Vpx (Vpr-related viral protein x of SIV; Lim et al., 2012) targets SAMHD1 (SAM domain and HD domain-containing protein 1), which poses an interferon-induced intracellular block to HIV-1 reverse transcription (Laguette et al., 2011, Hrecka et al., 2011). By its phosphohydrolytic activity (Powell et al., 2011; Goldstone et al., 2011), SAMHD1 depletes cytoplasmic nucleotide pools in monocytes, macrophages and dendritic cells (Laguette et al., 2011). Nef, on the other

hand, plays a critical role in suppressing the adaptive immune response against HIV-1 by downregulating the surface availability and exposure of Env, but also CD4, TCR (T-cell receptor)-CD3 and MHC-I (major histocompatibility complex class I) (Swigut et al., 2001). By limiting the availability of viral epitopes and mediators of adaptive immunity, Nef thus acts as a stealth factor, benefiting long-term systemic viral infectivity. Additionally, Vpr has been shown to induce G2 arrest in infected monocyte derived macrophages (MDMs), which increases HIV-1 transcription activity and efficiency (Goh et al., 1998; Hrecka et al., 2007). Vpr, incorporated into progeny virions via its interactions with the p6 domain within Gag during viral assembly, is also found to be associated with the PIC in the early phase of the HIV-1 infection and there have been reports assigning it a role in PIC nuclear import in macrophages (Vodicka et al., 1998; Popov et al., 1998)

C. HIV-1 replication cycle

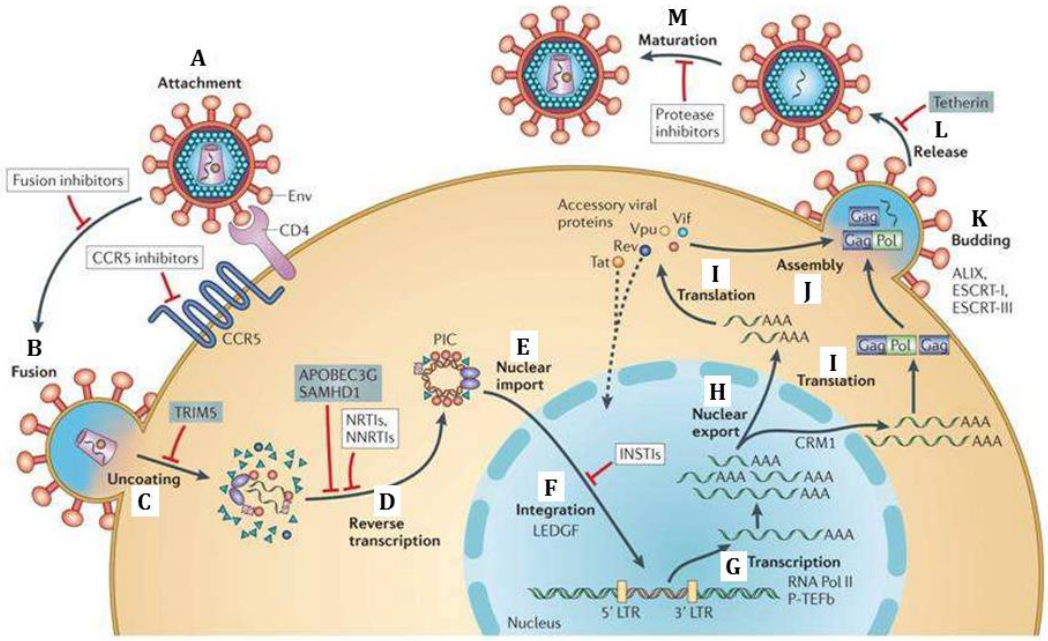

Figure 1.7 HIV-1 replication cycle. HIV-1 infection starts when the envelope (Env) proteins on mature viral particles attach to receptor (CD4) and coreceptor molecules (CCR5 or CXCR4) on a target cell (Figure 1.7A). Attachment triggers conformational changes in the envelope:receptor complex resulting in the juxtaposition of the viral and cellular membranes. This, in turn, leads to fusion of the membranes and the viral capsid core is released into the cytosol (Figure 1.7B). Upon entry, the protective capsid shell uncoats in a controlled fashion (Figure 1.7C), unless it is restricted by human TRIM5α that recognizes the mature capsid lattice and targets it for destruction. Concomitant with uncoating, viral RNA genome is reverse transcribed into a double-stranded DNA species by viral RT using cellular resources (Figure 1.7D). The viral life cycle can be inhibited at this stage by host restriction factor APOBEC3G that induces hypermutations in the viral genome; or SAMHD1, which depletes cytosolic nucleotide pools required for DNA synthesis. Upon successful completion of reverse transcription, the viral DNA is complexed with IN and other viral and cellular accessory factors, which are now dubbed the preintegration complex (PIC). This nucleoprotein complex is subsequently imported through nuclear pores into the nucleus allowing it access to host chromatin (Figure 1.7E). With the aid of the cellular LEDGF, the PIC is targeted to preferred genomic sites where viral IN catalyzes the integration of the two LTR ends of the viral DNA into the host DNA (Figure 1.7F), successfully generating a provirus. In the second half of the replication cycle, recruitment of cellular transcription factors such as P-TEFb mediate transcription of viral genes by host RNA polymerase II (Figure 1.7G). Alternatively spliced and subspliced viral transcripts are then exported into the cytosol via CRM1-mediated export pathway (Figure 1.7H), where the host protein translation machinery utilizes them to produce viral proteins (Figure 1.7I). Unspliced viral genomic RNAs, together with viral structural proteins, are then trafficked to viral assembly sites at the plasma membrane (Figure 1.7J), where they form immature particles that bud off from the cell with the help of the cellular ESCRT machinery (Figure 1.7K). Fully formed virions can then be released into the extracellular space, at which stage the host restriction factor tetherin can block them by membrane anchoring (Figure 1.7L). Viral budding and release trigger the nascent HIV-1 particle to undergo maturation that generates fully infectious particles (Figure 1.7M). Once this newly formed HIV-1 virion finds another target cell, a new round of the replication cycle can begin (Figure 1.7A-M). NRTI, nucleoside reverse transcriptase inhibitor; NNRTI, non-nucleoside reverse transcriptase inhibitor; INSTI, integrase strand transfer inhibitor. Adapted and modified from Engelman and Cherepanov, 2012.

C.i. Early phase events leading up to provirus formation

C.i.1. Attachment and Entry

As an enveloped virus, HIV-1 enters target cells via specific cell surface receptor (CD4) attachment followed by viral and plasma membrane fusion, which mediates entry. There has also been recent incidental evidence pointing to endocytic vesicles as the actual site of fusion upon viral uptake, though this observation awaits confirmation by independent research groups (Miyauchi et al., 2009). The globular envelope protein is a trimeric heterodimer composed of the SU gp120 subunit, which mediates initial binding, and TM gp41, which is responsible for triggering membrane fusion (**B.ii.3**). Upon binding to CD4 on target cells, gp120 undergoes conformational changes allowing critical recognition of specific coreceptors (CCR5 or CXCR4) (Figure 1.7A). This is followed by further conformational changes triggering gp41 (Finzi et al., 2010) to expose and insert its fusion peptide stably into the plasma membrane enabling juxtaposition of the two membranes. Finally gp41 subdomains snap unto themselves, pulling the two membranes together. Membrane fusion ensues and the viral capsid core is released into the cytosol (Figure 1.7B). This initial stage of the viral life cycle is successfully targeted by fusion/entry inhibitors in the clinic.

C.i.2. Uncoating

Upon entry into the cytosol the viral capsid core is believed to uncoat by losing its CA shell on its way to the nucleus, while the vRNA genome is reverse transcribed within. This leads to the maturation into a functional RTC (Iordansky et al., 2006). HIV-1 is believed to take advantage of cellular factors such as cyclophilin A (CypA) and PDZ domain containing 8 (PDZD8) (Guth et al., 2014) to regulate both viral core stability and disassembly allowing timely

progression into RTCs (Figure 1.7C). Uncoating and reverse transcription are tightly coordinated processes as evidenced by impediments to each brought forward by disabling the other: Family members of the host antiviral factor TRIM5 (Tripartite motif-containing Motif 5) recognize intact viral cores (Figure 1.5A) and lead to their accelerated uncoating, which in turn inhibits reverse transcription and subsequent formation of the PIC and nuclear entry (Stremlau et al., 2006). There are CA mutants with aberrant stability and disassembly kinetics that are also defective for reverse transcription. Similarly, inhibitors of reverse transcription have been shown to delay the kinetics of uncoating, pointing to a two-way regulatory mechanism (Hulme et al., 2011; Yang et al., 2013).

When exactly uncoating initiates, and whether it goes to completion while the core traverses the cytoplasm on its way to the nucleus, are still poorly understood. Whereas there is some evidence in support of gradual CA disassembly during reverse transcription up until nuclear entry, others have proposed that intact cores can reach the nuclear membrane and dock at the nuclear pore complexes (NPCs; Di Nunzio et al., 2012), and may only disassemble with the aid of nucleoporins (NUPs) like Nup358 (Bichel et al., 2013). Alternative models emphasize that uncoating may not strip the RTC/PIC of all the CA molecules attached, and some CA may even make its way into the nucleus along with the PIC (Zhou et al., 2011).

C.i.3. Reverse Transcription

Once in the cytosol, exposure to abundant levels of deoxyribonucleotides is hypothesized to trigger reverse transcription. This hypothesis garnered support by the recent discovery of a cellular restriction factor, SAMHD1, which blocks HIV-1 at the stage of reverse transcription by

depleting cytosolic nucleotide pools. Viral Vpr/Vpx has been shown to antagonize SAMHD1 activity by targeting it to proteosomal degradation (Lim et al., 2012).

In the core, vRNA is packaged together with tRNALys,3. Once the tertiary clover leaf structure of tRNALys,3 is chaperoned by NC to open up, it serves as a primer for RT thanks to its 3' end 18 nt sequence being complementary to the PBS on the vRNA.

The RT holoenzyme is solely responsible for all steps of reverse transcription (**B.ii.2**, Figure 1.7D); thus it serves as an RNA-dependent DNA polymerase (i), a nonspecific riboendonuclease (ii), and a DNA-dependent DNA polymerase (iii). The viral RT holoenzyme is responsible for (i) reverse transcribing the positive-sense single-stranded vRNA genome into a negative-sense single-stranded DNA (minus-strand). This is followed by (ii) the RNase H subdomain of RT degrading the original RNA template within this RNA/DNA genomic intermediate, except for two purine-rich sequences known as the polypurine tract (PPT) and the central PPT (cPPT). The PPT and the cPPT then prime the synthesis of the complementary positive-sense DNA strand (positive-strand) yielding a double-stranded genomic vDNA (iii). Mechanical intricacies during positive-strand DNA synthesis at the cPPT generate a temporary DNA triplex, the 'DNA flap', which is proposed to enhance viral infectivity in nondividing target cells (Zennou et al., 2000, Arhel et al., 2007) (possibly by kinetic enhancement of reverse transcription; Skasko et al., 2008) and which also possibly antagonizes host restriction factor APOBEC3G (Wurtzer et al., 2006; Hu et al., 2010).

APOBEC3G is incorporated into assempling virions in producer cells (Svarovskaia et al., 2004), only to restrict reverse transcription in target cells by inducing C → U mutations in the minus-strand, which result in G → A hypermutations in progeny gRNAs and thus destroy the coding and replicative capacity of the virus (Suspène et al., 2006). Viral protein Vif evolved to

counteract APOBEC3G by directing it to the ubiquitin-proteasome proteolytic pathway (**B.ii.5**, Figure 1.7D) (Marin et al., 2003; Sheehy et al., 2003; Newman et al., 2005).

Reverse transcription ultimately results in a double-stranded vDNA with two homologous LTRs at both the 3' and the 5' ends, which is then used as a substrate for IN to form an intasome (an IN–tetramer holding together the two LTR ends of a vDNA).

C.i.4. Nuclear import of the PIC

HIV-1, the prototypical lentivirus, can efficiently infect non-dividing cells (Lewis et al., 1992). It can import into the postmitotic nuclei of cells via active transport mechanisms (Bukrinsky et al., 1992) - a distinguishing property generally not shared by other genera of *Retroviridae,* such as the γ-retroviral MLV - rendering its infection cell cycle-independent (Lewis et al., 1994). Another exception is the β-retrovirus MMTV, which was recently shown to be able to transduce non-dividing dendritic cells (Konstantoulas et al., 2014).

Many viral RTC/PIC components and cellular nucleocytoplasmic shuttling proteins have been proposed to play a role in HIV-1 nuclear import, yet detailed investigations have been unable to definitively support these data (Suzuki et al., 2007). Studies involving partial *gag-pol* chimeras generated between cell cycle-dependent MLV (Roe et al., 1993) and cell cycle-independent HIV-1 (Katz et al., 2003) revealed CA to be the major determinant of this ability (Figure 1.7E; Yamashita and Emerman., 2004). Originally, biochemical characterization efforts failed to detect CA as a major constituent of HIV-1 RTC (Karageorgos et al., 1993; Miller et al., 1997; Fassati et al., 2001), the precursor of the PIC; and hence a potential functional role of CA in PIC nuclear import was unsupported. The MLV RTC, however, contained high levels of CA (Fassati et al., 1999), suggesting that a more stable and less uncoated MLV was being prevented from nuclear entry as opposed to a more extensively uncoated HIV-1. The viral determinant of

nuclear import and cellular factors that facilitate this step are of major interest, because some of the physiologically relevant targets of infection, such as differentiated macrophages and resting T lymphocytes (Weinberg et al., 1991), are non-dividing cells where HIV-1 exclusively relies on this pathway and may utilize it in other cycling target cells, as well. For a more detailed description of our current understanding of HIV-1 PIC nuclear import, please refer to section **D.ii.**

C.i.5. Integration

Once inside the nucleus, the HIV-1 PIC is ready to integrate the vDNA into the host chromatin in a reaction catalyzed by IN (**B.ii.2**), thus forming the provirus and completing the first phase of the viral replication cycle (Figure 1.7F). Integration site selection, however, is not a random process but rather favors weak palindromic sequences (Wu et al., 2005; Delelis et al., 2007) within regions of high transcriptional activity (Mitchell et al., 2004; Wang et al., 2007; Santoni et al., 2010). PIC targeting (Marshall et al., 2007; Shun et al., 2007b) and chromatin tethering (Llano et al., 2006) to these preferred sites is mediated by the lens epithelium-derived growth factor (LEDGF/p75) via direct interaction with IN (Ciuffi et al., 2005; Cherepanov et al., 2003; Cherepanov et al., 2004). More recently there has been accumulating evidence in favor of aditional cellular proteins playing roles in integration target site selection. Even though a direct binding to IN has been observed and thus a hypothetical mechanical explanation is available for some of these factors like for the more recently discovered transportin 3 (TNPO3/TRN-SR2/importin 12; Christ et al., 2008; Krishnan et al., 2010a; Larue et al., 2012; Taltynov et al., 2013) and Nup153 (Woodward et al., 2009; Matreyek et al,. 2011), a similar biochemical explanation is missing for CypA, Nup358, and the cleavage and polyadenylation specific factor 6

(CPSF6; mammalian cleavage factor I 68 kD subunit, CFIm68), which have also been shown to play regulatory roles in uncoating, nuclear import and integration site targeting. It is an attractive model that all these events are functionally linked to each other, where licensing or alternative path commitment in steps prior to nuclear import and integration may play critical roles in integration target site selection itself (Pryciak et al, 1992; Lewinski et al., 2006; Koh et al., 2013).

C.ii. Late phase events

C.ii.1. Gene expression

Following provirus formation, HIV-1 utilizes host transcription factors and host RNA Pol II to express its genome from the 5' LTR (Figure 1.3). The viral accessory protein Tat serves a crucial role at this step triggering transcriptional initiation via recruitment of the positive transcription elongation factor b (P-TEFb), which enhances RNA Pol II processivity and stimulates long vRNA synthesis (**B.ii.4**, Figure 1.7G). HIV-1 mRNAs are then transported into the cytoplasm using the CRM1 dependent nuclear mRNA export pathway. In the case of unspliced long vRNAs, the viral accessory protein Rev enables utilization of the same export pathway, which normally promotes export only if coupled to mRNA splicing (**B.ii.4**, Figure 1.7H). Viral structural proteins are expressed as polyproteins (Figure 1.7I) that rely on a post-release maturational step to yield functional particles. Viral accessory and regulatory proteins are expressed as final protein products (Figure 1.7I; Frankel et al., 1998).

C.ii.2. Production of progeny virions

Once viral proteins and genomic vRNA are expressed, they traffic to the plasma membrane to initiate the assembly process (Figure 1.7J). Gag is targeted to the membrane via its N-terminal myristoylated MA domain (Ono et al., 2000), while the NC domain of the polyprotein enables Gag self-assembly and also mediates viral gRNA encapsidation via direct interaction with the ψ signal. CA-CTD also serves a critical role in immature Gag multimerization (**B.ii.1**). HIV-1 glycoprotein precursor gp160 is synthesized on the rough endoplasmic reticulum (ER), where it is threaded into the ER-lumen accessing the secretory pathway to reach the cell surface. En route to the cell surface the gp120 domain is heavily glycosylated within the trans-Golgi network before getting cleaved by furin or a related host protease into gp120 and gp41 to yield mature Env glycoprotein trimers (**B.ii.3**) (Vollenweider et al., 1996; Moulard et al., 2000). Embedded in the plasma membrane, the cytoplasmic tail of gp41 interacts with the MA domain of Gag, enabling its own incorporation into assembling virions (Figure 1.7J) (Checkley et al., 2011). Viral budding is then facilitated by the host ESCRT machinery that is recruited to assembly sites with the aid of the p6 protein (**B.ii.5**, Figure 1.7K). Virion release into the surroundings, however, may not necessarily ensue freely, as budded virions can still be trapped by the host restriction factor tetherin via membrane anchoring (Van Damme et al., 2008) (Figure 1.7L). The viral accessory factor Vpu counteracts tetherin function by inducing its proteosomal degradation by targeting it for polyubiquitination (**B.ii.5**) (Van damme et al., 2008; Neil et al., 2008).

C.ii.3. Virion maturation

Presumably mediated by an increase in its local concentration within an assembled virion, the activation of the PR domain of Gag-Pol initiates autocleavage of Gag-Pol molecules and cleavage of Gag polyproteins (Figure 1.7M). The series of these maturational cleavages result in an infectious progeny virion, thus completing the viral life cycle (**B.ii.1-2**, Figure 1.7A-M).

D. HIV-1 PIC nuclear import

D.i. Nucleocytoplasmic transport and the Ran-GTP cycle

HIV-1 is believed to gain access to the nucleoplasm by passing through aqueous channels created by NPCs on the nuclear envelope, which act as selective passageways actively regulating bidirectional nucleocytoplasmic shuttling of molecules in eukaryotic cells (Stewart et al., 2007). NPCs are multiprotein complexes built from both permanent and dynamic structural components named NUPs (Paulillo et al., 2005; Strambio-De-Castillia et al., 2010). They coordinate molecular trafficking together with members of the ancient solenoid HEAT repeat containing soluble karyopherin β (KPN β) superfamily of nuclear transport receptors (Figure 1.8A; O'Reilly et al., 2011) that transiently associate with NPCs (O'Reilly *et al.*, 2011).

Size limitations of NPCs allow passive diffusion of small enough molecules (with a diameter less than ~ 9 nm), whereas large cargo (with a diameter up to ~ 39 nm; Pante et al., 2002) require facilitated active transport that is mediated by members of the KPN β superfamily. Importins are KPN β proteins responsible for transport into the nucleus, whereas exportins enable nucleocytoplasmic export (Figure 1.8A, B). Accordingly, the quest for NUPs and soluble importins playing a role in HIV-1 PIC nuclear import has been a subject of much research.

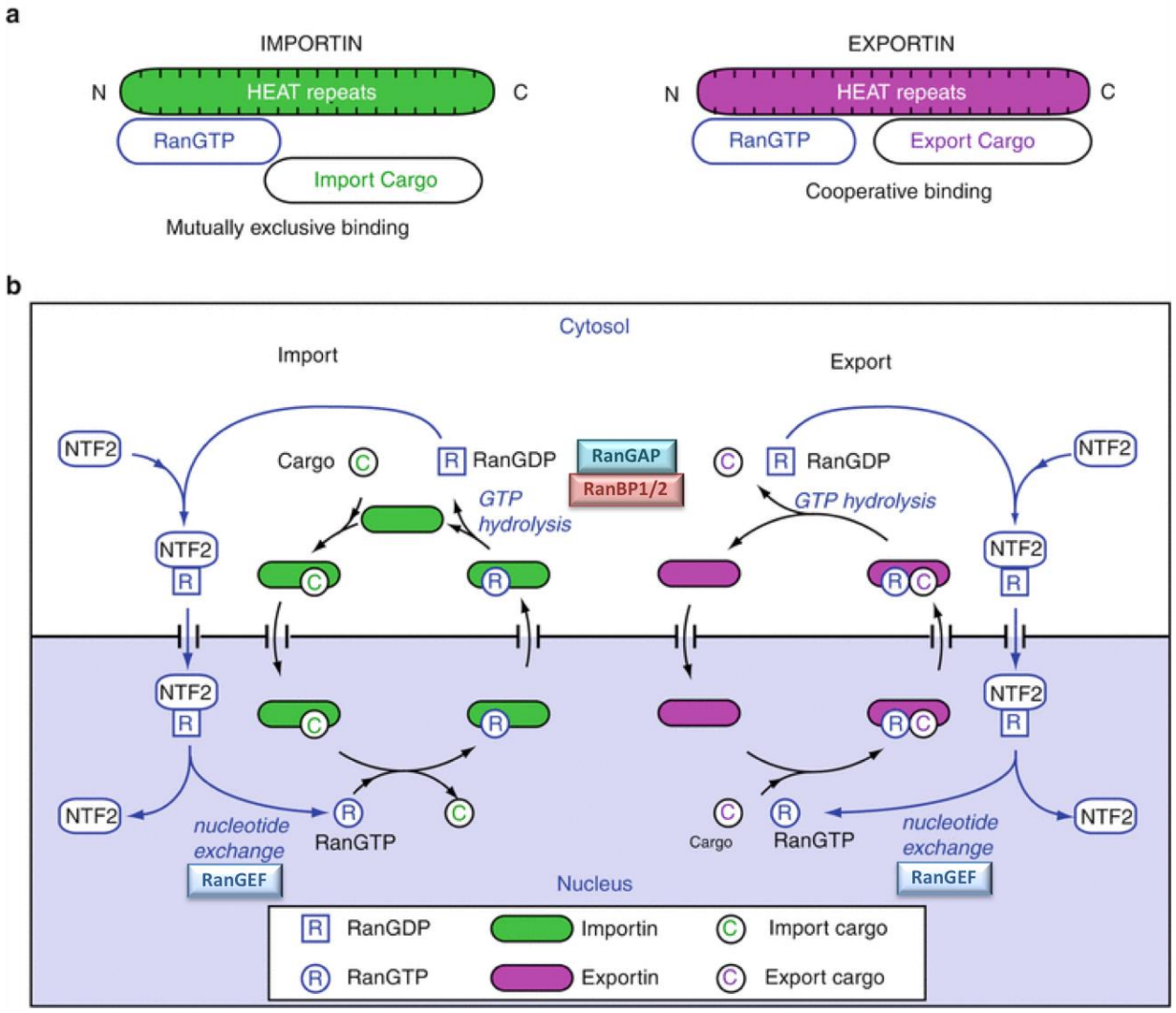

Figure 1.8 Nucleocytoplasmic transport and the Ran cycle. **(A)** Importins and exportins differ from each other in their ability to bind RanGTP and their cargo either competitively or cooperatively. **(B)** A schematic showing the maintenance mechanism of the Ran gradient across the nuclear barrier and the regulation of Ran-dependent nuclear transport of both import and export cargoes. Please refer to the main text for a detailed description. Adapted and modified from Petosa, 2012.

Cargo binding to KPN β proteins is regulated by the small Ras-related nuclear protein (Ran) GTPase. Directionality of nucleocytoplasmic shuttling is established by actively maintaining an asymmetric gradient of the guanosine diphosphate (GDP)- or guanosine triphosphate (GTP)-bound Ran across the nuclear barrier (Figure 1.8B). Two Ran co-factors, situated on opposite sides of the nuclear envelope enable this: Regulator of chromosome condensation 1 (RCC1, Ran guanine nucleotide exchange factor, RanGEF) resides in the

nucleus, is associated with nucleosomes (Nemergut et al., 2001), promotes the conversion of RanGDP to RanGTP; Ran GTPase-activating protein (RanGAP) is located on the cytoplasmic side of NPCs, is associated with Nup358 filaments (Wilken et al., 1995), and stimulates the GTPase activity of Ran in cooperation with the Ran binding protein 1/2 (RanBP1/2), inducing RanGTP to RanGDP catalysis (Bischoff et al., 1994). RanGTP is the predominant form inside the nucleus, whereas RanGDP is more abundant in the cytosol (Figure 1.8B).

Ran preferentially binds KPN β proteins in its GTP-bound state (inside the nucleus), and GTP to GDP hydrolysis by Ran causes its dissociation from KPN β proteins (on the cytoplasmic side of NPCs; Melchior et al., 1995). By means of nuclear localization signal (NLS) sequences nuclear-bound cargoes preferentially bind importins (Fontes et al., 2000) in their Ran-free state in the cytosol, and are then ferried inward through the NPCs with the aid of the phenylalanine-glycine (FG)-repeat containing NUPs, that line the NPC (Terry et al., 2009). Cargo and RanGTP binding to importins is competitive due to steric hindrance caused by overlapping binding sites (Figure 1.8A), and, thus, once at the nucleoplasmic side of the NPCs the high concentration of RanGTP enables cargo release. Importins, now complexed with RanGTP, are ferried back to the cytoplasmic side of NPCs, where Nup358 associated RanGAP and RanBP1/2 stimulate the conversion of RanGTP to RanGDP and induce Ran dissociation, successfully recycling the karyopherin (Figure 1.8B).

In the case of exportins such as exportin 1 (CRM1, XPO1), cargo and RanGTP binding is cooperative (Figure 1.8A), allowing cargo to preferentially bind the transport protein inside the nucleus. This binding is mediated by nuclear export signal (NES) sequences present within export cargo. Following outward transit through the NPC, this ternary complex again dissociates upon RanGAP/RanBP1-stimulated Ran GTPase activity (Kehlenbach et al., 1999). This releases

both the cargo protein and hydrolyzed RanGDP into the cytosol, at which point the free exportin can transit back into the nucleus (Figure 1.8B). Nuclear transport factor 2 (NTF2) then selectively imports free RanGDP into the nucleus, where RanGEF can exchange the GDP with GTP, thereby replenishing the nuclear RanGTP pools. This allows the maintenance of the original Ran gradient (Figure 1.8B). Biochemical studies frequently employ a point mutant of Ran, i.e. RanQ69L, which is deficient in GTPase activity, and thus cannot hydrolyze the bound GTP. This enables stable karyopherin:RanGTP complex formation aiding characterization in binding studies, especially.

D.ii. Viral and cellular components of RTC/PIC mediating HIV-1 nuclear import

The RTC and the PIC are believed to be dynamic nucleoprotein complexes, with viral and cellular proteins associating with and dissociating from them en route to the chromatin to regulate uncoating, reverse transcription and nuclear import. RTCs and intact capsid cores are 100-200 nm long and have a 50-60 nm diameter across their narrow ends (Miller et al., 1997; Zhao et al., 2013), which exceed the 39 nm size limit of transport through NPCs. Accordingly, during their maturation into PICs, RTCs must undergo conformational changes such as capsid uncoating, and a reduction in their contents, in order to allow the nuclear entry of the intasome (vDNA and the active IN-tetramer) as part of a functional PIC with other associated proteins (Figure 1.7E). The PIC is estimated to have a diameter of 56 nm at this stage (Miller et al., 1997).

Many studies employed coordinated biochemical and functional assays to identify the protein components of these complexes at various stages of the infection, as monitored by the progress of bulk reverse transcription, nuclear import and *in vitro* integration activity. RTCs are

more suitable for characterization thanks to their cytoplasmic abundance and specific enzymatic activity. When measuring RT activity, the functional readout, namely the amount of early/late stage reverse transcripts (ERT/LRT) formed, is already established inside cells before carrying out quantification, which minimizes experimental manipulations and increases the accuracy of the assay.

Biochemical identification of viral and cellular components of RTC/PICs before and after nuclear import, however, poses a formidable task. Due to low retroviral titers, at physiologically relevant experimental conditions with a multiplicity of infection (MOI) of ≤1, as per definition, only ≤1 functional RTC/PIC per cell will form, restricting biochemical resources. Also confounding is the fact that PIC activity is tracked by *in vitro* integration assays (Farnet et al., 1990), where IN alone will also score positive (Bushman et al., 1991), rendering the presence of PIC cofactors practically redundant. *In vitro* PIC integration assay requires partial purification of cytoplasmic and nuclear PICs prior to the assay (Engelman et al., 2009), which may be intrusive to structural PIC integrity, and thus skew the assay towards false negatives. This latter concern applies to biochemical characterization efforts of RTCs and PICs alike.

A second approach to monitor PIC-specific activity entails reconstituted nuclear import experiments, where isolated cellular fractions or purified cofactors can be added back to PICs and isolated nuclei to be assayed for their competence in inducing *in vitro* nuclear import. Use of cell extracts depleted of candidate cofactors provides a complementary approach. A third approach takes advantage of the phenomenon that vDNA and duplicate terminal LTR's (Figure 1.6), once inside the nucleus, can be used as a substrate by the DNA damage repair machinery. The homologous DNA recombination (Kilzer et al., 2003) and the non-homologous end-joining (NHEJ) pathways give rise to non-infectious, dead-end (albeit limited episomal transcription has

been observed) vDNA structures called 1-LTR and 2-LTR circles (Fritsch et al., 1977; Farnet et al., 1991), respectively, which can serve as surrogate markers for vDNA nuclear entry (Li et al., 2001). Yet another non-productive circular vDNA species is autointegrants, which may form as a result of prematurely activated IN that integrates the vDNA into itself (Yan et al., 2009), giving rise to circular forms that harbor two LTR sequences. Careful selection of qPCR primers is needed to properly distinguish these species from actual 2-LTR circles with defined junctions (De Iaco et al., 2013).

Similarly, following adequate and validated subcellular fractionation, cytoplasmic vs. nuclear distribution of LRTs can be measured, though a limited ability to distinguish between nucleoplasmic (truly inside the nucleus) vs. nuclear membrane associated (technically outside the nucleus) vDNA can make such an analysis difficult. Lastly, real-time confocal microscopy of fluorescently labeled RTC/PICs (Jun et al., 2011; Lelek et al., 2012; Pereira et al., 2012) and immunofluorescent labeling of fixed samples have been developed with the aim of quantitatively monitoring RTC/PIC trafficking (McDonald et al., 2002; Arhel et al., 2007) and even ultimate integration target site visualization (Di Primio et al., 2013). The inability to match labeled complexes with active, integration-competent PICs, however, puts some limitation on the interpretability of these assays.

These complications aside, and despite the lack of more direct methods, past research efforts consistently observed the copurification of MA, RT, and Vpr with active viral nucleoprotein complexes in fractionation experiments (Bukrinsky et al., 1993; Miller et al., 1997; Fassati et al, 2001). CA, the major structural constituent of the core upon delivery into the cytosol, was, however, either completely absent or only minimally present in the cytoplasmic/nuclear fractions that displayed reverse transcription activity – a striking difference

from MLV RTCs – even though there has been incidental detection of CA in actively reverse transcribing HIV-1 RTCs in immunofluorescence based assays (McDonald et al., 2002). Disregarding the possibility that loosely attached components like CA may have been stripped off of RTC/PICs during purification, the absence of CA in biochemical characterization efforts was interpreted as HIV-1 cores uncoating to completion prior to PIC formation. Later efforts, however, managed to detect CA both in cytoplasmic RTCs (McDonald et al., 2002; Albanese et al., 2008), in association with NPCs (Arhel et al., 2007), in crude biochemical nuclear fractions (Zhou et al., 2011) and even inside the nucleus (Di Nunzio et al., 2012), though it is hard to comment whether there is any functionality to its presence in these settings due to the limitations of the assays discussed before.

Many of the viral elements identified as PIC components have transferable karyophilic signals dubbed NLSs, as determined in ectopic expression assays (Haffar et al., 2000; Bouyac-Bertoia et al., 2001). Even though the isolated expression separate from a PIC may not necessarily recapitulate the conditions a functional PIC encounters during infection, each of these viral elements (MA; IN; Vpr) have each been proposed to be responsible for PIC nuclear import to some extent (Bukrinsky et al., 1993a; Heinzinger et al., 1994; Freed et al., 1995; Gallay et al., 1995; Gallay et al., 1997; Bouyac-Bertoia et al., 2001). This is mediated by recruiting members of the nuclear transport machinery: Basic type NLSs within IN can bind to importin α adaptors and KPN β members themselves, e.g. importin 7 (Fassati et al., 2003), importin α3 (Ao et al., 2010) and TNPO3 (Christ et al., 2008; Krishnan et al., 2010a; Larue et al., 2012). IN and Vpr have been shown to bind NUPs directly (Fouchier et al., 1998; Le Rouzic et al.; 2002; Woodward et al., 2009), which would allow them to by-pass a need for soluble KPN β import receptors (Jenkins et al., 1998). Point mutations to IN are known to have pleiotropic effects

including defects in PIC nuclear import (Limón et al., 2002a; Lu et al,. 2004); and finally a non-proteinacious PIC component, namely the genomic triple-stranded DNA flap element generated by the cPPT and the central termination signal (CTS), has been proposed to facilitate HIV-1 PIC nuclear import by an unknown mechanism (DeRijk et al., 2006). However, none of these individual elements are indispensable to PIC nuclear import during the course of a successful infection as shown by subsequent studies (Freed et al., 1997; Fouchier et al., 1997; Limón et al., 2002b; Dvorin et al., 2002; Zielske et al., 2005., Yamashita et al., 2005; Marsden et al., 2007; Rivière et al., 2010) - and in the case of IN, it has been impossible to distinguish specific nuclear import defects from indirect ones due to the pleiotropic nature of IN mutations.

As far as the cellular machinery that HIV-1 exploits on its way into the nucleus goes, many nuclear-associated factors including importin-β, importin-7, TNPO3, importin-α (Kamata et al., 2005; Hearps et al., 2006), importin-α3 (Ao et al., 2010; Jayappa et al., 2011); Nup98 (Ebina et al., 2004), Nup153 (DiNunzio et al., 2013; Matreyek et al., 2011), Nup358 (RanBP2; with a C-terminal cyclophilin domain; Zhang et al., 2010; Ocwieja et al., 2011) have come into the spotlight. Even tRNAs with defective 3' CCA ends have been implicated in PIC nuclear transport (Zaitseva et al., 2006), though many of these factors and their potential functional roles in HIV-1 biology await confirmation (Figure 1.7E).

D.ii.1. The role of HIV-1 CA in PIC nuclear import

In a rather ingenious experiment, growth-arrested, non-dividing cells were infected with chimeric viruses that were generated by swapping partial *gag/pol* domains between nuclear import capable HIV-1 and nuclear import deficient MLV (Yamashita et al 2004; Yamashita et al., 2005). The experiment pinpointed CA as the viral determinant of efficient transport of vDNA

across the nuclear barrier (as assayed indirectly via 2-LTR circle formation) before proceeding with integration. The presence of MLV CA rendered chimeric viruses cell cycle-dependent in all genomic contexts, mirroring the parental MLV. Follow up studies identified point mutations in CA facing the interhexameric space that resulted in low-titer, cell cycle dependent defective viruses with aberrant core stability; e.g. T54A/N57A and Q63A/Q67A (Figure 1.9A-C) (Dismuke et al., 2006., Yang et al., 2007; Qi et al., 2008). T54A/N57A virus displayed a rather unique post-nuclear entry, pre-integration defect. Q63A/Q67A had both poor core stability and restricted nuclear import, although there are confounding studies claiming extended core integrity. While the cell cycle dependence of these two mutants have been observed in all cell lines tested, other studies identified additional CA mutants with growth arrest phenotypes in a cell type dependent fashion.

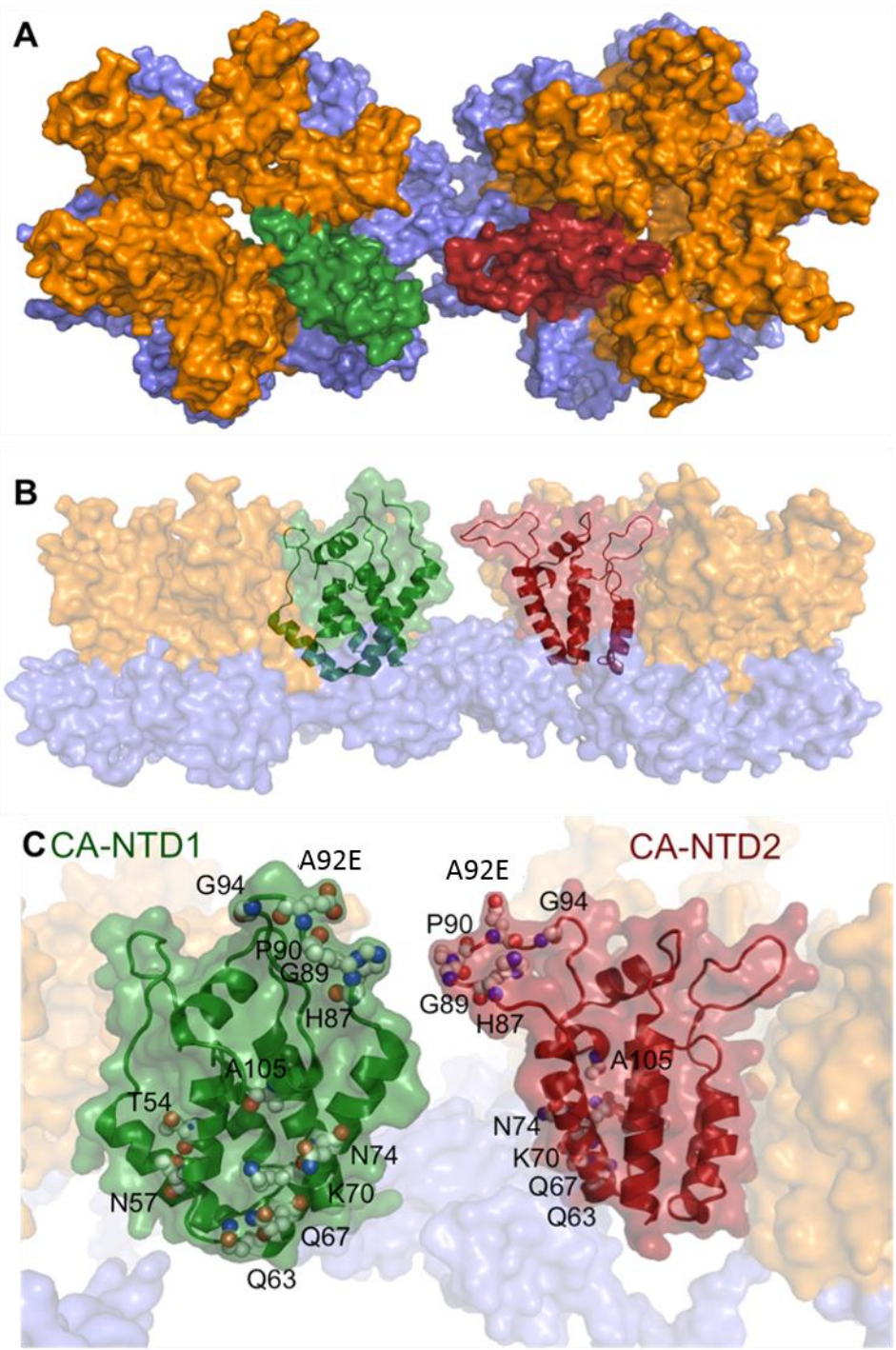

Figure 1.9 CA mutants with defective core stability, PIC nuclear import and growth arrest phenotypes define a novel CA surface pocket at the hexamer:hexamer interface. **(A)** 3D structure of the A92E HIV-1 core determined by single particle cryo-EM tomography reveals the interface between two CA hexamers. Two CA molecules, each on an adjoining hexamer facing each other at the interhexameric space, are highlighted in this series of surface renderings. Top view. **(B)** Side view with highlighted CA secondary structures. **(C)** Individual amino acid residues with uncoating, nuclear import growth arrest phenotypes are highlighted on two CAs facing each other at the hexamer interface. CA-NTDs, *orange;* CA-CTDs, *blue;* CA-NTD1, *green;* CA-NTD2, *red*. PDB: 1VU5 (Zhao *et al.*, 2013)

Two such mutations are A92E and G94D, where both residues extend over to the interhexameric space on a mature core (Figure 1.9A-C). They lie on a surface-exposed flexible loop that mediates binding to CypA (*PPIA*), an 18 kD prolyl isomerase (Bosco et al., 2002) that recognizes the ^{89}GP^{90} dipeptide within the CypA binding loop (Braaten et al., 1996; Gamble et al., 1996; Yoo et al., 1997), ^{85}PVHAGPIAPG^{94} of HIV-1 CA (Figure 1.9A-C), and gets incorporated into the virion via this interaction (Thali et al., 1994; Franke et al., 1994). The initial interaction between CypA and HIV CA takes place at the stage of viral assembly where CypA gets incorporated into assembling virions during Gag multimerization at a Gag:CypA ratio of 10:1 (Gross et al., 1998). It was later shown, however, that CypA plays a functional role during the early phase of infection in the target cell (Sokolskaja et al., 2004). The CA:CypA interaction can be inhibited by cyclosporine A (CsA), a small molecule drug that competitively binds and blocks the CypA active site (Handschumacher et al., 1984), which curbs HIV-1 infectivity in many natural target cell lines (Wainberg et al., 1998). A92E and G94D are mutations within the CypA-loop of CA that evolved under suboptimal CsA selection (Aberham *et al.*, 1996), rendering mutant viruses not only CsA-resistant but also CsA-dependent in some cell lines. A series of studies have extensively characterized A92E and G94D viruses from a functional perspective. They display a growth arrest phenotype with a reversible post-nuclear import block to infection and may also affect capsid core stability. A CsA-dependent infection profile is suggestive of a CypA-dependent restriction in untreated non-permissive cell lines with high CypA content (Yin et al., 1998; Ylinen et al., 2009). The infectivity defect of these mutants observed in the absence of CsA can similarly be relieved upon combining A92E or G94D with CypA binding mutants G89V or P90A. Yet even after the atomic structure of the CypA:CA-NTD complex was solved, the underlying mechanistic details of how A92E or G94D function

have eluded investigators, because the mutations do not seem to affect CA-NTD binding to the attached CypA molecule (In Appendix A, a novel hypothetical superstructural model will be discussed that bears a potential to explain these opposing CypA phenotypes, thanks to a proposed noncanonical interaction surface between CypA and the CA hexameric lattice). A recently identified mutant CA N121K also bears similar CsA-dependent phenotypes, even though N121 does not lie on the CypA loop of CA (Takemura et al,. 2013).

D.ii.2 Other cellular factors modulating HIV-1 CA and PIC nuclear import

Until recently the only other CA-interacting family of host factors with effects on HIV-1 core stability and downstream steps was the species-specific TRIM5α innate restriction proteins that act as barriers to cross-species transmission of primate lentiviruses (Hofmann et al., 1999). Upon the release of the viral core into the cytoplasm, TRIM5α acts by recognizing the hexagonal capsid lattice at a macroconformational rather than a residue-specific level (Ohkura et al., 2011; McCarthy et al., 2013) and by targeting it for proteasomal degradation in a series of not fully delineated steps that involve potential polyubiquitination (Danielson et al., 2012) and innate immune signaling mediated by unattached K63-linked ubiquitin chains (Pertel et al., 2011). This cellular block prevents the core from maturing into functional RTCs, which can be relieved upon MG132 proteasomal inhibitor treatment, allowing reverse transcription to ensue only to form nuclear import-deficient RTCs (Anderson et al., 2006; Wu et al., 2006). Similary, several natural (TRIMCyp; Yap et al., 2006) and engineered (Friend virus susceptibility 1 (Fv1)-Cyp; Schaller et al., 2007) CypA fusion constructs (facilitating CA recognition via CypA:CA interactions) have been shown to result in post-reverse transcription and post-nuclear import infectivity defects. The recently identified HIV-1 restriction factor myxovirus resistance 2 (Mx2, MxB) (Goujon et

al., 2013; Kane 2013; Liu et al., 2013) seems to target the incoming core at this stage as well, also evidenced by the presence of Mx2-resistant CA-CTD mutants (Busnadiego et al., 2014). These observations suggest that the HIV-1 core disassembles in a regulated fashion both in a positive and negative way and facilitates a functional connection between reverse transcription, nuclear trafficking and possibly beyond as evidenced by post-nuclear import blocks encountered by several capsid core mutants with aberrant stability/uncoating phenotypes, which may stem from a decreased ability to interact with regulatory host factors.

The importance of cellular factors in mediating HIV-1 infection has most recently been explored further by employing human RNAi screens (Brass et al., 2008; Koenig et al., 2008; Zhou et al., 2008; Yeung et al., 2009). These screens identified hundreds of potential new HIV-1 dependency factors, one of which, a nucleo-cytoplasmic shuttling protein, the importin-β TNPO3/TRN-SR2, sparked great interest. Depleting TNPO3 resulted in an HIV-1 infectivity defect in two of these screens (Brass et al., 2008; Koenig et al., 2008) and this infectivity defect was mapped to a step in the viral life cycle post-reverse transcription and pre- or at integration. As a nucleo-cytoplasmic SR protein transporter, whose depletion resulted in an infectivity defect that is compatible with a hypothetical role in HIV-1 nuclear import, TNPO3 has quickly become a popular research subject.

Independent research efforts identified CPSF6/CFIm68, a pre-mRNA splicing factor that is a member of the SR protein family (Ruegsegger et al., 1996), to potentially play a role in HIV-1 PIC nuclear import in a CA-dependent way. Overexpression and cytoplasmic localization of a truncation mutant of CPSF6, CPSF6-358, which lacks the original C-terminal domain, was shown to cause a novel, CA-targeting restriction of HIV-1 PIC nuclear import in mammalian cells (Lee et al., 2010). It was noteworthy that the truncation removed the C-terminal RS domain

of CPSF6, which pointed to a hypothetical model that CPSF6 might be a potential cargo of TNPO3, and the restriction caused by CPSF6-358 may have stemmed from its potential inability to interact with and to be shuttled into the nucleus by TNPO3.

The discovery of these two novel host factors, TNPO3 and CPSF6, which exerted CA-dependent phenotypes in core uncoating, nuclear import and integration site targeting piqued our interest to study their function, leading to this dissertation.

CHAPTER 2

HIV-1 CA IS THE FUNCTIONAL TARGET OF TNPO3 AND CPSF6

Adapted and modified from:

Krishnan L*, Matreyek KA*, **Oztop I***, Lee K, Tipper CH, Li X, Dar MJ, Kewalramani VN, Engelman A. The requirement for cellular transportin 3 (TNPO3 or TRN-SR2) during infection maps to human immunodeficiency virus type 1 capsid and not integrase. J Virol. 2010 Jan; 84(1):397-406. *Equal contribution

Lee K, Ambrose Z*, Martin TD*, **Oztop I**, Mulky A, Julias JG, Vandegraaff N, Baumann JG, Wang R, Yuen W, Takemura T, Shelton K, Taniuchi I, Li Y, Sodroski J, Littman DR, Coffin JM, Hughes SH, Unutmaz D, Engelman A, KewalRamani VN. Flexible use of nuclear import pathways by HIV-1. Cell Host & Microbe. 2010 Mar 18; 7(3):221-33. *Equal contribution

Ambrose Z, Lee K, Ndjomou J, Xu H, **Oztop I**, Matous J, Takemura T, Unutmaz D, Engelman A, Hughes SH, KewalRamani VN. Human immunodeficiency virus type 1 capsid mutation N74D alters Cyclophilin A dependence and impairs macrophage infection. J Virol. 2012 Apr; 86(8):4708-14.

Please refer to Appendix B for a detailed description of author contributions.

A. Abstract

Recent genome-wide screens have highlighted an important role for TNPO3 in HIV-1 infection and PIC nuclear import. Moreover, HIV-1 IN interacted with recombinant TNPO3 under conditions whereby MLV IN failed to do so, suggesting that IN:TNPO3 interactions might underscore active retroviral PIC nuclear import. Here we compared infectivity defects in TNPO3 knockdown (KD) cells with *in vitro* TNPO3 binding affinities to INs of an expanded set of retroviruses. Our results fail to support the hypothesis that TNPO3:IN interactions play a critical role in TNPO3 dependency of retroviral infection. In addition to IN, CA has also been highlighted as a retroviral nuclear import determinant. By utilizing MLV/HIV-1 chimera viruses we pinpointed the genetic determinant of sensitization to TNPO3 knockdown to the HIV-1 CA protein. We therefore conclude that CA, not IN, is the dominant viral factor that dictates TNPO3 dependency during HIV-1 infection. Under conditions where the expression of CPSF6 is enriched in the cytoplasm, be it by overexpression or mutation, we discovered a block to HIV-1 PIC nuclear import. We gathered evidence that the underlying mechanism is direct binding of CPSF6 to CA. The Asn74Asp (N74D) mutation of HIV-1 CA led to a loss of interaction with CPSF6 and evasion of the nuclear import restriction. The same mutation rendered HIV-1 TNPO3 independent, pointing to a functional link between TNPO3 and CPSF6. We show that compared to wild-type (WT) HIV-1, N74D HIV-1 is more sensitive to cyclosporine, and this is accompanied with a reduced affinity for ectopically expressed CypA, suggesting an indirect functional interplay between CPSF6 action and CypA as well.

B. Introduction

B.i. TNPO3 has a positive functional role in HIV-1 infection at a post reverse transcription / preintegration step

The importance of cellular interactors in mediating HIV-1 infection has been extensively described by human RNAi screens (Brass et al., 2008; Koenig et al., 2008; Zhou et al., 2008; Yeung et al., 2009) that identified hundreds of potential new HIV-1 dependency factors. Although there was little overlap between these studies (Bushman et al., 2009), a nucleo-cytoplasmic shuttling protein, the importin-β TNPO3/TRN-SR2 resulted in a HIV-1 infectivity defect upon its knockdown in two of these screens (Brass et al., 2008; Koenig et al., 2008). The requirement for TNPO3 for efficient HIV-1 infection was also confirmed in an independent study, where it was identified in a yeast-2-hybrid screen as an HIV-1 IN interactor. The same study proposed that TNPO3 may be responsible for mediating the nuclear import of HIV-1 PICs, as TNPO3 was not seen to bind the IN of MLV that lacks the ability for nuclear import. Even though it was uniformly established in all these studies that TNPO3 knockdown did not affect reverse transcription, assays looking for the nuclear presence of HIV-1 DNA products, either by quantifying total vDNA in nuclear vs cytoplasmic fractions or by assessing the levels of 2-LTR circles, failed to agree whether there was a nuclear import defect. As described in Chapter 1; **D.ii**, 2-LTR circles are accepted as a surrogate marker for nuclear import of HIV-1 PICs because their formation depends on the host nuclear NHEJ machinery, which joins the two viral terminal LTRs together.

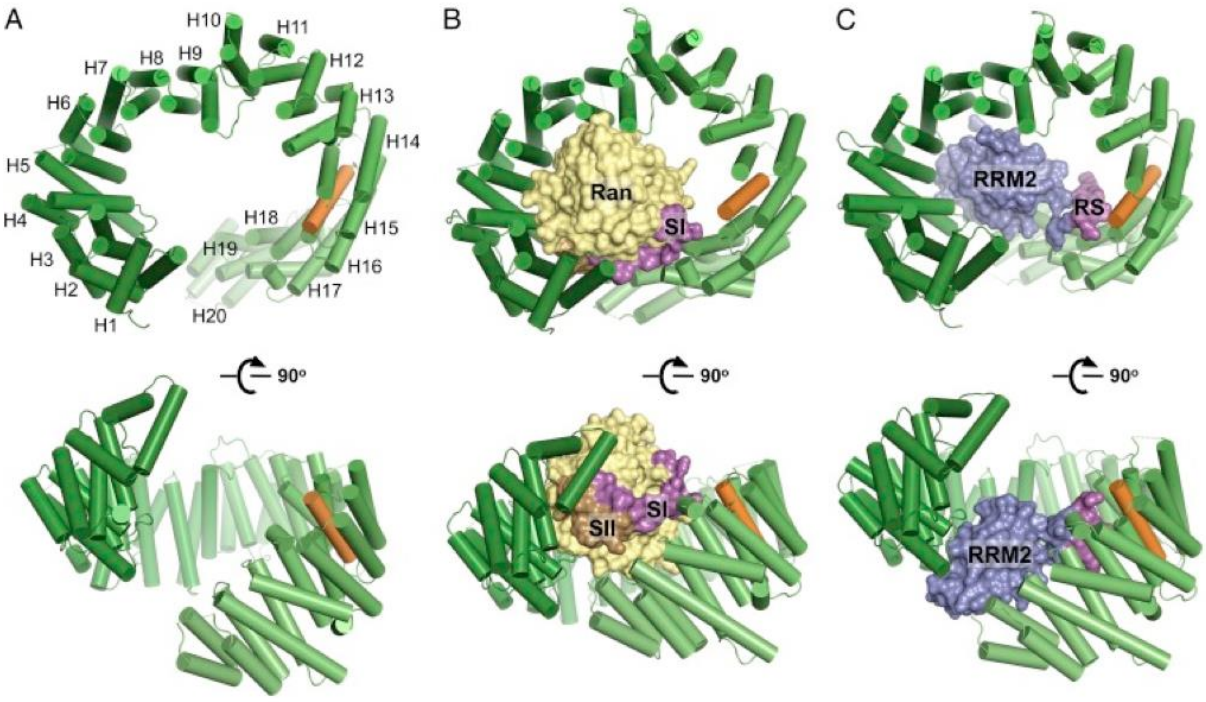

Figure 2.1 Overview of the crystal structures of unliganded TNPO3 **(A)**, TNPO3:RanQ69L-GTP **(B)**, and TNPO3:ASF/SF2 RRM2-RS **(C)** complexes. TNPO3 is shown as a cartoon, and the RRM2-RS domain of ASF/SF2 and Ran are depicted in space-filling surface rendering mode. TNPO3 is colored green except for the orange arginine rich R-helix responsible for cargo binding; Ran is colored yellow; and RRM2 and RS domains of ASF/SF2 are blue and magenta, respectively. H; helix. (Maertens et al., 2014).

TNPO3 is a transporter of serine-arginine rich (SR) protein family of splicing factors (Kataoka et al., 1999; Allemand et al., 2002) that mediates energy-dependent nuclear import of cargo molecules containing arginine-serine/arginine-aspartate/arginine-glutamate (RS/RD/RE) rich domains (Maertens et al., 2014). The Ran cycle responsible for energy generation is described in Chapter 1; **D.i**.

The recently solved X-Ray structures of TNPO3, TNPO3:RanQ69L-GTP and TNPO3:ASF/SF2 RRM2 (serine-arginine rich splicing factor 1 / pre-mRNA splicing factor 2 RNA recognition motif 2)-RS (arginine-serine rich) domain revealed atomic level mechanistic insight into (i) how cargo binding is established by pulling in the solenoid karyopherin TNPO3 (Figure 2.1A) unto itself via multiple interactions (Figure 2.1C) and into (ii) how cargo is

released upon RanQ69L-GTP binding via steric hindrance (Figure 2.1B). This particular study highlighted the importance of an arginine rich R-helix (specifically R661, R664, R667 and R671) and additional residues (R620, R754, R758) in TNPO3 for mediating critical interactions with phosphorylated serine residues on ASF/SF2, a canonical SR protein.

TNPO3-mediated import had been shown to be dependent on the cellular kinase mediated phosphorylation of serine residues within RS-domains, as exemplified in the case of the splicing factor ASF/SF2 (Colwill et al., 1996; Lai et al., 2000; Lai et al., 2001). However, phosphorylation-independent cargo binding has also been observed (Lai et al., 2003; Yun et al., 2003). The observation that TNPO3, a nucleocytoplasmic shuttling protein that may play a functional role at the step of PIC nuclear import or beyond in integration site targeting (Ocwieja et al., 2011) and its initial identification as an HIV-1 and lentiviral-specific IN - a PIC component - interacting protein garnered interest due to a potential interaction with the PIC in infected cells. This observation was, however, at odds with the finding that CA rather than IN is the functional determinant of PIC nuclear import (Chapter 1; **D.ii**) and thus prompted further study.

B.ii. Identification of a novel HIV-1 restriction factor, CPSF6-358

Additional laboratory evidence supporting a functional role of CA in PIC nuclear import came from a study in which we participated. The discovery of a novel, yet artificial, CA-mediated restriction of HIV-1 PIC nuclear import in mammalian cells, induced upon overexpression and cytoplasmic localization of a C-terminally truncated form of the SR protein, CPSF6-358, was noteworthy due to the loss of its RS domain and its potential ability to be recognized by TNPO3, the SR protein transporter (Lee et al., 2010). CPSF6/CFIm68 is a pre-

mRNA splicing factor that is a member of the SR-protein family (Ruegsegger et al., 1996) and bears a noncanonical C-terminal RS/RD/RE domain spanning residues 526-588 (Figure 2.2). Other discernible structural features are an N-terminal RNA recognition motif and a central proline rich domain (Figure 2.2) that is predicted to be devoid of secondary structure.

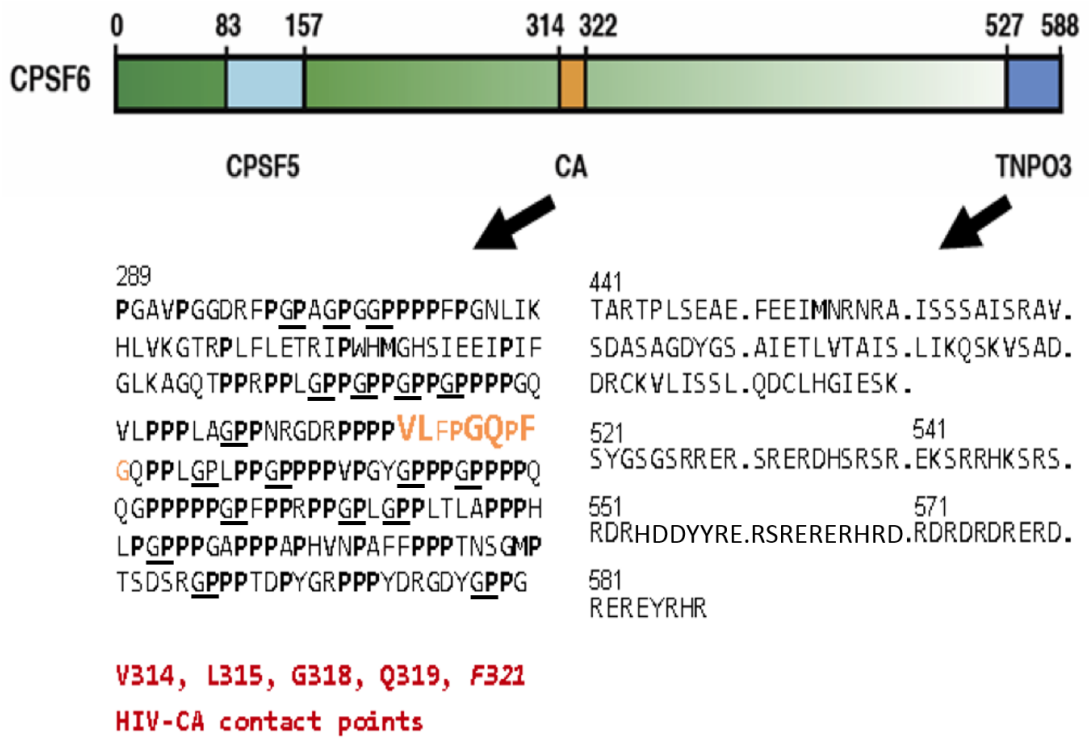

Figure 2.2 A schematic of CPSF6. Domains identified so far important for CPSF6 function have been highlighted. The N-terminal CPSF6 domain spanning 83-157 aa, highlighted in light blue, has been demonstrated to mediate intermolecular interactions with CPSF5, another splicing factor CPSF6 forms heterodimers with, mediating their joint nuclear localization (Yang *et al.*, 2011). The central 9-mer peptide sequence spanning 314-322 aa, highlighted in orange, is buried within a predictably nonstructured proline-rich region and mediates CA-recognition (Lee *et al.*, 2012), as confirmed in a co-crystal with HIV-1 CA-NTD (Price *et al.*, 2012), revealing a novel surface binding pocket on CA-NTD that CPSF6/CPSF6-358 presumably buries itself into. The C-terminal RS domain spanning 527-588 aa, harbors many RS/RD/RE repeats and is predicted to be responsible for TNPO3 binding.

CPSF6 is found in the nucleus, whereas the restrictive form, CPSF6-358 resides in the cytoplasm (Lee et al., 2010). The susceptibility of HIV-1 to CPSF6-358-mediated restriction was mapped to CA, because a resistant virus that evolved during passage in CPSF6-358 expressing cells harbored a single point mutation in CA, N74D, which is found in a well conserved surface

pocket on primate lentiviral CAs (Lee et al., 2010; Price et al,. 2012). In fact, N74 and adjoining CA residues are invariant among known HIV-1 isolates (Lee et al., 2010). A co-crystal structure of CA-NTD and a 15-mer peptide within the central proline-rich domain corresponding to 313-327 aa of CPSF6 was solved, identifying a direct interaction between the two. The CA contact points in the structure were N57, Q67, K70, N74, A105, T107 and S109, all grouping together on the CA-NTD (Figure 1.9C) in a surface pocket that faces the interhexameric space described in Chapter 1; **D.ii.1**.

B.iii. Preintegrative steps of HIV-1 infection are subject to modulation by CypA, a CA interacting protein

As described in **D.ii.1,** pinpointing the specific role of CypA in HIV-1 infection has been difficult. In lymphocyte-derived cell lines with low CypA concentrations, CypA seems to have a positive effect on HIV-1, possibly by increasing incoming core stability for a critical time window, whereas in cell lines such as HeLa cells or lymphocyte derived cell lines with high CypA content (Yin et al., 1998; Ylinen et al., 2009), it may reversibly impede infection by several HIV-1 CA mutants such as E45A, A92E, G94D, T54A/N57A and Q63A/Q67A, which can be relieved by CsA treatment (Song et al., 2007; Qi et al., 2008). Other studies highlighted the dual nature of CypA modulation on incoming RTC/PICs even with WT HIV-1 pointing to a possible positive effect on reverse transcription although a cell type-dependent, CypA-related dominant restriction at the stage of nuclear import (Song et al., 2007; Yamashita et al., 2009) had the potential to override such enhancement (De Iaco et al., 2014). CypA exerts an effect as early as at the stage of uncoating, causing early capsid disassembly as evidenced in the case of CA A92E (Li et al., 2009), but it also has downstream effects on integration site targeting (Schaller

et al., 2011). These functional observations with mostly CA mutants in cell-type dependent experimental conditions resulted in a rather complicated picture. Depending on the time of uncoating CypA may or may not be stably associated with the RTC/PIC, and such observations may be downstream effects of CypA modulation rather than due to a structural, stable CypA:CA interaction.

One other complication has been a lack of a quaternary understanding of how CypA interacts with the viral core, as all structural characterization efforts to date have focused on individual CypA:CA-NTD interactions without questioning how the surface topology of the hexagonal lattice with several CA hexamers, each displaying a CypA binding loop in close proximity to each other, might add to the picture.

C. Materials and Methods

Cells, viruses, and infections. HeLa, HEK293T, HeLa-T4 (Maddon et al., 1986), GHOST (Mörner et al., 1999) and MAGI (Chackerian et al., 1997) cell lines and its derivatives were cultured in Dulbecco's modified Eagle's medium (DMEM) supplemented with 10% fetal bovine serum (FBS), 100 IU/ml penicillin, and 100 μg/ml streptomycin. For cell cycle arrest experiments, HeLa cells were growth-arrested by incubation in complete medium containing 2 g/ml aphidicolin (Sigma) for 24 h, and maintained in this concentration of the drug during the infection. HeLa cells stably transduced with empty lentiviral vector pLKO.1 or pLKO.1 expressing TNPO3-specific short hairpin RNA (shRNA) (GGCGCACAGAAATTATAGAA) were additionally grown in 1 μg/ml puromycin. HeLa-T4 cells were transfected with 100 nM TNPO3-directed CGACAUUGCAGCUCGUGUA or mismatched control CGCCUAUGUAGCUCGUGUA (changes are underlined) siRNA by using RNAiMax or Oligofectamine.

Viral inocula used in Figures 2.3-5 were pseudotyped with the vesicular stomatitis virus G glycoprotein (VSV-G). The virus-specific molecular clones used were as follows: pBH2 and pBS-BC4MGppt for bovine immunodeficiency virus (BIV) (obtained from Michael Kaleko, Advanced Vision Therapies), pEV53 and an equine infectious anemia virus (EIAV)-green fluorescence protein (GFP) transfer vector for EIAV (gifts from John Olsen, University of North Carolina), pNL4-3env-GFP for HIV-1 (kindly provided by Dana Gabuzda, Dana-Farber Cancer Institute), pRCAS-GFP for Rous sarcoma virus (RSV) (Addgene plasmid # 13878, obtained from Constance Cepko via Addgene, Cambridge, MA), pFP93 and pGINSIN for feline immunodeficiency virus (FIV) (gifts from Eric Poeschla, Mayo Clinic), pFB-hrGFP (obtained from Joseph Sodroski, DFCI) and pCG-GagPol (provided by Richard Mulligan, Harvard

Medical School) for MLV. Simian immunodeficiency virus (SIV)-based pSIVmac239ΔnefΔenvEGFP (donated by J. Sodroski) was derived from pSIVΔnefEGFP (a kind gift from Ronald Desrosiers, Harvard Medical School) as follows. Env sequences were deleted by first changing the ATG start codon to TCC to create a BspE1 site. The 1.1-kb fragment between this and the native BspE1 site at position 8013 (GenBank accession # M33262.1) was excised, leaving Tat, Rev, and the Rev-responsive element intact.

The MLV-based retroviral vector, MIGR1, encoding a mouse thymus derived cDNA library was used for the cDNA overexpression screen mentioned in **D.ii**. The MLV vectors MIGR1, MX, and LPCX were used to generate stable cell lines. All HIV-1 reporter vectors encoding fluorescent proteins or firefly luciferase were NL4-3 derived. Reporter particles incorporated VSV-G, murine amphotropic Env, or HIV-1 Env glycoproteins. HIV-1, HIV-2, and SIV replication competent virus isolates, as listed in Figure 2.6, were also used in infection assays. Mouse and human CPSF6 cDNAs were purchased from Open Biosystems and Origene, respectively. Antibodies were from Abcam.

Viral vector particles were generated by transfecting 293T cells in 10-cm plates with 10 μg total of various ratios of virus production plasmids together with the VSV-G expression vector pMD.G using Fugene 6. Cells were washed at 16 h after transfection, and supernatants collected 28 to 72 h thereafter were clarified by centrifugation, filtered through 0.45 μm filters, and concentrated by ultracentrifugation at 53,000 × *g* for 2 h at 4 °C. HIV-1 CA p24 ELISA assay (Beckman Coulter) was performed per the manufacturer's recommendations. Infectious titers for luciferase- or Tat- expressing vectors were determined with GHOST cells.

GFP reporter virus infections were conducted in triplicate in 48-well plates. Cells were replenished with fresh medium following 16 h of virus absorption, and the percentage of positive

cells was determined at 48 h postinfection by using a FACsCanto flow cytometer equipped with FACSDIVA software. Inocula were adjusted to yield ~30 to 40% GFP-positive cells in control samples, with all infections scoring between 5 and 60% positive. For single-cycle viral infections, infection was measured by firefly luciferase activity (Promega) or fluorescence by FACS 2-3 days later.

Env-deleted MHIV chimera plasmids MHIV-mMA12CA-Luc, MHIV-mMA12-Luc, MHIV-mIN-Luc, and MHIV-mMA12CA/mIN-Luc as well as parental HIV-1_{LAI}-based pLaiΔenvLuc2 were generous gifts from Michael Emerman and Masahiro Yamashita (Yamashita et al., 2004). Viruses were generated by co-transfecting 293T cells with pCG-VSV-G using Fugene 6. Supernatants collected at 36 and 60 h posttransfection were pooled and spin concentrated as described above. Single-round MLV-Luc was produced as described previously (Shun et al 2007a). Cells infected in duplicate in 12-well plates for 12 h were rinsed with phosphate-buffered saline and replenished with fresh medium. At 2 days postinfection, resulting levels of luciferase activity in cell extracts were normalized to corresponding levels of total protein as described previously (Shun et al, 2007a). Inocula were adjusted such that control cells yielded 1×10^3 to 1.2×10^4 relative light units (RLU)/μg.

Western blotting. Cells were lysed with radioimmunoprecipitation assay buffer (20 mM HEPES [pH 7.5], 150 mM NaCl, 1% NP-40, 1% sodium deoxycholate, 0.1% sodium dodecyl sulfate, 0.5 M EDTA, protease inhibitors) at the time of infection. Following protein concentration determinations by Bradford assay, 50 μg or various dilutions were fractionated through 10 to 20% Tris-glycine gels. Proteins transferred onto a polyvinylidene fluoride membrane were blotted with a 1:100 dilution of mouse anti-TNPO3 antibody (Abcam), followed by a 1:10,000 dilution of rabbit anti-mouse horseradish peroxidase (HRP)-conjugated secondary

antibody (Dako). HRP-conjugated anti-β-actin antibody (1:10,000 dilution; Abcam) was used to control for gel loading.

Recombinant protein purification. All INs were studied as His_6-tagged fusion proteins; expression and purification were performed essentially as previously described (Dar *et al.*, 2009). Briefly, shaker flasks of *E. coli* strain BL21 or its PC2 derivative were grown in LB medium at 28 °C to an A_{600} of 0.6 to 0.8 prior to induction with 0.4 mM isopropyl-thio-β-d-galactopyranoside (IPTG) for 4 h, after which cells were harvested and lysed by sonication in buffer A {1 M NaCl, 7.5 mM 3-[(3-cholamidopropyl)dimethylammonio]-2-hydroxy-1-propanesulfonate (CHAPS), 0.5 mM phenylmethanesulfonyl fluoride, 25 mM Tris-HCl [pH 7.4]}. Lysates were clarified by centrifugation at 40,000 × *g* for 30 min at 4 °C and incubated with 2 ml Ni-nitrilioacetate (NTA) agarose beads (Qiagen, Valencia, CA) for 3 h at 4 °C in buffer A containing 25 mM imidazole. After extensive washing, bound protein was eluted with buffer A-200 mM imidazole. IN-containing fractions diluted with 4 volumes of 7.5 mM CHAPS-50 mM Tris-HCl [pH 7.4] were injected into a 1-ml HiTrap heparin column (GE Healthcare), and bound proteins were eluted with a linear gradient of 0.25 to 1 M NaCl in 7.5 mM CHAPS-50 mM Tris-HCl [pH 7.4]. MLV IN was further purified by gel filtration on a Superdex-200 column in buffer A, whereas Mason-Pfizer monkey virus (MPMV) IN was purified using just Ni-NTA beads. IN proteins concentrated by ultrafiltration using Amicon ultracentrifugal filters with a 10,000-molecular-weight cutoff (Millipore) were dialyzed against buffer A-10% (wt/vol) glycerol, flash-frozen in liquid N_2, and stored at −80 °C.

BL21 cells transformed with pGEX6P3-TNPO3 were grown at 37 °C to an A_{600} of 0.35 to 0.45 prior to 4 h of induction with 0.4 mM IPTG. Bacteria were harvested and lysed by sonication in cold buffer B (150 mM NaCl, 1 mM EDTA, 1 mM dithiothreitol [DTT], 50 mM

Tris-HCl [pH 7.4]). The crude extract, incubated with 25 U/ml Benzonase nuclease (EMD Biosciences) for 30 min at 25 °C to degrade bulk *E. coli* DNA, was clarified by centrifugation at 40,000 × *g* for 30 min at 4 °C, and the supernatant was incubated with 2 ml glutathione-Sepharose beads (GE Healthcare) for 3 h at 4 °C. After washing in excess buffer B, a 50% gel slurry was incubated with 20 U PreScission protease (GE Healthcare) at 4 °C for 16 to 24 h to remove the GST tag. Flowthrough and wash fractions containing tagless TNPO3 were pooled, concentrated, flash-frozen in liquid N_2, and stored at −80 °C. Recombinant Glutathione S-transferase (GST) protein was purified following bacterial expression as previously described (Cherepanov et al., 2004).

GST pulldown assays. GST-TNPO3 protein concentrations were determined by densitometric scans of Coomassie-R250 stained gel images relative to bovine serum albumin (BSA) standard curves. GST-TNPO3 (12 μg, which corresponded to 0.46 μM during binding) or control GST (12 μg) absorbed onto glutathione-Sepharose beads (30-μl settled volume) was resuspended in 200 μl of PD buffer (150 mM NaCl, 5 mM $MgCl_2$, 5 mM DTT, 0.1% Nonidet P40, 25 mM Tris-HCl [pH 7.4]) containing 10 μg BSA. IN (0.4 μM) was added, and the mixture was gently rocked for 3 h at 4 °C. After aspiration of the supernatant, the settled were beads resuspended in 600 μl PD buffer were allowed to sediment without centrifugation. The wash was repeated twice, and bound proteins were eluted in Laemmli sample buffer containing 50 mM EDTA-50 mM DTT. IN pulldown was confirmed in some experiments by blotting with a 1:1,000 dilution of HRP-conjugated anti-His_6 antibody (Clontech, Mountain View, CA).

Ni-NTA pulldown assays. INs were adsorbed onto Ni-NTA agarose beads in NTA-PD buffer (150 mM NaCl, 2 mM $MgCl_2$, 25 mM imidazole, 0.1% Nonidet P40, 50 mM Tris-HCl [pH 7.4]). Beads (25-μl settled volume containing 0.4 μM IN) resuspended in 300 μl NTA-PD

buffer containing 10 μg of BSA were incubated without (input controls) or with 0.4 μM TNPO3 for 3 h at 4 °C. Following supernatant aspiration, beads washed three times in ice-cold NTA-PD buffer were boiled in Laemmli sample buffer as described above. IN proteins were detected by staining with Coomassie-R250, whereas TNPO3 was detected by Western blotting.

Viral DNA Quantitation by qPCR (Figure 2.6). Cells challenged with DNaseI-treated HIV-1 vectors were lysed at different time points. As a control, a reverse transcription inhibitor [(150 nM efavirenz (EFV)] was added at the time of infection. Total DNA was extracted using the QIAmp Blood Mini Kit (Qiagen) and assayed by qPCR using Platinum qPCR SuperMix-UDG (Invitrogen) with primers and conditions as previously described (Julias et al., 2001). For quantification of PCR products, duplicate samples of serial dilutions of plasmid DNAs containing the target sequences were used to generate a standard curve.

High Molecular Weight HIV-1 CA-NC Complex Binding Assay. Recombinant wild-type and N74D HIV-1 CA-NC were expressed in bacteria, purified, and assembled in vitro as described previously for wild-type HIV-1 CA-NC (Ganser et al, 1999). Lysates containing CPSF6-358-HA, CPSF6-300-HA, or rhTRIM5α-HA were obtained from transiently transfected 293T cells via successive freeze/thaws in hypotonic buffer. CA-NC complexes were mixed with cell extracts for 1 hr at room temperature before ultracentrifugation through a 70% sucrose cushion (Stremlau et al., 2006). HA-tagged proteins were detected by Western blotting using HRP-conjugated anti-HA, whereas CA-NC was detected by Coomassie R-250 staining.

D. Results

D.i. The requirement for TNPO3 maps to HIV-1 CA but not IN

Original studies pointed to a functional role for TNPO3 in HIV-1 infection (Brass et al., 2008; Koenig et al., 2008), possibly at nuclear import of the PIC (Christ et al., 2008). The gammaretrovirus MLV, in contrast, had no dependence on this karyopherin, and biochemical studies showed that MLV IN failed to interact with recombinant TNPO3 under conditions where HIV-1 IN interaction was evident (Christ et al., 2008). To test the model that TNPO3 might be a lentiviral-specific factor that serves an IN-mediated function in lentiviral infection, such as PIC nuclear import, we set out to test additional lentiviral and non-lentiviral vectors for their dependence on TNPO3 in HeLa-T4 cells. Our expanded set of lentiviral vectors included SIV, BIV, EIAV, and FIV, as well as the α-retrovirus RSV. Recombinantly expressed and purified INs of these retroviruses, together with those of HIV-2 and β-retroviral MPMV, were simultaneously assayed for TNPO3 binding. A high percentage of homology (≥98%, not shown) among TNPO3 proteins of the respective species was considered safe to allow the assessment of TNPO3 dependence in HeLa cells.

Our results did not support the previously proposed model that TNPO3 interacts with lentiviral specific INs to mediate nuclear import of the PIC. Not all lentiviruses tested were dependent on TNPO3 under the assay conditions, and several non-lentiviral INs also had observable affinities to recombinant TNPO3 (**D.i.1**). Additionally, a functional assay employing MLV/HIV (MHIV) *gag-pol* chimerae identified the viral determinant of TNPO3 dependence as CA rather than IN (**D.i.2**).

D.i.1. TNPO3 : retroviral IN binding profiles do not reflect the dependency of respective retroviruses on TNPO3

Infections were staged to yield ~30 to 40% transduction of target HeLa cells, corresponding to an MOI of ~0.35 to 0.5. TNPO3 expression was then knocked down both stably (by means of a pLKO.1-shRNA vector) yielding an approximate 7- to 10-fold reduction in TNPO3 protein levels compared to control cells (Figure. 2.3A) or transiently (by means of siTNPO3 transfection) yielding a stronger, 14- to 20-fold decrease in protein levels (Figure 2.3C). Infectivities were assessed by GFP expression in infected cells as driven from retroviral vectors. As seen in Figure 2.3B and Figure 2.3D, various retroviruses displayed a wide range of sensitivity to TNPO3 knockdown, which did not correlate with the lentiviral- or nonlentiviral origin of the respective vectors. Replicating previously published results, HIV-1 infectivity was significantly impaired by stable TNPO3 knockdown, whereas MLV was unaffected (Figure 2.3B). RSV, an α-retrovirus, mimicked MLV. SIV, BIV, and EIAV exhibited considerable ~6.9-fold, 1.6-fold, and 1.9-fold infection defects, respectively, whereas infectivity of the lentiviral FIV vector was not impaired upon TNPO3 depletion (Figure 2.3B). The transient and stronger knockdown achieved with siTNPO3 treatment of HeLa-T4 cells replicated the defects in infectivity profiles of the vectors tested (cf. Figures 2.3B, D). Primate lentiviral SIV was the most affected and thus the most dependent on TNPO3 under both stable and transient knockdown conditions, whereas another lentivirus, FIV, only had a mild TNPO3 dependence in either condition. The overall order of TNPO3 dependency of the tested viruses was accordingly: SIV > HIV-1 > BIV and EIAV > MLV, RSV, and FIV.

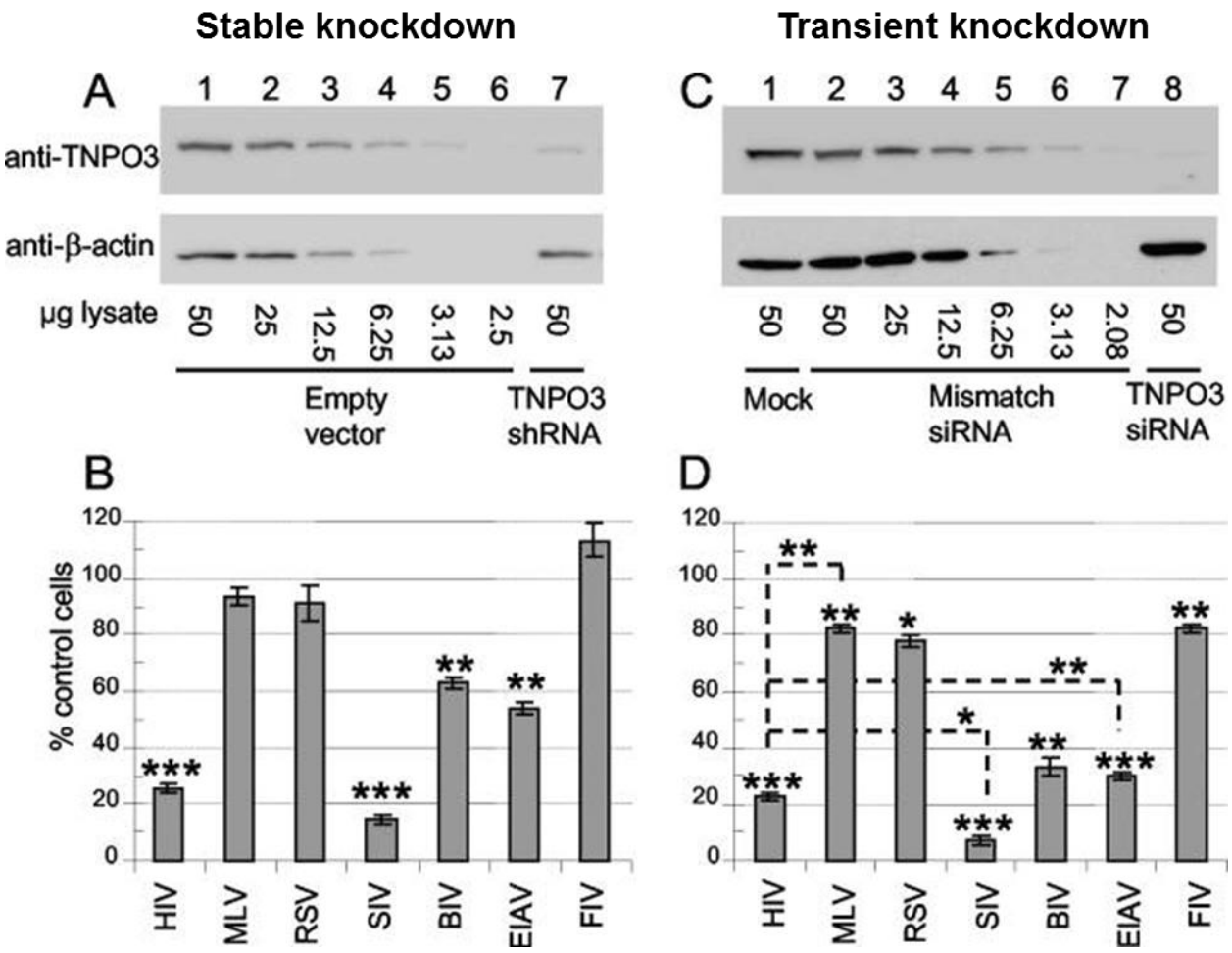

Figure 2.3 Retroviral infectivity profiles of TNPO3 knockdown cells. **(A)** TNPO3 levels in shRNA transduced cells were reduced 7- to 10-fold (lane 7) as revealed by the comparison to a gradient dilution of control cells (lane 1-6); β-actin served as a gel loading control. **(B)** Infectivity defects incurred by viral vectors upon stable TNPO3 knockdown as shown by mean percentages compared to empty control shRNA transduced cells (n=5; ± standard errors of the means [SEM]) **(C)** Western blotting showing the levels of TNPO3 depletion in transiently knocked down HeLa-T4 cells: Comparison of mock (lane 1) or mismatch control transfected (lanes 2 to 7) cells with siTNPO3-treated cell (lane 8) revealed a 14- to 20-fold decrease in steady state TNPO3 levels. **(D)** Infectivities (n=4; ± SEM) of indicated retroviral vectors, expressed as percent infectivity in TNPO3 knockdown cells compared to mismatch siRNA-transfected controls. Statistical significance values shown in **(B)** and **(D)** were calculated by using a Student's two-sided *t* test. Asterisks directly above bars indicate differences between knockdown and control cells for a given virus, whereas asterisks above dotted lines indicate differences between indicated viruses. ***, $P < 0.0001$; **, $P < 0.001$; *, $P < 0.01$. This particular dataset was generated by Kenneth Matreyek (Krishnan et al., 2010a).

To test whether the sensitivities of each retrovirus to TNPO3 knockdown correlated with the ability of their respective INs to bind recombinant TNPO3, we carried out reciprocal pulldown assays with either His_6-tagged IN or GST-tagged TNPO3 proteins immobilized onto

beads. Initially, GST-TNPO3 was assayed for its ability to bind soluble IN. Replicating earlier observations, HIV-1 IN was pulled down by GST-TNPO3 (Figure 2.4A, cf. lane 7 to lane 6; HIV-1 IN=32kD). Contrary to data from the previous report, however (Christ et al., 2008), MLV IN bound GST-TNPO3 readily as well (lane 8). GST-TNPO3 recovered SIV IN (lane 9) at levels similar to that of HIV-1 IN, whereas EIAV IN was not pulled down under these conditions (lane 10; deeper inspection by Western blotting revealed a low-level EIAV IN binding to GST-TNPO3, data not shown). GST alone did not pull down any of the IN proteins, confirming specificity of the binding to TNPO3 (Figure 2.4A, lanes 12 to 17).

Reciprocal pulldowns employed His_6-tagged IN proteins immobilized on Ni-NTA beads and assessed their ability to capture tag-free TNPO3 (Figure 2.4B). Similar results were obtained compared to Figure 2.4A: HIV-1 and MLV IN had the highest recovery of TNPO3, while SIV and EIAV did less so, and FIV IN bound TNPO3 better in the Ni-NTA assay than in the GST pulldown assay (cf. Figure 2.5B, lanes 7-11 to Figure 2.5A, lanes 7-11). The lack of TNPO3 recovery on empty Ni-NTA beads validated the specificity of the interactions detected (lane 12). Additional IN proteins (of which the respective retroviral vectors were not tested in the infectivity assays) from HIV-2, BIV, RSV also displayed detectable TNPO3 binding, whereas MPMV IN failed to do so (lanes 19 to 24). Overall, our data revealed a lack of lentiviral specifity for the ability of TNPO3 to bind INs; TNPO3 readily bound INs derived from both γ- and α-retroviruses in addition to lentiviruses. Control Ni-NTA pulldowns of LEDGF/p75 confirmed the conformational integrity of each His_6-tagged IN tested in the pull downs (data not shown).

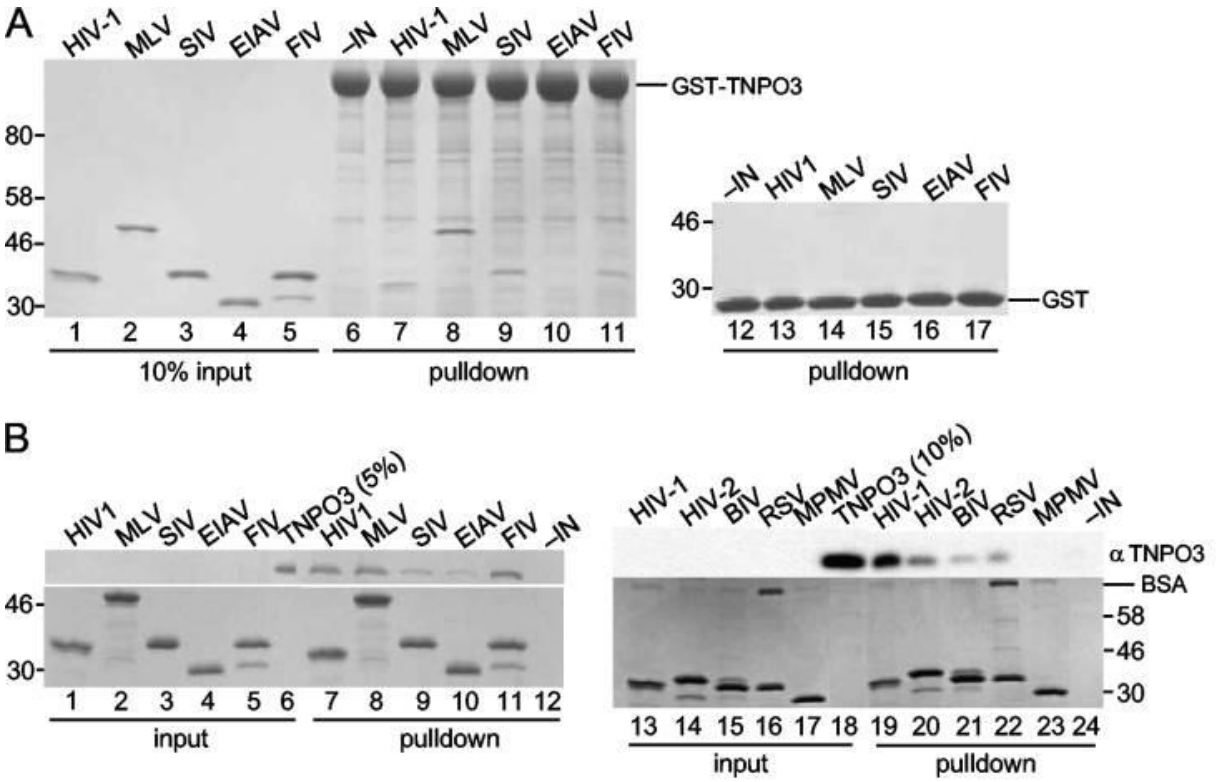

Figure 2.4 Pulldown analyses of IN-TNPO3 binding. **(A)** GST pulldowns. Lanes 1 to 5 contained 10% of input IN protein. Proteins bound to GST-TNPO3 (lanes 6 to 11) or GST (lanes 12 to 17) immobilized on Glutathione Sepharose beads were recovered by boiling and visualized by Coomaassie staining. Samples 6 and 12 served as negative controls by omitting IN from binding reactions. **(B)** Reciprocal pulldowns with Ni-NTA bound INs: mock pulldowns (lanes 1-5 and 13-17) or TNPO3-pulldowns are shown (lanes 7-12 and 19-24) Eluted proteins were detected by Western blotting (top) or Coomassie R-250 staining (bottom). Input levels of TNPO3 were analyzed in lanes 6 and 18. Lanes 12 and 24 are negative controls. Molecular weight markers depicted to the side of the gels. This particular dataset was generated by Lavanya Krishnan (Krishnan et al., 2010a).

To assess TNPO3:IN binding more quantitatively and with higher sensitivity, surface plasmon resonance measurements were carried out with chip-immobilized TNPO3 and soluble INs. The data obtained confirmed the lentiviral nonspecificity of the interaction as revealed by binding affinities of respective INs ranking from strongest to weakest: FIV, HIV-1, and BIV > SIV and MLV > EIAV (data not shown).

D.i.2. HIV-1 CA determines the requirement for TNPO3 during HIV-1 infection

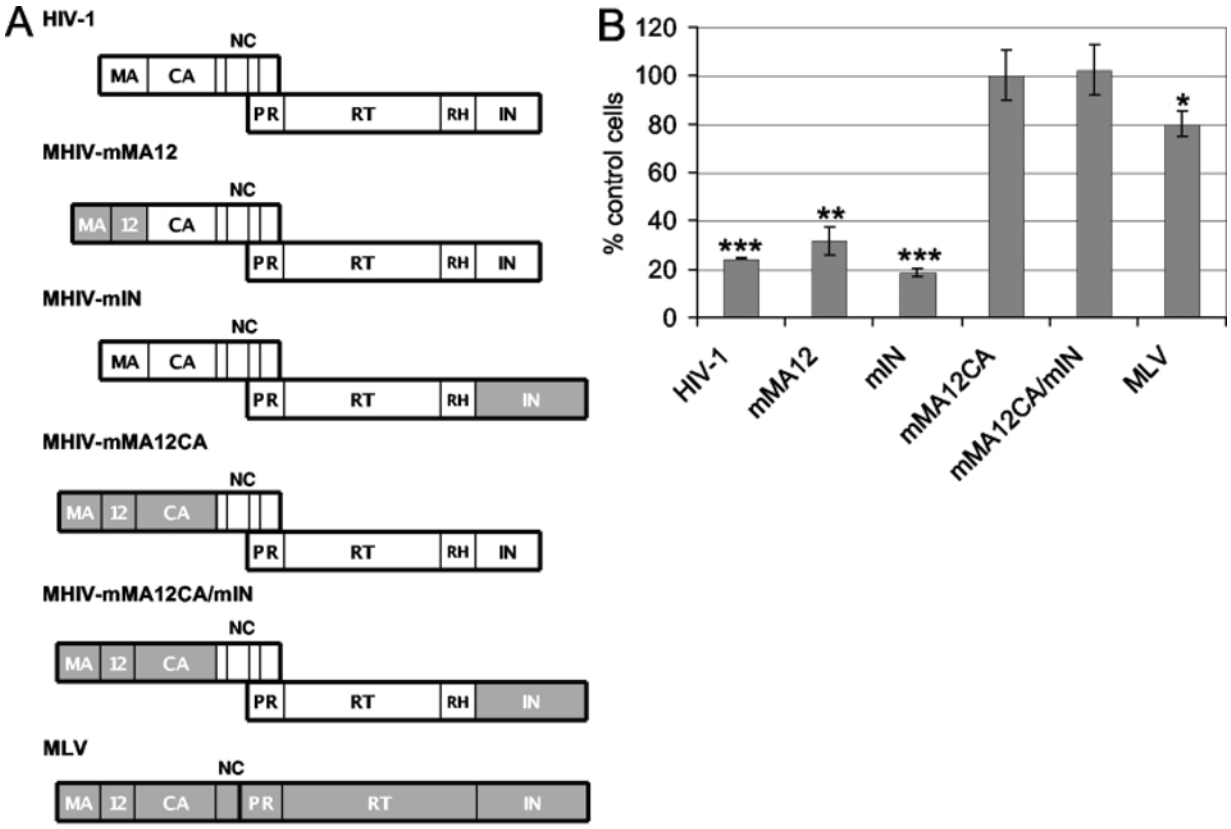

Figure 2.5 Infectivity profiles of MHIV chimera viruses versus HIV-1 and MLV. **(A)** Schematics of HIV-1 (white), MLV (gray), and chimera viral Gag and Pol proteins. NC, nucleocapsid; PR, protease; RT, reverse transcriptase; RH, RNase H. **(B)** Results of two independent experiments (means ± SEM) expressed as the percent infectivity on TNPO3-depleted compared to control cells. Student's two-sided *t* test comparisons of these values revealed significance parameters (***, $P < 0.001$; **, $P < 0.01$; *, $P < 0.05$). In contrast, relative MHIV-mMA12 and MHIV-mIN titers did not significantly differ ($P > 0.05$) from the HIV-1 value.

Our findings indicated that IN-TNPO3 binding affinities did not correlate with the respective retroviral dependencies on TNPO3 during infection. We therefore sought to determine other viral factors that might contribute to the phenotype. As TNPO3 knockdown preferentially inhibited infection by HIV-1 over MLV (Figure 2.3B, D), previously described MHIV chimera viruses (Yamashita et al., 2007), which swap various parts of MLV *gag-pol* for the corresponding ones in HIV-1 (Figure 2.5A), were investigated. As described in Chapter 1; **D.ii.1**, these hybrid constructs were previously used to highlight a dominant role for HIV-1 CA in

conferring infectivity on growth-arrested cells. The following chimera viruses were utilized in our studies: MHIV-mMA12CA, where MLV MA, p12, and CA replaced HIV-1 MA and CA (p12 is specific to MLV); MHIV-mMA12, harboring MLV MA and p12 in place of HIV-1 MA; MHIV-mIN, where MLV IN replaced the HIV-1 protein; and MHIV-mMA12CA/mIN, where MLV Gag and IN determinants were combined in the same construct (Figure 2.5A). Parental luciferase reporter viruses were VSV-G pseudotyped alongside the chimerae, and the resulting infectivities in HeLa cells stably knocked down for TNPO3 were expressed as percentages of control cell infection levels.

Replacing HIV-1 MA and CA with the corresponding MLV determinants strikingly rendered the MHIV-mMA12CA chimera insensitive to TNPO3 knockdown. Swapping the CA of this virus back to the HIV-1 protein, however, resensitized MHIV-mMA12 to the knockdown, highlighting a role for CA in determining TNPO3 dependency during HIV-1 infection (Figure 2.5B). The MHIV-mIN chimera, which harbored MLV IN alongside HIV-1 Gag determinants, was accordingly sensitive to the knockdown. Moreover, the combined MHIV-mMA12CA/mIN chimera virus behaved in a TNPO3-independent manner (Figure 2.5B). Thus, all viruses that harbored HIV-1 CA depended on TNPO3 for optimal infectivity regardless of whether they carried HIV-1 or MLV IN, pinpointing HIV-1 CA as the viral determinant of TNPO3 function.

D.ii. CPSF6-358 is an HIV-1 restriction factor that targets HIV-1 CA

D.ii.1. CPSF6-358, a primate lentiviral specific restriction factor of PIC nuclear import, can be overcome by a single point mutation, N74D, in HIV-1 CA

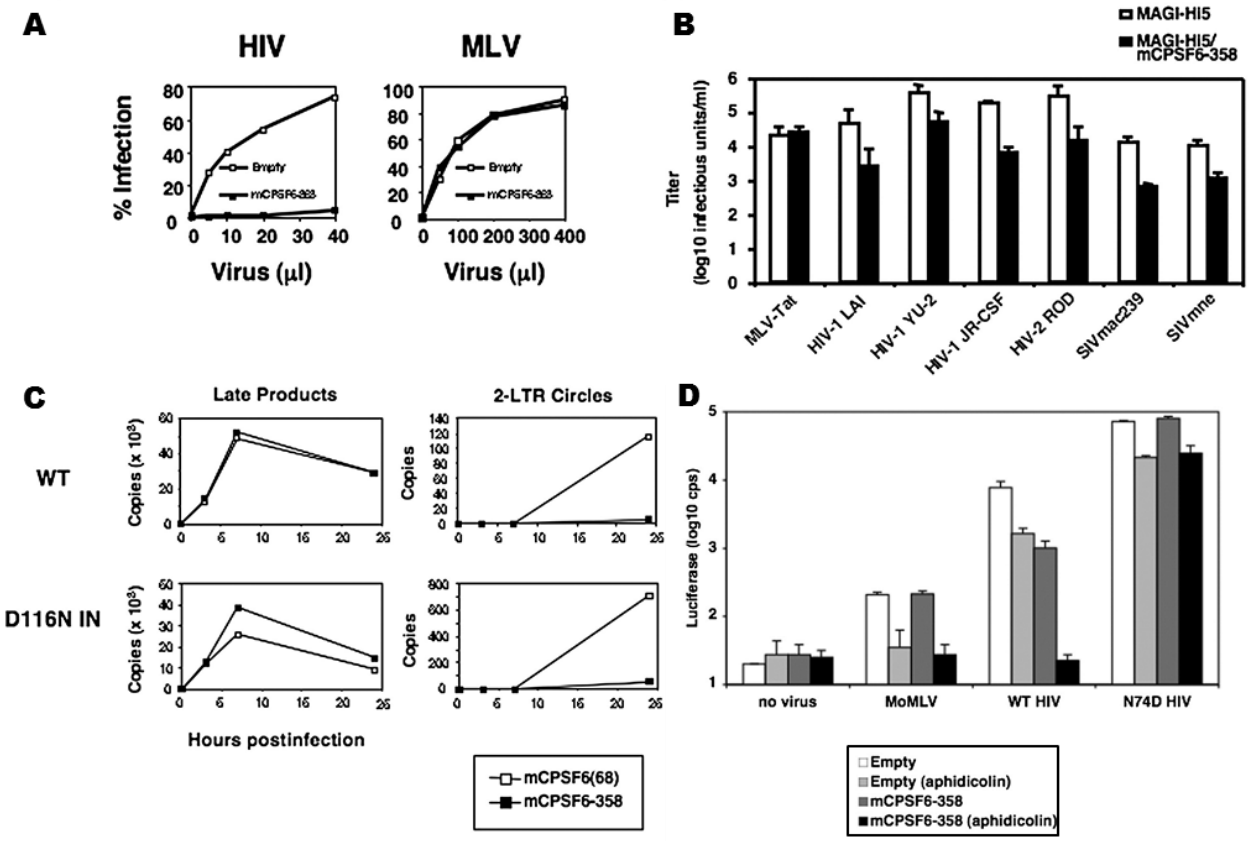

Figure 2.6 CPSF6-358 restricts primate lentiviruses at the nuclear import step and can be overcome by CA N74D **(A)** Infection of HeLa cells expressing mCPSF6-358 with HIV-RFP/VSV-G and MLV-RFP/VSV-G vectors. Infectivity was quantified by FACS for the expression of red fluorescent protein (RFP). **(B)** mCPSF6-358 readily inhibits replication competent primate lentiviruses under single-cycle conditions using MAGI cells expressing CCR5. VSV-G pseudotyped MLV expressing HIV-1 Tat was used as a control. **(C)** qPCR profiling of HIV-1 DNA species. 293T cells expressing control mCPSF6 or mCPSF6-358 were infected with VSV-G pseudotyped HIV or integration deficient HIV/D116N IN and whole cell lysates were probed at different time points post-infection to quantify viral reverse transcription products (ERT, not shown; LRT, shown) and 2-LTR circles. (D) HIV-1 CA N74D efficiently infects nondividing HeLa cells arrested with aphidicolin and infection is resistant to mCPSF6-358 restriction as opposed to WT HIV-1. Control infections are carried out in cycling HeLa and HeLa-mCPSF6-358 cells with MLV. All viruses are pseudotyped with VSV-G. This particular dataset was generated by the KewalRamani laboratory (Lee et al., 2010).

In a joint study with the KewalRamani Lab, a mouse thymic cDNA expression library was screened in NIH3T3.hCycT1 cells (Michel et al., 2009) to identify factors that limit the

infection of VSV-G pseudotyped HIV-1. From this we identified mouse CPSF6-358 (mCPSF6-358), a C-terminal truncation product of the cellular nuclear splicing factor CPSF6 that only harbors the N-terminal 358 amino acids (Lee et al., 2010). The parental protein, mCPSF6, did not show a restrictive phenotype upon overexpression. A similarly truncated human CPSF6-358 also restricted HIV-1 infection (data not shown). mCPSF6 was shown to localize to the nucleus, whereas mCPSF6-358 and other restrictive CPSF6 species were enriched in the cytoplasm as assessed by nucleocytoplasmic fractionation followed by immunoblotting in NIH3T3.hCycT1 cells (data not shown). To confirm the specificity of the restriction, control and mCPSF6-358-expressing HeLa cells were challenged with VSV-G pseudotyped HIV-RFP or MLV-RFP (Figure 2.6A). HIV-1, but not MLV infection, was strongly impaired by mCPSF6-358.

To further characterize the retroviral specificity of the restriction several primate lentiviruses were assayed for their susceptibility to mCPSF6-358 interference in control and mCPSF6-358-expressing MAGI-Hi5 cells. Different strains of replication competent HIV-1 (HIV-1_{LAI}, HIV-1_{YU-2}, HIV-1_{JR-CSF}) and HIV-2, SIV_{mac239} or $SIV_{mne\ cl.8}$ were all susceptible to mCPSF6-358 mediated restriction displaying approximately 10-fold or greater infectivity defects (Figure 2.6B). Even stronger infectivitry defects were observed in continuous replication assays such that over the course of three weeks or longer, HIV-1_{NL4-3}, HIV-$1_{NL4-AD8}$, HIV-1_{YU-2}, and HIV-1_{JR-CSF} did not replicate to detectable levels in HUT-R5- mCPSF6-358 cells as opposed to parental control HUT-R5 cells (data not shown).

Quantification of vDNA species by quantitative PCR (qPCR) revealed that the mCPSF6-358 block impaired HIV-1 at a step post reverse transcription (as implied by unaffected kinetics and steady state levels of LRT levels), whereas overexpression of the full length mCPSF6 had no effect (Figure 2.6C). However, the accumulation of the 2-LTR circular form of vDNA, a dead-

end form produced in the nucleus, was reduced upon mCPSF6-358 expression, even in the case of $HIV_{IN/D116N}$ (an integration deficient IN active site mutant) that normally generates elevated levels of 2-LTRs due to accumulation of unintegrated vDNA species inside the nucleus (Figure 2.6C). In vitro integration assays with isolated PICs from either control NIH3T3.hCycT1 or NIH3T3.hCycT1-mCPSF6-358 cells revealed no defect to integration competence, mapping the infectivity defect at a pre-integration and post/at-nuclear import step (data not shown).

To further confirm the nuclear import defect imposed by mCPSF6-358 restriction, control HeLa cells and HeLa cells expressing mCPSF6-358 were challenged with VSV-G pseudotyped HIV-1 both under cycling and aphidicolin-treated, growth-arrested non-mitotic conditions. Aphidicolin is an inhibitor of DNA polymerase α and δ that results in cell cycle arrest at the G1/S phase (Ikegami et al., 1978; Goscin et al., 1982). Growth arrest intensified the mCPSF6-358 HIV-1 infectivity defect more than one order of magnitude bringing it down to a ~70-fold decrease when compared to untreated parental HeLa cells (Figure 2.6D). MLV, a γ-retrovirus that depends on mitosis to gain access to target nucleus (Roe et al, 1993) served as a negative control; its already decimated infectivity in growth-arrested cells was unaffected by mCPSF6-358 overexpression.

In a parallel viral evolution assay, replication-competent $HIV\text{-}1_{NL4\text{-}3/BaL}$ was passaged in HUT-R5.mCPSF6-358 cells and gave rise to a single point CA mutant, N74D, which rendered the virus completely resistant to mCPSF6-358 restriction with no observable fitness cost in these cells (data not shown). Introducing the mutation into HIV_{NLdE} and infecting growth-arrested HeLa cells with VSV-G pseudotyped HIV_{NLdE} CA N74D then revealed that this CA mutant virus was still unaffected by the combination of cell-cycle arrest and mCPSF6-358 expression (Figure 2.6D).

D.ii.2. CPSF6-358 is a novel CA-interacting protein, and CA N74D abolishes this interaction

The ability of the N74D mutant to evade mCPSF6-358 restriction suggested that this antiviral protein might directly target viral CA. To assay for an interaction of CPSF6-358 to CA, we employed the high molecular weight (HMW) CA-NC 'tube' binding assay, where *in vitro* reconstituted tubular CA-NC assemblies are used to recapitulate the surface configuration of the CA hexagonal lattice (Ganser et al., 1999). The HMW CA-NC complexes can then be incubated with target factors either in the form of ectopically expressed or recombinant proteins. Ultracentrifugation through a sucrose cushion then separates CA-binding partners from the rest of the mixture by allowing their co-pelleting with the CA-NC tubes (Stremlau et al., 2006).

We assembled WT and N74D CA-NC complexes *in vitro*. Pre-assembled complexes were then incubated with 293T cell lysates transfected with human CPSF6-358; the non-restrictive larger deletion variant, CPSF6-300; or rhTRIM5α which served as positive control. As shown previously (Stremlau et al., 2006), WT CA-NC complexes pellet rhesus rhTRIM5α, a known CA interactor, under these conditions (Figure 2.7, right panel) (interestingly, N74D CA-NC complexes more efficiently precipitated rhTRIM5α - about two-fold - than wild-type CA-NC complexes in four separate trials). Non-restrictive CPSF6-300 pelleted with WT and N74D CA-NC complexes at an equal efficiency (Figure 2.7, middle panel). By contrast, CPSF6-358 co-purified more efficiently with WT vs. N74D CA-NC cores (Figure 2.7, left panel), at an average difference of 3.9-fold over four trials (data not shown), revealing a mechanistic explanation to N74D evasion of CPSF6-358 restriction.

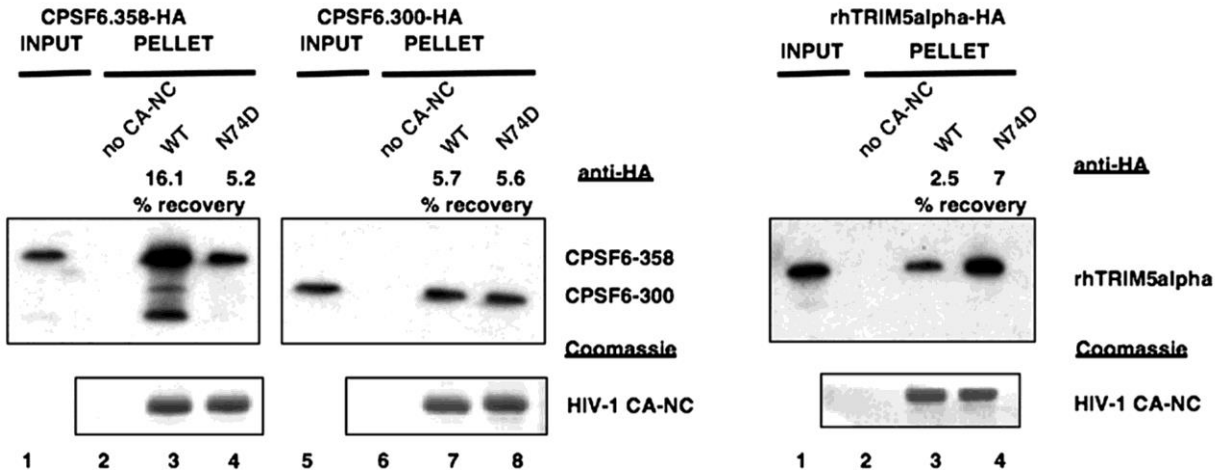

Figure 2.7 CPSF6-358 is a novel CA-binding protein and N74D inhibits binding. Enhanced binding of CPSF6-358 to WT CA-NC complexes. Recombinant WT and N74D CA-NC complexes were incubated with lysates from 293T cells transfected with HA-tagged constructs expressing CPSF6-300, CPSF6-358, or rhTRIM5α. Mixtures were then layered on top of a 70% sucrose cushion followed by ultracentrifugation. Top panels are Western blots using anti-HA; bottom panels are Coomassie R-250 stains of pelleted material. Lanes 1 and 5 depict lysate inputs that were not subjected to ultracentrifugation. Lanes 2 and 6 are pelleted material in the absence of CA-NC complexes. Recovery of HA-tagged proteins in pellet fractions following coincubation with CA-NC complexes (50% of total loaded) relative to input samples (10% of total loaded) was measured by densitometry.

D.ii.3. CPSF6-358 restriction and TNPO3-requirement have different cell cycle dependencies

Following the observation that mCPSF6-358 restricted HIV-1 infection at the stage of nuclear import and a single point mutant of HIV-1 CA, N74D, could overcome this restriction with no apparent fitness cost in HeLa cells (Figure 2.6D untreated cells, WT vs N74D), the two viruses were assayed for their dependence on several karyopherins, including TNPO3 (Figure 2.8), that may have functional importance for HIV-1 PIC nuclear import.

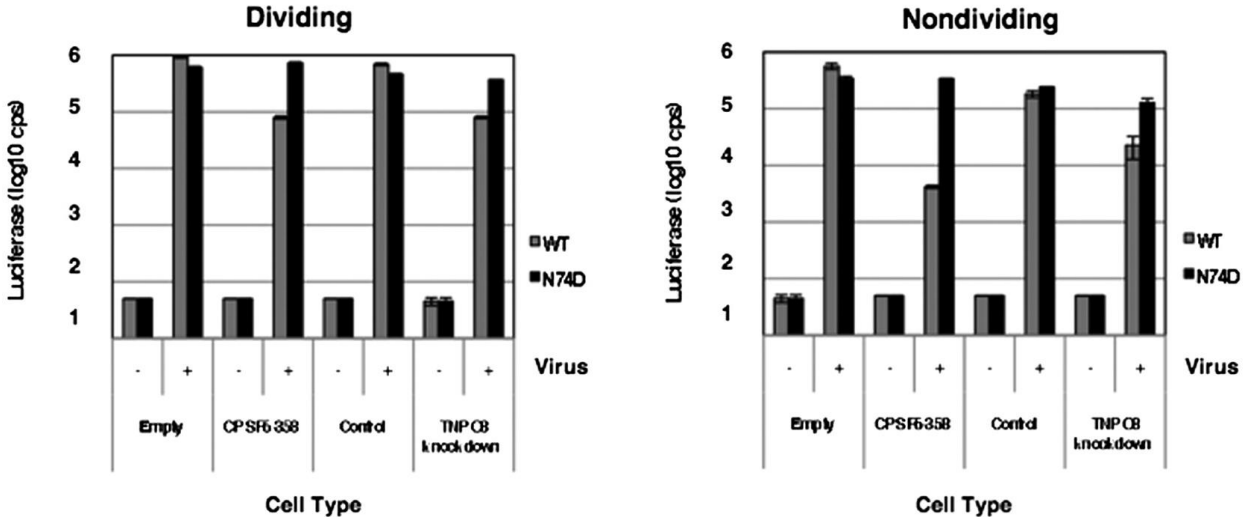

Figure 2.8 Cell growth arrest does not increase the dependency of WT HIV-1 on TNPO3. HeLa cells that contain only the empty vector or cells that express mCPSF6-358 and HeLa cells transduced with control shRNA vector or TNPO3 shRNA were infected with either WT HIV-1 or N74D mutant vectors that express a luciferase reporter (HIV_{NLdE}-luc/VSV-G or $HIV_{NLdE\ CA\ N74D}$-luc/VSV-G, respectively). Cell lysates were measured for luciferase activity 48 h after infection. Luciferase values reflect averages of duplicate infections with standard deviations. The data in the right panel were from cells treated with aphidicolin. This particular dataset was generated by the KewalRamani laboratory (Lee et al., 2010).

HeLa cells stably depleted of TNPO3 were similar to mCPSF6-358 expressing cells in that both types of cells were about 10-fold less susceptible to infection by WT HIV-1 than were control cell lines during normal growth (Figure 2.8, left panel). Infection by N74D HIV-1 was not only unimpaired upon mCPSF6-358 expression, but also upon TNPO3 depletion, indicating that CA N74D rendered HIV-1 not only mCPSF6-358 resistant but TNPO3 independent, as well. Upon aphidicolin-induced growth arrest in the same set of cells (Figure 2.8, right panel), the mCPSF6-358 restriction and TNPO3 knockdown phenotypes differed, however. As previously observed in Figure 2.6D, nondividing cells that express mCPSF6-358 strongly restricted infection by WT HIV-1 (~ two orders of magnitude) but not by N74D HIV-1. In contrast, the HIV-1 infectivity defect in TNPO3-depleted cells remained similar upon growth arrest. Thus, the dependence on TNPO3 in HIV-1 infection was the same in dividing and nondividing cells, whereas HIV-1 was differentially more vulnerable to mCPSF6-358 in nondividing cells.

Additional karyopherins such as Nup153 and Nup155 were also tested in similar assays, revealing differential NUP requirements for N74D and WT HIV-1 (data not shown).

D.iii. HIV-1 N74D has increased sensitivity to CsA and lowered binding to CypA

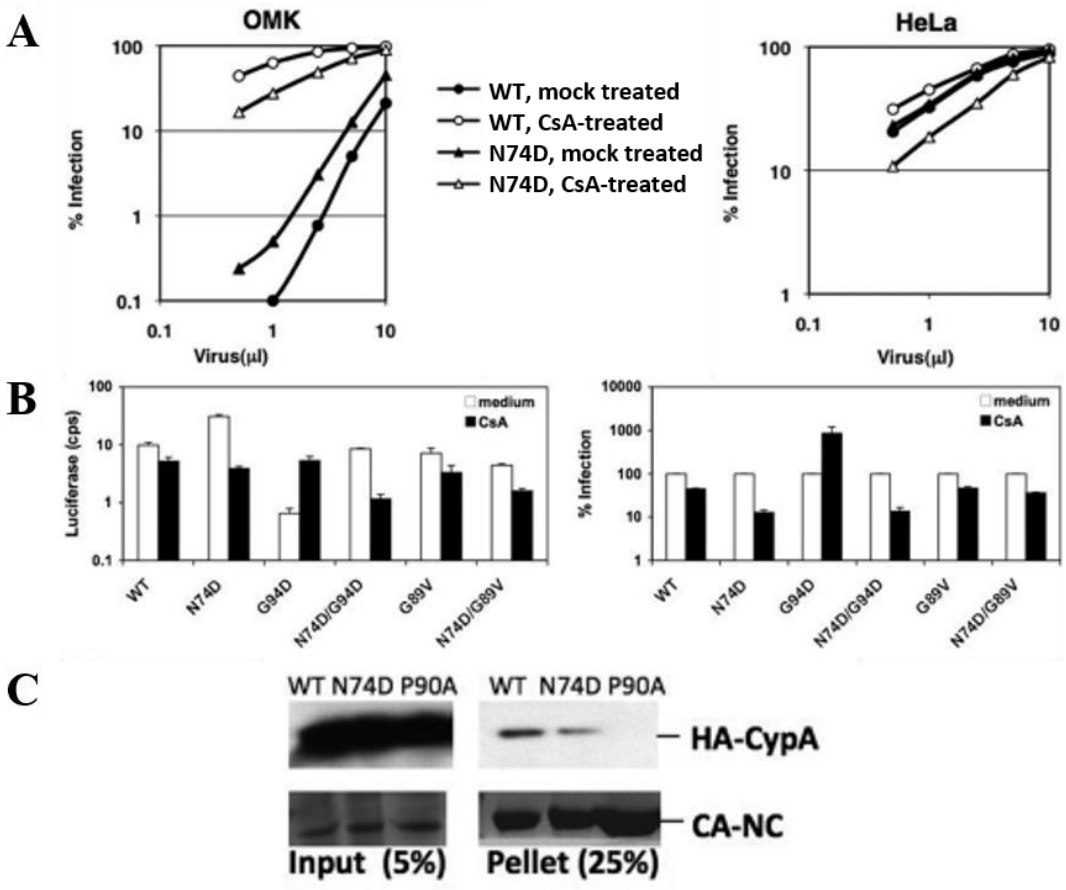

Figure 2.9 HIV-1 N74D CA has increased sensitivity to CsA and shows reduced binding to CypA. **(A)** OMK or HeLa cells incubated with or without 2.5 μM CsA were infected with different volumes of VSV-G pseudotyped WT or N74D HIV-1-RFP 48 h before FACS analysis. **(B)** HeLa cells were infected with VSV-G pseudotyped WT or N74D, G94D, N74D/G94D, G89V, and N74D/G89V HIV-1-luc with or without 2.5 μM CsA for 48 h before bioluminescence analysis. Infectivity data are presented both in absolute counts per second (left) and as normalized percentages based on WT infectivity without CsA treatment (right). **(C)** WT, N74D, and P90A CA-NC complexes were incubated with 293T cell extracts expressing HA-tagged CypA. HA-CypA in the pellet is detected by immunoblotting, whereas CA-NC pellet amounts are visualized by Coomassie R-250 staining. Image is representative of two independent experiments. Panels A and B were generated by the KewalRamani laboratory (Lee et al., 2010).

Owl monkey kidney (OMK) cells express a Trim5 restriction factor variant, TrimCyp that recognizes incoming capsids via its C-terminal Cyp domain (Sayah et al., 2004). N74D

impairs CPSF6-358 recognition without causing gross changes in the capsid core as observed by normal levels of rhesus TRIM5α restriction in HeLa cells (data not shown). To test for changes in CypA recognition, N74D HIV-1 sensitivity to TRIMCyp was assayed (Figure 2.9A). N74D, which bears no fitness cost to HIV-1 in HeLa cells, was restricted in OMK cells similar to WT HIV-1 over a titration curve; however, it was 2- to 5-fold less susceptible overall (solid data points), suggestive of decreased binding to TRIMCyp. Notably, when these cells were treated with CsA, ablating interaction between CA and both TrimCyp and CypA alike (empty data points), WT HIV-1 infection increased to a greater extent (20- to 600-fold over the titration curve) than N74D HIV-1 (5-to 50-fold). Parallel infections in HeLa cells, where there is no TRIMCyp expression but CypA, revealed that whereas WT HIV-1 was virtually unaffected by CsA treatment, N74D HIV-1 infectivity decreased up to 3-fold, suggestive of an increased dependence on normal levels of CypA.

To better characterize its lowered sensitivity to TrimCyp, higher sensitivity to CsA and increased requirement for CypA, N74D was assessed alongside other CA mutant viruses with known CypA dependence. G89V that abolishes CypA binding and G94D that renders HIV-1 CsA-dependence were tested in presence and absence of CsA (Figure 2.9B). As expected, G89V rendered HIV-1 insensitive to CsA in absence of CypA binding with or without the N74D mutation compared to WT HIV-1. Confirming the previous observation in Figure 2.9A, N74D HIV-1 infectivity was decreased and, in line with the literature (Aberham et al., 1996), the infectivity of G94D HIV-1 was increased upon CsA treatment. Combining N74D with G94D led to a complete relief of the CypA-dependent restriction of G94D, and the resulting double mutant was as dependent on CypA / as sensitive to CsA as N74D was by itself.

To test for a biochemical basis to why N74D has an increased dependence on CypA that can even override the CypA-dependent restriction of G94D, we employed the *in vitro* CA-NC binding assay to assess CypA binding to N74D compared to WT CA (Figure 2.9C). In cell extracts, N74D bound 65 to 70% less CypA than WT CA-NC in two independent assays, P90A CA-NC served as a negative control. This result suggests that N74D HIV-1 cores in infected cells may bind CypA with less affinity, which may render the virus more sensitive to CsA treatment.

Our results overall pinpoint to CA as the functional target of two novel HIV-1 determinants in infected cells. Corroborated by structural efforts from independent research efforts we have not only identified CPSF6 as a novel CA binding protein that may also regulate the previously established interaction between CA and CypA, but also a novel conserved surface pocket on capsid at the CA hexamer:hexamer interface. Our results emphasize the importance of evaluating biochemical and functional observations on CA binding proteins within the context of the quaternary capsid lattice, where different interactions may take place not only simultaneously but also cooperatively or in a coregulated manner.

E. Discussion

E.i The capsid cone displays a multifaceted surface regulating HIV-1 PIC nuclear import where several host factors converge

Since TNPO3 and CPSF6 became players in the field of HIV-1 PIC nuclear import and preintegration trafficking, their functional role has been extensively studied. Price et al. (2012) solved the co-crystal structure of CA-NTD:CPSF6$_{313-327}$, revealing how the surface pocket created by CA-NTD helix 3 and 4 present critical contact points to the CPSF6 15-mer (Figure 1.9C: CA residues N57, Q67, K70, N74, A105, T107 and S109), and how N74D would thus abrogate binding to CPSF6 rendering the virus CPSF6-independent / CPSF6-358 resistant. It is noteworthy that at the time of our publications no critical function could be ascribed to endogenous CPSF6, as cellular depletion by RNAi failed to show either a negative or positive effect on HIV-1 infectivity in the cells tested. Modeling a CypA molecule onto this co-crystal structure (see Appendix B), which is projected here onto the hexamer:hexamer interface as resolved by Zhao et al., 2013 (Figure 1.9), reveals the context in which CPSF6$_{313-327}$ would need to bind CA with regards to CypA (Figure 2.10).

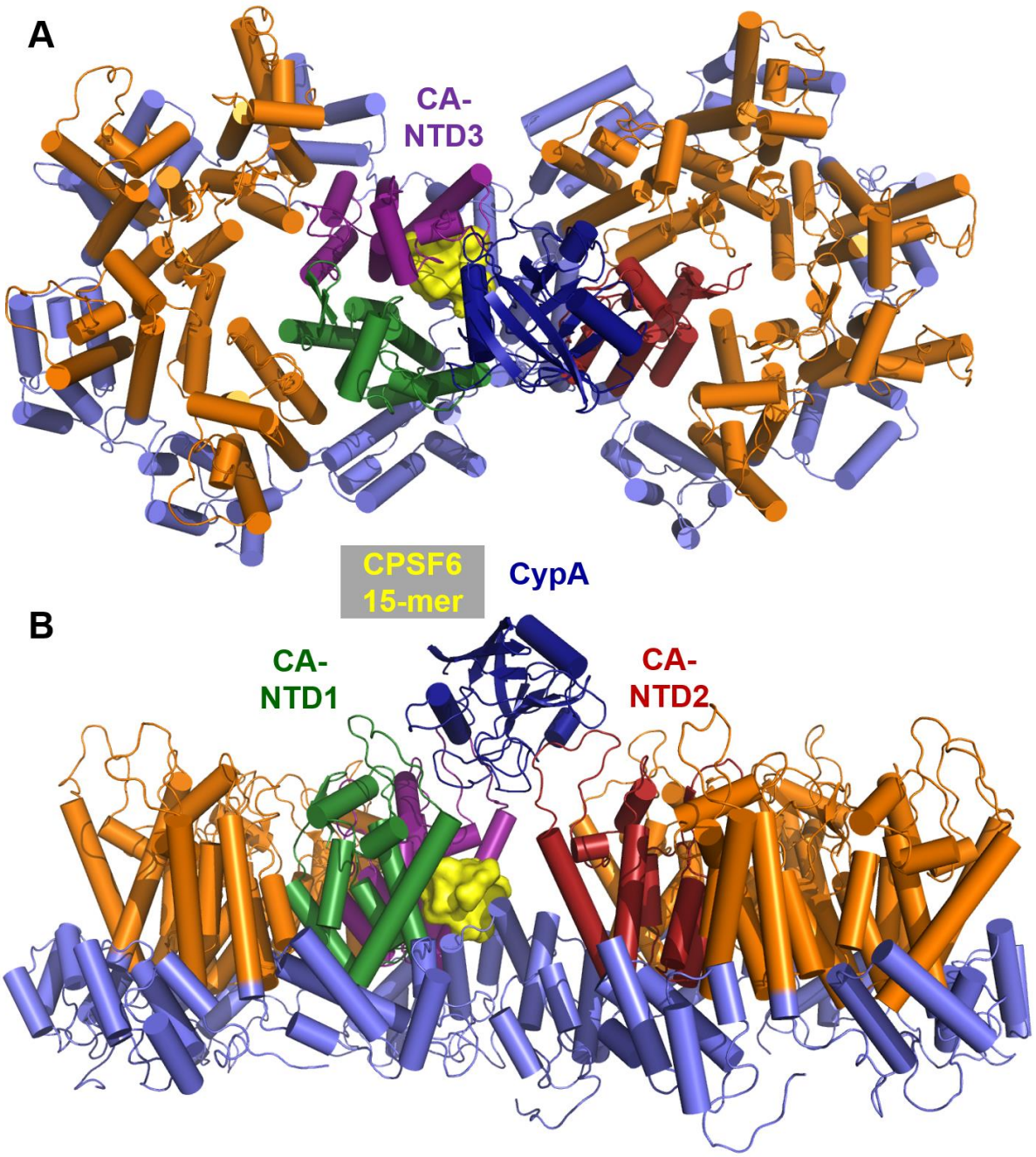

Figure 2.10 Structural modeling of CypA and CPSF6$_{313-327}$ onto the hexameric lattice. The context of CA-NTD:CypA (PDB: 1AK4; Gamble et al., 1996) aligned with CA-NTD2 (Appendix A), and CA-NTD:CPSF6$_{313-327}$ (PDB: 4B4N; Price et al., 2012) aligned with CA-NTD3 of the CA hexamer:hexamer dimer described in Figure 1.9 (PDB: 1VU5) predicts a CypA molecule flexibly attached to the CA-NTD2 CypA-loop that hypothetically extends over the CA-CTD:CA-CTD dimer bridging the CA interhexameric space. It may be reaching over to the adjacent CA-NTD1/3 wedge (please see Appendix A for a detailed discussion), which is also home to the surface pocket that CPSF6$_{313-327}$ binds to. Though the ways of regulation between these three molecules might be myriad, and the joint configuration described herein only hypothetical, the model nevertheless provides a spatial understanding of the quaternary interaction surface that determines the fate of PIC nuclear import. **(A)** Top view. **(B)** Side view.

Additional research efforts identified Coumermycin-A1 (C-A1; Vozzolo et al., 2010), a small molecule drug that was originally characterized to be a gyrase B inhibitor, blocked HIV-1 infection at the step of integration as assessed by 2-LTR circle formation. Interestingly, however, when replication competent HIV-1 virus was subjected to a viral evolution assay under C-A1 selection, the rescuant clone had acquired a single point mutation in HIV-1 CA, namely A105S, another residue lining the CPSF6-binding pocket. As was the case with N74D in our hands, the C-A1 resistant A105S was also proven to be insensitive to TNPO3 knockdown adding to the functional relationship between TNPO3 and CPSF6. The difference in the infection block; postnuclear in the case of C-A1 and at or before nuclear import in the case of CPSF6-358, is not well understood. We observed that TNPO3 dependence of HIV-1 is independent of cell cycle state (Figure 2.8) even though both N74D and A105S can override this dependence.

A third restriction targeting HIV-1 CA was induced by another small molecule drug, PF-3450074 (PF74; Blair et al., 2010). Mechanistic studies revealed that PF74 bound HIV-1 CA within the same surface pocket lined by helices 3 and 4 and that it acted by destabilizing the incoming viral capsid in the cytoplasm as revealed by fate-of-capsid assays (Shi et al., 2011), inducing premature and detrimental uncoating. A viral evolution assay under drug selection isolated a resistant clone, 5mut, with 5 missense mutations in CA, three of which (Q67H, K70R, T107N) are located near N74 and shared by the CPSF6 15mer as contact points as previously described (Price et al., 2012). Of the remaining two CA mutations (H87P, L111I) that were required to render the virus PF74 resistant, H87P had been previosly described to cause reduced CypA incorporation into progeny virions (Gatanaga et al., 2006). This observation was corroborated by the fact that CypA knockdown or CsA treatment rendered PF74 less potent,

implying that by reducing its affinity to CypA, 5mut may have gained partial resistance to PF74 (Shi et al., 2011).

The overlap between binding sites for PF74 and $CPSF6_{313-327}$ prompted us to look into whether PF74 might affect the CPSF6:CA interaction. We confirmed such an antagonistic relationship between PF74 and CPSF6/CPSF6-358 in HMW CA-NC binding assays (data not shown) *in vitro*. The fact that endogenous CPSF6 is nuclear and does not readily display an HIV-1 infectivity phenotype, and also that PF74 impairs HIV-1 infection by accelerated uncoating presumably in the cytosol, prevented us from making a conclusive interpretation that CPSF6 may be the natural target of PF74 in infected cells.

As seen in the hypothetical structural model in Figure 2.10, where both CA-interactors CPSF6-313-327 and CypA are depicted on an A92E CA hexamer:hexamer interface (Zhou et al., 2013), CypA may be extending over across the interhexameric space to CA-NTD1/3 of the adjacent CA-hexamer, potentially capping the surface pocket where CPSF6 is believed to bind CA (Price et al, 2012). A rather hypothetical structural configuration of one CypA molecule modeled onto a hexamer:hexamer dimer right above the interhexameric juncture thus displays further secondary interaction possibilities with both neighbouring CA-NTDs and a putative CPSF6 molecule binding the surface pocket generated by helices 3 and 4. Such intermolecular interactions at the surface of incoming RTC/PICs may explain how CypA can modulate core stability and how the quaternary capsid structure can coordinate different cellular nuclear import determinants. One should note that at the time of these studies no function was ascribed to endogenous CPSF6. If and where TNPO3 would fit into this superstructure is currently unknown.

E.ii. CA is a functional PIC component targeted by both TNPO3 and CPSF6-358

Compositional analyses of cytoplasmic and nuclear HIV-1 RTCs had revealed that on the way from plasma membrane to the nucleus, HIV-1 RTCs shed CA, which coincides with increased reverse transcription. However, (i) trace amounts of CA could still be detected in nuclear fractions (Miller et al., 1997), (ii) the detection limit for HIV-1 CA in early studies may have been limited (the intact viral capsid prior to uncoating is thought to be comprised of ~1056 p24 CA molecules; Pornillos et al., 2011; Zhou et al., 2013) (iii) imaging studies detected co-localization of p24 CA with *de novo* reverse transcripts pointing at a possibility that some CA may remain associated with HIV-1 RTCs (McDonald et al., 2002). Another group even observed intact HIV-1 capsid cores at the nuclear envelope upon infection (Arhel et al., 2007), and yet others reported evidence for nuclear presence of HIV-1 CA that is exported by means of TNPO3 activity (Zhou et al., 2011)

In this regard, the finding that CA plays a dominant role in nuclear import of the PIC, and that TNPO3, CPSF6 and CypA all converge on CA (at least functionally as revealed by CA mutant phenotypes) is critical. A biochemical basis to CPSF6:CA and CypA:CA interaction is evident, and our observation that N74D, a CPSF6-358 binding mutant, also affects CypA interactions in cells - either due to intrinsic changes in CA structure or impaired CPSF6 binding - both functionally and biochemically suggests a link between these two factors. N74D, and thus CPSF6-binding, may modulate CypA binding to the extent that a CypA-dependent restriction can be alleviated as observed in the case of G94D. An alternative explanation could be intrinsic changes in the viral capsid core that affect such a restriction.

Whether TNPO3 and its functional target CA are biochemically linked to each other, however, needs further elucidation. The observation that CA is a functional determinant of PIC

nuclear import and exerts this function possibly via its interactions with cellular cofactors, raises the possibility that it may be a structural component of the PIC even past the nuclear barrier; or it may simply modulate and 'imprint' the PIC in a way with the aid of cofactors along the path, which determine the downstream fate of the PIC.

The observation that integration site targeting is affected by TNPO3 KD and RanBP2 KD (Ocwieja et al., 2011), CsA treatment (Schaller et al., 2011), and also by CA mutations (Schaller et al., 2011) point to a critical role of CA in dictating postnuclear events, be it by its direct presence at or beyond NPCs, or by its ability to commit the HIV-1 PIC to differential nuclear import and targeting pathways via deterministic interactions that take place at the cytoplasmic side of the NPCs with downstream effects.

E.iii. Differences between TNPO3 and CPSF6-358 phenotypes

The observation that the infectivity defect upon TNPO3 KD and CPSF6-358 overexpression can both be bypassed by common CA mutants, yet respond differently to cell cyle arrest, point to a possibility that TNPO3 may also perform an additional function separate from the one that it may exert through CPSF6 and its direct interaction with CA. This function would be required for successful infection in cells regardless of their cell cycle state, bringing up the possibility that PIC nuclear 'import' may rather refer to PIC utilization of nuclear transport machinery which may involve physical transport or not through the NPCs. The fact that the virus can use alternative import pathways as shown by altered dependencies of WT versus CA mutant viruses on nuclear import factors (Lee et al., 2010) and by altered integration site targeting phenotypes, TNPO3 may simply be playing a licensing role, in that it commits HIV-1 PIC to one or the other delivery lines that is not only used in the postmitotic phase. Yet another explanation

is that pharmacologically induced cell-cyle arrest may result in additional mislocalized – spatially and/or temporarily – CPSF6-interacting HIV-1 dependency factors, that may be specifically getting sequestered by the ectopic overexpression of CPSF6-358 differentially compared to under conditions of TNPO3 knockdown.

CHAPTER 3

DIRECT INTERACTION OF TNPO3 WITH CPSF6 BUT NOT WITH HIV-1 CA DETERMINES THE REQUIREMENT FOR TNPO3 IN HIV-1 INFECTION

This chapter is in preparation for publication as:

Oztop I, Cook N, Lee K, Matreyek K, Ahn J, Cherepanov P, KewalRamani VN, Engelman A. Direct interaction with CPSF6 but not with HIV-1 CA determines the requirement for TNPO3 in HIV-1 infection (Work in progress)

Please refer to Appendix B for a detailed description of author contributions.

A. Abstract

HIV-1 infection is dependent on the β-karyopherin TNPO3, which is responsible for nuclear transport of SR proteins involved in mRNA splicing. Characterizing the infection block in cells depleted for TNPO3 has yielded disparate findings. Some groups have reported significant reductions in the formation of viral DNA 2-LTR circles, which is indicative of a block in the nuclear import of the PIC, whereas others found no effect on 2-LTR circle formation. CPSF6 is an SR protein that contains a C-terminal RS/RD/RE domain. We showed previously that expression of a C-terminal truncation mutant of CPSF6, CPSF6-358, which is missing the RS/RD/RE domain, restricted HIV-1 infection at the step of nuclear import without affecting the intrinsic activity of the PIC to integrate into a target plasmid DNA in vitro. We also showed that a single point mutation in CA, N74D, overcame CPSF6-358 restriction and TNPO3 dependency during HIV-1 infection, and diminished the binding of CPSF6-358 protein to recombinant CA-NC tubes that mimic the surface structure of intact viral cores. Although TNPO3 also binds CA-NC tubes, the N74D change does not alter this interaction. We expanded the size of our panel of HIV-1 CA mutant viruses in both infectivity and biochemical binding assays and correlated their sensitivity to CPSF6-358 restriction and dependence on TNPO3 with the ability of the respective CA-NC tubes to bind the two factors. The correlation between TNPO3 dependency and sensitivity to CPSF6-358 mediated restriction of several HIV-1 CA mutant viruses, the lack of correlation between TNPO3 dependency and TNPO3 binding to CA-NC as opposed to CPSF6-358 sensitivity and CA-NC binding within this panel, combined with the observation that the RS domain is missing from CPSF6-358 prompted us to test for a direct interaction between CPSF6 and TNPO3 to explain the functional link between these two factors and HIV-1 CA. We show specific binding between recombinant TNPO3 and the RS domain of

CPSF6 and also mapped this interaction to subdomains of CPSF6.RS. The interaction is downmodulated by RanQ69L-GTP, suggesting that CPSF6 is a *bona fide* import substrate of TNPO3. Our results are in accordance with a model where the functional link between TNPO3 and HIV-1 CA is based on the ability of TNPO3 to interact with and shuttle CPSF6, which can restrict HIV-1 infection by direct targeting of CA.

B. Introduction

B.i. The role of TNPO3 in HIV-1 infection

After the identification of TNPO3 as a positive factor for HIV-1 replication (Brass et al., 2008; Christ et al., 2008; Koenig et al., 2008), the field could not immediately resolve the issue at which stage TNPO3 acted in the HIV-1 replication cycle. One camp proposed a role in nuclear import of the PIC, as determined by quantitative imaging of fluorescently labeled PICs (Christ et al., 2008) and reduced 2-LTR levels upon TNPO3 knockdown (Schaller et al., 2011; Logue et al., 2011; De Iaco et al., 2013), whereas others assigned TNPO3 a postnuclear role, again primarily relying on 2-LTR data (Koenig et al., 2008; De Iaco et al., 2011; Cribier et al., 2011; Zhou et al,. 2011; Valle-Casuso et al., 2012), and also on vDNA distribution in fractionated cells (Zhou et al,. 2011). The discrepancy in 2-LTR quantification by independent research groups was most recently attributed to the selection of nonspecific qPCR primers unable to differentiate between *bona fide* 2-LTR circles and heterogenous autointegration products that may still bear 2 LTR sequences in close enough proximity to allow qPCR amplification (De Iaco et al., 2013). Careful modification of primers and sequencing-based characterization of qPCR amplicons resolved this confounding phenomenon and revealed a true reduction in 2-LTR formation upon TNPO3 knockdown, which strongly supported a role for TNPO3 in PIC nuclear import (De Iaco et al., 2013) even though the 2-LTR defect was not as strong as the infectivity defect under the conditions tested.

The identification of CA as the functional determinant of TNPO3 dependency of a retrovirus (Chapter 1; **D.i.2**, **D.ii.1**) prompted to investigate the biochemical basis for this functional link. One study could not detect a biochemical interaction between tubular assembles of HIV-1 CA and TNPO3 under conditions where CypA served as a positive control (Larue et

al., 2012); whereas an independent study reported binding to HIV-1 WT CA-NC HMW complexes under conditions where HIV-1 N74D CA-NC displayed a modest ~1.5-fold reduced binding compared to WT CA-NC. This was proposed as the biochemical basis for the relative TNPO3 independence of N74D HIV-1, albeit with the caveat that TNPO3 knockdown caused an 8-fold infectivity defect in the case of WT HIV-1 (Valle-Casuso et al., 2012). Such opposing observations led us to systematically assess a panel of CA mutants with varying dependencies on TNPO3 for their ability to bind TNPO3 in the context of CA-NC.

B.ii. Molecular details of the partial CPSF6:CA interface

The highly non-structured central proline-rich domain complicates quantitative purification and structural determination of the full length CPSF6. Previous efforts solved the atomic structure of CPSF6 N13-235 in a heterotetrameric complex with a truncated form of CPSF5 composed of one CPSF5 dimer and two CPSF6 monomers (Yang et al., 2011). Research on CPSF6-358, however, instead focused on a central stretch of amino acids spanning 314-322 aa, which was shown to be responsible for the restriction of HIV-1 as revealed by functional mapping upon deletion and alanine-scanning mutagenesis (Lee et al., 2012). Based on this finding, a co-crystal structure of CA-NTD and $CPSF6_{313-327}$ was solved, revealing critical contact points between the two molecules and the biochemical basis of interaction (Price et al., 2012). Specifically, N57, Q67, K70, N74, A105, T107 and S109 were critical for binding. These residues line the surface pocket on CA generated by helices 3 and 4, and as previously explained they face the interhexameric space described in Chapter 1; **D.ii.1** (Figure 1.9C).

At the time of our studies, evidence for a role in HIV-1 replication had been scarce for endogenous CPSF6. Exceptions to this were functional studies providing indirect evidence for a

possible coordination between CPSF6 and CypA as revealed by the ability of CPSF6-358-resistant CA mutations also rescuing a CypA-mediated restriction several CA mutants are subject to: CA N74D/G94D (Ambrose et al,. 2012); CA A92E/A105T and CA R132K/A105T (Qi et al., 2008), and CA T54A/A105T (Yang et al., 2007; Qi et al., 2008) are rescued from their respective CypA-sensitive, cell cycle-dependent phenotypes characteristic of CA G94D, A92E, R132K and T54A. Both N74D and A105T render HIV-1 CPSF6-358 resistant (De Iaco et al., 2013) and both residues are shown to mediate contact between $CPSF6_{313-327}$ and CA (Price et al., 2012). We had previously shown that N74D reduced binding to CPSF6-358 in Figure 2.7 (Lee et al., 2010). An opposite effect, namely a role for CypA in CPSF6-358 mediated restriction, however, has not been observed.

These findings are suggestive of endogenous CPSF6 having a potential role in the cell-cycle dependent restriction of some HIV-1 CA mutants. This prompted us to screen a panel of HIV-1 CA mutants for their sensitivity to CPSF6-358 and compare these results to their ability to bind CPSF6-358 and full length CPSF6. We also wanted to test whether these interactions were subject to modulation by CypA, as probed by CsA treatment.

B.iii. Nucleocytoplasmic localization of CPSF6 species affects their restriction phenotype

It was originally observed that the restrictive ability of ectopically expressed CPSF6 and CPSF6-358 species may correlate with their nucleocytoplasmic localization (Lee et al., 2010). Independent research efforts gathered further evidence to support this claim. It was shown that engineering a full length CPSF6 construct with an NES, which forced cytoplasmic localization upon this normally nuclear protein, conferred upon this construct the ability to restrict HIV-1

infection in a CA N74-dependent fashion (De Iaco et al., 2013). The same group also showed that redirecting the normally cytoplasmic CPSF6-358 into the nucleus by means of an SV40 NLS counteracted CPSF6-358 restriction.

B.iv. CPSF6, an SR protein, is potential cargo for TNPO3

The CPSF6.RS domain (spanning amino acids 526-588) is noncanonical in that it harbors RD/RE requences besides RS dipeptides that have been shown to require phosphorylation for recognition by TNPO3. RD/RE on the other hand, may already mimic such a phosphorylation event due to the negative charge carried by Asp and Glu carboxyl side chains.

The presence of a C-terminal RS-domain in nuclear CPSF6 and the lack thereof in cytoplasmic CPSF6-358 that restricts HIV-1 at the stage of nuclear import by targeting CA directly; the observation that depleting the SR-protein transporter TNPO3 impairs HIV-1 infectivity possibly at the stage of nuclear import in a CA-dependent fashion; and the overlap between CPSF6-358 resistance and TNPO3 independence of several CA mutants all together strongly imply a model where TNPO3 may simply be responsible for determining the cellular localization of the CPSF6 species. Such regulation may be disrupted upon inhibiting transporter:cargo recognition either through TNPO3 knockdown or removal of the RS-domain, as in the case of CPSF6-358.

Evidence for such a model is already present in the literature. It was shown that TNPO3 knockdown relocalizes endogenous CPSF6 from the nucleoplasm into the cytoplasm in transformed fibroblasts, albeit partially (De Iaco et al., 2013). Further support came from double knockdown studies where the infectivity defect incurred upon WT HIV-1 due to TNPO3 depletion could be rescued by depleting endogenous CPSF6 (De Iaco et al., 2013). This result is

also supportive of the model, where the infectivity defect WT HIV-1 encounters upon TNPO3 knockdown may be due to cytoplasmically relocalized CPSF6, whose depletion then relieves the CA-targeting restriction.

C. Materials and Methods

Cells, viruses and infections. HeLa, HEK293T and their derivative cell lines were cultured in DMEM supplemented with 10% FBS, 100 IU/ml penicillin and 100 μg/ml streptomycin. For infection experiments with the CypA active site inhibitor CsA, cells were treated with 4 μM CsA during the course of infection. For infectivity assays, HeLa and HEK293T cells stably transduced with empty lentiviral vector pLKO.1 or pLKO.1 expressing TNPO3-specific shRNA (GGCGCACAGAAATTATAGAA), and HeLa and HEK293T cells stably transduced with empty lentiviral vector pLKO.1 or pLKO.1 expressing CPSF6-358-HA, were additionally grown in 1 μg/ml puromycin. HEK293T cells were transfected with pCP-HA-TNPO3, pLKO.1-CPSF6-HA or pLKO.1-CPSF6-358-HA using Lipofectamine (Invitrogen), and cultured for 2 days prior to lysis to be used in HMW CA-NC binding assays.

Single round viral vector particles were generated by transfecting HEK293T cells in 10-cm plates with 6 μg pCMV cells in GagPol (HXB2; Parolin et al., 1996) packaging plasmid, 3 μg HIV-1 transfer vector pHI.Luc (Nakajima et al., 2001), 1 μg pRev, and 1 μg VSV-G expression vector pCG-VSV-G using Fugene 6 as previously described (Hofmann et al., 1999). Cells were washed 16 h after transfection, and supernatants collected twice, once at 24 h and once at 48 h posttransfection. Viral supernatants were clarified by centrifugation, filtered through 0.45 μm filters, and titered via ^{32}P RT assay.

Plasmid construction. HIV-1 CA mutants were generated by Quick Lightning (Stratagene) site directed mutagenesis (SDM) of the pCMVe agene) sGagPol (HXB2) packaging plasmid. Human TNPO3 sequence was subcloned between BglII and XhoI sites of pCPHA-NLS (Cherepanov et al., 2004), generating pCP-HA-TNPO3. The GST-CPSF6.RS$_{441-588}$ expression plasmid was obtained by subcloning a DNA fragment encoding residues 441-588 of human CPSF6 between BamHI and EcoRI sites of pGEX6P3 (GE Healthcare). GST-CPSF6.RS C-terminal truncations were generated by introducing in-frame stop codons after the coding sequence of CPSF6 residues 526, 540, 553 and 568 SDM of pGEX6P3-CPSF6.RS$_{441-588}$. GST-CPSF6.RS N-terminal truncations were generated by introducing internal deletions within pGEX6P3-CPSF6.RS$_{441-588}$ by SDM using internal deletion primers that omitted the coding sequences for CPSF6.RS$_{441-526}$, CPSF6.RS$_{441-553}$, and CPSF6.RS$_{441-568}$, respectively. pGEX6P3-CPSF6.RS$_{\Delta 541-553}$ and pGEX6P3-CPSF6.RS$_{\Delta 541-568}$ were generated similarly by SDM. pGEX6P3-CPSF6.RS$_{541-568}$ fusion construct was generated by subcloning a DNA fragment encoding residues 541-568 of human CPSF6 between BamHI and EcoRI sites of pGEX6P3. All constructs were confirmed by sequence verification.

The pET11a HIV-1 CA-NC expression vector was described previously (Ganser et al,. 1999). pET11a HIV-1 CA-NC CA mutants were generated by SDM. The sequence encoding full-length human TNPO3 was cloned into the pET-SUMO vector (Invitrogen) generating pET-His$_6$-SUMO-TNPO3. The coding sequence of RanQ69L was subcloned in between the XmaI and XhoI sites of pCPH6P (Cherepanov, 2007) to generate pCP-His$_6$-RanQ69L.

Recombinant baculovirus expressing His$_6$-CPSF6-358 was generated using the Bac-to-Bac system (Invitrogen) following the manufacturer's instructions. For construction of the transfer vector, the CPSF6-358 region was amplified by PCR using primers that introduced an

N-terminal His_6-epitope into the construct in between 5'-EcoRI and a 3'-BamHI sites. The His_6-CPSF6-358 amplicon was then cloned into the EcoRI and BamHI sites of the pFAST-BAC-DUAL vector according to the protocol of the manufacturer (Invitrogen), which also expresses RFP from its second promoter to aid with titering. After sequence confirmation, the pFAST-BAC-DUAL-His_6-CPSF6-358 vector was recombined into the bacmid by transformation of DH10 Bac cells (Invitrogen). Transformed bacterial colonies were grown by multiple antibiotic selection (50 mg/ml kanamycin, 7 mg/ml gentamicin, and 10 mg/ml tetracycline) and positive clones were identified by restriction digest and DNA sequencing.

Recombinant protein purification. Rosetta2 (DE3) pLacI cells (Novagen), transformed with pET-His_6-SUMO-TNPO3, were grown at 28 °C in Terrific Broth medium (Melford) supplemented with 50 µg/ml kanamycin and 0.4% glycerol. Expression was induced with IPTG (0.01% final concentration) for 5 h at 25 °C. Bacteria, re-suspended in core buffer (25 mM Tris-HCl [pH 7.4], 0.5 M NaCl) containing 1 mM PMSF and 1 mg/ml lysozyme, were disrupted by sonication. The lysates were pre-cleared by centrifugation at 13,000 rpm (SS-34 rotor) for 30 min at 4 °C. The supernatants were incubated with Ni-NTA agarose (Qiagen) in the presence of 20 mM imidazole. After extensive washing in core buffer containing 20 mM imidazole, the protein was eluted in core buffer with 200 mM imidazole. Following overnight incubation with SUMO protease to remove the His_6-SUMO tag, the protein was captured on a HiTrap Q Sepharose column (GE Healthcare). The protein, eluted with a linear 0.1-1 M NaCl gradient, was further purified by size exclusion chromatography (Superdex 200, GE Healthcare) in 150 mM NaCl, 25 mM Tris-HCl [pH 7.4]. TNPO3 containing fractions were pooled, supplemented with 10 mM DTT and 10% glycerol, concentrated to 3-8 mg/ml, snap frozen in liquid nitrogen and stored at -80 °C.

An overnight culture of PC2 cells (Cherepanov 2007) transformed with pGEX6P3-CPSF6.RS constructs was diluted 1:100 and grown to an A_{600} of 0.6 at 37 °C, followed by 1 mM IPTG induction for 4 h. Bacteria were harvested and lysed by sonication in buffer A (50 mM Tris-HCl [pH 7.4], 500 mM NaCl, 1 mM EDTA, 1 mM DTT). The lysate was treated with 25 U/ml Benzonase nuclease (EMD Biosciences) for 30 min on ice prior to centrifugation at 40,000 g for 30 min at 4 °C, and the supernatant was incubated with glutathione-Sepharose beads (GE Healthcare) for 2 h at 4 °C. The beads were washed extensively in buffer B (50 mM Tris-HCl [pH 7.4], 1 M NaCl, 1 mM EDTA, 1 mM DTT), resuspended in 50% bead slurry in the same buffer, and used in pulldown assays following total protein quantification by titration against BSA standard curves visualized by Coomassie R-250. Recombinant GST was purified as previously described (Cherepanov et al., 2004).

Recombinant WT and 9 mutant (E45A, K70R, N74D, G89V, P90A, A92E, G94D, A105T, and A105S) HIV-1 CA-NC proteins were expressed in PC2 cells (Cherepanov 2007) and purified as described previously (Ganser et al., 1999; Lee et al., 2010), concentrated to 20 mg/ml and snap frozen in liquid nitrogen and stored at -80 °C.

To make recombinant RanQ69L, PC2 cells were transformed with pCPH6P- RanQ69L and grown at 30 °C in LB medium supplemented with 120 µg/ml ampicillin to an A_{600} of 0.9-1.0, after which the temperature was shifted to 25 °C and protein expression was induced with 0.01% IPTG for 4 h. Bacterial pellets resuspended in ice-cold core buffer supplemented with 1 mM PMSF were disrupted by sonication, and the lysates were cleared by centrifugation at 27,000 g for 30 min at 4 °C. Supernatants were incubated with NiNTA resin in the presence of 20 mM imidazole; after extensive washing in core buffer containing 20 mM imidazole His_6-tagged proteins were eluted in core buffer supplemented with 200 mM imidazole. The proteins

were further purified by gel filtration over a HiLoad 16/60 Superdex 200 column in 150 mM NaCl, 25 mM Tris-HCl [pH 7.4] and supplemented with 5 mM DTT. To charge RanQ69L with GTP, purified proteins were incubated on ice for 30 min in the presence of 10 mM EDTA and 2 mM GTP, after which 25 mM $MgCl_2$ was added. RanQ69LGTP complexes were supplemented with 10% glycerol, frozen in liquid nitrogen and stored at -80 °C.

The bacmid expressing His6-CPSF6-358 was transfected into *Spodoptera frugiperda 9* (SF9) cells using Cellfectin II reagent (Invitrogen). Cells were incubated and passaged at 28 °C in SF-900 II serum-free insect cell medium (SFM-II, Invitrogen) for 3 days, and recombinant viruses were harvested (P1 viral stock). Following a viral plaque assay, as per the guidelines of the manufacturer (Invitrogen), three plaques (clones) were isolated and expanded by infecting SF21 cells. After culturing the cells for 3 days at 28 °C in SFM-II, the cells are lysed and subjected to Coomassie R-250 staining and His6-immunoblotting to determine the highest expressor, which was amplified further by another round of passaging. The P2 virus was subjected to another round of clonal selection via viral plaque assays to increase expression levels. The highest expressor was selected and amplified in SF21 cells (P3), and used for protein expression and purification. His6-CPSF6-358 was purified by Ni-NTA followed by size exclusion chromatography, concentrated up to 0.180 mg/ml, dialyzed against 25 mM Tris-HCl [pH 7.4], 150 mM NaCl, 2 mM DTT, 0.02% sodium azide (v/v%), 10% glycerol (v/v%), snap frozen in liquid nitrogen and stored at -80 °C.

In vitro assembly of *TNPO3-RanQ69L-GTP*. TNPO3-RanQ69LGTP complexes were assembled by mixing TNPO3 with His_6-RanQ69L-GTP at a 1:4 molar ratio and incubating the mixure for 1 h at 18 °C in binding buffer (BB: 150 mM NaCl, 25 mM Tris-HCl [pH 7.4]). The complex was then bound to a 1 ml HisTrap column (GE Healthcare) and eluted in 150 mM

NaCl, 200 mM imidazole, 25 mM Tris-HCl [pH 7.4]. The tag was removed by incubation with His_6-tagged human rhinovirus 3C protease. The protein was diluted 5-fold in BB and filtered through a HisTrap column. The protein was further purified by size exclusion chromatography on a HiLoad 16/60 Superdex 200 column operated in 150 mM NaCl, 25 mM Tris-HCl [pH 7.4].

In vitro assembly of HMW HIV-1 CA-NC complexes. HIV-1 CA-NC particles were assembled *in vitro* by diluting the CA-NC protein to a concentration of 10 mg/ml in 50 mM Tris-HCl (pH 8.0), 0.5 M NaCl and 2 mg/ml DNA oligo-$(TG)_{50}$. The mixture was incubated at 4 °C overnight and spun at 9000 g at for 5 min at 4 °C on a tabletop centrifuge. Pellets containing assembled CA-NC complexes were then resuspended in assembly buffer (50 mM Tris-HCl [pH 8.0], 0.5 M NaCl), diluted to an apparent concentration of 10 mg/ml based on OD_{280}, and used in binding assays.

HMW CA-NC binding assays. HEK293T cells transiently transfected with CPSF6-358-HA, CPSF6-HA, or HA-TNPO3 were lysed in hypotonic lysis buffer (10 mM Tris-HCl [pH 7.4], 1.5 mM MgCl2, 10 mM KCl, 1 mM DTT) by successive freeze/thaws (in liquid nitrogen / 37 °C water bath) and diluted to 1 mg/ml total protein concentration as determined by Bradford Assay (BioRad). The lysates were adjusted to contain 150 mM NaCl, and incubated with 5 µM WT or mutant CA-NC complexes for 30 min at room temperature before ultracentrifugation (1 h; 200,000 x g, 4 °C) through a 60% (HA-TNPO3, TNPO3) or 50% (CPSF6-358-HA, CPSF6-HA, His_6-CPSF6-358) sucrose cushion (Stremlau et al., 2006). Following removal of the supernatants, the pellets were resuspended 2 x SDS Loading Buffer (SLB). Input and pellet samples were subjected to HA immunoblotting (CPSF6-358-HA, CPSF6-HA, or HA-TNPO3), His_6 immunoblotting (His_6-CPSF6-358) or TNPO3 immunoblotting to detect binding proteins. Coomassie R-250 staining was performed to visualize CA-NC in the pellets. Band intensities

were quantified by gel densitometry using BioRad ChemieDoc and associated Image Lab ™ software.

GST pulldown assays. Semi-purified GST-CPSF6.RS constructs, along with GST control, were immobilized on glutathione sepharose beads. Protein concentrations were determined by comparing gradient dilutions of loaded glutathione-sepharose beads to BSA standard curves. Each binding reaction was set up to contain 1 µM bait protein. Settled beads (adjusted to 10 µl total) loaded with GST-CPSF6.RS constructs were incubated with 1 µM TNPO3 in a final volume of 100 µl buffer A (25 mM Tris-HCl [pH 7.4], 200 mM NaCl, 5 mM DTT, 0.1 mM EDTA, 0.5% CHAPS and protease inhibitors) containing 10 µg BSA. Following gentle rocking at 4 °C for 45 min the supernatant was removed from all samples and the beads were washed three times in 1 ml pulldown buffer (PDB; 25 mM Tris-HCl, [pH 7.4]), 200 mM NaCl, 5 mM DTT, 0.5% CHAPS). Bound proteins were eluted in 2 x SLB. Following SDS-PAGE, proteins in input and pulldown samples were visualized by Coomassie R-250 staining. Band intensities were quantified by gel densitometry using BioRad ChemieDoc and associated Image Lab ™ software.

D. Results

D.i. Correlation between TNPO3 dependence and CPSF6-358 sensitivity of a panel of HIV-1 CA mutants

We tested a panel of 9 HIV-1 CA mutants alongside WT HIV-1 for their dependence on TNPO3 and sensitivity to CPSF6-358 to assess how the two phenotypes might be related. Our panel consisted of the following CA mutants: G89V and P90A that render HIV-1 CypA-independent due to mutations in the CypA binding site (G89V, P90A; Braaten et al., 1996), mutants C-terminal to the CypA-loop that render the virus CsA-dependent in HeLa cells (A92E, G94D; Aberham et al., 1996), mutants in the CPSF6 binding pocket that alleviate CPSF6-358 sensitivity and presumably abrogate binding to $CPSF6_{313-327}$ (K70R, N74D, A105T; Price et al., 2012), a mutant that renders HIV-1 resistant to the integration inhibitor Coumermycin-A1 (A105S; Vozzolo et al., 2010), and another CsA-dependent mutant that lies outside of both the CypA binding loop and and the CPSF6 binding pocket that renders the capsid core hyperstable (E45A; Forshey et al., 2002). Infection assays were carried out in stably transduced HeLa and HEK293T cells, yielding similar data (Figure 3.1) (results in HEK293T cells not shown), both in presence and absence of CsA, to assess a potential role of CypA in utilizing TNPO3 and/or interacting with CPSF6.

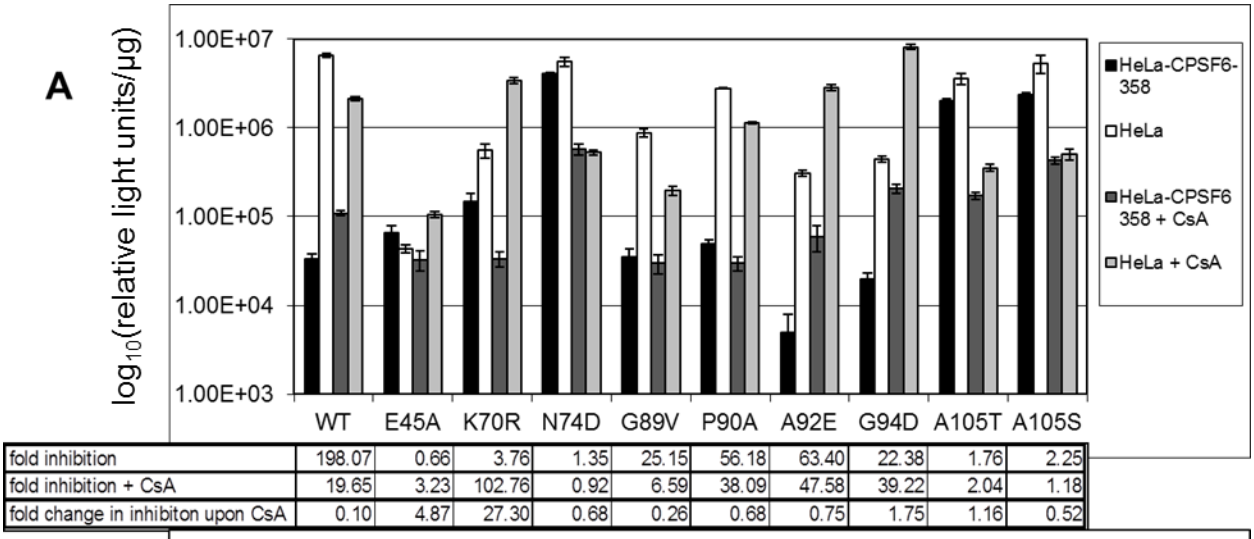

	WT	E45A	K70R	N74D	G89V	P90A	A92E	G94D	A105T	A105S
fold inhibition	198.07	0.66	3.76	1.35	25.15	56.18	63.40	22.38	1.76	2.25
fold inhibition + CsA	19.65	3.23	102.76	0.92	6.59	38.09	47.58	39.22	2.04	1.18
fold change in inhibiton upon CsA	0.10	4.87	27.30	0.68	0.26	0.68	0.75	1.75	1.16	0.52

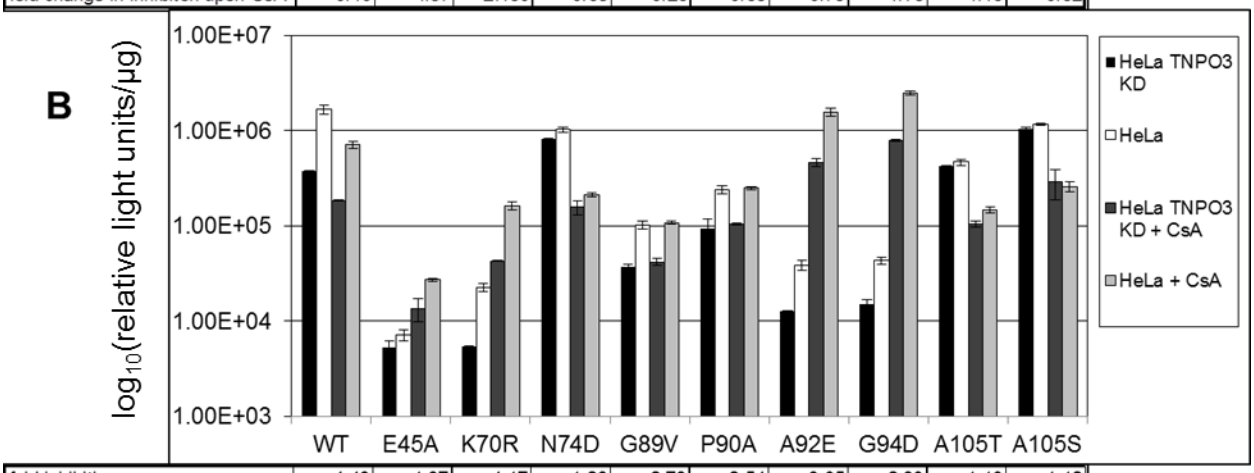

	WT	E45A	K70R	N74D	G89V	P90A	A92E	G94D	A105T	A105S
fold inhibition	4.43	1.37	4.17	1.26	2.76	2.54	3.05	2.90	1.10	1.12
fold inhibition + CsA	3.85	2.03	3.83	1.34	2.58	2.37	3.35	3.12	1.42	0.90
fold change in inhibiton upon CsA	0.87	1.48	0.92	1.07	0.94	0.93	1.10	1.08	1.29	0.80

Figure 3.1 Infectivity profiles of HIV-1 CA WT and 9 mutants upon CPSF6-358 restriction and TNPO3 KD. Stably transduced empty vector HeLa-CTRL vs HeLa-TNPO3 KD (upper panel) and stably transduced empty vector HeLa-CTRL vs HeLa-CPSF6-358 cells (lower panel) were infected with RT matched inocula of single round HIV-1 vectors expressing luciferase; either in presence or absence of 4 µM CsA. Bioluminescence readings were taken at 48 h post infection. Results of two independent experiments (mean ± standard error of the mean, SEM) are depicted as $\log_{10}$(relative light units/µg) per sample. Mean fold inhibition upon CPSF6-358 restriction / TNPO3 depletion in presence of DMSO control; mean fold inhibition upon CPSF6-358 restriction / TNPO3 depletion in presence of 4 µM CsA; and the ratio of each is tabulated below each graph. **(A)** HeLa CTRL DMSO (white); HeLa CPSF6-358 DMSO (black); HeLa CTRL 4 µM CsA (light grey); HeLa CPSF6-358 4 µM CsA (dark grey). **(B)** HeLa CTRL DMSO (white); HeLa TNPO3 KD DMSO (black); HeLa CTRL 4 µM CsA (light grey); HeLa TNPO3 KD 4 µM CsA (dark grey).

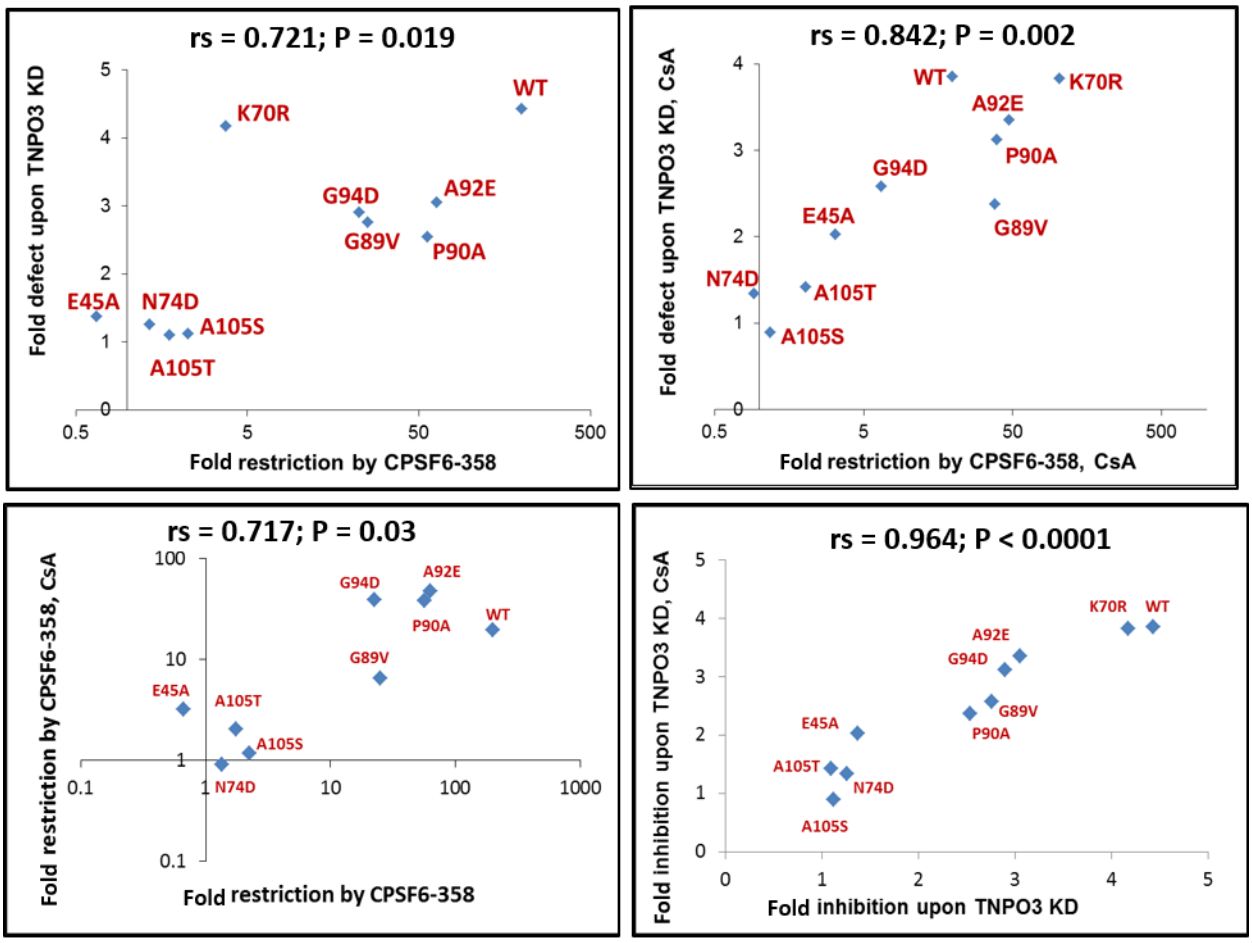

Figure 3.2 Correlation of TNPO3 dependence and CPSF6-358 sensitivity of a panel of HIV-1 CA mutants. Correlation between CPSF6-358 sensitivity and TNPO3 dependence in DMSO control (top left) and upon CsA treatment (top right). Correlation between CPSF6-358 sensitivity in DMSO control vs. CsA-treated cells (bottom left; K70R is omitted from the analysis). Correlation between TNPO3 dependence in DMSO control vs. CsA-treated cells (bottom right). Graphs are plotted and Spearman's rank correlation coefficients (rs) and the strength of significance (P) were calculated using Figure 3.1 data.

CPSF6-358 sensitivity and TNPO3 dependence correlated in DMSO-treated cells (Figure 3.2; top left; Spearman's rho coefficient, rs = 0.721, P<0.02), and in CsA-treated cells (Figure 3.2; top right; rs = 0.842, P<0.01). TNPO3 dependence of HIV-1 was completely independent of CsA-treatment and CypA modulation under these conditions (Figure 3.2; bottom right; rs = 0.964, P<0.0001). CPSF6-358 sensitivity in the absence and presence of CsA correlated less strongly, yet significantly (Figure 3.2; bottom left; rs = 0.717, P<0.05) when K70R was left out of calculation, which became significantly CPSF6-358 sensitive upon CsA treatment (Figure

3.1).

As seen in Figure 3.2, there is a strong correlation between TNPO3 dependence and CPSF6-358 sensitivity of the full set of CA mutants both under DMSO- and CsA-treated conditions. CPSF6-358 restriction itself is independent of CsA treatment for all mutants except for K70R, which seems to reverse its CPSF6-358 sensitivity phenotype under drug treatment. As can be seen in Figure 3.1, K70R displays a severe infectivity defect in the HeLa cell line tested (10-100 fold) when compared to WT HIV-1. It has been reported previously that K70R may display a CypA-modulated stability defect (Li et al., 2009), and such defects may render the incoming quaternary capsid surface in a way that may affect CPSF6-358 interactions in the cytosol. Additionally, further testing at equal MOIs rather than RT-matched conditions may be necessary to reveal the true phenotype of defective mutants such as E45A and K70R

WT HIV-1 lost sensitivity to CPSF6-358 upon CsA treatment (Figure 3.2; cf. top left vs. top right), but was still restricted strongly. Mutation of $CPSF6_{313-327}$ contact residues (K70R, N74D, A105T, and A105S) significantly conferred resistance to CPSF6-358 as did E45A, which lies outside of the CPSF6-CA interface, in the absence of CsA. These mutants also infected cells similarly regardless of TNPO3 depletion, except for HIV-1 CA K70R, whose dependence on TNPO3 was as strong as that of HIV-1 WT. All four CypA loop mutants displayed moderate CPSF6-358 sensitivity and TNPO3 dependence, albeit to a lesser extent compared to WT HIV-1.

D.ii. CPSF6-358 sensitivity of HIV-1 correlates with CA binding to CPSF6

D.ii.1. CPSF6-358 sensitivity of HIV-1 correlates with CA binding to CPSF6-HA

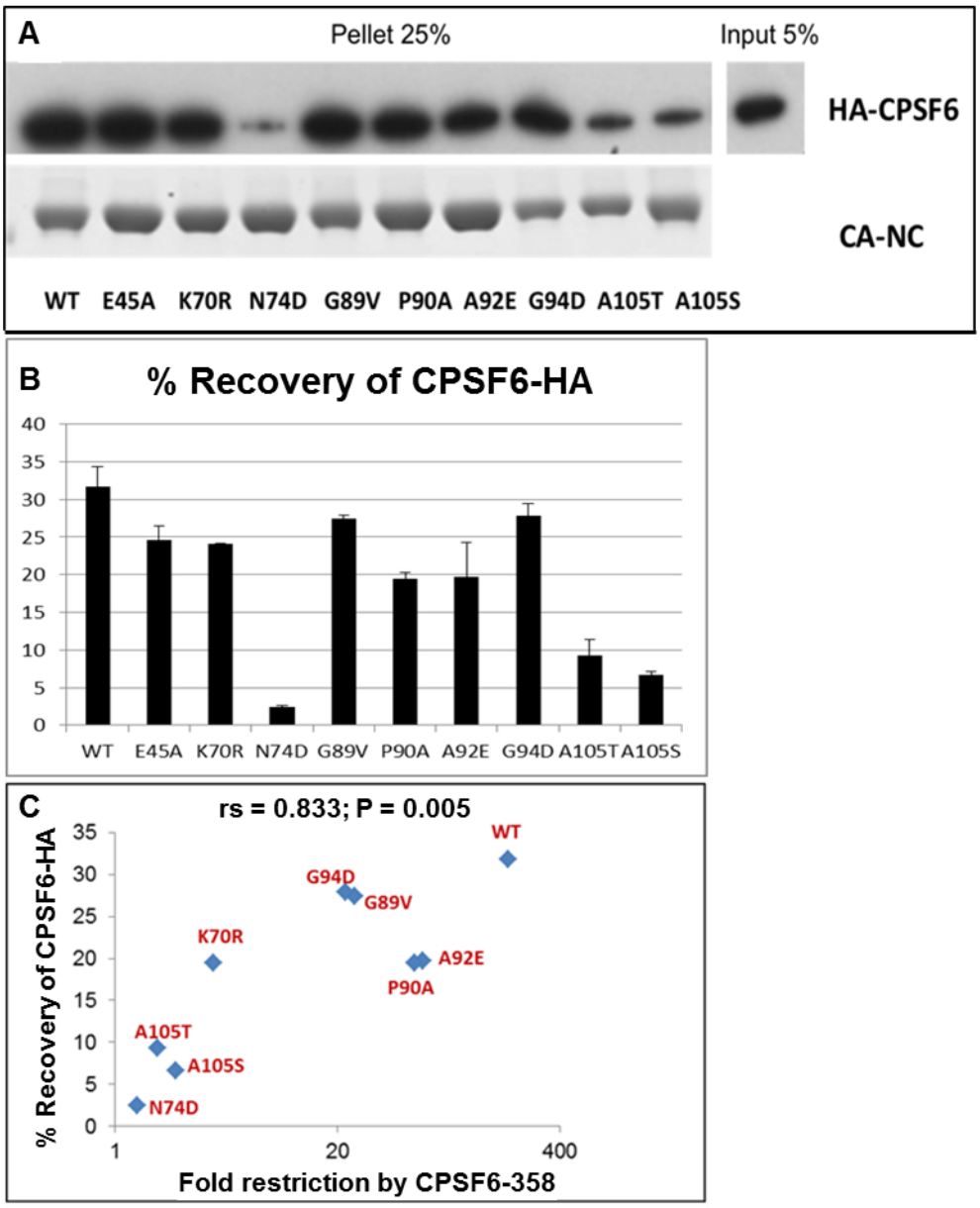

Figure 3.3 CPSF6-358 sensitivity of HIV-1 correlates with CA binding to CPSF6-HA. HMW CA-NC binding assays were carried out with the panel of HIV-1 CA mutants to test their ability to bind ectopically expressed CPSF6-HA in 293T cell extracts. **(A**) Top panel shows HA- immunoblot of CA-bound CPSF6-HA and Coomassie R-250 stain of CA-NC pellets. **(B)** Mean % recovery of CPSF6-HA (+/- SEM) from two independent experiments were graphed and **(C)** correlated with CPSF6-358 sensitivity (no CsA treatment) of each respective CA mutant vector from Figure 3.1. HIV-1 CA E45A was omitted from the calculations.

To gain insight into the determinants of CPSF6-358 sensitivity and TNPO3 dependency of HIV-1 CA mutants, we carried out HMW HIV-1 CA-NC tube binding assays that employ *in vitro* assembled HIV-1 CA lattices as a bait. The assay - as opposed to monomeric CA pulldowns - allows testing candidate cellular interactors as they would encounter the incoming quaternary capsid core in the cytosol.

We tested both ectopically overexpressed CPSF6 species (CPSF6-HA, Figure 3.3; CPSF6-358-HA, Figure 3.4) that were present abundantly in hypotonic cytoplasmic lysates (data not shown); and recombinant His_6-CPSF6-358, obtained via baculoviral expression in insect cells (Figure 3.5) in the absence of other cytoplasmic proteins.

The ability of HIV-1 CA mutants to bind ectopically expressed CPSF6 species correlated strongly and significantly with the CPSF6-358 sensitivity of each respective mutant - with the caveat that the dresults for HIV-1 CA E45A had to be omitted in our analysis to reveal such a correlation (CPSF6-HA:CA rs= 0.833, $P<0.01$, Figure 3.3C; CPSF6-358-HA:CA rs= 0.8, $P<0.01$, Figure 3.4C). E45A is fully resistant to CPSF6-358 restriction (Figure 3.1) yet retains the ability to bind CPSF6 species *in vitro*, unlike the CPSF6-358 resistant HIV-1 CA mutants N74D, A105T and A105S (Figures 3.3, 4). E45A is also a severely defective CA mutant when it s absolute infectivity is compared to WT HIV-1 (Figure 3.1). Such gross defects complicate a comparative analysis, especially E45A is known to be an intrinsic stability mutant (Forshey et al., 2002), which may stem from large scale conformational changes at the CA hexamer:hexamer interspace, where CPSF6 interactions also take place. Thus *in vitro* binding assays looking at CPSF6-358/CPSF6 interactions with E45A within the context of a CA-NC construct as tested in out studies may not reflect the quaternary surface structure that is exposed in an infected cell, which led us to omit E45A in our statistical analysis.

K70R, another CPSF6 resistant HIV-1 CA mutant, also retained the ability to bind both CPSF6 species *in vitro* under the experimental conditions tested. HIV-1 CA-NC binding profiles to CPSF6-HA and CPSF6-358-HA were strongly correlated ($r_s = 0.83$, $P<0.01$; data not shown), supporting the notion that the major determinant of the CA:CPSF6 interaction is shared between CPSF6 and CPSF6-358 (Price et al., 2012).

D.ii.2. CPSF6-358 sensitivity of HIV-1 correlates with CA binding to CPSF6-358-HA

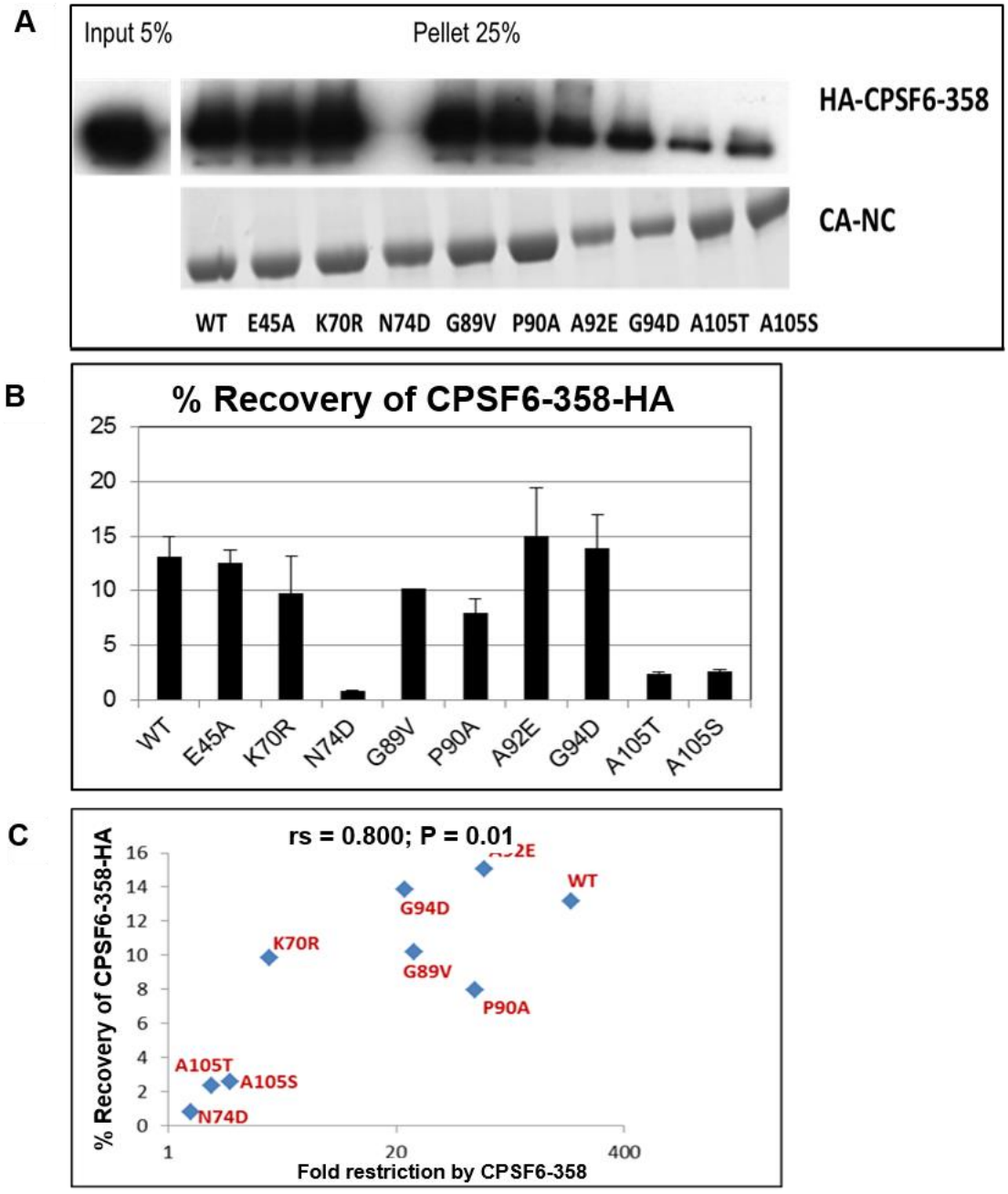

Figure 3.4 CPSF6-358 sensitivity of HIV-1 correlates with CA binding to CPSF6-358-HA. HMW CA-NC binding assays were carried out with the panel of HIV-1 CA mutants to test their ability to bind ectopically expressed CPSF6-358-HA in 293T cell extracts. **(A**) Top panel shows a representative HA-immunoblot of CA-bound CPSF6-358-HA and Coomassie R-250 stain of CA-NC pellets. **(B)** Mean % recovery of CPSF6-358-HA (+/- SEM) from two independent experiments were graphed and **(C)** correlated with CPSF6-358 sensitivity (in absence of CsA treatment) of each respective CA mutant vector from Figure 3.1. HIV-1 CA E45A was omitted from this analysis.

D.ii.3. CPSF6-358 sensitivity of HIV-1 correlates with CA binding to recombinant His_6-CPSF6-358

To assess whether the direct interaction between HIV-1 CA and CPSF6 (Price et al., 2012) and the binding phenotypes we observed in our assays could still be modulated by other cellular factors, we assessed binding between recombinant His_6-CPSF6-358 and HIV-1 assemblies (Figure 3.5).

Similar to the observations with cytoplasmic CPSF6-HA and CPSF6-358-HA, the CPSF6-358 sensitivities of HIV-1 CA mutant viruses mirrored their ability to bind recombinant His_6-CPSF6-358 protein; although this correlation was somewhat weaker, it yet still gained statistical significance ($r_s = 0.7$, $P<0.05$; cf. Figures 3.3, 4).

One immediate observation was that the CypA-sensitive, CsA-dependent HIV-1 CA mutants, A92E and G94D, displayed reduced affinity to His_6-CPSF6-358 when compared to when the protein was assayed as a cell lysate.

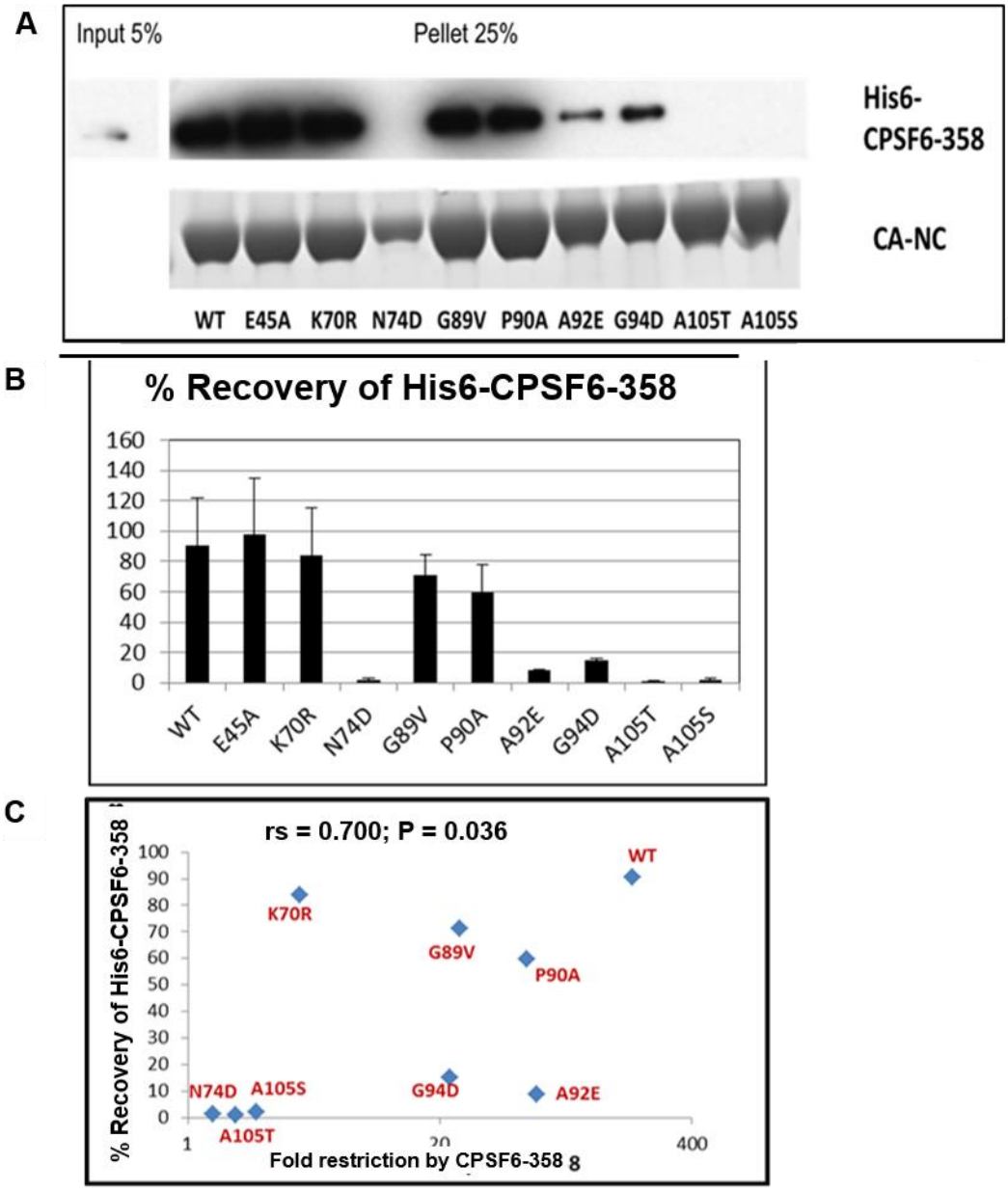

Figure 3.5 CPSF6-358 sensitivity of HIV-1 correlates with CA binding to recombinant His_6-CPSF6-358. HMW CA-NC binding assays were carried out with the panel of HIV-1 CA mutants (5 µM) to test their ability to bind recombinant His_6-CPSF6-358 (1 µM) in isotonic buffer. **(A)** Top panel shows a representative His_6- immunoblot of CA-bound His_6-CPSF6-358 and Coomassie R-250 stain of CA-NC pellets. **(B)** Mean % recovery of His_6-CPSF6-358 (+/- SEM) from two independent experiments were graphed and **(C)** correlated with CPSF6-358 sensitivity (in absence of CsA treatment) of each respective CA mutant vector from Figure 3.1. HIV-1 CA E45A was omitted from calculations.

D.iii. TNPO3 dependence of HIV-1 does not correlate with CA binding to TNPO3

Following our observations that TNPO3 dependence and CPSF6-358 sensitivity of HIV-1 CA mutants correlated and that CPSF6-358 sensitivity of HIV-1 CA mutants in turn strongly correlated with the ability of all but one mutant to bind CPSF6, we tested whether TNPO3 interacted with.

We detected binding between ectopically expressed HA-TNPO3 and HIV-1 CA WT (Figure 3.6A). This interaction, however, displayed no correlation with the dependence of the respective HIV-1 CA mutants on TNPO3 in infected cells (Figure 3.6C; rs= -0.4, P=0.286) Similar results were obtained in binding assays using recombinant TNPO3 in isotonic buffer (data not shown).

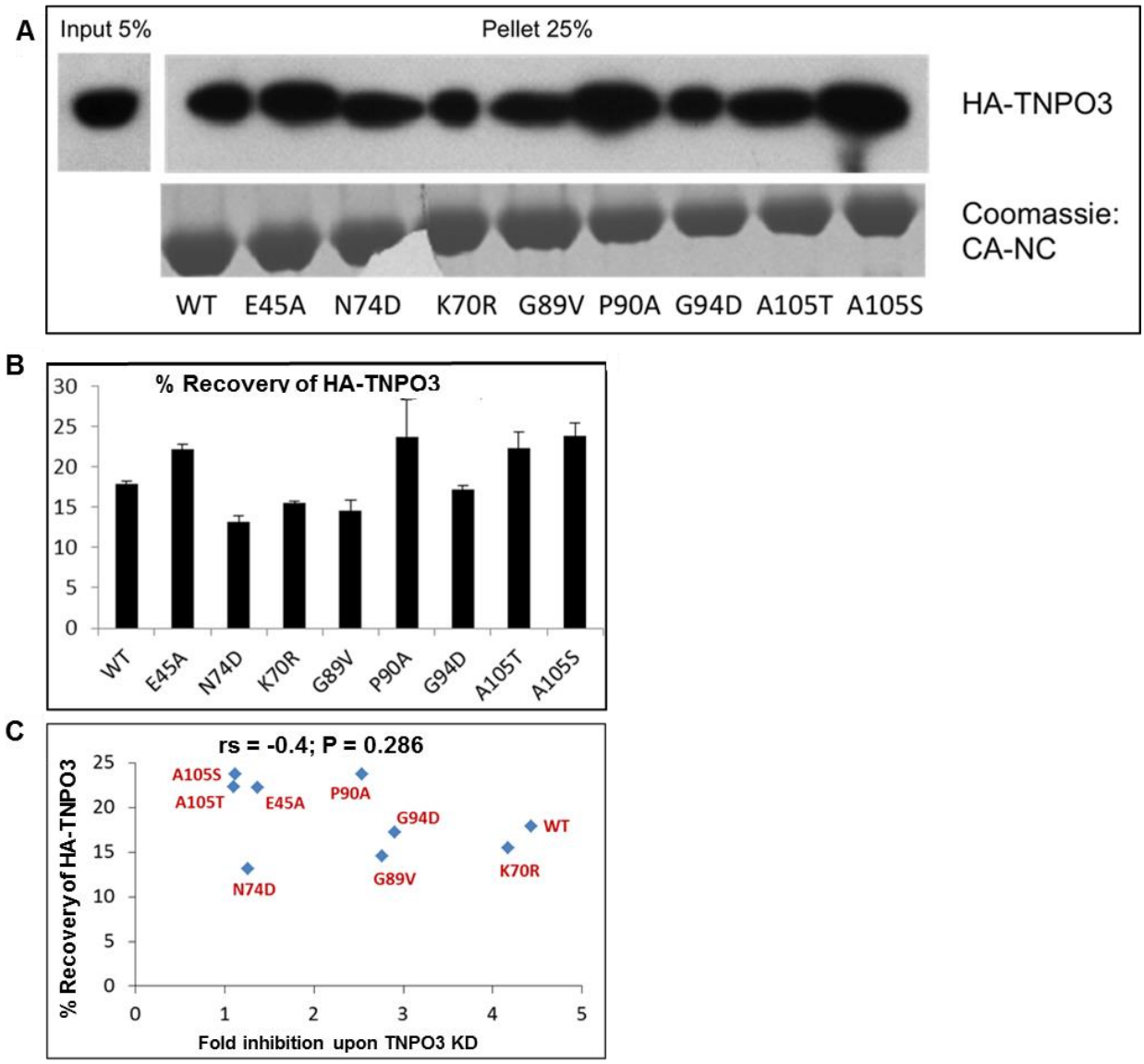

Figure 3.6 TNPO3 dependence of HIV-1 does not correlate with CA binding to HA-TNPO3. HMW CA-NC binding assays were carried out with the panel of HIV-1 CA mutants to test their ability to bind ectopically expressed HA-TNPO3 in 293T cell extracts. **(A**) Top panel shows a representative HA-immunoblot of CA-bound HA-TNPO3 and Coomassie R-250 stain of CA-NC pellets. **(B)** Mean % recovery of HA-TNPO3 (+/- SEM) from two independent experiments were graphed but **(C)** lacked a correlation with TNPO3 dependence (in absence of CsA treatment) of each respective CA mutant vector (data from Figure 3.1).

D.iv. CPSF6.RS is potential import cargo of TNPO3

D.iv.1. TNPO3 binds CPSF6.RS directly and specifically

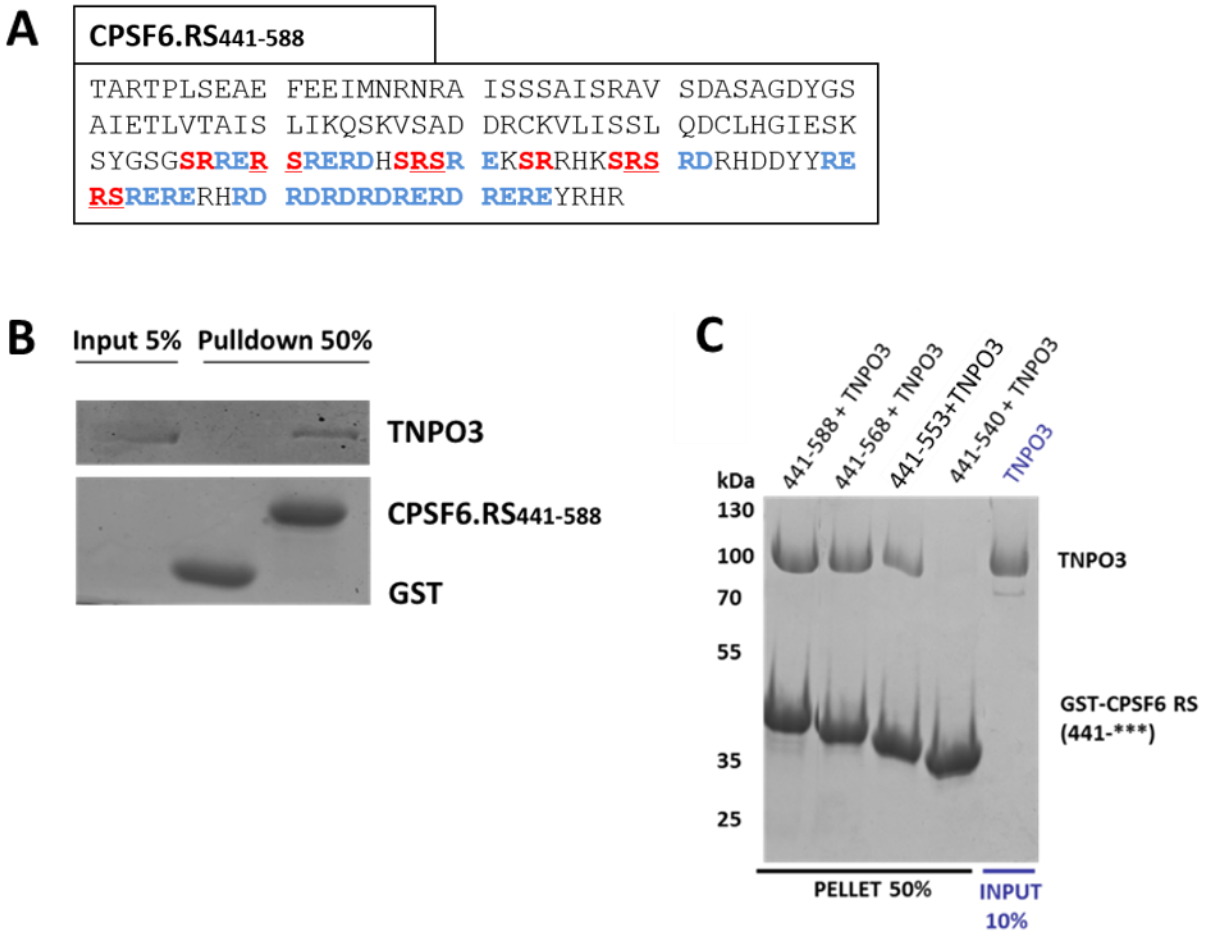

Figure 3.7 TNPO3 binds CPSF6.RS directly and specifically. **(A)** The primary sequence of the C-terminal RS-domain of CPSF6. Canonical RS repeats, and non-canonical RD/RE repeats are highlighted in red and blue respectively. **(B)** GST-CPSF6$_{441-588}$ can pull down recombinant TNPO3 out of solution. **(C)** Initial mapping studies with CPSF6.RS C-terminal truncations and recombinant TNPO3. Images are representative of two independent binding assays. In each case total protein staining is done with Coomassie R-250.

The lack of correlation between TNPO3 dependence of HIV-1 CA mutants and their ability to bind TNPO3 prompted us to test the hypothesis that TNPO3 may exert its function in HIV-1 replication indirectly through an interaction with CPSF6, which is predicted to be an import cargo for TNPO3 in cells (Maertens et al., 2014).

To assess whether there is direct binding between recombinant TNPO3 and CPSF6, as

expected from a transporter:cargo pair, we set out to test for binding between these two factors. Extensive efforts to express and purify full length CPSF6 in quantitative amounts conducive for biochemical analysis failed (bacterial expression, *in vitro* transcription and translation and baculoviral expression in insect cells; data not shown). We instead decided to work with a truncation construct, GST-CPSF6.RS$_{441-588}$, that harbors the putative TNPO3 recognition domain, the C-terminal SR-rich CPSF6.RS, spanning CPSF6 residues 526-588 as predicted from primary sequence analysis (Figure 3.7A). The GST fusion protein GST-CPSF6.RS$_{441-588}$ proved to be highly soluble and conducive to purification, thus this domain was used in pull down studies with recombinant TNPO3.

As seen in Figure 3.7B, GST-CPSF6.RS$_{441-588}$ pulled down recombinant TNPO3, whereas GST by itself did not, indicating the binding was specific to the CPSF6.RS$_{441-588}$ domain. To determine the subdomains of CPSF6.RS that mediate binding, we designed consecutive CPSF6 C-terminal truncation mutants and tested them in the pulldown assay side by side with GST-CPSF6.RS$_{441-588}$ (Figure 3.7.C, lane 1). Of the three CPSF6 truncation mutants that lacked the C-terminal 20 aa (GST-CPSF6.RS$_{441-568}$), 34 aa (GSTCPSF6.RS$_{441-554}$) or 48 aa (CPSF6.RS$_{441-540}$), (lanes 2-4); GST-CPSF6.RS$_{441-540}$ lost binding to TNPO3 completely, whereas GST-CPSF6.RS$_{441-554}$ displayed reduced binding and GST-CPSF6.RS$_{441-568}$ was unaffected. Thus one determinant of binding to TNPO3 was mapped to CPSF6 residues 540-554 aa, with residues spanning 554-568 aa playing a potential secondary role under these assay conditions.

D.iv.2. TNPO3:CPSF6.RS binding is mediated may be mediated by multiple points of contact

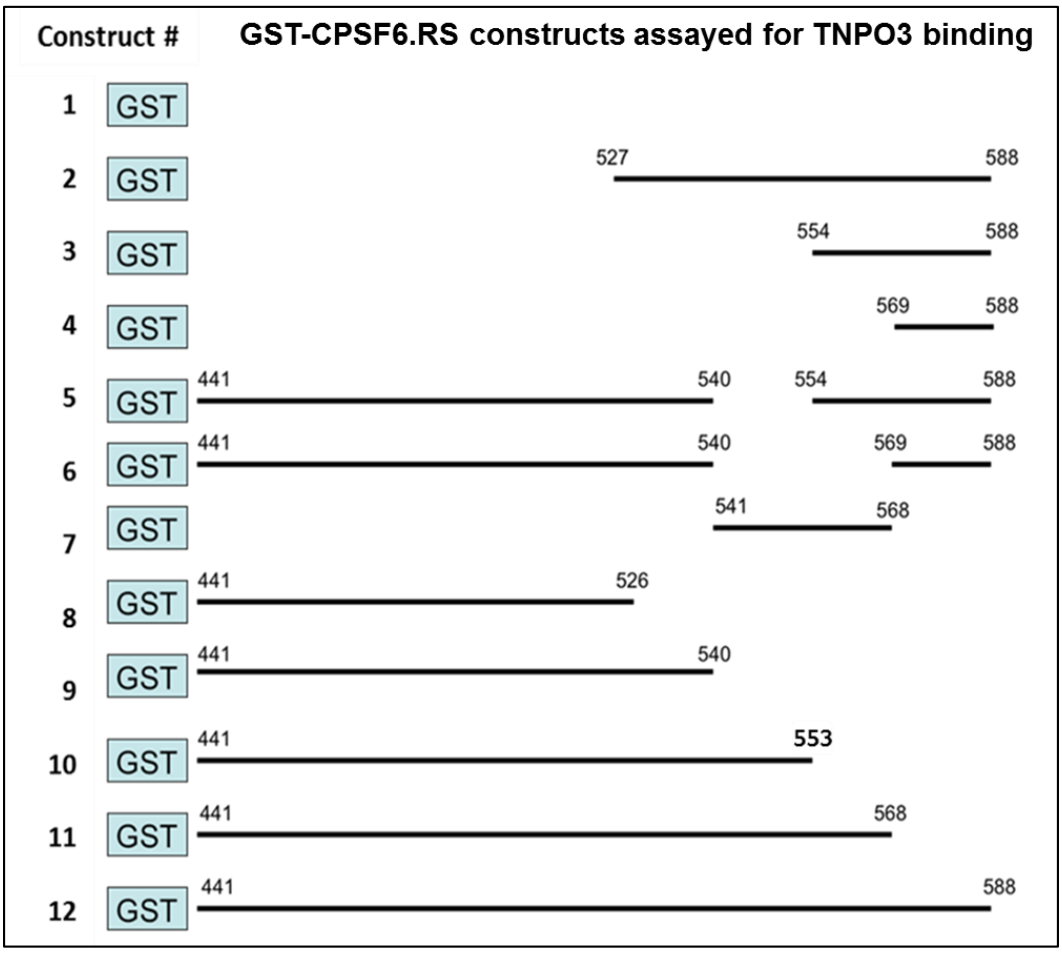

Figure 3.8 The extended CPSF6.RS mutagenesis scheme.

To fine-map the interaction between TNPO3 and GST-CPSF6.RS$_{441-588}$ we expanded our set of CPSF6.RS mutants (Figure 3.8) to include a larger C-terminal deletion (CPSF6.RS$_{441-526,}$ #8), internal RS domain deletions (Δ541-553, #5; Δ541-568, #6) and N-terminal deletions of CPSF6.RS (CPSF6.RS$_{527-588,}$ #2; CPSF6.RS$_{554-588,}$ #3; CPSF6.RS$_{569-588}$, #4), along with the internal 541-568 aa sequence fused to GST (CPSF6.RS$_{541-568}$, #7) that we had preliminarily identified to be critical for binding in Figure 3.7. The results are shown in Figure 3.9.

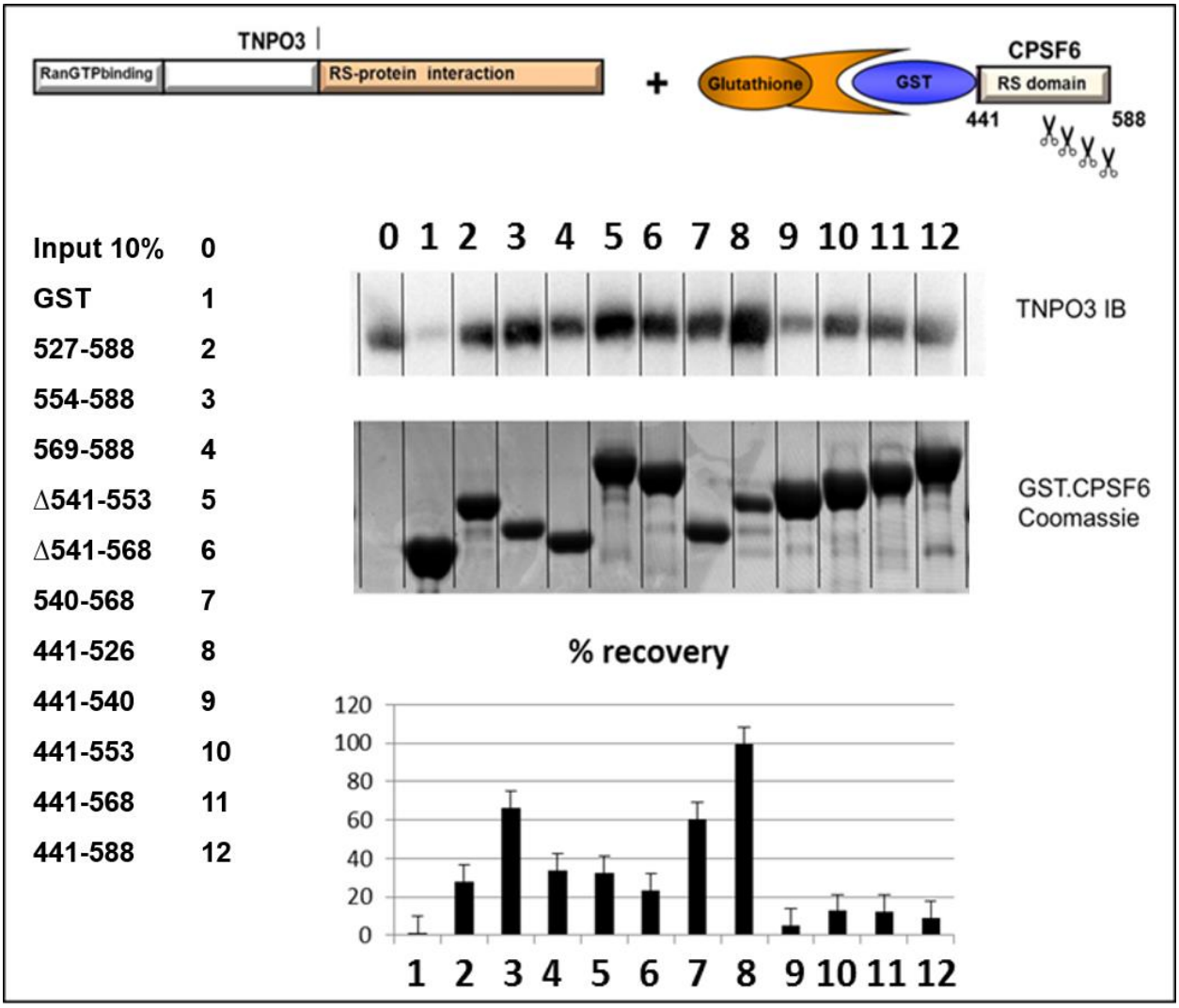

Figure 3.9 TNPO3:CPSF6.RS binding is mediated by multiple points of contact. GST.CPSF6.RS mutants were individually expressed and purified while immobilized on Glutathione sepharose beads. GST pulldowns are carried out following incubation with equal amounts of TNPO3. TNPO3 was visualized by immunoblotting (upper panel), whereas GST-CPSF6.RS proteins were stained with Coomassie R-250 (central panel). The amount of pulled down TNPO3 was normalized by the amount of GST.CPSF6.RS in each pulldown and graphed (lower panel). The images are representative of two independent experiments. The graph shows %recovery of TNPO3 (means +/- standard errors of the means) after normalization for the bead-immobilized GST-CPSF6.RS constructs in two independent experiments.

Surprisingly, all of the constructs tested recovered TNPO3 at least as much as GST-CPSF6.RS$_{441\text{-}588}$ (lane 12), except for GST-CPSF6.RS$_{441\text{-}540}$ (lane 9). Extending the C-terminal truncations down to CPSF6 residue 526 (constructs #8-12 in Figure 3.8 & 3.9) revealed that in absence of the 540-568 aa sequence, GST-CPSF6.RS$_{441\text{-}526}$ pulled down TNPO3 strongly,

recovering all of TNPO3 used as input. GST-CPSF6.RS$_{441-526}$ along with GST-CPSF6.RS$_{554-588}$ recovered the highest amounts of TNPO3, implying that both domains bear residues important for TNPO3 binding. The 8-10-fold increased recovery of TNPO3 by GST-CPSF6.RS$_{441-526}$ compared to CPSF6.RS$_{441-553,}$ CPSF6.RS$_{441-568,}$ and CPSF6.RS$_{441-588}$, together with the observation that CPSF6.RS$_{554-588}$ also efficiently pulled down TNPO3, implied that CPSF6.RS residues spanning 527-553 aa may have a negative affect on TNPO3 binding in the context of this partial CPSF6 construct.

The N-terminal truncation mutant CPSF6.RS$_{527-588}$ (construct #2 in Figure 3.8 & 3.9)l bound TNPO3. Larger N-terminal truncations that removed residues spanning 527-553 (construct #3 in Figure 3.8 and 3.9) and 527-568 (construct #4 in Figure 3.8 and 3.9) also scored positive for binding TNPO3 in this assay, contradicting our previous finding that residues spanning CPSF6.RS 540-568 aa constituted the major binding site to TNPO3 (Figure 3.7).

Internal deletions of 540-554 and 540-568 (constructs #5, 6 in Figure 3.8 and 3.9) still bound TNPO3, implying that the residues within these deletion constructs were not essential to bind TNPO3.

Overall, CPSF6 residues 441-526 and 554-588 conferred binding to TNPO3, whereas CPSF6 residues 540-553 conferred a negative effect under these assay conditions.

D.v. The TNPO3:CPSF6.RS interaction is modulated by RanQ69L-GTP

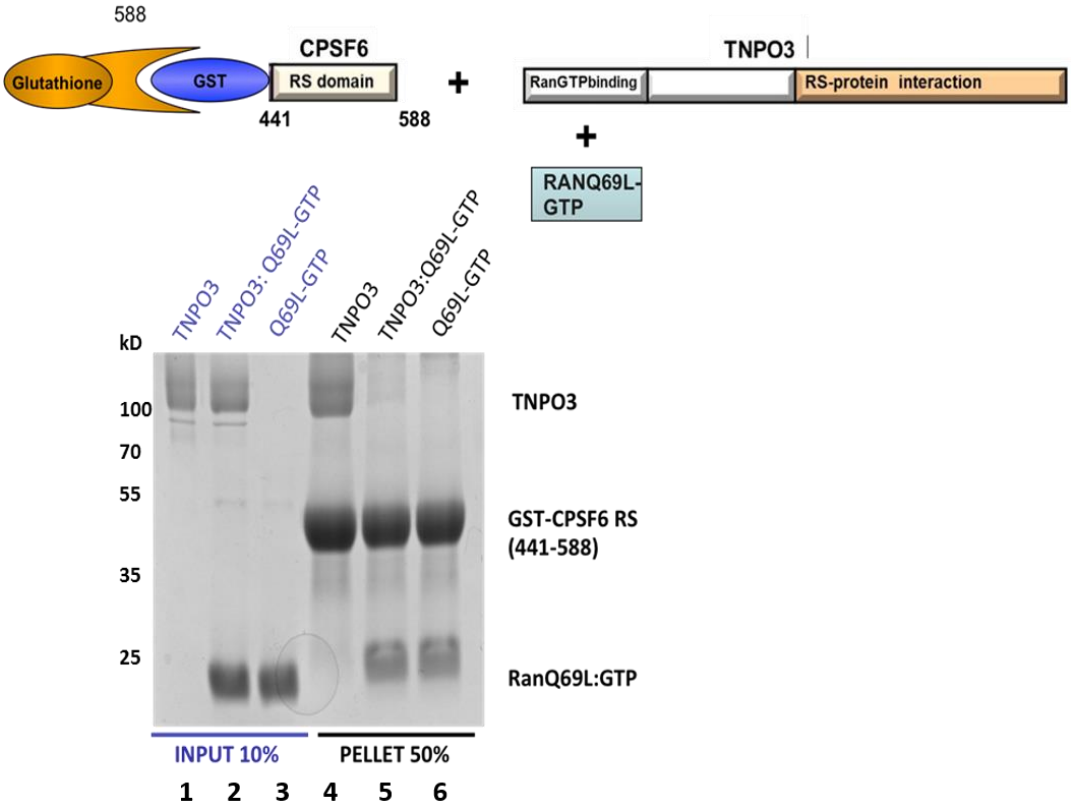

Figure 3.10 Coincubation with RanQ69LGTP impairs TNPO3:CPSF6.RS domain interaction. Image is representative of two independent binding assays. Total protein staining is done with Coomassie R-250.

High concentrations of intranuclear RanGTP disrupts transportin:import cargo complexes by binding to transportins competitively, which results in cargo release (Chapter 1, **D.i**; Figure 1.8). To assess whether the specific binding we observed *in vitro* between TNPO3 and GST-CPSF6.RS$_{441\text{-}588}$ (Figure 3.7) constituted a *bona fide* transport:import cargo interaction between TNPO3 and the CPSF6.RS domain, we tested whether pre-formed stable TNPO3:RanQ69L-GTP complexes would impair this binding. As seen in Figure 3.10, GST-CPSF6.RS$_{441\text{-}588}$ was either incubated with TNPO3 alone (lane 1), the pre-formed TNPO3:RanQ69L-GTP complex (lane 2) or RanQ69L-GTP (lane 3). TNPO3 pulldown by GST-CPSF6.RS$_{441\text{-}588}$ was completely inhibited upon coincubation with TNPO3:RanQ69L-GTP complexes compared to TNPO3 alone (cf. lanes 4 and 5), suggesting that RanQ69L-GTP inhibited the interaction.henning

E. Discussion

As shown in **D.i,** Figure 3.2; TNPO3 dependency of HIV-1 CA mutants correlated with sensitivity to CPSF6-358. Inhibiting the CA:CypA interaction pharmacologically with CsA flipped the CPSF6-358 sensitivity of HIV-1 CA K70R (i.e., from being resistant to sensitive). CPSF6-358 sensitivities of HIV-1 CA mutants correlated in both the absence and presence of CsA (Figure 3.2), implying that CypA modulation played little role in the CA:CPSF6 interaction under these conditions, except for K70R as mentioned above.

All CypA loop mutants, CA G89V, P90A, A92E and G94D, moderately reduced the TNPO3 dependency and CPSF6-sensitivity of HIV-1. HIV-1 CA E45A proved to be an outlier in our studies due to its ability to bind CPSF6 as well as CA WT *in vitro*, yet this virus was not restricted in infectivity assays. A potential explanation of this phenomenon can be that CPSF6-358 restriction relies on yet another factor in the cell and that E45A cannot interact with it. Alternatively, intrinsic changes in core stability (Forshey et al., 2002) may affect interactions with cellular factors, or due to differential blocks in its replication HIV-1 E45A may not encounter CPSF6 inside cells, presumably due to a differential uncoating kinetics that may preclude endogenous CPSF6 species from coming in contact with the quaternary CA hexamer:hexamer interface in a timely manner.

HIV-1 CA A92E and G94D displayed reduced binding to recombinant His_6-CPSF6-358, which could imply that binding to ectopically expressed CPSF6 species may be enhanced by the CypA-dependent restriction these mutants encounter in infected cells. In preliminary assays, we did not observe an effect of CsA on the binding of CPSF6 to WT or K70A CA-NC. Use of CA double mutants such as ones that combine CPSF6 and CypA-related phenotypes in binding

assays may enhance out understanding of whether there is functional interplay between CPSF6 and CypA.

Our mapping studies of the binding between TNPO3 and CPSF6.RS proved to be indeterminate (Figures 3.6-8). Confounding factors may have been the lack of full length CPSF6 used in binding assays and that GST-CPSF6.RS$_{441-588}$ may not have recapitulated the tertiary structure of the CPSF6.RS domain, either as part of CPSF6 itself, and/or as part of other cellular complexes CPSF6 may be found in (Yang et al., 2011). Anither plausible explanation may be the lack of phosphorylation of our binding construct, which is required for most cargo proteins such as ASF/SF2 to bind TNPO3 (Lai et a., 2000; Lai et al., 2001; Maertens et al., 2014). Indeed, it has been reported that phosphorylation enhances the solubility of ASF/SF2 RRM2-RS and CPSF6.RS domains (Maertens et al., 2014). Accordingly, the lack of phosphorylation may have resulted in nonspecific binding between TNPO3 and partially insoluble CPSF6.RS under our experimental conditions. An alternative explanation could be that partial deletions and truncations may be disrupting the tertiary protein structure within the CPSF6.RS domain to different extents, confounding our analysis. Our results could, however, also imply that TNPO3 binding may be modulated negatively and positively by multiple points of contact on CPSF6.RS, rather than by a defined set of amino acids within a specific subdomain. Such multi-contact TNPO3:cargo binding has precedence in the literature. For example, the co-crystal structure of TNPO3:ASF/SF2 RRM2-RS domain revealed multiple residues both in the RS and RRM domains that play important roles in TNPO3 binding (Maertens et al., 2014).

E.i. A potential role of TNPO3 in HIV-1 infection that is mediated by CPSF6

The finding that the HIV-1 infectivity defect upon TNPO3 depletion can largely be alleviated by simultaneous knockdown of endogenous cytoplasmic CPSF6 (De Iaco., 2013; Fricke et al., 2013) is strong evidence that the role TNPO3 plays in the HIV-1 life cycle is mediated through cytoplasmic CPSF6; an intermediary factor that directly targets HIV-1 CA. The correlation between binding profiles of HIV-1 CA mutants with CPSF6/CPSF6-358 and their respective sensitivities to CPSF6-358 (**D.ii**), but the lack thereof with TNPO3 and their respective dependencies on TNPO3 (**D.iii**) are supportive of a model where CPSF6 is the biochemical link that ties TNPO3 functionally to HIV-1 CA. The observation that TNPO3-insensitive CA mutants (e.g. N74D, A105S, A105T) are actual CPSF6-binding mutants (Figures 3.3-5) gives credence to this hypothesis. In this regard it seems that the binding we detected between TNPO3 and HIV-1 CA-NC is nonspecific.

According to this model (Figure 3.11) TNPO3 and CPSF6 are *bona fide* transporter : nuclear import cargo partners, where TNPO3 exerts a positive effect on incoming HIV-1 virions by ensuring nuclear sequesteration of endogenous CPSF6. Cytosolic accumulation of CPSF6, be it either due to TNPO3 depletion of recognition RS domain removal, will then pose a restrictive phenotype at the stage of HIV-1 PIC nuclear import. Thus, the positive role of TNPO3 in HIV-1 infection stems from its ability to sequester an otherwise nuclear HIV-1 capsid interactor that can become detrimental to HIV-1 infection upon untimely mislocalization to the cytosol. Our current understanding of TNPO3 strongly favors such a model, with the caveat that (i) there are CA mutants such as K70R that are resistant to CPSF6-358 yet depend on TNPO3; and (ii) the cell cycle dependencies of TNPO3 and CPSF6-358 phenotypes are disparate (Chapter 2; **D.iii**).

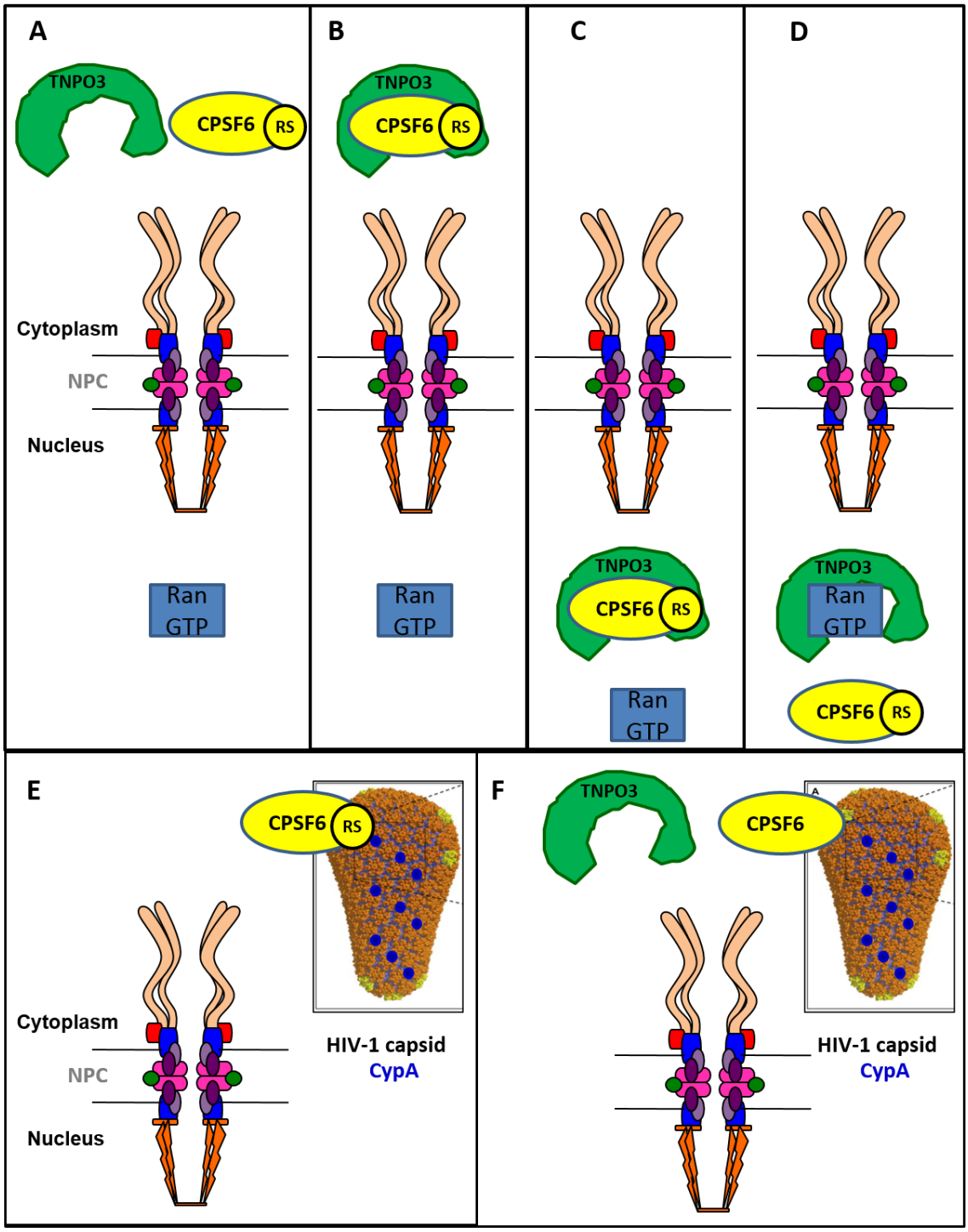

Figure 3.11. The model depicting the role of TNPO3 in HIV-1 infection. TNPO3 recognizes **(A)** and binds CPSF6 via its RS domain in the cytosol **(B)**, ferries it through the NPCs into the nucleus **(C)**, where upon competitive RanGTP binding CPSF6 is then released into the nucleoplasm **(D)**. CPSF6 cannot be shuttled into the nucleus when TNPO3 is depleted, and instead binds and restricts the incoming HIV-1 capsid in the cytosol **(E).** Truncation of the C-terminal RS domain prevents TNPO3 recognition and nuclear transport of CPSF6-358, which then instead binds and restricts the incoming HIV-1 capsid in the cytosol.

E.ii. Is there a tertiary complex between TNPO3, CPSF6, CypA and CA?

The *in vitro* evidence that CPSF6.RS is a specific binding partner of TNPO3 and that this binding is abrogated upon TNPO3:RanQ69L-GTP complex formation suggests that CPSF6 is a *bona fide* import cargo for TNPO3. As described in Chapter 1; **D.i**, the β-karyopherin TNPO3 is supposed to bind its import cargo, CPSF6, in the cytoplasm, ferry it across the NPC and once at the nuclear side of NPCs release it upon competitive RanGTP binding. Thus, even if it may be transitory mid-shuttling, a TNPO3:CPSF6 complex is expected to form on the cytosolic side of an NPC, where CPSF6 species can bind incoming HIV-1 capsids. It is currently not known, however, whether binding to CA (mediated by CPSF6 residues 314-322 aa) and binding to TNPO3 (mediated by the RS domain) can affect each other within the context of full length endogenous CPSF6. If both are specific *in vivo*, the two binding events may be mutually exclusive due to steric hindrance, cooperative, or independent. Unfortunately, the lack of access to quantitative amounts of recombinant CPSF6 species harboring both domains hindered our studies in this regard.

Cooperative binding, for example, could explain the observation that ectopically expressed TNPO3 bound CA-NC complexes non-specifically (Figure 3.6), if it were mediated by residual amounts of CPSF6 present in cell lysates. Our finding that recombinant TNPO3 also displayed similar nonspecificity when it comes to binding CA-NC in absence of cell lysate (results not shown), however, allows the alternative interpretation that the observed binding may be non-specific in nature and an artifact of the *in vitro* binding system, or that direct TNPO3 binding may be mediated by an as yet to be described domain on HIV-1 CA. The strong genetic evidence obtained with present CA mutants that render HIV-1 TNPO3-independent and cluster around the CPSF6-binding pocket, suggest otherwise, however.

At first sight, the tertiary model presented in Chapter 2; **E.i** (Figure 2.10) is suggestive of possible intermolecular interactions between CPSF6 and CypA and that their simultaneous binding to the capsid surface would require some coordination. The lack of conclusive evidence for such a link in our functional and biochemical assays, however, needs to be weighed carefully. *In vitro* binding assays employ a rather high concentration of HIV-1 CA-NC complexes, potentially making it impossible to observe effects on e.g. cooperativity, due to the saturating levels of CA binding sites present. This may in turn prevent occupation of all CPSF6- and CypA binding sites, diminishing the probability of joint binding events. Similarly, *in vivo*, not all CA hexamer:hexamer interfaces may be occupied by cytoplasmic binding factors, precluding cooperation or any other functional link. Observing such interaction may require all interactors involved in recombinant form to allow quantitative saturation of all binding sites.

Under our experimental conditions, we have not been able to observe an effect of CsA on CPSF6-binding to WT CA, implying that liberation of CypA-loops from endogenous levels of CypA in a cell extract does not affect ectopically expressed CPSF6 binding to CA (data not shown; also addressed in Henning et al., 2014). This was also the case for the CA K70R mutant (results not shown), which in infectivity assays revealed a functional role of CypA, since CsA treatment / altered CypA binding modulated the infectivity of this particular virus (Figure 3.1). An alternative approach could be to saturate CypA-loops with excess recombinant CypA. However, (i) we have not been able to detect recombinant CypA binding to HMW CA-NC complexes efficiently (results not shown), and (ii) saturating CA tubes with recombinant CypA has been known to destabilize and induce their disassembly (Graettinger et al., 1999), which may thus require the use of CA A14C/E45C disulfide cross-linked stable CA tubes instead (Pornillos

et al., 2009). Similarly, quantitative production of recombinant CPSF6 species bearing the CA interaction domain should enable reverse competition assays.

CHAPTER 4

GENERAL DISCUSSION

A. The convergence of CPSF6 and CypA on the CA hexamer:hexamer interface

Since the atomic structures of CA-NTD (Gitti et al., 1996) and the CA-NTD:CypA (Gamble et al., 1996) complex were solved, investigators working on HIV-1 CA and its role in HIV-1 replication have used this monomeric structure as a reference base to map amino acid residues with aberrant biological phenotypes onto it. Even after the atomic structural of the CA hexameric unit was solved (Pornillos et al., 2009), functional and biochemical CA mutations were highlighted on a CA-NTD monomer or on a single CA-hexamer to aid with interpretations about how their structural context may tie in to their observed biology.

However, since CA was identified as the main structural component of the viral core in ultrastructural and immunoelectron microscopic studies of HIV-1 (Gelderblom et al., 1987), it has been known that the capsid core forms a conical topology within a virion, which was later revealed to be constructed by CA hexamer and pentamer interactions (Jin et al., 1999; Ganser et al., 1999). Accumulating structural data on full length CA (Ganser-Pornillos et al., 2007) and its oligomers (Pornillos et al., 2009; Pornillos et al., 2011) finally allowed full conical modeling of the capsid core (Figure 1.5; Pornillos et al., 2011), which was confirmed in atomic detail most recently (Zhao et al., 2013).

The identification of cellular factors such as CypA, TNPO3, CPSF6, Nup358 and Nup153 that enable CA-mediated functions emphasizes the need to understand their interaction interface with capsid, which presents a multimeric and multifaceted lattice to the cytosol. On the capsid, CA hexamers and biologically important CA residues are found within the context of other CA hexamers and their surface exposed residues. This requires a superstructural understanding of their relative positions on capsid (Figure 1.9), and a superstructural projection of CA interactors (Figure 2.10); something the field had largely omitted so far.

We and others have shown, for example, that CPSF6 binds CA within a surface pocket defined by CA-NTD helices 3 and 4 (Lee et al., 2010; Price et al., 2012). It is only revealed within the context of a CA hexamer:hexamer interface, however, that the minimal CA binding portion, $CPSF6_{313-327}$, finds itself within this interhexameric space, access to which may require coordination with CypA and neighboring CA molecules (Figure 2.10). Such a hypothetical coordination may explain our observation that the CPSF6 binding mutant N74D increases CsA-sensitivity of HIV-1, as well, and that this may be a result of a decreased binding affinity to CypA (Figure 2.9; Ambrose et al 2012). This model will be discussed in further detail under section **E** of this chapter.

B. A multiplicity of nuclear import/preintegration targeting pathways and their potential roles of TNPO3, CPSF6 and CypA in pathway commitment

TNPO3, Nup358 (Ocwieja et al., 2011) and Nup153 (Koh et al., 2013) have been shown to reduce HIV-1 integration frequency in regions dense with transcriptional units (TUs). CA mutants N74D and N57A, which are CPSF6 and Nup153 binding mutants, respectively, also display reduced dependence on the aforementioned nuclear transport proteins, integrate not only in regions of low TUs but also of low gene density, showing some difference from the targeting phenotype under knockdown conditions listed above (Schaller et al., 2011). CypA binding mutants (G89V, P90A) or CsA treatment of WT virus results in yet another different targeting phenotype, namely into regions with higher than normal gene density and with higher transcriptional activity (Schaller et al., 2011). Intriguingly, CsA treatment does not affect the targeting phenotype of N74D and N57A, in line with a model that these mutations lead to a different import/integration pathway than of WT HIV-1. Indeed, compared to WT HIV-1, N74D

employs a different set of NPC components (Lee et al., 2010).

The N74D mutation confers resistance to CPSF6-358, reduces dependency on TNPO3, Nup358 and Nup153, all of which have been shown to interact with HIV-1 CA (Figure 2.7; Lee et al., 2010; Price et al., 2012; Figure 3.6; Valle-Casuso et al., 2011; Schaller et al., 2011; Matreyek et al., 2013) (our results in Figure 3.6, however, argue for such binding to be nonspecific in the case of TNPO3). Biochemically, however, N74D has only been proven to have a direct negative effect on CPSF6 binding to CA, whereas the functional independence from Nup153 of this mutation did not manifest itself in the form of altered Nup153 binding to CA (Matreyek et al., 2013) or TNPO3 (Figure 3.6). Similar to $CPSF6_{313-327}$ (Price et al., 2012), however, Nup153-CTD also binds the same CA surface pocket – and can compete with CPSF6 binding - suggestive of a need to coordinate their interaction with the CA lattice on an incoming PIC. It is possible that the PIC may be handed over from one factor to another; overlapping binding sites, and cytoplasmic localization and local concentrations of each factor may ensure directionality of transport and temporal regulation. Alternatively, both factors may be able to bind an incoming capsid core at the same time, either intact or partially uncoated, in different pockets available on the quaternary CA hexamer lattice.

Similar coordination may exist between soluble CypA in the cytosol and the NPC component Nup358 that has a CTD homologous to CypA (Wu et al., 1995), which has been shown to bind CA-NTD (Bichel et al., 2013) akin to CypA. As discussed above, such shared binding may enable directionality and temporal regulation to PIC transport to and across the NPC, where multiple exposed CypA loops may coordinate these events.

C. Does the TNPO3:IN interaction play a role post-nuclear import ?

The HIV-1 infectivity defect observed upon TNPO3 depletion has been reproducibly around 5-20-fold in experimental systems tested so far (Brass et al., 2008; Christ et al., 2008; Krishnan et al., 2010a; Schaller et al., 2011; De Iaco et al., 2011; Valle-Casuso et al., 2012; Shah et al., 2013), and in the case of another primate lentivirus, SIV, the defect can be up to 20-fold. Additionally, the TNPO3 dependency of WT HIV-1 does not depend on the cell cycle state of target cells, as pharmacological induction of growth arrest at the stage of G2->S phase with aphidicolin does not render HIV-1 more sensitive to the depletion of the protein (Figure 2.8; Schaller et al., 2011). This may imply that the role TNPO3 plays in HIV-1 PIC nuclear import is independent of the cell cycle state, and that it can perform its function whether or not the nuclear envelope is intact. This may hint at (i) an integrative step common to both cell cycle arrested and cycling cells, or (ii) a role of the NPC that TNPO3 may regulate, such as nuclear import and licensing different integration site targeting pathways. CPSF6-358 restriction, on the other hand, is accentuated upon growth arrest, which may be reflective of the expression levels of endogenous CPSF6 that is released upon TNPO3 knockdown vs. ectopically over-expressed CPSF6-358 that readily accumulates in the cytosol. Further comparison of the different phenotypes were discussed in Chapter 2; **E.iii**.

The initial controversy regarding whether TNPO3 depletion resulted in a 2-LTR circle formation (‘nuclear import’) defect was resolved by correcting for confounding autointegration events, which revealed an absolute 2-4-fold decrease (Chapter 3, **B.i**; De Iaco et al., 2013). This, however, is lower than the observed 5-20-fold infectivity defect caused by TNPO3 depletion in respective cell lines tested. Again, a potential explanation of this observation could be that there may be an independent component to TNPO3 function post-nuclear import, such as a role in

integration as mediated by a TNPO3:IN interaction (Christ et al., 2008; Krishnan et al., 2010a) that may take place within the context of the intasome (Larue et al., 2012) once inside the nucleus. This additional role may then synergize with the nuclear import defect imposed by cytoplasmically relocalized endogenous CPSF6 (Chapter 3; **E.i**) and thus result in higher infectivity defects observed across the board in TNPO3 depleted cells. Preliminary results from our research group imply that recombinant TNPO3 may marginally enhance the in vitro integration activity of HIV-1 IN, yet this phenomenon awaits a more detailed study.

D. Timing of uncoating and nuclear import: Does the incoming capsid core play a licensing role or a direct structural role? How far into the nucleus might CA reach?

As described previously in Chapter 1; **D.ii.1**, it is generally accepted that uncoating, to an indeterminate extent, takes place in the cytosol when the HIV-1 core traverses the cytoplasm headed to the nucleus. This process is believed to be highly regulated in a cell-type specific fashion both by positive stabilizing factors; e.g. PDZD8, CypA, CPSF6 (cell-type dependent; see below in **E**) and negative destabilizing factors; e.g. TRIM5α, possibly Mx2, CypA (may be concentration dependent), and CPSF6 (described in detail in Chapter 1; **D.ii.1-2**). It has been reported that intact capsid cores could be detected on the cytosolic face of NPCs by electron microscopy (Arhel et al., 2007). Employing a functional assay that takes advantage of the TRIMCyp sensitivity of the incoming capsid only when it displays the quaternary CA lattice (Hulme et al., 2014) was used as a surrogate for uncoating, and a half-life of about 40 min was calculated for uncoating, with the process going to completion by 2 h post infection (Hulme et al., 2011). On the other hand, fate-of-capsid assays that are used to quantify pelletable, intact

incoming cores in infected cells readily detect CA+ high molecular weight complexes at 24 h post infection (Stremlau et al., 2006). These findings mark the extremes of the generally accepted timeline of HIV-1 early phase events where uncoating is believed to happen around 6-8 h post infection, readying the PIC for nuclear import. It is also worth mentioning that biochemical detection of HMW CA complexes may not be taken as functional evidence for being precursors to mature PICs, since ~ 85% of viral particles entail non-infectious events (Thomas et al., 2007).

Additionally, the observation that CA can play a functional role in PIC nuclear import and integration site targeting (Ocwieja et al., 2011), as described earlier in **C**, may or may not be taken as evidence for a structural presence of CA in these processes when they actually take place. By 'matching' the incoming PIC with differential NPC components at the stage of import, CA and its interactors; e.g. CypA, CPSF6 (Schaller et al., 2011), Nup153 (Koh et al., 2013), may be functioning as master regulators of distinct PIC import pathways, which lead to different integration site targeting. As such, CA may perform a licensing function at a pre-import stage with farther reaching consequences at post-import steps - even if CA may not be physically there inside the nucleus.

E. The role of endogenous CPSF6 in HIV-1 infection

Initial studies on the protein could not ascribe any function to endogenous CPSF6 in HIV-1 replication, because depleting it via RNAi in experimental cell lines had neither a positive nor a negative effect on HIV-1 infectivity (Lee et al., 2010; De Iaco et al., 2013). Additionally, the CPSF6-binding mutant N74D (Figure 2.7; Lee et al., 2010) repeatedly displayed WT levels of infectivity, implying that loss of CPSF6 binding did not bear any discernable fitness cost to

the virus (Lee et al., 2010; De Iaco et al., 2011; Schaller et al., 2011; Zhou et al., 2011; Price et al., 2012; Koh et al., 2013). This was challenged, however, upon finding that N74D replicated poorly in primary macrophages, and that it was blocked prior to reverse transcription in these cells (Schaller et al., 2011; Towers, 2011; Ambrose et al., 2012) along with the CypA binding mutant P90A. It is had been shown that CypA may increase the stability of incoming viral cores (Li et al., 2009; De Iaco et al., 2013; Fricke et al., 2013; Shah et al., 2013) and endogenous CPSF6 in macrophages may serve a similar function potentially playing a role as an HIV-1 dependency factor that promotes capsid core integrity and reverse transcription together with CypA.

In a similar vein we had shown that N74D displayed an impaired affinity to CypA and that it was rendered more susceptible to pharmacological inhibition by CsA, again lending support to the hypothesis that CPSF6 and CypA interactions with the incoming capsid core may be coregulated. Prior evidence for such coordination came indirectly as several CA mutants affected by a CypA-dependent cellular restriction at or after nuclear import could be rescued by introducing secondary mutations that we now know abrogate CPSF6 binding: CA N74D/G94D (Ambrose et al,. 2012), CA A92E/A105T and T54A/A105T (Yang et al., 2007; Qi et al., 2008) are all rescue mutants that do not display the original CypA-sensitive phenotype of G94D, A92E, and T54A, respectively.

The reciprocal phenotypes, i.e. loss of CypA binding leading to the rescue of the endogenous CPSF6-dependent restriction of a HIV-1 CA mutant was recently observed in a physiologically relevant HIV-1 mutant (Henning et al., 2014). R132K in the cytotoxic T-lymphocyte (CTL) response escape mutant HIV-1 CA R132K/L136M (RKLM) isolated *in vivo* from human leukocyte antigen (HLA)-B27+ individuals – the R132K mutation prevents

recognition by the HLA-B27 allele, which is part of the human major histocompatibility complex class I (MHC I) (Goulder et al., 2001) – was known to be linked to a cell cycle arrest phenotype (Qi et al., 2008). In this recent study, it was revealed that the restriction imposed on CA RKLM can be lifted upon CPSF6 knockdown as well as introducing CPSF6-binding mutations; N74D and A105T, but also by CsA treatment or CypA depletion (Henning et al., 2014), again highlighting the functional significance of endogenous CPSF6. It is important to mention, however, that HIV-1 does not prefer this escape pathway *in vivo;* namely losing the ability to bind CPSF6, as evidenced by late CTL variants that can sustain high levels of viral replication that still bind CPSF6, can be restricted by CPSF6-358 in vitro (Henning et al., 2014). These observations point to a second and positive role of CPSF6, yet these two opposing functions have not been elucidated in detail.

Further evidence for CPSF6 playing a positive role in HIV-1 replication was again detected in macrophages (Rasaiyah et al., 2013). The investigators observed that endogenous CPSF6 may be acting like a protective cloak against an interferon–induced cytoplasmic restriction in macrophages that would otherwise attack the incoming capsid core causing premature disassembly and impaired reverse transcription (as opposed to the impaired nuclear import reported by Lee et al., 2010). The CPSF6 isoform they claim to be studying however is different than the one tested in our assays (Figures 2.6-8, 3.1; Lee et al., 2010), which lacks the 37 codon long exon 6 corresponding to residues 231-267 on CPSF6 that lie upstream of the CA binding site within the proline-rich domain (Figure 2.2). It is interesting to note that an independent study confirmed this unique phenotypic difference (Hori et al., 2013), i.e. a block to reverse transcription vs. nuclear import of the PIC, determined by the absence or presence of exon 6. Accordingly, further investigation into differential cytoplasmic pulldown partners of

each individual CPSF6 isoforms, and of the 37 codon long exon 6 itself is warranted, along with studies looking for effects of potential minimal CPSF6 constructs that harbor exon6 and the CA-binding domain of CPSF6 (231-322 aa; 1-321 aa, Fricke et al., 2013). As opposed to our previous failed attempts at expressing and purifying full length CPSF6 quantitatively (data not shown), we currently have an optimized protocol that may allow us to study further the role of exon6 within the context of recombinant full length CPSF6.

CPSF6-358 impairs nuclear import of the HIV-1 PIC by directly binding and targeting CA (Lee et al., 2010; Lee et al., 2012; Price et al., 2012), and we have shown that full length CPSF6 also has the ability to interact with the CA lattice (Figure 3.3). Others have shown that CPSF6 may play a role in stabilizing the incoming capsid since ectopically expressed, and cytoplasmically localized CPSF6 (De Iaco et al., 2013) and recombinantly expressed and purified CPSF6 (1-321 aa; Fricke et al., 2013) seem to enhance pelletability of intact HMW capsid cores, evidenced by *in vitro* fate-of-capsid and CA-NC pelleting assays, respectively. Our observation that N74D CA-NC tubes, which do not bind CPSF6, reproducibly pellet less than WT CA-NC tubes (Figure 3.5) in absence of an otherwise stabilizing cellular extract (Guth et al., 2014) is in line with this model, yet one cannot disregard the possibility that these mutations may also cause intrinsic capsid stability defects leading to increased and premature uncoating as well.

REFERENCES

Aberham C, Weber S, Phares W. Spontaneous mutations in the human immunodeficiency virus type 1 gag gene that affect viral replication in the presence of cyclosporins. J Virol. 1996 Jun; 70(6):3536-44.

Albanese A, Arosio D, Terreni M, Cereseto A. HIV-1 pre-integration complexes selectively target decondensed chromatin in the nuclear periphery. PLoS One. 2008 Jun 11; 3(6):e2413.

Alkhatib G, Combadiere C, Broder CC, Feng Y, Kennedy PE, Murphy PM, Berger EA. CC CKR5: a RANTES, MIP-1alpha, MIP-1beta receptor as a fusion cofactor for macrophage-tropic HIV-1. Science. 1996 Jun 28; 272(5270):1955-8.

Allemand E, Dokudovskaya S, Bordonné R, Tazi J. A conserved Drosophila transportin-serine/arginine-rich (SR) protein permits nuclear import of Drosophila SR protein splicing factors and their antagonist repressor splicing factor 1. Mol Biol Cell. 2002 Jul; 13(7):2436-47.

Ambrose Z, Lee K, Ndjomou J, Xu H, Oztop I, Matous J, Takemura T, Unutmaz D, Engelman A, Hughes SH, KewalRamani VN. Human immunodeficiency virus type 1 capsid mutation N74D alters cyclophilin A dependence and impairs macrophage infection. J Virol. 2012 Apr; 86(8):4708-14.

Anderson JL, Campbell EM, Wu X, Vandegraaff N, Engelman A, Hope TJ. Proteasome inhibition reveals that a functional preintegration complex intermediate can be generated during restriction by diverse TRIM5 proteins. J Virol. 2006 Oct; 80(19):9754-60.

Ao Z, Danappa Jayappa K, Wang B, Zheng Y, Kung S, Rassart E, Depping R, Kohler M, Cohen EA, Yao X. Importin alpha3 interacts with HIV-1 integrase and contributes to HIV-1 nuclear import and replication. J Virol. 2010 Sep; 84(17):8650-63.

Arhel NJ, Souquere-Besse S, Munier S, Souque P, Guadagnini S, Rutherford S, Prévost MC, Allen TD, Charneau P. HIV-1 DNA Flap formation promotes uncoating of the pre-integration complex at the nuclear pore. EMBO J. 2007 Jun 20; 26(12):3025-37.

Baltimore D. RNA-dependent DNA polymerase in virions of RNA tumour viruses. Nature. 1970 Jun 27; 226(5252):1209-11

Barré-Sinoussi F, Chermann JC, Rey F, Nugeyre MT, Chamaret S, Gruest J, Dauguet C, Axler-Blin C, Vézinet-Brun F, Rouzioux C, Rozenbaum W, Montagnier L. Isolation of a T-lymphotropic retrovirus from a patient at risk for acquired immune deficiency syndrome (AIDS). Science. 1983 May 20; 220(4599):868-71.

Berkowitz RD, Ohagen A, Höglund S, Goff SP. Retroviral nucleocapsid domains mediate the specific recognition of genomic viral RNAs by chimeric Gag polyproteins during RNA packaging in vivo. J Virol. 1995 Oct; 69(10):6445-56.

Berthet-Colominas C, Monaco S, Novelli A, Sibaï G, Mallet F, Cusack S. Head-to-tail dimers and interdomain flexibility revealed by the crystal structure of HIV-1 capsid protein (p24) complexed with a monoclonal antibody Fab. EMBO J. 1999 Mar 1; 18(5):1124-36.

Bichel K, Price AJ, Schaller T, Towers GJ, Freund SM, James LC. HIV-1 capsid undergoes coupled binding and isomerization by the nuclear pore protein NUP358. Retrovirology. 2013 Jul 31; 10:81.

Bieniasz PD. Late budding domains and host proteins in enveloped virus release. Virology. 2006 Jan 5; 344(1):55-63.

Bischoff FR, Klebe C, Kretschmer J, Wittinghofer A, Ponstingl H. RanGAP1 induces GTPase activity of nuclear Ras-related Ran. Proc Natl Acad Sci USA 1994 Mar 29; 91(7):2587-91.

Bishop KN, Holmes RK, Sheehy AM, Malim MH. APOBEC-mediated editing of viral RNA. Science. 2004 Jul 30; 305(5684):645.

Blair WS, Pickford C, Irving SL, Brown DG, Anderson M, Bazin R, Cao J, Ciaramella G, Isaacson J, Jackson L, Hunt R, Kjerrstrom A, Nieman JA, Patick AK, Perros M, Scott AD, Whitby K, Wu H, Butler SL. HIV capsid is a tractable target for small molecule therapeutic intervention. PLoS Pathog. 2010 Dec 9; 6(12):e1001220.

Bosco DA, Eisenmesser EZ, Pochapsky S, Sundquist WI, Kern D. Catalysis of cis/trans isomerization in native HIV-1 capsid by human cyclophilin A. Proc Natl Acad Sci USA. 2002 Apr 16; 99(8):5247-52.

Bouyac-Bertoia M, Dvorin JD, Fouchier RA, Jenkins Y, Meyer BE, Wu LI, Emerman M, Malim MH. HIV-1 infection requires a functional integrase NLS. Mol Cell. 2001 May; 7(5):1025-35.

Braaten D, Aberham C, Franke EK, Yin L, Phares W, Luban J. Cyclosporine A-resistant human immunodeficiency virus type 1 mutants demonstrate that Gag encodes the functional target of cyclophilin A. J Virol. 1996 Aug; 70(8):5170-6.

Braaten D, Ansari H, Luban J. The hydrophobic pocket of cyclophilin is the binding site for the human immunodeficiency virus type 1 Gag polyprotein. J Virol. 1997 Mar; 71(3):2107-13

Brass AL, Dykxhoorn DM, Benita Y, Yan N, Engelman A, Xavier RJ, Lieberman J, Elledge SJ. Identification of host proteins required for HIV infection through a functional genomic screen. Science. 2008 Feb 15; 319(5865):921-6.

Briggs JA, Wilk T, Welker R, Kräusslich HG, Fuller SD. Structural organization of authentic, mature HIV-1 virions and cores. EMBO J. 2003 Apr 1; 22(7):1707-15.

Briggs JA, Grünewald K, Glass B, Förster F, Kräusslich HG, Fuller SD. he mechanism of HIV-1 core assembly: insights from three-dimensional reconstructions of authentic virions. Structure. 2006 Jan; 14(1):15-20.

Briggs JA, Kräusslich HG. The molecular architecture of HIV. J Mol Biol. 2011 Jul 22; 410(4):491-500.

Brown PO, Bowerman B, Varmus HE, Bishop JM. Retroviral integration: structure of the initial covalent product and its precursor, and a role for the viral IN protein. Proc Natl Acad Sci USA. 1989 Apr; 86(8):2525-9.

Buckman JS, Bosche WJ, Gorelick RJ. Human immunodeficiency virus type 1 nucleocapsid zn(2+) fingers are required for efficient reverse transcription, initial integration processes, and protection of newly synthesized viral DNA. J Virol. 2003 Jan; 77(2):1469-80.

Bukrinsky MI, Sharova N, Dempsey MP, Stanwick TL, Bukrinskaya AG, Haggerty S, Stevenson M. Active nuclear import of human immunodeficiency virus type 1 preintegration complexes. Proc Natl Acad Sci USA. 1992 Jul 15; 89(14):6580-4.

Bukrinsky MI, Haggerty S, Dempsey MP, Sharova N, Adzhubel A, Spitz L, Lewis P, Goldfarb D, Emerman M, Stevenson M. A nuclear localization signal within HIV-1 matrix protein that governs infection of non-dividing cells. Nature. 1993a Oct 14; 365(6447):666-9.

Bukrinsky MI, Sharova N, McDonald TL, Pushkarskaya T, Tarpley WG, Stevenson M. Association of integrase, matrix, and reverse transcriptase antigens of human immunodeficiency virus type 1 with viral nucleic acids following acute infection. Proc Natl Acad Sci USA. 1993b Jul 1; 90(13):6125-9.

Burniston MT, Cimarelli A, Colgan J, Curtis SP, Luban J. Human immunodeficiency virus type 1 Gag polyprotein multimerization requires the nucleocapsid domain and RNA and is promoted by the capsid-dimer interface and the basic region of matrix protein. J Virol. 1999 Oct; 73(10):8527-40.

Bushman FD, Craigie R. Activities of human immunodeficiency virus (HIV) integration protein in vitro: specific cleavage and integration of HIV DNA. Proc Natl Acad Sci USA. 1991 Feb 15;88(4):1339-43.

Bushman FD, Malani N, Fernandes J, D'Orso I, Cagney G, Diamond TL, Zhou H, Hazuda DJ, Espeseth AS, König R, Bandyopadhyay S, Ideker T, Goff SP, Krogan NJ, Frankel AD, Young JA, Chanda SK. Host cell factors in HIV replication: meta-analysis of genome-wide studies. PLoS Pathog. 2009 May; 5(5):e1000437."

Busnadiego I, Kane M, Rihn SJ, Preugschas HF, Hughes J, Blanco-Melo D, Strouvelle VP, Zang TM, Willett BJ, Boutell C, Bieniasz PD, Wilson SJ. Host and viral determinants of Mx2 antiretroviral activity. J Virol. 2014 Jul;88(14):7738-52.

Buzon V, Natrajan G, Schibli D, Campelo F, Kozlov MM, Weissenhorn W. Crystal structure of HIV-1 gp41 including both fusion peptide and membrane proximal external regions. PLoS Pathog. 2010 May 6; 6(5):e1000880.

Chackerian B, Long EM, Luciw PA, Overbaugh J. Human immunodeficiency virus type 1 coreceptors participate in postentry stages in the virus replication cycle and function in simian immunodeficiency virus infection. J Virol. 1997 May; 71(5):3932-9.

Checkley MA, Luttge BG, Freed EO. HIV-1 envelope glycoprotein biosynthesis, trafficking, and incorporation. J Mol Biol. 2011 Jul 22; 410(4):582-608.

Cherepanov P, Maertens G, Proost P, Devreese B, Van Beeumen J, Engelborghs Y, De Clercq E, Debyser Z. HIV-1 integrase forms stable tetramers and associates with LEDGF/p75 protein in human cells. J Biol Chem. 2003 Jan 3; 278(1):372-81.

Cherepanov P, Devroe E, Silver PA, Engelman A. Identification of an evolutionarily conserved domain in human lens epithelium-derived growth factor/transcriptional co-activator p75 (LEDGF/p75) that binds HIV-1 integrase. J Biol Chem. 2004 Nov 19; 279(47):48883-92.

Cherepanov P. LEDGF/p75 interacts with divergent lentiviral integrases and modulates their enzymatic activity in vitro. Nucleic Acids Res. 2007; 35(1):113-24.

Christ F, Thys W, De Rijck J, Gijsbers R, Albanese A, Arosio D, Emiliani S, Rain JC, Benarous R, Cereseto A, Debyser Z. Transportin-SR2 imports HIV into the nucleus. Curr Biol. 2008 Aug 26; 18(16):1192-202.

Chun TW, Stuyver L, Mizell SB, Ehler LA, Mican JA, Baseler M, Lloyd AL, Nowak MA, Fauci AS. Presence of an inducible HIV-1 latent reservoir during highly active antiretroviral therapy. Proc Natl Acad Sci USA. 1997 Nov 25; 94(24):13193-7.

Ciuffi A, Llano M, Poeschla E, Hoffmann C, Leipzig J, Shinn P, Ecker JR, Bushman F. A role for LEDGF/p75 in targeting HIV DNA integration. Nat Med. 2005 Dec; 11(12):1287-9.

Coffin JM, Hughes SH, Varmus HE. The Interactions of Retroviruses and their Hosts. Retroviruses. Cold Spring Harbor, NY. Cold Spring Harbor Laboratory Press, 1997. http://www.ncbi.nlm.nih.gov/books/NBK19465

Colwill K, Pawson T, Andrews B, Prasad J, Manley JL, Bell JC and Duncan PI. The Clk/Sty protein kinase phosphorylates SR splicing factors and regulates their intranuclear distribution. EMBO J. 1996; 15(2):265–275.

Compton AA, Malik HS, Emerman M. Host gene evolution traces the evolutionary history of ancient primate lentiviruses. Philos Trans R Soc Lond B Biol Sci. 2013 Aug 12; 368(1626):20120496.

Cradick TJ, Fine EJ, Antico CJ, Bao G. CRISPR/Cas9 systems targeting β-globin and CCR5 genes have substantial off-target activity. Nucleic Acids Res. 2013 Nov 1; 41(20):9584-92.

Cribier A, Ségéral E, Delelis O, Parissi V, Simon A, Ruff M, Benarous R, Emiliani S. Mutations affecting interaction of integrase with TNPO3 do not prevent HIV-1 cDNA nuclear import. Retrovirology. 2011 Dec 16; 8:104.

Dalgleish AG, Beverley PC, Clapham PR, Crawford DH, Greaves MF, Weiss RA. The CD4 (T4) antigen is an essential component of the receptor for the AIDS retrovirus. Nature. 1984 Dec 20-1985 Jan 2;312(5996):763-7.

Danielson CM, Cianci GC, Hope TJ. Recruitment and dynamics of proteasome association with rhTRIM5α cytoplasmic complexes during HIV-1 infection. Traffic. 2012 Sep; 13(9):1206-17.

Dar MJ, Monel B, Krishnan L, Shun MC, Di Nunzio F, Helland DE, Engelman A. Biochemical and virological analysis of the 18-residue C-terminal tail of HIV-1 integrase. Retrovirology. 2009 Oct 19; 6:94.

Davis TL, Walker JR, Campagna-Slater V, Finerty PJ, Paramanathan R, Bernstein G, MacKenzie F, Tempel W, Ouyang H, Lee WH, Eisenmesser EZ, Dhe-Paganon S. Structural and biochemical characterization of the human cyclophilin family of peptidyl-prolyl isomerases.PLoS Biol. 2010 Jul 27; 8(7):e1000439.

De Iaco A, Luban J. Inhibition of HIV-1 infection by TNPO3 depletion is determined by capsid and detectable after viral cDNA enters the nucleus. Retrovirology. 2011 Dec 6; 8:98.

De Iaco A, Santoni F, Vannier A, Guipponi M, Antonarakis S, Luban J. TNPO3 protects HIV-1 replication from CPSF6-mediated capsid stabilization in the host cell cytoplasm. Retrovirology. 2013 Feb 15; 10:20.

De Iaco A, Luban J. Cyclophilin A promotes HIV-1 reverse transcription but its effect on transduction correlates best with its effect on nuclear entry of viral cDNA. Retrovirology. 2014 Jan 30; 11:11.

De Rijck J, Debyser Z. The central DNA flap of the human immunodeficiency virus type 1 is important for viral replication. Biochem Biophys Res Commun. 2006 Oct 27; 349(3):1100-10.

Delelis O, Parissi V, Leh H, Mbemba G, Petit C, Sonigo P, Deprez E, Mouscadet JF. Efficient and specific internal cleavage of a retroviral palindromic DNA sequence by tetrameric HIV-1 integrase. PLoS One. 2007 Jul 11; 2(7):e608.

Deng H, Liu R, Ellmeier W, Choe S, Unutmaz D, Burkhart M, Di Marzio P, Marmon S, Sutton RE, Hill CM, Davis CB, Peiper SC, Schall TJ, Littman DR, Landau NR. Identification of a major co-receptor for primary isolates of HIV-1. Nature. 1996 Jun 20; 381(6584):661-6.

Di Marzo Veronese F, Copeland TD, DeVico AL, Rahman R, Oroszlan S, Gallo RC, Sarngadharan MG. Characterization of highly immunogenic p66/p51 as the reverse transcriptase of HTLV-III/LAV. Science. 1986 Mar 14; 231(4743):1289-91.

Di Nunzio F, Danckaert A, Fricke T, Perez P, Fernandez J, Perret E, Roux P, Shorte S, Charneau P, Diaz-Griffero F, Arhel NJ. Human nucleoporins promote HIV-1 docking at the nuclear pore, nuclear import and integration. PLoS One. 2012; 7(9):e46037.

Di Nunzio F, Fricke T, Miccio A, Valle-Casuso JC, Perez P, Souque P, Rizzi E, Severgnini M, Mavilio F, Charneau P, Diaz-Griffero F. Nup153 and Nup98 bind the HIV-1 core and contribute to the early steps of HIV-1 replication. Virology. 2013 May 25; 440(1):8-18.

Di Primio C, Quercioli V, Allouch A, Gijsbers R, Christ F, Debyser Z, Arosio D, Cereseto A. Single-cell imaging of HIV-1 provirus (SCIP). Proc Natl Acad Sci USA. 2013 Apr 2; 110(14):5636-41.

Diaz-Griffero F, Vandegraaff N, Li Y, McGee-Estrada K, Stremlau M, Welikala S, Si Z, Engelman A, Sodroski J. Requirements for capsid-binding and an effector function in TRIMCyp-mediated restriction of HIV-1. Virology. 2006 Aug 1; 351(2):404-19.

Dismuke DJ, Aiken C. Evidence for a functional link between uncoating of the human immunodeficiency virus type 1 core and nuclear import of the viral preintegration complex. J Virol. 2006 Apr; 80(8):3712-20.

Duggal NK, Emerman M. Evolutionary conflicts between viruses and restriction factors shape immunity. Nat Rev Immunol. 2012 Oct;12(10):687-95.

Dvorin JD, Bell P, Maul GG, Yamashita M, Emerman M, Malim MH. Reassessment of the roles of integrase and the central DNA flap in human immunodeficiency virus type 1 nuclear import. J Virol. 2002 Dec; 76(23):12087-96.

Dyda F, Hickman AB, Jenkins TM, Engelman A, Craigie R, Davies DR. Crystal structure of the catalytic domain of HIV-1 integrase: similarity to other polynucleotidyl transferases. Science. 1994 Dec 23; 266(5193):1981-6.

Ebina H, Aoki J, Hatta S, Yoshida T, Koyanagi Y. Role of Nup98 in nuclear entry of human immunodeficiency virus type 1 cDNA. Microbes Infect. 2004 Jul; 6(8):715-24.

Emerman M, Vazeux R, Peden K. The rev gene product of the human immunodeficiency virus affects envelope-specific RNA localization. Cell. 1989 Jun 30; 57(7):1155-65.

Engelman A, Mizuuchi K, Craigie R. HIV-1 DNA integration: mechanism of viral DNA cleavage and DNA strand transfer. Cell. 1991 Dec 20; 67(6):1211-21.

Engelman A, Craigie R. Identification of conserved amino acid residues critical for human immunodeficiency virus type 1 integrase function in vitro. J Virol. 1992 Nov; 66(11):6361-9.

Engelman A, Bushman FD, Craigie R. Identification of discrete functional domains of HIV-1 integrase and their organization within an active multimeric complex. EMBO J. 1993 Aug; 12(8):3269-75.

Engelman A, Oztop I, Vandegraaff N, Raghavendra NK. Quantitative analysis of HIV-1 preintegration complexes. Methods. 2009 Apr; 47(4):283-90.

Engelman A, Cherepanov P. The structural biology of HIV-1: mechanistic and therapeutic insights. Nat Rev Microbiol. 2012 Mar 16; 10(4):279-90.

Farnet CM, Haseltine WA. Integration of human immunodeficiency virus type 1 DNA in vitro. Proc Natl Acad Sci USA. 1990 Jun; 87(11):4164-8.

Farnet CM, Haseltine WA. Circularization of human immunodeficiency virus type 1 DNA in vitro. J Virol. 1991 Dec; 65(12):6942-52.

Fassati A, Goff SP. Characterization of intracellular reverse transcription complexes of Moloney murine leukemia virus. J Virol. 1999 Nov; 73(11):8919-25.

Fassati A, Goff SP. Characterization of intracellular reverse transcription complexes of human immunodeficiency virus type 1. J Virol. 2001 Apr; 75(8):3626-35.

Fassati A, Görlich D, Harrison I, Zaytseva L, Mingot JM. Nuclear import of HIV-1 intracellular reverse transcription complexes is mediated by importin 7. EMBO J. 2003 Jul 15; 22(14):3675-85.

Feinberg MB, Jarrett RF, Aldovini A, Gallo RC, Wong-Staal F. HTLV-III expression and production involve complex regulation at the levels of splicing and translation of viral RNA. Cell. 1986 Sep 12; 46(6):807-17.

Feng Y, Broder CC, Kennedy PE, Berger EA. HIV-1 entry cofactor: functional cDNA cloning of a seven-transmembrane, G protein-coupled receptor. Science. 1996 May 10; 272(5263):872-7.

Finzi A, Xiang SH, Pacheco B, Wang L, Haight J, Kassa A, Danek B, Pancera M, Kwong PD, Sodroski J. Topological layers in the HIV-1 gp120 inner domain regulate gp41 interaction and CD4-triggered conformational transitions. Mol Cell. 2010 Mar 12; 37(5):656-67.

Follenzi A, Ailles LE, Bakovic S, Geuna M, Naldini L. Gene transfer by lentiviral vectors is limited by nuclear translocation and rescued by HIV-1 pol sequences. Nat Genet. 2000 Jun; 25(2):217-22.

Fontes MR, Teh T, Kobe B. Structural basis of recognition of monopartite and bipartite nuclear localization sequences by mammalian importin-alpha. J Mol Biol. 2000 Apr 14; 297(5):1183-94.

Forshey BM, von Schwedler U, Sundquist WI, Aiken C. Formation of a human immunodeficiency virus type 1 core of optimal stability is crucial for viral replication. J Virol. 2002 Jun; 76(11):5667-77.

Fouchier RA, Meyer BE, Simon JH, Fischer U, Malim MH. HIV-1 infection of non-dividing cells: evidence that the amino-terminal basic region of the viral matrix protein is important for Gag processing but not for post-entry nuclear import. EMBO J. 1997 Aug 1; 16(15):4531-9.

Fouchier RA, Meyer BE, Simon JH, Fischer U, Albright AV, González-Scarano F, Malim MH. Interaction of the human immunodeficiency virus type 1 Vpr protein with the nuclear pore complex. J Virol. 1998 Jul; 72(7):6004-13.

Franke EK, Yuan HE, Luban J. Specific incorporation of cyclophilin A into HIV-1 virions. Nature. 1994 Nov 24; 372(6504):359-62.

Frankel AD and Young JA. HIV-1: fifteen proteins and an RNA. Annu Rev Biochem. 1998; 67:1-25.

Freed EO, Englund G, Martin MA. Role of the basic domain of human immunodeficiency virus type 1 matrix in macrophage infection. J Virol. 1995 Jun; 69(6):3949-54.

Freed EO, Martin MA. Domains of the human immunodeficiency virus type 1 matrix and gp41 cytoplasmic tail required for envelope incorporation into virions. J Virol. 1996 Jan; 70(1):341-51.

Freed EO, Englund G, Maldarelli F, Martin MA. Phosphorylation of residue 131 of HIV-1 matrix is not required for macrophage infection. Cell. 1997 Jan 24; 88(2):171-3; discussion 173-4

Fricke T, Valle-Casuso JC, White TE, Brandariz-Nuñez A, Bosche WJ, Reszka N, Gorelick R, Diaz-Griffero F. The ability of TNPO3-depleted cells to inhibit HIV-1 infection requires CPSF6. Retrovirology. 2013 Apr 26; 10:46.

Fritsch E, Temin HM Formation and structure of infectious DNA of spleen necrosis virus. J Virol. 1977 Jan; 21(1):119-30.

Fujiwara T, Mizuuchi K. Retroviral DNA integration: structure of an integration intermediate. Cell. 1988 Aug 12; 54(4):497-504.

Furuta RA, Wild CT, Weng Y, Weiss CD. Capture of an early fusion-active conformation of HIV-1 gp41. Nat Struct Biol. 1998 Apr; 5(4):276-9.

Gallay P, Swingler S, Song J, Bushman F, Trono D. HIV nuclear import is governed by the phosphotyrosine-mediated binding of matrix to the core domain of integrase. Cell. 1995 Nov 17; 83(4):569-76.

Gallay P, Hope T, Chin D, Trono D. HIV-1 infection of nondividing cells through the recognition of integrase by the importin/karyopherin pathway. Proc Natl Acad Sci USA. 1997 Sep 2; 94(18):9825-30.

Gallo RC, Sarin PS, Gelmann EP, Robert-Guroff M, Richardson E, Kalyanaraman VS, Mann D, Sidhu GD, Stahl RE, Zolla-Pazner S, Leibowitch J, Popovic M. Isolation of human T-cell leukemia virus in acquired immune deficiency syndrome (AIDS). Science. 1983 May 20; 220(4599):865-7.

Gamble TR, Vajdos FF, Yoo S, Worthylake DK, Houseweart M, Sundquist WI, Hill CP. Crystal structure of human cyclophilin A bound to the amino-terminal domain of HIV-1 capsid. Cell. 1996 Dec 27; 87(7):1285-94.

Gamble TR, Yoo S, Vajdos FF, von Schwedler UK, Worthylake DK, Wang H, McCutcheon JP, Sundquist WI, Hill CP. Structure of the carboxyl-terminal dimerization domain of the HIV-1 capsid protein. Science. 1997 Oct 31; 278(5339):849-53.

Ganser BK, Li S, Klishko VY, Finch JT, Sundquist WI. Assembly and analysis of conical models for the HIV-1 core. Science. 1999 Jan 1; 283(5398):80-3.

Ganser-Pornillos BK, von Schwedler UK, Stray KM, Aiken C, Sundquist WI. Assembly properties of the human immunodeficiency virus type 1 CA protein. J Virol. 2004 Mar; 78(5):2545-52.

Ganser-Pornillos BK, Cheng A, Yeager M. Structure of full-length HIV-1 CA: a model for the mature capsid lattice. Cell. 2007 Oct 5; 131(1):70-9.

Gao F, Bailes E, Robertson DL, Chen Y, Rodenburg CM, Michael SF, Cummins LB, Arthur LO, Peeters M, Shaw GM, Sharp PM, Hahn BH. Origin of HIV-1 in the chimpanzee Pan troglodytes troglodytes. Nature. 1999 Feb 4; 397(6718):436-41.

Garrus JE, von Schwedler UK, Pornillos OW, Morham SG, Zavitz KH, Wang HE, Wettstein DA, Stray KM, Côté M, Rich RL, Myszka DG, Sundquist WI. Tsg101 and the vacuolar protein sorting pathway are essential for HIV-1 budding. Cell. 2001 Oct 5;107(1):55-65.

Gartner S, Markovits P, Markovitz DM, Kaplan MH, Gallo RC, Popovic M. The role of mononuclear phagocytes in HTLV-III/LAV infection. Science. 1986 Jul 11; 233(4760):215-9.

Gatanaga H, Das D, Suzuki Y, Yeh DD, Hussain KA, Ghosh AK, Mitsuya H. Altered HIV-1 Gag protein interactions with cyclophilin A (CypA) on the acquisition of H219Q and H219P substitutions in the CypA binding loop. J Biol Chem. 2006 Jan 13; 281(2):1241-50.

Gaynor R. Cellular transcription factors involved in the regulation of HIV-1 gene expression. AIDS. 1992 Apr; 6(4):347-63.

Gelderblom HR, Hausmann EH, Ozel M, Pauli G, Koch MA. Fine structure of human immunodeficiency virus (HIV) and immunolocalization of structural proteins. Virology. 1987 Jan;156(1):171-6.

Gheysen D, Jacobs E, de Foresta F, Thiriart C, Francotte M, Thines D, De Wilde M. Assembly and release of HIV-1 precursor Pr55gag virus-like particles from recombinant baculovirus-infected insect cells. Cell. 1989 Oct 6; 59(1):103-12.

Gitti RK, Lee BM, Walker J, Summers MF, Yoo S, Sundquist WI: Structure of the amino-terminal core domain of the HIV-1 capsid protein. Science 1996, 273:231-235.

Goettlinger HG, Dorfman T, Sodroski JG, Haseltine WA. Effect of mutations affecting the p6 gag protein on human immunodeficiency virus particle release. Proc Natl Acad Sci USA. 1991 Apr 15; 88(8):3195-9.

Goh WC, Rogel ME, Kinsey CM, Michael SF, Fultz PN, Nowak MA, Hahn BH, Emerman M. HIV-1 Vpr increases viral expression by manipulation of the cell cycle: a mechanism for selection of Vpr in vivo. Nat Med. 1998 Jan;4(1):65-71.

Goldgur Y, Dyda F, Hickman AB, Jenkins TM, Craigie R, Davies DR. Three new structures of the core domain of HIV-1 integrase: an active site that binds magnesium. Proc Natl Acad Sci USA. 1998 Aug 4; 95(16):9150-4.

Goldstone DC, Ennis-Adeniran V, Hedden JJ, Groom HC, Rice GI, Christodoulou E, Walker PA, Kelly G, Haire LF, Yap MW, de Carvalho LP, Stoye JP, Crow YJ, Taylor IA, Webb M. HIV-1 restriction factor SAMHD1 is a deoxynucleoside triphosphate triphosphohydrolase. Nature. 2011 Nov 6; 480(7377):379-82.

Goscin LP, Byrnes JJ. DNA polymerase delta: one polypeptide, two activities. Biochemistry. 1982 May 11;21(10):2513-8.

Goujon C, Moncorgé O, Bauby H, Doyle T, Ward CC, Schaller T, Hué S, Barclay WS, Schulz R, Malim MH. Human MX2 is an interferon-induced post-entry inhibitor of HIV-1 infection. Nature. 2013 Oct 24; 502(7472):559-62.

Goulder PJ, Brander C, Tang Y, Tremblay C, Colbert RA, Addo MM, Rosenberg ES, Nguyen T, Allen R, Trocha A, Altfeld M, He S, Bunce M, Funkhouser R, Pelton SI, Burchett SK, McIntosh K, Korber BT, Walker BD. Evolution and transmission of stable CTL escape mutations in HIV infection. Nature. 2001 Jul 19; 412(6844):334-8.

Graettinger M, Hohenberg H, Thomas D, Wilk T, Müller B, Kräusslich HG. In vitro assembly properties of wild-type and cyclophilin-binding defective human immunodeficiency virus capsid proteins in the presence and absence of cyclophilin A. Virology. 1999 Apr 25;257(1):247-60.

Gross I, Hohenberg H, Kräusslich HG. In vitro assembly properties of purified bacterially expressed capsid proteins of human immunodeficiency virus. Eur J Biochem. 1997 Oct 15; 249(2):592-600.

Gross I, Hohenberg H, Huckhagel C, Kräusslich HG. N-Terminal extension of human immunodeficiency virus capsid protein converts the in vitro assembly phenotype from tubular to spherical particles. J Virol. 1998 Jun; 72(6):4798-810.

Guo F, Cen S, Niu M, Javanbakht H, Kleiman L. Specific inhibition of the synthesis of human lysyl-tRNA synthetase results in decreases in tRNA(Lys) incorporation, tRNA(3)(Lys) annealing to viral RNA, and viral infectivity in human immunodeficiency virus type 1. J Virol. 2003 Sep; 77(18):9817-22.

Guth CA, Sodroski J. Contribution of PDZD8 to stabilization of the human immunodeficiency virus type 1 capsid. J Virol. 2014 May; 88(9):4612-23.

Haffar OK, Popov S, Dubrovsky L, Agostini I, Tang H, Pushkarsky T, Nadler SG, Bukrinsky M. Two nuclear localization signals in the HIV-1 matrix protein regulate nuclear import of the HIV-1 pre-integration complex. J Mol Biol. 2000 Jun 2; 299(2):359-68.

Hahn BH, Shaw GM, De Cock KM, Sharp PM. Review AIDS as a zoonosis: scientific and public health implications. Science. 2000 Jan 28; 287(5453):607-14.

Handschumacher RE, Harding MW, Rice J, Drugge RJ, Speicher DW. Cyclophilin: a specific cytosolic binding protein for cyclosporin A. Science. 1984 Nov 2; 226(4674):544-7.

Hare S, Gupta SS, Valkov E, Engelman A, Cherepanov P. Retroviral intasome assembly and inhibition of DNA strand transfer. Nature. 2010 Mar 11; 464(7286):232-6.

Harris RS, Bishop KN, Sheehy AM, Craig HM, Petersen-Mahrt SK, Watt IN, Neuberger MS, Malim MH. DNA deamination mediates innate immunity to retroviral infection. Cell. 2003 Jun 13; 113(6):803-9.

Hatziioannou T, Perez-Caballero D, Cowan S, Bieniasz PD. Cyclophilin interactions with incoming human immunodeficiency virus type 1 capsids with opposing effects on infectivity in human cells. J Virol. 2005 Jan; 79(1):176-83.

Hauber I, Hofmann-Sieber H, Chemnitz J, Dubrau D, Chusainow J, Stucka R, Hartjen P, Schambach A, Ziegler P, Hackmann K, Schröck E, Schumacher U, Lindner C, Grundhoff A, Baum C, Manz MG, Buchholz F, Hauber J. Highly significant antiviral activity of HIV-1 LTR-specific tre-recombinase in humanized mice. PLoS Pathog. 2013; 9(9):e1003587.

He J, Chen Y, Farzan M, Choe H, Ohagen A, Gartner S, Busciglio J, Yang X, Hofmann W, Newman W, Mackay CR, Sodroski J, Gabuzda D. CCR3 and CCR5 are co-receptors for HIV-1 infection of microglia. Nature. 1997 Feb 13; 385(6617):645-9.

Hearps AC, Jans DA. HIV-1 integrase is capable of targeting DNA to the nucleus via an importin alpha/beta-dependent mechanism. Biochem J. 2006 Sep 15; 398(3):475-84.

Heinzinger NK, Bukinsky MI, Haggerty SA, Ragland AM, Kewalramani V, Lee MA, Gendelman HE, Ratner L, Stevenson M, Emerman M. The Vpr protein of human immunodeficiency virus type 1 influences nuclear localization of viral nucleic acids in nondividing host cells. Proc Natl Acad Sci USA. 1994 Jul 19; 91(15):7311-5.

Henning MS, Dubose BN, Burse MJ, Aiken C, Yamashita M. In vivo functions of CPSF6 for HIV-1 as revealed by HIV-1 capsid evolution in HLA-B27-positive subjects. PLoS Pathog. 2014 Jan;10(1):e1003868.

Hill CP, Worthylake D, Bancroft DP, Christensen AM, Sundquist WI. Crystal structures of the trimeric human immunodeficiency virus type 1 matrix protein: implications for membrane association and assembly. Proc Natl Acad Sci USA. 1996 Apr 2; 93(7):3099-104.

Hirsch VM, Olmsted RA, Murphey-Corb M, Purcell RH, Johnson PR. An African primate lentivirus (SIVsm) closely related to HIV-2. Nature. 1989 Jun 1; 339(6223):389-92.

Hofmann W, Schubert D, LaBonte J, Munson L, Gibson S, Scammell J, Ferrigno P, Sodroski J. Species-specific, postentry barriers to primate immunodeficiency virus infection. J Virol. 1999 Dec; 73(12):10020-8.

Hori T, Takeuchi H, Saito H, Sakuma R, Inagaki Y, Yamaoka S. A carboxy-terminally truncated human CPSF6 lacking residues encoded by exon 6 inhibits HIV-1 cDNA synthesis and promotes capsid disassembly. J Virol. 2013 Jul; 87(13):7726-36.

Hrecka K, Gierszewska M, Srivastava S, Kozaczkiewicz L, Swanson SK, Florens L, Washburn MP, Skowronski J. Lentiviral Vpr usurps Cul4-DDB1[VprBP] E3 ubiquitin ligase to modulate cell cycle. Proc Natl Acad Sci USA. 2007 Jul 10; 104(28):11778-83

Hrecka K, Hao C, Gierszewska M, Swanson SK, Kesik-Brodacka M, Srivastava S, Florens L, Washburn MP, Skowronski J. Vpx relieves inhibition of HIV-1 infection of macrophages mediated by the SAMHD1 protein. Nature. 2011 Jun 29; 474(7353):658-61.

Hu C, Saenz DT, Fadel HJ, Walker W, Peretz M, Poeschla EM. The HIV-1 central polypurine tract functions as a second line of defense against APOBEC3G/F. J Virol. 2010 Nov; 84(22):11981-93.

Hu WS, Hughes SH. HIV-1 reverse transcription. Cold Spring Harb Perspect Med. 2012 Oct 1; 2(10). pii: a006882.

Huang M, Orenstein JM, Martin MA, Freed EO. p6Gag is required for particle production from full-length human immunodeficiency virus type 1 molecular clones expressing protease. J Virol. 1995 Nov; 69(11):6810-8.

Hulme AE, Perez O, Hope TJ. Complementary assays reveal a relationship between HIV-1 uncoating and reverse transcription. Proc Natl Acad Sci USA. 2011 Jun 14; 108(24):9975-80.

Hulme AE, Hope TJ. The cyclosporin A washout assay to detect HIV-1 uncoating in infected cells. Methods Mol Biol. 2014; 1087:37-46.

Hütter G, Nowak D, Mossner M, Ganepola S, Müssig A, Allers K, Schneider T, Hofmann J, Kücherer C, Blau O, Blau IW, Hofmann WK, Thiel E. Long-term control of HIV by CCR5 Delta32/Delta32 stem-cell transplantation. N Engl J Med. 2009 Feb 12; 360(7):692-8.

Ikegami S, Taguchi T, Ohashi M, Oguro M, Nagano H, Mano Y. Aphidicolin prevents mitotic cell division by interfering with the activity of DNA polymerase-alpha. Nature. 1978 Oct 5; 275(5679):458-60.

Iordanskiy S, Berro R, Altieri M, Kashanchi F, Bukrinsky M. Intracytoplasmic maturation of the human immunodeficiency virus type 1 reverse transcription complexes determines their capacity to integrate into chromatin. Retrovirlogy. 2006 Jan 12; 3:4.

Jacks T, Power MD, Masiarz FR, Luciw PA, Barr PJ, Varmus HE. Characterization of ribosomal frameshifting in HIV-1 gag-pol expression. Nature. 1988 Jan 21; 331(6153):280-3.

Jayappa KD, Ao Z, Yang M, Wang J, Yao X. Identification of critical motifs within HIV-1 integrase required for importin α3 interaction and viral cDNA nuclear import. J Mol Biol. 2011 Jul 29; 410(5):847-62.

Jenkins Y, McEntee M, Weis K, Greene WC. Characterization of HIV-1 vpr nuclear import: analysis of signals and pathways. J Cell Biol. 1998 Nov 16; 143(4):875-85.

Jin Z, Jin L, Peterson DL, Lawson CL. Model for lentivirus capsid core assembly based on crystal dimers of EIAV p26. J Mol Biol. 1999 Feb 12;286(1):83-93.

Julias JG, Ferris AL, Boyer PL, Hughes SH. Replication of phenotypically mixed human immunodeficiency virus type 1 virions containing catalytically active and catalytically inactive reverse transcriptase. J Virol. 2001 Jul; 75(14):6537-46

Julien JP, Cupo A, Sok D, Stanfield RL, Lyumkis D, Deller MC, Klasse PJ, Burton DR, Sanders RW, Moore JP, Ward AB, Wilson IA. Crystal structure of a soluble cleaved HIV-1 envelope trimer. Science. 2013 Dec 20; 342(6165):1477-83.

Jun S, Ke D, Debiec K, Zhao G, Meng X, Ambrose Z, Gibson GA, Watkins SC, Zhang P. Direct visualization of HIV-1 with correlative live-cell microscopy and cryo-electron tomography. Structure. 2011 Nov 9; 19(11):1573-81.

Kamata M, Nitahara-Kasahara Y, Miyamoto Y, Yoneda Y, Aida Y. Importin-alpha promotes passage through the nuclear pore complexof human immunodeficiency virus type 1 Vpr. J Virol. 2005 Mar; 79(6):3557-64.

Kane M, Yadav SS, Bitzegeio J, Kutluay SB, Zang T, Wilson SJ, Schoggins JW, Rice CM, Yamashita M, Hatziioannou T, Bieniasz PD. MX2 is an interferon-induced inhibitor of HIV-1 infection. Nature. 2013 Oct 24; 502(7472):563-6.

Kao SY, Calman AF, Luciw PA, Peterlin BM. Anti-termination of transcription within the long terminal repeat of HIV-1 by tat gene product. Nature. 1987 Dec 3-9; 330(6147):489-93.

Karacostas V, Wolffe EJ, Nagashima K, Gonda MA, Moss B. Overexpression of the HIV-1 gag-pol polyprotein results in intracellular activation of HIV-1 protease and inhibition of assembly and budding of virus-like particles. Virology. 1993 Apr;193(2):661-71

Karageorgos L, Li P, Burrell C. Characterization of HIV replication complexes early after cell-to-cell infection. AIDS Res Hum Retroviruses. 1993 Sep; 9(9):817-23.

Kataoka N, Bachorik JL, Dreyfuss G. Transportin-SR, a nuclear import receptor for SR proteins. J Cell Biol. 1999 Jun 14; 145(6):1145-52.

Katz RA, Greger JG, Boimel P, Skalka AM. Human immunodeficiency virus type 1DNA nuclear import and integration are mitosis independent in cycling cells. J Virol. 2003 Dec; 77(24):13412-7.

Kehlenbach RH, Dickmanns A, Kehlenbach A, Guan T, Gerace L. A role for RanBP1 in the release of CRM1 from the nuclear pore complex in a terminal step of nuclear export. J Cell Biol. 1999 May 17; 145(4):645-57.

Kelly BN, Howard BR, Wang H, Robinson H, Sundquist WI, Hill CP. Implications for viral capsid assembly from crystal structures of HIV-1 Gag(1-278) and CA(N)(133-278). Biochemistry. 2006 Sep 26;45(38):11257-66.

Khayat R, Lee JH, Julien JP, Cupo A, Klasse PJ, Sanders RW, Moore JP, Wilson IA, Ward AB. Structural characterization of cleaved, soluble HIV-1 envelope glycoprotein trimers. J Virol. 2013 Sep; 87(17):9865-72.

Kilzer JM, Stracker T, Beitzel B, Meek K, Weitzman M, Bushman FD. Roles of host cell factors in circularization of retroviral DNA. Virology. 2003 Sep 15; 314(1):460-7.

Kim FJ, Battini JL, Manel N, Sitbon M. Emergence of vertebrate retroviruses and envelope capture. Virology. 2004 Jan 5; 318(1):183-91

Knipe DM and Howley PM. Retroviridae: Retroviruses and Their Replication. Fields Virology. 5th ed. Philadelphia, Pa.: Lippincott Williams & Wilkins, 2006. p2004.

Koenig R, Zhou Y, Elleder D, Diamond TL, Bonamy GM, Irelan JT, Chiang CY, Tu BP, De Jesus PD, Lilley CE, Seidel S, Opaluch AM, Caldwell JS, Weitzman MD, Kuhen KL, Bandyopadhyay S, Ideker T, Orth AP, Miraglia LJ, Bushman FD, Young JA, Chanda SK. Global

analysis of host-pathogen interactions that regulate early-stage HIV-1 replication. Cell. 2008 Oct 3; 135(1):49-60.

Koh Y, Haim H, Engelman A. Identification and characterization of persistent intracellular human immunodeficiency virus type 1 integrase strand transfer inhibitor activity. Antimicrob Agents Chemother. 2011 Jan; 55(1):42-9.

Koh Y, Wu X, Ferris AL, Matreyek KA, Smith SJ, Lee K, KewalRamani VN, Hughes SH, Engelman A. Differential effects of human immunodeficiency virus type 1 capsid and cellular factors nucleoporin 153 and LEDGF/p75 on the efficiency and specificity of viral DNA integration. J Virol. 2013 Jan; 87(1):648-58.

Kohl NE, Emini EA, Schleif WA, Davis LJ, Heimbach JC, Dixon RA, Scolnick EM, Sigal IS. Active human immunodeficiency virus protease is required for viral infectivity. Proc Natl Acad Sci USA. 1988 Jul; 85(13):4686-90.

Kohlstaedt LA, Wang J, Friedman JM, Rice PA, Steitz TA. Crystal structure at 3.5 A resolution of HIV-1 reverse transcriptase complexed with an inhibitor. Science. 1992 Jun 26; 256(5065):1783-90.

Kondo E, Göttlinger HG: A conserved LXXLF sequence is the major determinant in p6gag required for the incorporation of human immunodeficiency virus type 1 Vpr. J Virol 1996, 70(1):159-164.

Konstantoulas CJ, Indik S. Mouse mammary tumor virus-based vector transduces non-dividing cells, enters the nucleus via a TNPO3-independent pathway and integrates in a less biased fashion than other retroviruses. Retrovirology. 2014 Apr 30; 11(1):34.

Korber B, Muldoon M, Theiler J, Gao F, Gupta R, Lapedes A, Hahn BH, Wolinsky S, Bhattacharya T. Timing the ancestor of the HIV-1 pandemic strains. Science. 2000 Jun 9; 288(5472):1789-96.

Kovaleski BJ, Kennedy R, Hong MK, Datta SA, Kleiman L, Rein A, Musier-Forsyth K. In vitro characterization of the interaction between HIV-1 Gag and human lysyl-tRNA synthetase. J Biol Chem. 2006 Jul 14; 281(28):19449-56.

Kowalski M, Potz J, Basiripour L, Dorfman T, Goh WC, Terwilliger E, Dayton A, Rosen C, Haseltine W, Sodroski J. Functional regions of the envelope glycoprotein of human immunodeficiency virus type 1. Science. 1987 Sep 11; 237(4820):1351-5.

Krishnan L, Matreyek KA, Oztop I, Lee K, Tipper CH, Li X, Dar MJ, Kewalramani VN, Engelman A. The requirement for cellular transportin 3 (TNPO3 or TRN-SR2) during infection maps to human immunodeficiency virus type 1 capsid and not integrase. J Virol. 2010a Jan; 84(1):397-406.

Krishnan L, Li X, Naraharisetty HL, Hare S, Cherepanov P, Engelman A. Structure-based modeling of the functional HIV-1 intasome and its inhibition. Proc Natl Acad Sci USA. 2010b Sep 7; 107(36):15910-5.

Kwong PD, Wyatt R, Robinson J, Sweet RW, Sodroski J, Hendrickson WA. Structure of an HIV gp120 envelope glycoprotein in complex with the CD4 receptor and a neutralizing human antibody. Nature. 1998 Jun 18; 393(6686):648-59.

Laguette N, Sobhian B, Casartelli N, Ringeard M, Chable-Bessia C, Ségéral E, Yatim A, Emiliani S, Schwartz O, Benkirane M. SAMHD1 is the dendritic- and myeloid-cell-specific HIV-1 restriction factor counteracted by Vpx. Nature. 2011 May 25; 474(7353):654-7.

Lai MC, Lin RI, Huang SY, Tsai CW, Tarn WY. A human importin-beta family protein, transportin-SR2, interacts with the phosphorylated RS domain of SR proteins. J Biol Chem. 2000 Mar 17; 275(11):7950-7.

Lai MC, Lin RI, Tarn WY. Transportin-SR2 mediates nuclear import of phosphorylated SR proteins. Proc Natl Acad Sci USA. 2001 Aug 28; 98(18):10154-9.

Lai MC, Kuo HW, Chang WC, Tarn WY. A novel splicing regulator shares a nuclear import pathway with SR proteins. EMBO J. 2003 Mar 17; 22(6):1359-69.

Larue R, Gupta K, Wuensch C, Shkriabai N, Kessl JJ, Danhart E, Feng L, Taltynov O, Christ F, Van Duyne GD, Debyser Z, Foster MP, Kvaratskhelia M. Interaction of the HIV-1 intasome with transportin 3 protein (TNPO3 or TRN-SR2). J Biol Chem. 2012 Oct 5; 287(41):34044-58.

Lasky LA, Nakamura G, Smith DH, Fennie C, Shimasaki C, Patzer E, Berman P, Gregory T, Capon DJ. Delineation of a region of the human immunodeficiency virus type 1 gp120 glycoprotein critical for interaction with the CD4 receptor. Cell. 1987 Sep 11; 50(6):975-85.

Laspia MF, Rice AP, Mathews MB. HIV-1 Tat protein increases transcriptional initiation and stabilizes elongation. Cell. 1989 Oct 20; 59(2):283-92.

Le Rouzic E, Mousnier A, Rustum C, Stutz F, Hallberg E, Dargemont C, Benichou S. Docking of HIV-1 Vpr to the nuclear envelope is mediated by the interaction with the nucleoporin hCG1. J Biol Chem. 2002 Nov 22; 277(47):45091-8.

Lee K, Ambrose Z, Martin TD, Oztop I, Mulky A, Julias JG, Vandegraaff N, Baumann JG, Wang R, Yuen W, Takemura T, Shelton K, Taniuchi I, Li Y, Sodroski J, Littman DR, Coffin JM, Hughes SH, Unutmaz D, Engelman A, KewalRamani VN. Flexible use of nuclear import pathways by HIV-1. Cell Host Microbe. 2010 Mar 18; 7(3):221-33.

Lee K, Mulky A, Yuen W, Martin TD, Meyerson NR, Choi L, Yu H, Sawyer SL, Kewalramani VN. HIV-1 capsid-targeting domain of cleavage and polyadenylation specificity factor 6. J Virol. 2012 Apr; 86(7):3851-60.

Lelek M, Di Nunzio F, Henriques R, Charneau P, Arhel N, Zimmer C. Superresolution imaging of HIV in infected cells with FlAsH-PALM. Proc Natl Acad Sci USA. 2012 May 29; 109(22):8564-9.

Levin JG, Mitra M, Mascarenhas A, Musier-Forsyth K. Role of HIV-1 nucleocapsid protein in HIV-1 reverse transcription. RNA Biol. 2010 Nov-Dec; 7(6):754-74.

Levy JA, Hoffman AD, Kramer SM, Landis JA, Shimabukuro JM, Oshiro LS. Isolation of lymphocytopathic retroviruses from San Francisco patients with AIDS. Science. 1984 Aug 24; 225(4664):840-2.

Lewinski MK, Yamashita M, Emerman M, Ciuffi A, Marshall H, Crawford G, Collins F, Shinn P, Leipzig J, Hannenhalli S, Berry CC, Ecker JR, Bushman FD. Retroviral DNA integration: viral and cellular determinants of target-site selection. PLoS Pathog. 2006 Jun; 2(6):e60.

Lewis P, Hensel M, Emerman M. Human immunodeficiency virus infection of cells arrested in the cell cycle. EMBO J. 1992 Aug; 11(8):3053-8.

Lewis PF, Emerman M. Passage through mitosis is required for oncoretroviruses but not for the human immunodeficiency virus. J Virol. 1994 Jan; 68(1):510-6.

Li L, Olvera JM, Yoder KE, Mitchell RS, Butler SL, Lieber M, Martin SL, Bushman FD. Role of the non-homologous DNA end joining pathway in the early steps of retroviral infection. EMBO J. 2001 Jun 15; 20(12):3272-81.

Li L, Krymskaya L, Wang J, Henley J, Rao A, Cao LF, Tran CA, Torres-Coronado M, Gardner A, Gonzalez N, Kim K, Liu PQ, Hofer U, Lopez E, Gregory PD, Liu Q, Holmes MC, Cannon PM, Zaia JA, DiGiusto DL. Genomic editing of the HIV-1 coreceptor CCR5 in adult hematopoietic stem and progenitor cells using zinc finger nucleases. Mol Ther. 2013 Jun; 21(6):1259-69.

Li M, Mizuuchi M, Burke TR Jr, Craigie R. Retroviral DNA integration: Reaction pathway and critical intermediates. EMBO J. 2006 Mar 22; 25(6):1295-304.

Li Y, Kar AK, Sodroski J. Target cell type-dependent modulation of human immunodeficiency virus type 1 capsid disassembly by cyclophilin A. J Virol. 2009 Nov; 83(21):10951-62.

Lim ES, Fregoso OI, McCoy CO, Matsen FA, Malik HS, Emerman M. The ability of primate lentiviruses to degrade the monocyte restriction factor SAMHD1 preceded the birth of the viral accessory protein Vpx. Cell Host Microbe. 2012 Feb 16; 11(2):194-204.

Limón A, Devroe E, Lu R, Ghory HZ, Silver PA, Engelman A. Nuclear localization of human immunodeficiency virus type 1 preintegration complexes (PICs): V165A and R166A are pleiotropic integrase mutants primarily defective for integration, not PIC nuclear import. J Virol. 2002a Nov; 76(21):10598-607.

Limón A, Nakajima N, Lu R, Ghory HZ, Engelman A. Wild-type levels of nuclear localization and human immunodeficiency virus type 1 replication in the absence of the central DNA flap. J Virol. 2002b Dec; 76(23):12078-86.

Liu R, Paxton WA, Choe S, Ceradini D, Martin SR, Horuk R, MacDonald ME, Stuhlmann H, Koup RA, Landau NR. Homozygous defect in HIV-1 coreceptor accounts for resistance of some multiply-exposed individuals to HIV-1 infection. Cell. 1996 Aug 9; 86(3):367-77.

Liu Z, Pan Q, Ding S, Qian J, Xu F, Zhou J, Cen S, Guo F, Liang C. The interferon-inducible MxB protein inhibits HIV-1 infection. Cell Host Microbe. 2013 Oct 16; 14(4):398-410.

Llano M, Vanegas M, Hutchins N, Thompson D, Delgado S, Poeschla EM. Identification and characterization of the chromatin-binding domains of the HIV-1 integrase interactor LEDGF/p75. J Mol Biol. 2006 Jul 21; 360(4):760-73.

Logue EC, Taylor KT, Goff PH, Landau NR. The cargo-binding domain of transportin 3 is required for lentivirus nuclear import. J Virol. 2011 Dec; 85(24):12950-61

Los Alamos National Laboratory. Genome Maps. HIV Sequence Compendium 2013 http://www.hiv.lanl.gov/content/sequence/HIV/COMPENDIUM/2013/frontmatter.pdf

Lu R, Limón A, Devroe E, Silver PA, Cherepanov P, Engelman A. Class II integrase mutants with changes in putative nuclear localization signals are primarily blocked at a postnuclear entry step of human immunodeficiency virus type 1 replication. J Virol. 2004 Dec; 78(23):12735-46.

Lyumkis D, Julien JP, de Val N, Cupo A, Potter CS, Klasse PJ, Burton DR, Sanders RW, Moore JP, Carragher B, Wilson IA, Ward AB. Cryo-EM structure of a fully glycosylated soluble cleaved HIV-1 envelope trimer. Science. 2013 Dec 20; 342(6165):1484-90.

Maddon PJ, Dalgleish AG, McDougal JS, Clapham PR, Weiss RA, Axel R. The T4 gene encodes the AIDS virus receptor and is expressed in the immune system and the brain. Cell. 1986 Nov 7;47(3):333-48.

Maertens GN, Hare S, Cherepanov P. The mechanism of retroviral integration from X-ray structures of its keyintermediates. Nature. 2010 Nov 11; 468(7321):326-9

Maertens GN, Cook NJ, Wang W, Hare S, Gupta SS, Öztop I, Lee K, Pye VE, Cosnefroy O, Snijders AP, KewalRamani VN, Fassati A, Engelman A, Cherepanov P. Structural basis for nuclear import of splicing factors by human Transportin 3. Proc Natl Acad Sci U S A. 2014 Feb 18; 111(7):2728-33

Malik HS, Henikoff S, Eickbush TH. Poised for contagion: evolutionary origins of the infectious abilities of invertebrate retroviruses. Genome Res. 2000 Sep; 10(9):1307-18

Malim MH, Hauber J, Le SY, Maizel JV, Cullen BR. The HIV-1 rev trans-activator acts through a structured target sequence to activate nuclear export of unspliced viral mRNA. Nature. 1989 Mar 16; 338(6212):254-7

Malim MH, Emerman M. HIV-1 accessory proteins -- ensuring viral survival in a hostile environment. Cell Host Microbe. 2008 Jun 12; 3(6):388-98.

Mancebo HS, Lee G, Flygare J, Tomassini J, Luu P, Zhu Y, Peng J, Blau C, Hazuda D, Price D, Flores O. P-TEFb kinase is required for HIV Tat transcriptional activation in vivo and in vitro. Genes Dev. 1997 Oct 15; 11(20):2633-44.

Manjunath N, Yi G, Dang Y, Shankar P. Newer gene editing technologies toward HIV gene therapy. Viruses. 2013 Nov 14; 5(11):2748-66.

Mao Y, Wang L, Gu C, Herschhorn A, Désormeaux A, Finzi A, Xiang SH, Sodroski JG. Molecular architecture of the uncleaved HIV-1 envelope glycoprotein trimer. Proc Natl Acad Sci USA. 2013 Jul 23; 110(30):12438-43.

Marin M, Rose KM, Kozak SL, Kabat D. HIV-1 Vif protein binds the editing enzyme APOBEC3G and induces its degradation. Nat Med. 2003 Nov; 9(11):1398-403.

Marsden MD, Zack JA. Human immunodeficiency virus bearing a disrupted central DNA flap is pathogenic in vivo. J Virol. 2007 Jun; 81(11):6146-50.

Marshall HM, Ronen K, Berry C, Llano M, Sutherland H, Saenz D, Bickmore W, Poeschla E, Bushman FD. Role of PSIP1/LEDGF/p75 in lentiviral infectivity and integration targeting. PLoS One. 2007 Dec 19; 2(12):e1340.

Matreyek KA, Engelman A. The requirement for nucleoporin NUP153 during human immunodeficiency virus type 1 infection is determined by the viral capsid. J Virol. 2011 Aug; 85(15):7818-27.

Matreyek KA, Yücel SS, Li X, Engelman A. Nucleoporin NUP153 phenylalanine-glycine motifs engage a common binding pocket within the HIV-1 capsid protein to mediate lentiviral infectivity. PLoS Pathog. 2013; 9(10):e1003693.

McCarthy KR, Schmidt AG, Kirmaier A, Wyand AL, Newman RM, Johnson WE. Gain-of-sensitivity mutations in a Trim5-resistant primary isolate ofpathogenic SIV identify two independent conserved determinants of Trim5α specificity. PLoS Pathog. 2013 May; 9(5):e1003352

McDonald D, Vodicka MA, Lucero G, Svitkina TM, Borisy GG, Emerman M, Hope TJ. Visualization of the intracellular behavior of HIV in living cells. J Cell Biol. 2002 Nov 11; 159(3):441-52.

McDougal JS, Kennedy MS, Sligh JM, Cort SP, Mawle A, Nicholson JK. Binding of HTLV-III/LAV to T4+ T cells by a complex of the 110K viral protein and the T4 molecule. Science. 1986 Jan 24;231(4736):382-5.

Melchior, F, T Guan, N Yokoyama, T Nishimoto, and L Gerace. "GTP Hydrolysis by Ran Occurs at the Nuclear Pore Complex in an Early Step of Protein Import." The Journal of Cell Biology 131, no. 3 (November 1995): 571–81.

Melikyan GB, Markosyan RM, Hemmati H, Delmedico MK, Lambert DM, Cohen FS. Evidence that the transition of HIV-1 gp41 into a six-helix bundle, not the bundle configuration induces membrane fusion. J Cell Biol. 2000 Oct 16; 151(2):413-23.

Michel N, Goffinet C, Ganter K, Allespach I, Kewalramani VN, Saifuddin M, Littman DR, Greene WC, Goldsmith MA, Keppler OT. Human cyclin T1 expression ameliorates a T-cell-specific transcriptional limitation for HIV in transgenic rats, but is not sufficient for a spreading infection of prototypic R5 HIV-1 strains ex vivo. Retrovirology. 2009 Jan 13; 6:2.

Miller MD, Farnet CM, Bushman FD. Human immunodeficiency virus type 1 preintegration complexes: studies of organization and composition. J Virol. 1997 Jul; 71(7):5382-90.

Mitchell RS, Beitzel BF, Schroder AR, Shinn P, Chen H, Berry CC, Ecker JR, Bushman FD. Retroviral DNA integration: ASLV, HIV, and MLV show distinct target site preferences. PLoS Biol. 2004 Aug; 2(8):E234.

Miyauchi K, Kim Y, Latinovic O, Morozov V, Melikyan GB. HIV enters cells via endocytosis and dynamin-dependent fusion with endosomes. Cell. 2009 May 1; 137(3):433-44.

Morellet N, Jullian N, De Rocquigny H, Maigret B, Darlix JL, Roques BP. Determination of the structure of the nucleocapsid protein NCp7 from the human immunodeficiency virus type 1 by 1H NMR. EMBO J. 1992 Aug; 11(8): 3059-65.

Mörner A, Björndal A, Albert J, Kewalramani VN, Littman DR, Inoue R, Thorstensson R, Fenyö EM, Björling E. Primary human immunodeficiency virus type 2 (HIV-2) isolates, like HIV-1 isolates, frequently use CCR5 but show promiscuity in coreceptor usage. J Virol. 1999 Mar; 73(3):2343-9.

Mortuza GB, Haire LF, Stevens A, Smerdon SJ, Stoye JP, Taylor IA. High-resolution structure of a retroviral capsid hexameric amino-terminal domain. Nature. 2004 Sep 23; 431(7007):481-5.

Moulard M, Decroly E. Maturation of HIV envelope glycoprotein precursors by cellular endoproteases. Biochim Biophys Acta. 2000 Nov 10; 1469(3):121-32.

Nakajima N, Lu R, Engelman A. Human immunodeficiency virus type 1 replication in the absence of integrase-mediated DNA recombination: definition of permissive and nonpermissive T-cell lines. J Virol. 2001 Sep; 75(17):7944-55.

National Institute of Allergy and Infectious Diseases. Structure of HIV. January, 2009. http://www.niaid.nih.gov/topics/hivaids/understanding/howhivcausesaids/pages/howhiv.aspx

Neil S, Bieniasz P. Human immunodeficiency virus, restriction factors, and interferon. J Interferon Cytokine Res. 2009 Sep; 29(9):569-80.

Neil SJ, Zang T, Bieniasz PD. Tetherin inhibits retrovirus release and is antagonized by HIV-1 Vpu. Nature. 2008 Jan 24; 451(7177):425-30.

Nemergut ME, Mizzen CA, Stukenberg T, Allis CD, Macara IG. Chromatin docking and exchange activity enhancement of RCC1 by histones H2A and H2B. Science. 2001 May 25; 292(5521):1540-3.

Newman EN, Holmes RK, Craig HM, Klein KC, Lingappa JR, Malim MH, Sheehy AM. Antiviral function of APOBEC3G can be dissociated from cytidine deaminase activity. Curr Biol. 2005 Jan 26; 15(2):166-70.

OARAC - Office of AIDS Research Advisory Council. Department of Health and Human Services. Guidelines for the Use of Antiretroviral Agents in HIV-1-Infected Adults and Adolescents. May, 2014. http://aidsinfo.nih.gov/ContentFiles/AdultandAdolescentGL.pdf

Ocwieja KE, Brady TL, Ronen K, Huegel A, Roth SL, Schaller T, James LC, Towers GJ, Young JA, Chanda SK, König R, Malani N, Berry CC, Bushman FD. HIV integration targeting: a pathway involving Transportin-3 and the nuclear pore protein RanBP2. PLoS Pathog. 2011 Mar; 7(3):e1001313.

Ohkura S, Goldstone DC, Yap MW, Holden-Dye K, Taylor IA, Stoye JP. Novel escape mutants suggest an extensive TRIM5α binding site spanning the entire outer surface of the murine leukemia virus capsid protein. PLoS Pathog. 2011 Mar; 7(3):e1002011.

Ono A, Orenstein JM, Freed EO. Role of the Gag matrix domain in targeting human immunodeficiency virus type 1 assembly. J Virol. 2000 Mar; 74(6):2855-66.

O'Reilly AJ, Dacks JB, Field MC. Evolution of the karyopherin-β family of nucleocytoplasmic transport factors; ancient origins and continued specialization. PLoS One. 2011 Apr 27; 6(4):e19308

Panganiban AT, Temin HM. The retrovirus pol gene encodes a product required for DNA integration: identification of a retrovirus int locus. Proc Natl Acad Sci USA. 1984 Dec; 81(24):7885-9.

Panté N, Kann M. Nuclear pore complex is able to transport macromolecules with diameters of about 39 nm. Mol Biol Cell. 2002 Feb; 13(2):425-34.

Parolin C, Taddeo B, Palú G, Sodroski J. Use of cis- and trans-acting viral regulatory sequences to improve expression of human immunodeficiency virus vectors in human lymphocytes. Virology. 1996 Aug 15; 222(2):415-22

Paulillo SM, Phillips EM, Köser J, Sauder U, Ullman KS, Powers MA, Fahrenkrog B. Nucleoporin domain topology is linked to the transport status of the nuclear pore complex. J Mol Biol. 2005 Aug 26; 351(4):784-98.

Pereira CF, Rossy J, Owen DM, Mak J, Gaus K. HIV taken by STORM: super-resolution fluorescence microscopy of a viral infection. Virol J. 2012 May 2; 9:84.

Persaud D, Gay H, Ziemniak C, Chen YH, Piatak M Jr, Chun TW, Strain M, Richman D, Luzuriaga K. Absence of detectable HIV-1 viremia after treatment cessation in an infant. N Engl J Med. 2013 Nov 7; 369(19):1828-35.

Persaud D, Luzuriaga K. Absence of HIV-1 after treatment cessation in an infant. N Engl J Med. 2014 Feb 13; 370(7):678.

Pertel T, Hausmann S, Morger D, Züger S, Guerra J, Lascano J, Reinhard C, Santoni FA, Uchil PD, Chatel L, Bisiaux A, Albert ML, Strambio-De-Castillia C, Mothes W, Pizzato M, Grütter MG, Luban J. TRIM5 is an innate immune sensor for the retrovirus capsid lattice. Nature. 2011 Apr 21; 472(7343):361-5.

Petosa C. Ran: Role in nucleocytoplasmic transport. Encyclopedia of Signaling Molecules. Springer eBook, NY. Springer, 2013. p1574-1581, Fig.3. Reuse License # 3384690688162
http://link.springer.com/referenceworkentry/10.1007/978-1-4419-0461-4_641

Ping YH, Rana TM. DSIF and NELF interact with RNA polymerase II elongation complex and HIV-1 Tat stimulates P-TEFb-mediated phosphorylation of RNA polymerase II and DSIF during transcription elongation. J Biol Chem. 2001 Apr 20; 276(16):12951-8.

Popov S, Rexach M, Zybarth G, Reiling N, Lee MA, Ratner L, Lane CM, Moore MS, Blobel G, Bukrinsky M. Viral protein R regulates nuclear import of the HIV-1 pre-integration complex. EMBO J. 1998 Feb 16; 17(4):909-17.

Popovic M, Sarngadharan MG, Read E, Gallo RC. Detection, isolation, and continuous production of cytopathic retroviruses (HTLV-III) from patients with AIDS and pre-AIDS. Science. 1984 May 4; 224(4648):497-500.

Pornillos O, Ganser-Pornillos BK, Kelly BN, Hua Y, Whitby FG, Stout CD, Sundquist WI, Hill CP, Yeager M. X-ray structures of the hexameric building block of the HIV capsid. Cell. 2009 Jun 26; 137(7):1282-92.

Pornillos O, Ganser-Pornillos BK, Yeager M. Atomic-level modelling of the HIV capsid. Nature. 2011 Jan 20; 469(7330):424-7.

Powell RD, Holland PJ, Hollis T, Perrino FW. Aicardi-Goutieres syndrome gene and HIV-1 restriction factor SAMHD1 is a dGTP-regulated deoxynucleotide triphosphohydrolase. J Biol Chem. 2011 Dec 23; 286(51):43596-600.

Price AJ, Fletcher AJ, Schaller T, Elliott T, Lee K, KewalRamani VN, Chin JW, Towers GJ, James LC. CPSF6 defines a conserved capsid interface that modulates HIV-1 replication. PLoS Pathog. 2012; 8(8):e1002896.

Pryciak PM, Varmus HE. Nucleosomes, DNA-binding proteins, and DNA sequence modulate retroviral integration target site selection. Cell. 1992 May 29; 69(5):769-80.

Qi M, Yang R, Aiken C. Cyclophilin A-dependent restriction of human immunodeficiency virus type 1 capsid mutants for infection of nondividing cells. J Virol. 2008 Dec; 82(24):12001-8.

Rasaiyaah J, Tan CP, Fletcher AJ, Price AJ, Blondeau C, Hilditch L, Jacques DA, Selwood DL, James LC, Noursadeghi M, Towers GJ. HIV-1 evades innate immune recognition through specific cofactor recruitment. Nature. 2013 Nov 21;503(7476):402-5.

Rivière L, Darlix JL, Cimarelli A. Analysis of the viral elements required in the nuclear import of HIV-1 DNA. J Virol. 2010 Jan; 84(2):729-39.

Roe T, Reynolds TC, Yu G, Brown PO. Integration of murine leukemia virus DNA depends on mitosis. EMBO J. 1993 May; 12(5):2099-108.

Ruegsegger U, Beyer K, Keller W. Purification and characterization of human cleavage factor Im involved in the 3' end processing of messenger RNA precursors. J Biol Chem. 1996 Mar 15;271(11):6107-13.

Santoni FA, Hartley O, Luban J. Deciphering the code for retroviral integration target site selection. PLoS Comput Biol. 2010 Nov 24; 6(11):e1001008.

Sayah DM, Sokolskaja E, Berthoux L, Luban J. Cyclophilin A retrotransposition into TRIM5 explains owl monkey resistance to HIV-1. Nature. 2004 Jul 29; 430(6999):569-73.

Schaller T, Ylinen LM, Webb BL, Singh S, Towers GJ. Fusion of cyclophilin A to Fv1 enables cyclosporine-sensitive restriction of human and feline immunodeficiency viruses. J Virol. 2007 Sep; 81(18):10055-63.

Schaller T, Ocwieja KE, Rasaiyaah J, Price AJ, Brady TL, Roth SL, Hué S, Fletcher AJ, Lee K, KewalRamani VN, Noursadeghi M, Jenner RG, James LC, Bushman FD, Towers GJ. HIV-1 capsid-cyclophilin interactions determine nuclear import pathway, integration targeting and replication efficiency. PLoS Pathog. 2011 Dec;7(12):e1002439.

Shah VB, Shi J, Hout DR, Oztop I, Krishnan L, Ahn J, Shotwell MS, Engelman A, Aiken C. The host proteins transportin SR2/TNPO3 and cyclophilin A exert opposing effects on HIV-1 uncoating. J Virol. 2013 Jan; 87(1):422-32.

Sharp PM, Hahn BH. Origins of HIV and the AIDS pandemic. Cold Spring Harb Perspect Med. 2011 Sep; 1(1):a006841.

Sheehy AM, Gaddis NC, Choi JD, Malim MH. Isolation of a human gene that inhibits HIV-1 infection and is suppressed by the viral Vif protein. Nature. 2002 Aug 8;418(6898):646-50.

Sheehy AM, Gaddis NC, Malim MH. The antiretroviral enzyme APOBEC3G is degraded by the proteasome in response to HIV-1 Vif. Nat Med. 2003 Nov; 9(11):1404-7.

Shi J, Zhou J, Shah VB, Aiken C, Whitby K. Small-molecule inhibition of human immunodeficiency virus type 1 infection by virus capsid destabilization. J Virol. 2011 Jan; 85(1):542-9.

Shun MC, Daigle JE, Vandegraaff N, Engelman A. Wild-type levels of human immunodeficiency virus type 1 infectivity in the absence of cellular emerin protein. J Virol. 2007a Jan; 81(1):166-72.

Shun MC, Raghavendra NK, Vandegraaff N, Daigle JE, Hughes S, Kellam P, Cherepanov P, Engelman A. LEDGF/p75 functions downstream from preintegrationcomplex formation to effect gene-specific HIV-1 integration. Genes Dev. 2007b Jul 15; 21(14):1767-78.

Skasko M, Kim B. Compensatory role of human immunodeficiency virus central polypurine tract sequence in kinetically disrupted reverse transcription. J Virol. 2008 Aug; 82(15):7716-20.

Sokolskaja E, Sayah DM, Luban J. Target cell cyclophilin A modulates human immunodeficiency virus type 1 infectivity. J Virol. 2004 Dec; 78(23):12800-8.

Song C, Aiken C. Analysis of human cell heterokaryons demonstrates that target cell restriction of cyclosporine-resistant human immunodeficiency virus type 1 mutants is genetically dominant. J Virol. 2007 Nov; 81(21):11946-56.

Stewart M. Molecular mechanism of the nuclear protein import cycle. Nat Rev Mol Cell Biol. 2007 Mar; 8(3):195-208.

Strack B, Calistri A, Craig S, Popova E, Göttlinger HG. AIP1/ALIX is a binding partner for HIV-1 p6 and EIAV p9 functioning in virus budding. Cell. 2003 Sep 19; 114(6):689-99.

Strambio-De-Castillia C, Niepel M, Rout MP. The nuclear pore complex: bridging nuclear transport and gene regulation. Nat Rev Mol Cell Biol. 2010 Jul; 11(7):490-501.

Stremlau M, Perron M, Lee M, Li Y, Song B, Javanbakht H, Diaz-Griffero F, Anderson DJ, Sundquist WI, Sodroski J. Specific recognition and accelerated uncoating of retroviral capsids by the TRIM5alpha restriction factor. Proc Natl Acad Sci USA. 2006 Apr 4; 103(14):5514-9.

Suspène R, Rusniok C, Vartanian JP, Wain-Hobson S. Twin gradients in APOBEC3 edited HIV-1 DNA reflect the dynamics of lentiviral replication. Nucleic Acids Res. 2006; 34(17):4677-84.

Suzuki Y, Craigie R. The road to chromatin - nuclear entry of retroviruses. Nat Rev Microbiol. 2007 Mar; 5(3):187-96.

Svarovskaia ES, Xu H, Mbisa JL, Barr R, Gorelick RJ, Ono A, Freed EO, Hu WS, Pathak VK. Human apolipoprotein B mRNA-editing enzyme-catalytic polypeptide-like 3G (APOBEC3G) is incorporated into HIV-1 virions through interactions with viral and nonviral RNAs. J Biol Chem. 2004 Aug 20; 279(34):35822-8.

Swigut T, Shohdy N, Skowronski J. Mechanism for down-regulation of CD28 by Nef. EMBO J. 2001 Apr 2; 20(7):1593-604.

Symons J, Vandekerckhove L, Hütter G, Wensing AM, van Ham PM, Deeks SG, Nijhuis M. Dependence on the CCR5 co-receptor for viral replication explains the lack of rebound of CXCR4-predicted HIV-variants in the Berlin Patient. Clin Infect Dis. 2014 Apr 23

Takemura T, Kawamata M, Urabe M, Murakami T. Cyclophilin A-dependent restriction to capsid N121K mutant human immunodeficiency virus type 1 in a broad range of cell lines. J Virol. 2013 Apr; 87(7):4086-90.

Taltynov O, Demeulemeester J, Christ F, De Houwer S, Tsirkone VG, Gerard M, Weeks SD, Strelkov SV, Debyser Z. Interaction of transportin-SR2 with Ras-related nuclear protein (Ran) GTPase. J Biol Chem. 2013 Aug 30; 288(35):25603-13.

Temin HM, Mizutani S. RNA-dependent DNA polymerase in virions of Rous sarcoma virus. Nature. 1970 Jun 27;226(5252):1211-3.

Terry LJ, Wente SR. Flexible gates: dynamic topologies and functions for FG nucleoporins in nucleocytoplasmic transport. Eukaryot Cell. 2009 Dec; 8(12):1814-27.

Thali M, Bukovsky A, Kondo E, Rosenwirth B, Walsh CT, Sodroski J, Göttlinger HG. Functional association of cyclophilin A with HIV-1 virions. Nature. 1994 Nov 24; 372(6504):363-5.

Thomas JA, Ott DE, Gorelick RJ. Efficiency of human immunodeficiency virus type 1 postentry infection processes: evidence against disproportionate numbers of defective virions. J Virol. 2007 Apr;81(8):4367-70.

Towers GJ, Hatziioannou T, Cowan S, Goff SP, Luban J, Bieniasz PD. Cyclophilin A modulates the sensitivity of HIV-1 to host restriction factors. Nat Med. 2003 Sep; 9(9):1138-43.

Towers GJ. HIV, cyclophilins and nuclear entry: going under the radar. Retrovirology 2011, 8 (Suppl 2):O7.

Tsuchihashi Z, Brown PO. DNA strand exchange and selective DNA annealing promoted by the human immunodeficiency virus type 1 nucleocapsid protein. J Virol. 1994 Sep; 68(9):5863-70.

Valle-Casuso JC, Di Nunzio F, Yang Y, Reszka N, Lienlaf M, Arhel N, Perez P, Brass AL, Diaz-Griffero F. TNPO3 is required for HIV-1 replication after nuclear import but prior to integration and binds the HIV-1 core. J Virol. 2012 May; 86(10):5931-6.

Van Damme N, Goff D, Katsura C, Jorgenson RL, Mitchell R, Johnson MC, Stephens EB, Guatelli J. The interferon-induced protein BST-2 restricts HIV-1 release and is downregulated from the cell surface by the viral Vpu protein. Cell Host Microbe. 2008 Apr 17; 3(4):245-52.

Vishwanathan SA, Hunter E. Importance of the membrane-perturbing properties of the membrane-proximal external region of human immunodeficiency virus type 1 gp41 to viral fusion. J Virol. 2008 Jun; 82(11):5118-26.

Vodicka MA, Koepp DM, Silver PA, Emerman M. HIV-1 Vpr interacts with the nuclear transport pathway to promote macrophage infection. Genes Dev. 1998 Jan 15; 12(2):175-85.

Vollenweider F, Benjannet S, Decroly E, Savaria D, Lazure C, Thomas G, Chrétien M, Seidah NG. Comparative cellular processing of the human immunodeficiency virus (HIV-1) envelope glycoprotein gp160 by the mammalian subtilisin/kexin-like convertases. Biochem J. 1996 Mar 1; 314 (Pt 2):521-32.

von Schwedler U, Kornbluth RS, Trono D. The nuclear localization signal of the matrix protein of human immunodeficiency virus type 1 allows the establishment of infection in macrophages and quiescent T lymphocytes. Proc Natl Acad Sci USA. 1994 Jul 19; 91(15):6992-6.

von Schwedler UK, Stuchell M, Müller B, Ward DM, Chung HY, Morita E, Wang HE, Davis T, He GP, Cimbora DM, Scott A, Kräusslich HG, Kaplan J, Morham SG, Sundquist WI. The protein network of HIV budding. Cell. 2003 Sep 19; 114(6):701-13.

Vozzolo L, Loh B, Gane PJ, Tribak M, Zhou L, Anderson I, Nyakatura E, Jenner RG, Selwood D, Fassati A. Gyrase B inhibitor impairs HIV-1 replication by targeting Hsp90 and the capsid protein.J Biol Chem. 2010 Dec 10; 285(50):39314-28.

Waheed AA, Freed EO. Lipids and membrane microdomains in HIV-1 replication. Virus Res. 2009 Aug; 143(2):162-76.

Wainberg MA, Dascal A, Blain N, Fitz-Gibbon L, Boulerice F, Numazaki K, Tremblay M. The effect of cyclosporine A on infection of susceptible cells by human immunodeficiency virus type 1. Blood. 1988 Dec; 72(6):1904-10.

Wang GP, Ciuffi A, Leipzig J, Berry CC, Bushman FD. HIV integration site selection: analysis by massively parallel pyrosequencing reveals association with epigenetic modifications. Genome Res. 2007 Aug; 17(8):1186-94.

Weinberg JB, Matthews TJ, Cullen BR, Malim MH. Productive human immunodeficiency virus type 1 (HIV-1) infection of nonproliferating human monocytes. J Exp Med. 1991 Dec 1; 174(6):1477-82.

Weiss RA. The discovery of endogenous retroviruses. Retrovirology. 2006 Oct 3; 3:67.

Wilken N, Senécal JL, Scheer U, Dabauvalle MC. Localization of the Ran-GTP binding protein RanBP2 at the cytoplasmic side of the nuclear pore complex. Eur J Cell Biol. 1995 Nov; 68(3):211-9.

Wlodawer A, Miller M, Jaskólski M, Sathyanarayana BK, Baldwin E, Weber IT, Selk LM, Clawson L, Schneider J, Kent SB. Conserved folding in retroviral proteases: crystal structure of a synthetic HIV-1 protease. Science. 1989 Aug 11; 245(4918):616-21.

Woodward CL, Prakobwanakit S, Mosessian S, Chow SA. Integrase interacts with nucleoporin NUP153 to mediate the nuclear import of human immunodeficiency virus type 1. J Virol. 2009 Jul; 83(13):6522-33.

World Health Organization (WHO – UNAIDS). Epidemiology Slides. HIV 2013 Global Report, p2-4. September 2013.
http://www.unaids.org/en/media/unaids/contentassets/documents/epidemiology/2013/gr2013/201309_epi_core_en.pdf

Worobey M, Gemmel M, Teuwen DE, Haselkorn T, Kunstman K, Bunce M, Muyembe JJ, Kabongo JM, Kalengayi RM, Van Marck E, Gilbert MT, Wolinsky SM. Direct evidence of extensive diversity of HIV-1 in Kinshasa by 1960. Nature. 2008 Oct 2; 455(7213):661-4.

Worobey M, Telfer P, Souquière S, Hunter M, Coleman CA, Metzger MJ, Reed P, Makuwa M, Hearn G, Honarvar S, Roques P, Apetrei C, Kazanji M, Marx PA. Island biogeography reveals the deep history of SIV. Science. 2010 Sep 17; 329(5998):1487.

Wu J, Matunis MJ, Kraemer D, Blobel G, Coutavas E. Nup358, a cytoplasmically exposed nucleoporin with peptide repeats, Ran-GTP binding sites, zinc fingers, a cyclophilin A homologous domain, and a leucine-rich region. J Biol Chem. 1995 Jun 9; 270(23):14209-13.

Wu X, Li Y, Crise B, Burgess SM, Munroe DJ. Weak palindromic consensus sequences are a common feature found at the integration target sites of many retroviruses. J Virol. 2005 Apr; 79(8):5211-4.

Wu X, Anderson JL, Campbell EM, Joseph AM, Hope TJ. Proteasome inhibitors uncouple rhesus TRIM5alpha restriction of HIV-1 reverse transcription and infection. Proc Natl Acad Sci USA. 2006 May 9; 103(19):7465-70.

Wurtzer S, Goubard A, Mammano F, Saragosti S, Lecossier D, Hance AJ, Clavel F.Functional central polypurine tract provides downstream protection of the human immunodeficiency virus type 1 genome from editing by APOBEC3G and APOBEC3B. J Virol. 2006 Apr; 80(7):3679-83.

Wyatt R, Kwong PD, Desjardins E, Sweet RW, Robinson J, Hendrickson WA, Sodroski JG. The antigenic structure of the HIV gp120 envelope glycoprotein. Nature. 1998 Jun 18; 393(6686):705-11.

Yamashita M, Emerman M. Capsid is a dominant determinant of retrovirus infectivity in nondividing cells. J Virol. 2004 Jun; 78(11):5670-8.

Yamashita M, Emerman M. The cell cycle independence of HIV infections is not determined by known karyophilic viral elements. PLoS Pathog. 2005 Nov; 1(3):e18.

Yamashita M, Perez O, Hope TJ, Emerman M. Evidence for direct involvement of the capsid protein in HIV infection of nondividing cells. PLoS Pathog. 2007 Oct 26; 3(10):1502-10.

Yamashita M, Emerman M. Cellular restriction targeting viral capsids perturbs human immunodeficiency virus type 1 infection of nondividing cells. J Virol. 2009 Oct; 83(19):9835-43.

Yan N, Cherepanov P, Daigle JE, Engelman A, Lieberman J. The SET complex acts as a barrier to autointegration of HIV-1. PLoS Pathog. 2009 Mar; 5(3):e1000327.

Yang R, Aiken C. A mutation in alpha helix 3 of CA renders human immunodeficiency virus type 1 cyclosporin A resistant and dependent: rescue by a second-site substitution in a distal region of CA. J Virol. 2007 Apr; 81(8):3749-56.

Yang Q, Coseno M, Gilmartin GM, Doublié S. Crystal structure of a human cleavage factor CFI(m)25/CFI(m)68/RNA complex provides an insight into poly(A)site recognition and RNA looping. Structure. 2011 Mar 9; 19(3):368-77.

Yang Y, Fricke T, Diaz-Griffero F. Inhibition of reverse transcriptase activity increases stability of the HIV-1 core. J Virol. 2013 Jan; 87(1):683-7.

Yap MW, Dodding MP, Stoye JP. Trim-cyclophilin A fusion proteins can restrict human immunodeficiency virus type 1 infection at two distinct phases in the viral life cycle. J Virol. 2006 Apr; 80(8):4061-7.

Yeung ML, Houzet L, Yedavalli VS, Jeang KT. A genome-wide short hairpin RNA screening of jurkat T-cells for human proteins contributing to productive HIV-1 replication. J Biol Chem. 2009 Jul 17;284(29):19463-73.

Yin L, Braaten D, Luban J. Human immunodeficiency virus type 1 replication is modulated by host cyclophilin A expression levels. J Virol. 1998 Aug; 72(8):6430-6.

Ylinen LM, Schaller T, Price A, Fletcher AJ, Noursadeghi M, James LC, Towers GJ. Cyclophilin A levels dictate infection efficiency of human immunodeficiency virus type 1 capsid escape mutants A92E and G94D. J Virol. 2009 Feb; 83(4):2044-7.

Yoo S, Myszka DG, Yeh C, McMurray M, Hill CP, Sundquist WI. Molecular recognition in the HIV-1 capsid/cyclophilin A complex. J Mol Biol. 1997 Jun 27; 269(5):780-95.

Yukl SA, Boritz E, Busch M, Bentsen C, Chun TW, Douek D, Eisele E, Haase A, Ho YC, Hütter G, Justement JS, Keating S, Lee TH, Li P, Murray D, Palmer S, Pilcher C, Pillai S, Price RW, Rothenberger M, Schacker T, Siliciano J, Siliciano R, Sinclair E, Strain M, Wong J, Richman D, Deeks SG. Challenges in detecting HIV persistence during potentially curative interventions: a study of the Berlin patient. PLoS Pathog. 2013; 9(5):e1003347.

Yun CY, Velazquez-Dones AL, Lyman SK, Fu XD. Phosphorylation-dependent and -independent nuclear import of RS domain-containing splicing factors and regulators. J Biol Chem. 2003 May 16; 278(20):18050-5.

Zack JA, Arrigo SJ, Weitsman SR, Go AS, Haislip A, Chen IS. HIV-1 entry into quiescent primary lymphocytes: molecular analysis reveals a labile, latent viral structure. Cell. 1990 Apr 20; 61(2):213-22.

Zaitseva L, Myers R, Fassati A. tRNAs promote nuclear import of HIV-1 intracellular reverse transcription complexes. PLoS Biol. 2006 Oct; 4(10):e332.

Zennou V, Petit C, Guetard D, Nerhbass U, Montagnier L, Charneau P. HIV-1 genome nuclear import is mediated by a central DNA flap. Cell. 2000 Apr 14; 101(2):173-85.

Zhang R, Mehla R, Chauhan A. Perturbation of host nuclear membrane component RanBP2 impairs the nuclear import of human immunodeficiency virus -1 preintegration complex (DNA). PLoS One. 2010 Dec 14; 5(12):e15620.

Zhao G, Perilla JR, Yufenyuy EL, Meng X, Chen B, Ning J, Ahn J, Gronenborn AM, Schulten K, Aiken C, Zhang P. Mature HIV-1 capsid structure by cryo-electron microscopy and all-atom molecular dynamics. Nature. 2013 May 30; 497(7451): 643-6.

Zhou H, Xu M, Huang Q, Gates AT, Zhang XD, Castle JC, Stec E, Ferrer M, Strulovici B, Hazuda DJ, Espeseth AS. Genome-scale RNAi screen for host factors required for HIV replication. Cell Host Microbe. 2008 Nov 13; 4(5):495-504.

Zhou L, Sokolskaja E, Jolly C, James W, Cowley SA, Fassati A. Transportin 3 promotes a nuclear maturation step required for efficient HIV-1 integration. PLoS Pathog. 2011 Aug; 7(8):e1002194.

Zhu Y, Pe'ery T, Peng J, Ramanathan Y, Marshall N, Marshall T, Amendt B, Mathews MB, Price DH. Transcription elongation factor P-TEFb is required for HIV-1 tat transactivation in vitro. Genes Dev. 1997 Oct 15; 11(20):2622-32.

Zielske SP, Stevenson M. Importin 7 may be dispensable for human immunodeficiency virus type 1 and simian immunodeficiency virus infection of primary macrophages. J Virol. 2005 Sep; 79(17):11541-6.

Zou S, Glynn S, Kuritzkes D, Shah M, Cook N, Berliner N, NHLBI AIDS Blood Session Working Group. Hematopoietic cell transplantation and HIV cure: where we are and what next? Blood. 2013 Oct 31; 122(18):3111-5.

APPENDIX A

THE CA HEXAMER:HEXAMER INTERFACE AS A POTENTIAL MULTIFACETED BINDING SITE FOR CYPA

A. Introduction

We carried out preliminary structural modeling in Chapters 2 and 3 in order to project the full study set of CA mutants onto the incoming virion capsid surface to get a better grip of how they might relate to each other, to the multihexameric surface configuration of the conical capsid and also to other CA binding factors, CypA and CPSF6. The observation that a CypA molecule modeled onto the CA hexamer:hexamer interface was in close proximity of adjacent CA molecules it does not interact via CypA-loops prompted us to carefully analyze this hypothetical interface. As a result, we came up with structural predictions about how a CypA molecule may be coordinated and stabilized on a quaternary capsid surface with the aid of novel interactions mediated by neighboring surface CypA loops. We highlighted candidate CA and CypA residues that may play critical roles in this hypothetical interaction. Our predictions may have wider implications in that they provide a mechanistic explanation to the workings of several CypA-sensitive, CsA-dependent CA mutants present on CypA loops. Such multifaceted coordination of CypA in between two CA hexamers may also determine the mode of CPSF6 binding and other potential CA interacting proteins.

B. Methods

Modeling is carried out in PyMol (DeLano Scientific LLC®) using publicly available conical capsid structures and molecular CA hexamer structures described in Zhao *et al*, 2013 that used CA A92E mutant capsids for reference (PDB: 1VU5). The atomic structure of CypA was obtained from the CypA:CA-NTD crystal structure described in Gamble *et al.*,1996 (PDB: 1AK4).

Two adjacent CA hexamers (1VU5_hijklm & 1VU5_uvwxyz) together with a CypA:CA NTD structure (1AK4_BC) were modeled by aligning the Cα backbone of 1AK4_C (CA-NTD, not shown) with the Cα backbone of 1VU5_i (CA-NTD2). Accordingly, CypA (1AK4_B) is modeled onto the interhexameric space in the vicinity of two neighboring CA molecules; 1VU5_y (CA-NTD1) and 1VU5_z (CA-NTD3) of the adjacent CA-hexamer, 1VU5_uvwxyz.

C. Results

C.i. Molecular modeling of CypA onto the CA hexamer:hexamer interface and the description of the hypothetical secondary CA : CypA interface

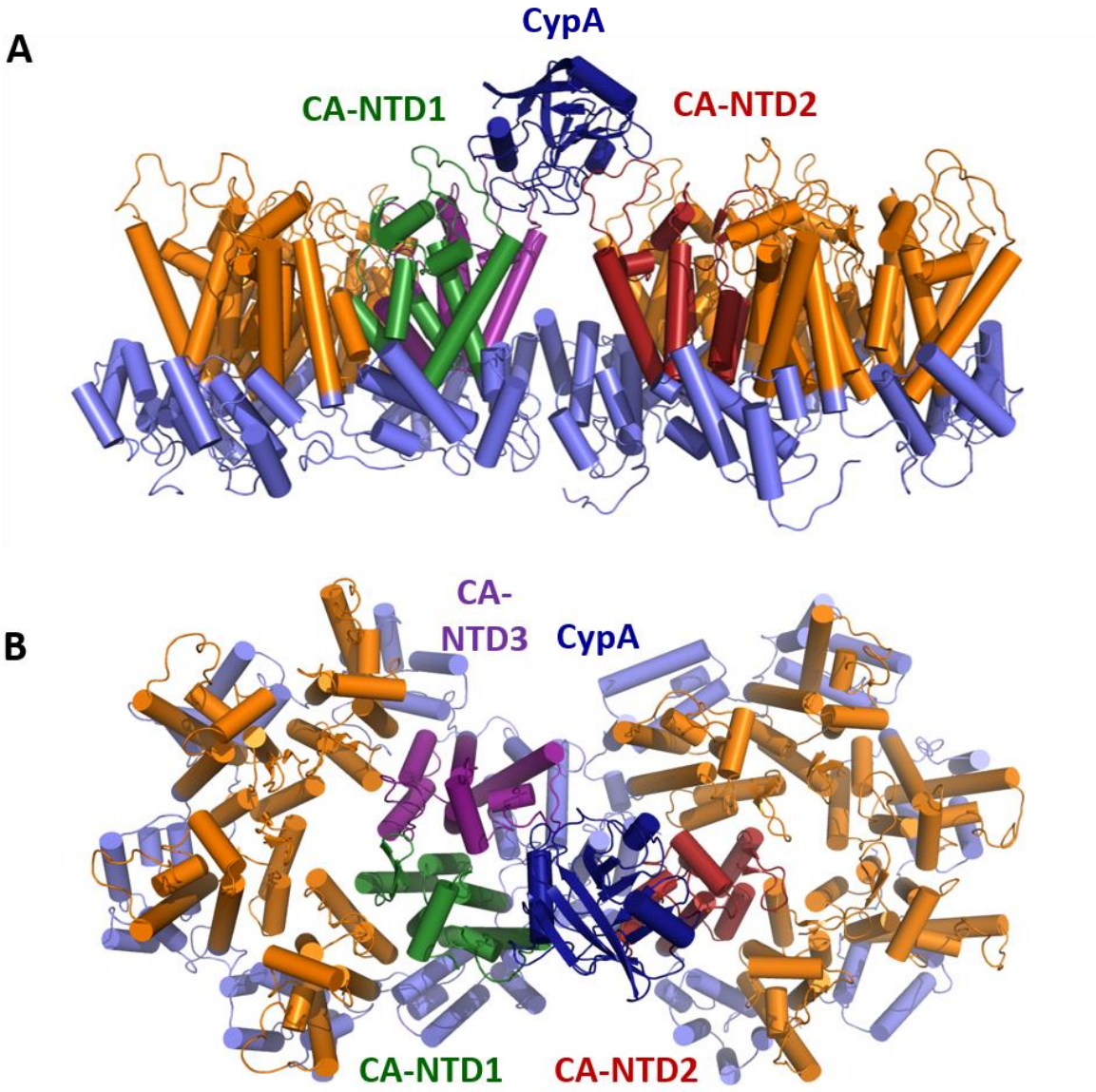

Figure A.1 The CA-NTD2:CypA:CA-NTD1/3 interhexamer bridging model. CypA (1AK4_B) that is attached to CA-NTD2 (upon alignment) within the CA hexamer on the right (1VU5_hijklm) is in close proximity of CA-NTD1 (1VU5_y) and CA-NTD3 (1VU5_z) on the adjacent CA hexamer to the left (1VU5_uvwxyz). **(A)** Side view depicting the hypothetical bridge. **(B)** Top view depicting the hypothetical interface between CypA:CA-NTD1/3

In this particular model (Figure A.1), the two adjacent CA hexamers, 1VU5_hijklm & 1VU5_uvwxyz are rather planar along the axis of the viral capsid cone and thus the interhexameric space is rather narrow allowing the modeled CypA molecule to bridge the two CA hexamers. A detailed view from the top of this hypothetical interface reveals how the CypA molecule (modeled as attached to CA-NTD2) is enclosed within the flexible surface loops of CA-NTD1 and CA-NTD3 that bear biologically significant residues with CypA-related phenotypes (Figure A.2).

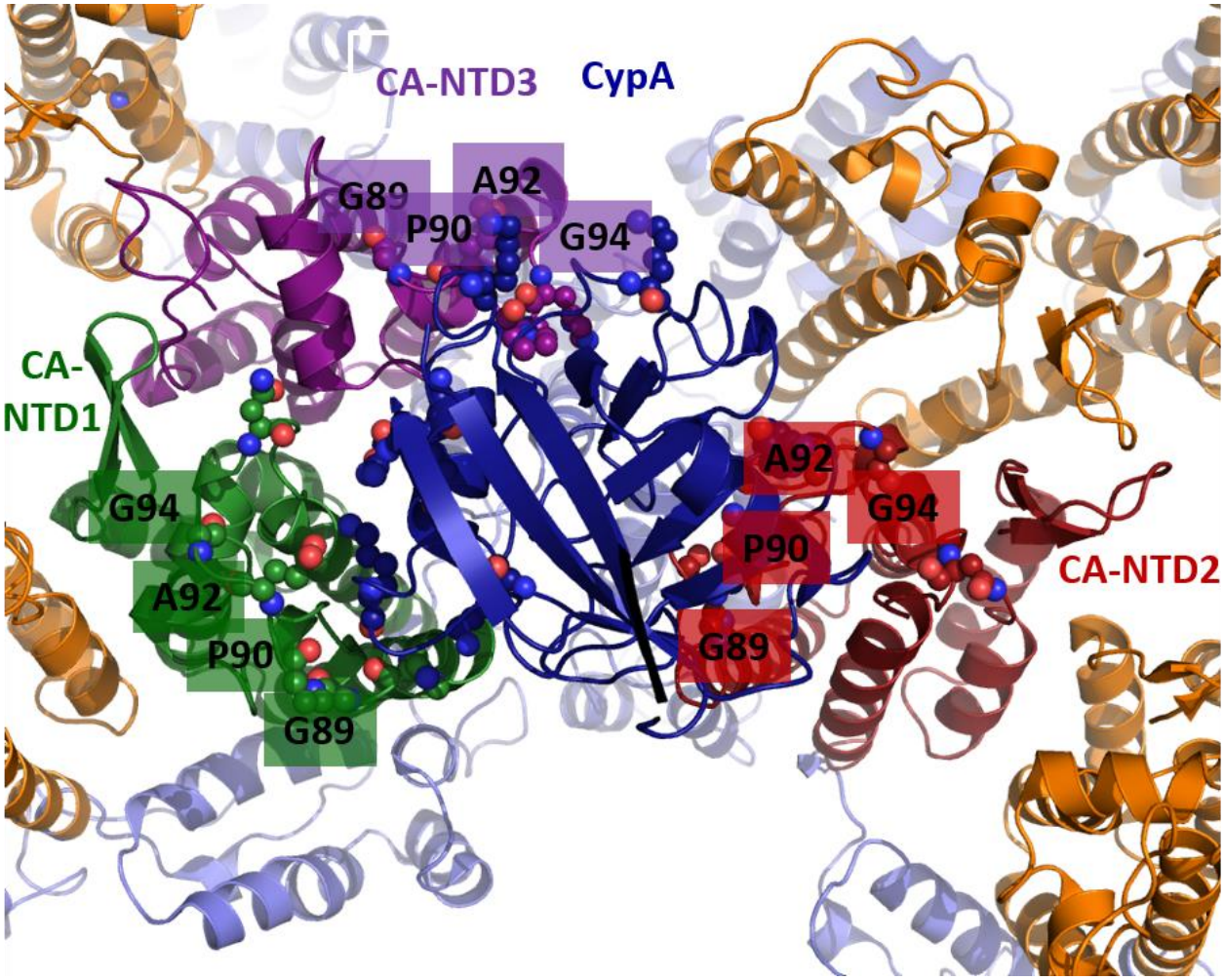

Figure A.2 The CA-NTD2:CypA:CA-NTD1/3 interhexamer bridging model, with CA residues responsible for CypA-related phenotypes highlighted. Top view.

The model, as it is, depicts a static configuration of all the individual molecules in relation to each other. The proposed secondary interface, in actuality, has three degrees of freedom: (i) the flexible CypA-loop of CA-NTD2 (1VU5_i) that the CypA molecule is attached to, (ii) the flexible CypA-loop of CA-NTD1 (1VU5_y), and (ii) the flexible CypA-loop of CA-NTD3 (1VU5_z) (Figure A.2).

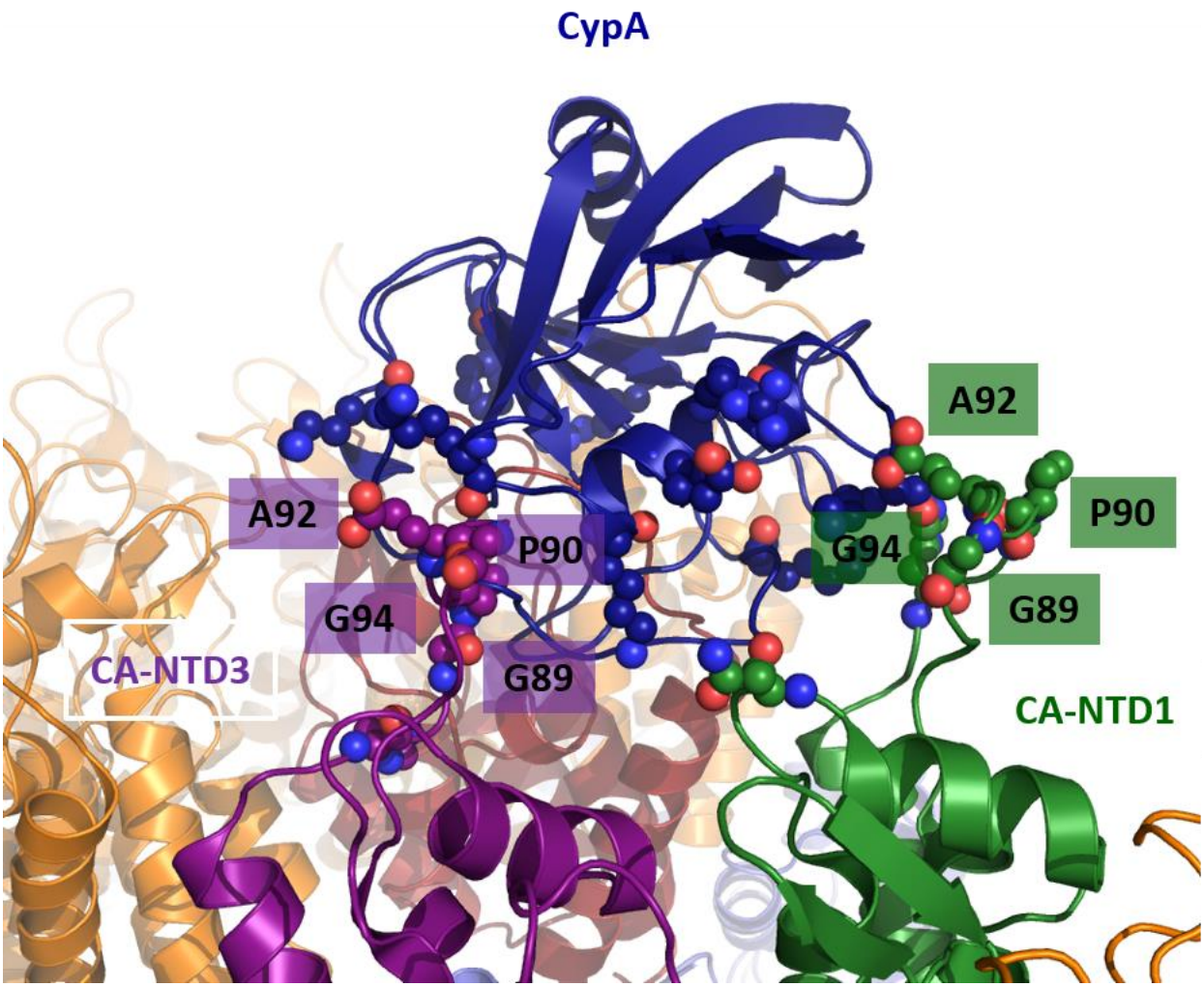

Figure A.3 The CA-NTD2:CypA:CA-NTD1/3 interhexamer bridging model, with potential CypA residues lining the secondary CypA:CA interface highlighted. Head on view to CypA from the perspective of the neighboring CA hexamer (CA-NTD1 & CA-NTD3).

According to the model, previously identified CA-NTD surface loop residues A92, G94 and N121, all of which can render HIV-1 CsA-dependent and CypA-sensitive upon mutation (A92E, G94D, N121K), surround the CypA molecule from the opposite side of where it is attached to the CA-NTD2 CypA loop (G89-P90) via its active site residue, F60 (Braaten et al., 1997). CA-NTD H87 is also found at this interface (Figure A.2), which upon mutating to H87P/Q can affect CypA incorporation into virions (Gatanaga et al., 2006).

Another perspective (Figure A.3) reveals the CypA residues facing this hypothetical interface. CypA residues K28, K31, R37, K44, K76, and K91 are highlighted due to their potential for electrostatic interactions with the CypA-loop mutants A92E and G94D on CA-NTD1 and CA-NTD3, taking into account the three degrees of structural freedom mentioned earlier. The most dramatic juxtaposition between CypA and the neighboring CA hexamer is where CypA K28 comes in close proximity of CA-NTD3 A92E (the ε-amino group of CypA K28 is ~ 4.6 Å from the γ carboxyl group of CA-NTD3 A92E) and where CypA R37 and K44 approach CA-NTD1 A92E (the guanidine group of CypA R37 and the ε-amino group CypA K44 are ~ 5.9 Å and ~ 4.6 Å away from CA-NTD1 A92E, respectively). Another CypA residue E34 may swing close enough to CA N121, potentially enabling electrostatic interactions with N121K; another CypA-dependent mutant of CA.

D. Discussion

As mentioned in the Introduction, research on the molecular architecture of the supramolecular CypA:capsid structure has been lagging behind our understanding of the quaternary capsid structure. CypA has been a prominent yet elusive cellular factor regulating HIV-1 infection via its interaction with CA resulting in phenotypes affecting almost all replicative steps leading up to provirus formation.

Given the known conical topology of the HIV-1 capsid coat (Zhao *et al.*, 2013), interhexameric spacing and angles vary along different axes of the capsid cone. Thus, the model does neither propose that all interhexameric spacings along the cone can accommodate such a bridging, nor does it predict that such a secondary interface will be formed by all CypA molecules attached to the core. But the capsid cone has a planar surface along its vertical axes (Figure 1.5) that minimizes the interhexameric spacing, and thus may support such bridging. From another perspective CypA is a cellular factor that may regulate core stability (Li et al., 2009; Shah et al., 2013), and it is intuitive that core (supramolecular intermultimeric) stability might be modulated by strengthening or weakening interhexameric interactions (CA-NTD2:CypA:CA-NTD1/3) rather than CA-NTD2:CypA only (Figure A.2).

In the case of WT HIV-1 capsid, the hypothetical secondary interface, enabled by neighboring flexible surface CypA loops, may aid interhexameric stability by hydrophobic or electrostatic interactions between CypA and adjoining CA-NTD1/3. The CypA residues highlighted in Figure A.3 may or may not be responsible for such interactions, even though the revelation that CypA-dependent mutants face these basic residues makes it tempting to speculate so. Thus the model predicts that CypA is held in place in between two hexamers by its canonical interaction with the CA-NTD2 CypA loop (G89-P90) at its active site (F60), and by

noncanonical - and probably weaker - interactions with the CypA loops of CA-NTD1/3 at its opposite end, independent from its active site.

It is worth emphasizing that while interpreting this hypothetical structure it was assumed that the reference CA A92E lattice and the positioning of the mutant CypA loops (Zhao et al., 2013) were a good fit for CA WT as reported previously for WT and A92E CA-NTDs (Kelly et al., 2006).

D.i. Implications for CypA-sensitive, CsA-dependent HIV-1 CA mutants

The two more established CypA-sensitive, CsA-dependent mutants of the CypA loop; i.e. A92E and G94D, both carry a negative charge. Our current knowledge refutes the hypothesis that these may be loss-of function mutants with regards to CypA binding. The alternative explanation, i.e. that the restricted phenotype of these mutants may be due to a gain of function such as CypA binding while under CsA selection (Aberham et al., 1996), has not been addressed. The negative charge on these two mutant residues prompted us to look for potential amino acids on CypA at this non-canonical interface, which may enable electrostatic interactions. In our static model, the ε-amino group of CypA K28 is in close proximity (~ 4.6 Å) of the γ carboxyl group of CA-NTD3 A92E; and the guanidine group of CypA R37 and the ε-amino group CypA K44 are ~ 5.9 Å and ~ 4.6 Å away from CA-NTD1 A92E, respectively. Though not as close, CypA K31, K76 and K91 also face the mutated CA-NTD CypA loops at this hypothetical interface. As mentioned before, CypA is attached to CA-NTD2 via a flexible CypA-loop, and both CA-NTD1 and CA-NTD3 CypA loops are flexible themselves, which may even allow closer spacing between CypA and the CA-NTD1/3 CypA loops.

Our working hypothesis is that by enabling electrostatic interactions these mutants may be stabilizing this hypothetical noncanonical interface to the detriment of HIV-1, since a rigid CypA bridge with both ends locked tight onto the hexameric lattice may cause aberrant stability or may limit exposure of CA surfaces beneath that may need to be utilized by other cellular cofactors (Figure A.2 & Figure 2.10). Similary, the recently identified CypA-sensitive, CsA-dependent phenotype of CA N121K (Takemura et al., 2013) might also stem from such an additional interaction with CypA at this interface. A potential point of interaction could be CypA E34 in this case.

Thus the model suggests that the CsA-dependent phenotype of HIV CA mutants such as A92E, G94D, N121K may be due to the need of HIV-1 for a single flexible CA-NTD2:CypA hinge only but not a rigid CA-NTD2:CypA:CA-NTD1/3 bridge. In the presence of CsA, CypA binding to CA-NTD2 would be inhibited, yet the aforementioned CsA-dependent mutations might allow continuing CypA association with the capsid core, albeit at a possibly weaker interface.

Supporting this model, there are two reports of functional evidence for A92E conferring an ability for CA to interact with CypA even when the primary interaction at the CypA active site is inhibited: CA P90A/A92E, which harbors P90A (a CypA binding mutant) is actually sensitive to Cyp-mediated TRIMCyp restriction in OMK cells when compared to P90A mutant virus (Hatziioannou *et al.*, 2004; Diaz-Griffero *et al.*, 2006). In the absence of CsA however, CypA would be locked onto its place, to the detriment of these mutants. The weak interactions allowed by WT CA may aid HIV-1 infectivity, though they may not be enough to utilize CypA in the presence of CsA, when primary binding to CA-NTD2 is inhibited (Figure A.3). The model may not account for the phenotypes of all CypA-sensitive mutants: T54A (hypostable cores) and

E45A (hyperstable cores) both face away from the CypA molecule spanning the CA-NTDs on the surface and their phenotype may be rather due to some intrinsic stability defect, which may indirectly affect PIC import and integration.

D.ii. Implications for other CA-binding proteins

As shown in a CA-NTD:CPSF6 15-mer cocrystal, and then modeled onto the hexamer:hexamer interface in Figure 2.10, CPSF6 is believed to bind CA-NTD within this surface pocket lined by helix 4 that faces the interhexameric space. With CypA potentially capping this interspace and with CPSF6 being much larger than the pocket itself (and possibly having to bury the CA-interacting loop into this pocket from above), it is probable that access of CPSF6 may be modulated by the CypA cap. Alternatively, CypA and CPSF6 may modulate or require the presence/function of each, even though we have not yet been able to find strong evidence suggestive of such modulation in Chapter 3. CypA has been shown to modulate TRIM5α recognition and activity (Stremlau et al., 2006b). This may stem from CypA having a stabilizing effect on the capsid lattice, whose superstructural integrity is required by TRIM5α for recognition (Towers et al., 2003).

The observation that CA N74D/G94D (Ambrose et al,. 2012) and CA A92E/A105T and T54A/A105T (Yang et al., 2007) are rescued from their respective CsA-dependent, CypA-sensitive phenotypes (G94D, A92E, T54A) is further support that there may be a functional talk between CPSF6 (both N74D and A105T render HIV-1 CPSF6-358 resistant by impaired binding, De Iaco et al., 2013) and CypA, though the details of such interaction is currently beyond our understanding. However the observation that A92E can either be rescued by N74D (a CPSF6-binding mutant; De Iaco et al., 2013) or P90A (a CypA binding mutant; Li et al., 2009)

in HeLa cells hints that this historically labeled CypA-dependent restriction may rather be CypA/CPSF6-dependence. Structural and biochemical efforts trying to understand this quaternary relationship on the CA hexamer:hexamer interface should be immensely informative to deepen our understanding.

It is noteworthy that RanBP2/Nup358, which has proposed roles in mediating HIV-1 PIC nuclear entry and integration site targeting (Zhang et al., 2010; Ocwieja et al., 2011), also harbors a C-terminal Cyp domain (Wu et al., 1995) and may also be utilizing such interhexameric bridging in its interaction with CA (Bichel et al., 2013). Additional cell type dependent cofactors (some of which may be harboring Cyp-domains themselves, Davis et al., 2010) may also be modulating CPSF6 and CypA binding to CA, adding yet another layer of complexity.

D.iii. Future experiments proposed to test the model

Biochemical assays testing for interaction would be most informative. The proposed secondary interface on a CA hexamer can be produced biochemically as a stable hexamer (Pornillos et al., 2009). One could then devise a binding assay between this construct and active site mutant CypA (F60A or R55A) wherein any binding to the CypA loop mediated by CypA active site would be precluded. The effect of proposed residues (**C.i**) on CA-NTD1/3 and CypA that may mediate secondary interactions can then be assayed. Given that such secondary interactions are strong enough, binding to mutant CA (A92E/G94D/N121K) may be detected even with an active site mutant of CypA (F60A).

Based on the hypothesis that the secondary interface may be strengthened/further stabilized in the case of A92E/G94D/N121K (gain of function/binding mutants), CypA binding

to these mutant CA hexamers may be less/not affected by CsA. Alternatively, CypA residues highlighted in Figure A.3 (K28, K31, R37, K44, K76, K91) can be mutated to reverse charges and then tested for binding to CA mutants A92E/G94D; or in the case of E34 to N121K.

Alternative structural determination methods such as 3D cryoEM imaging and NMR studies on CypA:CA complexes may shed light into the existence of such a noncanonical CypA:CA interaction. We set up a collaboration with Dr. Zhang (University of Pittsburgh – Department of Structural Biology) and Dr. Polenova (University of Delaware – Department of Chemistry and Biochemistry) to test the model employing these methods. Preliminary reports confirm the presence of such a novel noncanonical interaction between CypA and adjacent CA hexamer though the data awaits a careful analysis and independent confirmation and thus were not included in this dissertation.

APPENDIX B

LIST OF PUBLICATIONS I CONTRIBUTED TO OVER THE COURSE OF THIS DISSERTATION

8: **Oztop I**, Cook N, Lee K, Matreyek K, Ahn J, Cherepanov P, KewalRamani VN, Engelman A. Direct interaction with CPSF6 but not with HIV-1 CA determines the requirement for TNPO3 in HIV-1 infection (in preparation)

(Work in progress. Performed all of the experiments, for which some of the biochemical and cellular reagents were provided by collaborators.)

7: Maertens GN, Cook NJ, Wang W, Hare S, Gupta SS, **Oztop I**, Lee K, Pye VE, Cosnefroy O, Snijders AP, Kewalramani VN, Fassati A, Engelman A, Cherepanov P. Structural basis for nuclear import of splicing factors by human Transportin 3. Proc Natl Acad Sci USA. 2014 Feb 18; 111(7):2728-33.

(Contributed the GST-CPSF6-441-588 bacterial protein expression construct that was utilized to express and purify the protein used in Figs 4E and S10 in recombinant TNPO3 pull-down assays.)

6: Shah VB, Shi J, Hout DR, **Oztop I**, Krishnan L, Ahn J, Shotwell MS, Engelman A, Aiken C. The host proteins transportin SR2/TNPO3 and cyclophilin A exert opposing effects on HIV-1 uncoating. J Virol. 2013 Jan; 87(1):422-32.

(Contributed recombinant TNPO3 and 6xHis-RanQ69L protein reagents that were used in Figs 2, 4 and 6E in in vitro HIV-1 core uncoating assays)

5: Matreyek KA *, **Oztop I** *, Freed EO, Engelman A. Viral latency and potential eradication of HIV-1. Expert Rev Anti Infect Ther. 2012 Aug; 10(8):855-7. * Equal contribution

(Meeting review for Keystone Symposium: Frontiers in HIV Pathogenesis, Therapy and Eradication, March 2012 in Whistler, British Columbia, Canada. Contributed half the writing of the manuscript.)

4: Ambrose Z, Lee K, Ndjomou J, Xu H, **Oztop I**, Matous J, Takemura T, Unutmaz D, Engelman A, Hughes SH, KewalRamani VN. Human immunodeficiency virus type 1 capsid mutation N74D alters cyclophilin A dependence and impairs macrophage infection. J Virol. 2012 Apr; 86(8):4708-14.

(Generated and analyzed data for Fig 1E [Figure 2.9C in the dissertation]: Quantified the binding of ectopically expressed CypA to WT and mutant HIV-1 CA-NC assemblies to show that the increased CsA-sensitivity of N74D may stem from a reduced binding affinity to CypA.)

3: Lee K, Ambrose Z *, Martin TD *, **Oztop I**, Mulky A, Julias JG, Vandegraaff N, Baumann JG, Wang R, Yuen W, Takemura T, Shelton K, Taniuchi I, Li Y, Sodroski J, Littman DR, Coffin JM, Hughes SH, Unutmaz D, Engelman A, KewalRamani VN. Flexible use of nuclear import pathways by HIV-1. Cell Host & Microbe. 2010 Mar 18; 7(3):221-33. * Equal contribution

(Generated and analyzed data for Fig 5D [Figure 2.7 in the dissertation]: Quantified the binding of ectopically expressed CPSF6 and CPSF6-358 to WT and N74D CA-NC assemblies to show for the first time that CPSF6 is a CA-interacting protein and that N74D abolishes the interaction.)

2: Krishnan L *, Matreyek KA *, **Oztop I** *, Lee K, Tipper CH, Li X, Dar MJ, Kewalramani VN, Engelman A. The requirement for cellular transportin 3 (TNPO3 or TRN-SR2) during infection maps to human immunodeficiency virus type 1 capsid and not integrase. J Virol. 2010 Jan; 84(1):397-406. * Equal contribution

(Generated and analyzed data for Fig 5 [Figure 2.5 in the dissertation]: Quantified the infectivities of several HIV-MLV Gag-Pol chimerae on TNPO3 depleted cells to show for the first time that TNPO3 dependency is linked to the presence of HIV-1 CA but not HIV-1 IN within Gag-Pol. Contributed to writing the manuscript.)

1: Engelman A, **Oztop I**, Vandegraaff N, Raghavendra NK. Quantitative analysis of HIV-1 preintegration complexes. Methods. 2009 Apr; 47(4):283-90.

(Contributed to writing the manuscript.)